GEORGIA INSTITUTE OF TECHNOLOGY
OFFICE OF CONTRACT ADMINISTRATION
SPONSORED PROJECT INITIATION

Date: 9/9/80

Project Title: Products of the Chlorination and Ozonolysis of Synthetic Dyes

Project No: E-20-684 -B

Project Director: Dr. Joseph L. Gould

Sponsor: National Science Foundation

Agreement Period: From September 1, 1980 Until ~~February 28, 1983~~ ~~8-31-83~~ 9-16-86

Type Agreement: Grant No. DAR-7925722, dated August 5, 1980

Amount: $134,202 (E-20-684)
$ 1,390 (E-20-352)
$135,592 TOTAL

Reports Required: Annual Progress Report; Final Project Report

Sponsor Contact Person (s):

Technical Matters

Tapan Mukherjee
Program Manager for Chemistry & Chemical Applications
Applied Physical, Math & Bio Sci & Engr. Sect.
Division of Applied Research
National Science Foundation
Washington, D.C. 20550
(202) 357-7423

Contractual Matters
(thru OCA)

Al Rice
AAEO/EAS Branch
Division of Grants and Contracts
Directorate for Administration
National Science Foundation
Washington, D.C. 20550
(202) 357-9626

Defense Priority Rating: N/A

Assigned to: Civil Engineering (School/Laboratory)

COPIES TO:

Project Director
Division Chief (EES)
School/Laboratory Director
Dean/Director—EES
Accounting Office
Procurement Office
Security Coordinator (OCA)
Reports Coordinator (OCA)

Library, Technical Reports Section
~~Office of Computing Services~~
~~Director, Physical Plant~~ EES R+P
EES Information Office
Project File (OCA)
Project Code (GTRI)
Other C.E. Smith

CA—3 (3/76)

)RGIA INSTITUTE OF TECHNOLOGY OFFICE OF CONTRACT ADMINISTRATION

SPONSORED PROJECT TERMINATION/CLOSEOUT SHEET

Date 7-14-87

:t No. E-20-684 School/~~Lab~~ CE

ies Subproject No.(s) G-33-672/Moran

:t Director(s) Dr. Joseph L. Gould GTRC / ~~GIT~~

or National Science Foundation

Products of the Chlorination and Ozonolysis of Synthetic Dyes

ive Completion Date: 8/31/83 (Performance) 11/30/83 (Reports)

Contract Closeout Actions Remaining:

- [X] None
- [ ] Final Invoice or Final Fiscal Report
- [ ] Closing Documents
- [ ] Final Report of Inventions
- [ ] Govt. Property Inventory & Related Certificate
- [ ] Classified Material Certificate
- [ ] Other

ies Project No. Continued by Project No.

; TO:

Director
h Administrative Network
h Property Management
ting
ment/GTRI Supply Services
1 Security Services
Coordinator (OCA)
~~XXXX~~

Library
GTRC
~~Research Communications (2)~~
Project File
Other Duane H.
Angela DuBose
Russ Embry

)CA 69.285

C. K Rodgers

GEORGIA TECH RESEARCH INSTITUTE
ADMINISTRATION BUILDING
GEORGIA INSTITUTE OF TECHNOLOGY
ATLANTA, GEORGIA 30332
(404) 894-4820

November 11, 1982

Refer to: FGC/E-20-684, G-33-672

Division of Chemical and Process
Engineering
Directorate for Engineering
National Science Foundation
Washington, DC 20550

Attention: Tapan Mukherjee
Program Manager for Chemistry
and Chemical Applications

Subject: Grant No. DAR-7925722
"Products of the Chlorination and Ozonolysis
of Synthetic Dyes" under the direction of Joseph P. Gould

Dear Mr. Mukherjee:

As required by the General Conditions of the subject grant, NSF approval is requested to extend the grant period for six (6) months, or to August 31, 1983. No additional funding is required as a result of this time extension.

The research program funded by this grant has been delayed due to the following:

1) Due to low student enrollments during the past two years, it has been difficult to secure continuous student assistance. Breaks in the conduct of the research due to this factor have approximated nine months in duration. This has been the major problem.

2) The development of some of the needed analytical methodology has been unexpectedly time consuming.

3) Likewise aquisition purification and characterization of the commercial dyes have taken longer than anticipated.

As of October 1, 1982, the unexpended balance of the grant was $13,200. The remaining funds are distributed as follows:

Personal Services	$ 7,500
Fringe Benefits	200
Materials & Supplies	1,000
Overhead	4,500
TOTAL	$ 13,200

Telex: 542507 GTRIOCAATL Fax: 404-894-3120

The enclosed report from Dr. Gould gives the progress to date as well as the proposed study during the requested extension period.

We trust the above information and Dr. Gould's report will provide sufficient information for your consideration of this request for a six month no-cost time extension.

Thank you for your attention to this matter.

Sincerely,

Faith G. Costello
Contracting Officer

Joseph P. Gould, Ph.D
Assistant Professor
School of Civil Engineering

FGC/eb

Enclosure: As stated
xc: Al Rice
AAEO/EAS Branch
Division of Grants and Contracts
(w/o enclosure)

bxc: D. J. Gould
Dr. Moran
L. Murphy
D. Welch
O. Rodgers - with 2 copies enclosure
file - with enclosure
Suspense 12/20/82

Selection and Characterization of Dyes

While a bewildering array of commercial dyes was available to select from, it was decided to confine the choices to an industry characterized by a very large volume use of a fairly narrow range of dyes. In accordance with this standard, dyes used in substantial quantities in the paper dying industry were selected from a list supplied to the investigators by TAPPI. In addition, the dyes Direct Yellow 4 and Direct Yellow 12 were selected for this study on the basis of their interesting structural characteristics.

The dyes were obtained in the purest form available from commerical suppliers. Reference standards were prepared by crystallization from methanol. Purity was checked by both conventional and reverse phase thin layer chromatography (TLC). The percent purity of both the reference standards and the commercial dyes was established by total organic carbon (TOC). The reference standards were then used for the development of spectrometric parameters for analytical used.

Analytical Methodology

Analysis of synthetic dyes is being based on visible spectrometry. Since each dye presents its own unique problems and solutions in this regard no detailed discussion of the techniques developed will be presented here. Dye breakdown products are being monitored by TLC and liquid chromatography (HPLC).

The high color levels of the dye solutions was found, unsurprisingly, to render colorimetric chlorine analyses (DPD-FAS etc.) useless. All chlorine analyses are therefore being conducted by amperometric titrations using phenylarsine oxide. Ozone analyses are being performed iodometrically.

Results: Chlorination

Dye chlorination over a broad pH and chlorine to dye ratio range has been found empirically to adhere well to mixed second order kinetics. The reaction rates however are spread over a very substantial range of values. Broadly

speaking, these results meet expectations based on dye structures. For example, the chlorination rate of DY-12 with its moderately activating alkoxy groups was found to be at least an order of magnitude slower than was the case for the DY-4 with its strongly activating phenolic hydroxyls. Similar broad brush deductions based on structure have been found to be applicable to the other dyes as well.

Methodology for purification of individual products of the chlorination reactions utilizing TLC and HPLC has been developed with specific systems available for several dyes and near completion for the balance of the dyes. Techniques for identification of purified products will be discussed further on in the report.

Results: Ozonolysis

Treatment of the dyes with ozone has been carried out in semi-batch heterogeneous systems. In these gas flow systems dye consumption and ozone uptake have been recorded as a function of time. As is typical of such systems, dye consumption has followed a first order kinetic model with the rate constants relatively insensitive to structural features and pH in single solute systems. Concurrent dye ozonolysis studies by the investigator and a colleague using competative systems with several dyes have led to a model relating such competition to dye behavior at the gas liquid interface. A publication based on these results is pending.

Mass Spectrometric Studies

Pyrolysis-gas chromatography-mass spectrometry has proven to be a powerful tool for the analysis of involatile aniline based dyes. It has been used to quantify and characterize dyes in the 0.1 μg/liter concentration level. Although the pyrolysis approach is effective, we found it would be desirable to increase the sensitivity of our analysis as well as shorten the analysis time which is

controlled by the chromatographic elution times of the molecular subunits from the pyrolysis. These pyrolysis product compounds must be analyzed one at a time as they emerge from the chromatograph. In general, the larger molecular subunits from the pyrolysis process contain the most structural information but these are the compounds which have long elution times. Although classes of particular dyes can be identified by their pyrolysis products, i.e. aniline from aniline based dyes, etc., it is not possible always to unambiguously identify the original starting dye molecule. For example, isomeric molecules are difficult to distinguish using pyrolysis-gas chromatography-mass spectrometry.

In order to improve our analysis methodology we have been pursuing a new approach to dye molecule identification. This method involves desorption chemical ionization in which the dye to be analyzed is placed directly into the ion source plasma region of a spectrometer operated in the chemical ionization mode. The sensitivity of our mass spectrometer system can be quite high and it is probable that this direct desorption chemical ionization method will extend significantly the detection capability of our analysis well below the 0.1 µg/liter level attainable in the pyrolysis-GC-mass spectrometry method. Pyrolysis produces both volatile and involatile products and the latter are not passed through the chromatograph for detection. In our chemical ionization approach a small, fine wire extension to the direct probe in our Finnegan-MAT 112S mass spectrometer was built. The dye sampe to be analyzed is put into a micro-solution and a drop evaporated on this wire assembly. The probe is then inserted into the mass spectrometer ion source to a position where the fine wire

is centered in the ionizing electron beam. The source is operated at very high pressure with a chemical ionization gas such as pure isobutane. The small plasma, created by the electron beam ionization of high pressure isobutane, is used to flash heat and simultaneously desorb dye molecules on the fine wire.

Ion-molecule reactions of the type

a) $C_4H_9^+$ + Dye molecule → (Dye molecule + H)$^+$ + C_4H_8

occur between isobutane ions and desorbed dye molecules. Several other reaction paths occur such as ionization of the dye molecules

b) e + Dye molecule → (Ionic Fragments)$^+$ + 2e

as well as pyrolysis of the dye molecules in the plasma and desorption of neutral fragments. Neutral fragments undergo the following reactions

c) $C_4H_9^+$ + (Dye fragment molecules) → (Dye fragment molecules + H)$^+$ + C_4H_8

and

d) e + (Dye fragment molecules) → (Ionic Dye fragments)$^+$ + 2e

Of the four reactions above only reaction a) gives information on the molecular mass of the dye molecule. We have enjoyed a certain measure of success in observing reaction a) and are attempting to maximize this interaction at the expense of routes b), c) and d). Fragment ions have dominated the spectra we have obtained so far but steady improvements are being made to maximize reaction a) by variation of electron beam intensity, chemical ionization gas pressure, probe configuration, sample position in the plasma, etc. Although not indicated in reaction a), the ion-molecule reaction between $C_4H_9^+$ ions and dye molecules give rise to high molecular weight fragments which can be used to analyze the structural configuration of the starting molecules. Minimizing routes b, c and d shifts the locus of ion mass peaks from the low mass region to a small number of high mass ions of high information content. This will enable us to use selective ion monitoring with greater effectiveness and increase the detection capability and speed of our analysis.

E-20-684

CLAUSE 73

In addition to the reporting requirements specified in Article 13 of the FL 118, Grant General Conditions, a minimum of ten (10) copies of a detailed final technical report (addressed in Part III of NSF Form 98A) is to be submitted within 90 days of the expiration of this grant. The report should describe the research project activities and include a statement regarding the actual or potential utilization of the research results.

XC: OHR

AE-20-684

7. Consultant Services

Payments to individuals for consultant services under this grant shall not exceed the daily equivalent of the then current maximum rate paid to a GS-18 Federal employee (exclusive of indirect cost, travel, per diem, clerical services, vacation, fringe benefits, and supplies.) As of October 1979 this rate is $193 per day.

8. Project Income

a. Royalty Income. Unless otherwise specified in the grant letter, the grantee may retain royalties received as a result of copyrights produced during the life of the grant and for 3 years following the expiration of the grant, up to the amount of $10,000. Royalty income in excess of $10,000 earned during this period will to the extent practicable be maintained in an interest bearing account and remitted and reported annually to NSF.

b. Other Income. Unless otherwise specified in the grant letter, the Federal share of other project income may be retained by the grantee and added to the funds committed to the project by NSF and the grantee and be used to further project objectives. The grantee share may be used as desired by the grantee, including financing the non-Federal share of the project. The "Federal share" and the "grantee share" will reflect their respective contributions to the cost of the project.

9. Cost-Sharing and Cost-Sharing Records

a. The grantee must cost share under this grant in accordance with any specific requirements contained in or referenced by the grant letter. If the grant letter has no specific requirements and if the work supported by this grant is for research resulting from an unsolicited proposal, the grantee must share in the costs of the work at a rate of not less than one percent of total project costs.

b. The grantee must maintain records of all project costs that are claimed by the grantee as cost sharing as well as records of costs to be paid by the Government. Such records are subject to audit. If the grantee's cost participation includes in-kind contributions, the basis for determining the valuation for volunteer services and donated property must be documented.

c. If the grant is for only one or more of the purposes enumerated in GPM 643.1 as not supporting research, cost sharing is not required.

10. Acknowledgment of Support and Disclaimer

An acknowledgment of NSF support and a disclaimer must appear in any publication of any material, whether copyrighted or not, based on or developed under this project, in the following terms:

> "This material is based upon work supported by the National Science Foundation under Grant No. (Grantee should enter NSF grant number)."
>
> All materials, except scientific articles or papers published in scientific journals, must also contain the following:
>
> "Any opinions, findings, and conclusions or recommendations expressed in this publication are those of the author(s) and do not necessarily reflect the views of the National Science Foundation."

11. Reprints of Publications

At such time as any article resulting from work under the grant is published in a scientific, technical or professional journal or publication, two reprints of the publication should be sent to the cognizant NSF Program Officer, clearly labeled with the grant number and other appropriate identifying information.

12. Progress Reports

a. Content of Progress Reports. Unless otherwise specified in the grant letter, progress reports shall include:

(1) A summary of overall progress, including results obtained to date, and a comparison of actual accomplishments with proposed goals for the period;

(2) An indication of any current problems or favorable or unusual developments;

(3) A summary of work to be performed during the succeeding budget period, and

(4) Other information pertinent to the type of project being supported or as specified in the terms and conditions of the grant.

(5) For all grants (standard or continuing) involving human subjects (GPM 711), an updated annual certification is required by NSF as an appendix to the report.

b. Timing of Progress Reports. Unless otherwise specified in the grant letter, two copies of progress reports shall be submitted to the cognizant NSF Program Officer in the following frequency:

For grants with an award duration of 2 years or more, the first report should be submitted no later than 90 days after the anniversary of the effective date of the grant, with succeeding reports annually thereafter, except after the final year. If a request for renewed support is submitted during the final year, the progress report should be attached to such request. Otherwise, only a final project report need be submitted.

13. Final Report Requirements

Unless otherwise specified in the grant letter and within 90 days following the expiration of the grant, the grantee must furnish NSF with:

(a) two copies of the Final Project Report (NSF Form 98A, May 1978); and

(b) the Technical Information items listed in Part III of the Form 98A, as appropriate; and

(c) Final disbursement information on the Federal Cash Transaction Report (SF 272; see GPM 670); and

(d) any unique reports or other end products in accord with the grant letter, including report requirements set forth in any NSF brochure, guide, solicitation, etc., referenced in the grant letter as being directly related to either the award or administration of

cc: OHP

E-20-684

this grant. Technical information items shall be submitted to the NSF Program Officer or as specified in the grant letter.

14. Data Collection

Data collection activities performed under this grant are the responsibility of the grantee and NSF support of the project does not constitute NSF approval of the survey design, questionnaire content, or data collection procedures. The grantee shall not represent to respondents that such data are being collected for or in association with the National Science Foundation or any other Government agency without the specific written approval of such data collection plan or device by the Foundation. However, this requirement is not intended to preclude mention of NSF support of the project in response to an inquiry or acknowledgment of such support in any publication of this data.

15. Title to Equipment

Unless otherwise specified in the grant letter, title to equipment purchased or fabricated with NSF grant funds by a college or university, other nonprofit organization, or a unit of State or local government shall vest in the grantee institution, with the understanding that such equipment (or a suitable replacement obtained as a trade in) will remain in use for the specific project for which it was obtained.

16. Copyright

Unless otherwise provided in the grant letter, the grantee may copyright any books, publications, films, or other copyrightable materials developed in the course of or under this grant. However, any such copyrighted materials shall be subject to a royalty-free, irrevocable, worldwide, nonexclusive license in the United States Government to reproduce, perform, translate, and otherwise use and to authorize others to use such materials for Government purposes.

17. Rights in Inventions

a. Except as otherwise provided in the grant letter, or where an Institutional Patent Agreement has been executed with the grantee (unless the grant letter or the terms of IPA exclude the grant from the operation of the IPA), the following provisions will apply:

b. Whenever any invention that is, or may be, patentable is conceived or first actually reduced to practice in the course of or under this grant, the grantee shall furnish NSF with complete information thereon; and NSF shall have the right to determine whether or not and where a patent application shall be filed and to determine the disposition of the invention and title to and rights under any patent application or patent that may result. In making such a determination, NSF shall take into account the public interest and the equities of the grantee. In any case, NSF may arrange to have the invention described in a printed publication.

c. The grantee, for itself and for its employees, agrees that all documents will be executed and all other actions necessary or proper to carry out the determination of NSF will be taken.

d. Except as otherwise authorized in writing by the Grants Officer, the grantee shall insert in each subcontract having experimental, developmental, or research work as one of its purposes, provisions making this article applicable to the subcontractor and its employees.

e. Reports of inventions required under these provisions or requests for retention of rights in such inventions, as well as requests for guidance in these matters, should be addressed to the NSF Office of the General Counsel.

18. Rights in ADP Data Banks and Software

Unless otherwise provided in the grant letter, data banks and software, produced with the assistance of NSF grants, having utility to others in addition to the grantee shall be made available to users, at no cost to the grantee, by publication or, on request, by duplication or loan for reproduction by others. The investigator who produced the data or software shall have the first right of publication. Grantees will be allowed a reasonable amount of time to make necessary corrections or additions to finite data banks that are incomplete or contain errors, ambiguities or distortions. Privileged or confidential information will be released only in a form that protects the rights of privacy of the individuals involved. Any dispute over the release or use of data or software will be referred to the Foundation for resolution. Any out of pocket costs incurred by the grantee in providing information to third parties may be charged to the third party.

19. Standards for Financial Management Systems

NSF grantees, except State or local units of government, shall have financial management systems that meet the requirements of Attachment F to OMB Circular A-110. State and local units of government shall follow the comparable standards of OMB Circular A-102. Attachment F to OMB Circular A-110 is reproduced as Exhibit III-1 in the NSF *Grant Policy Manual*.

20. Procurement Standards

a. NSF grantees, except units of State or local government, shall follow the requirements of Attachment O to OMB Circular A-110. Units of State or local government shall follow the comparable requirements of OMB Circular A-102. Attachment O to OMB Circular A-110 is reproduced as Exhibit III-2 in the NSF *Grant Policy Manual*.

b. In addition, unless the grant letter provides otherwise, prior written approval shall be obtained from the NSF Grants Officer before:

(1) Any of the research or other substantive project effort is contracted or otherwise transferred.

(2) Contracting for the commercial production or distribution of books, films, or similar materials.

c. NSF approvals will be made by the Grants Officer, who will specify which requirements of this grant must be flowed-down to satisfy the purposes of OMB Circular A-110 or A-102.

XC: OHR
JWW
CES

E-20-684

31. Commercial Publication/Distribution of Grant Materials

Before the commercial publication/distribution of any materials developed under this grant, the grantee shall submit a publication plan for the approval of the Grants Officer.

The plan should include a description of the materials and the rationale for commercial publication and distribution as opposed to dissemination through National Technical Information Service, including an assessment of the potential market for the materials. The plan must address the selection of publishers/distributors, including identification of the firms to be approached so as to assure reasonable competition, and the criteria to be used in the selection.

Further, upon selection of a firm, the Foundation may require that the proposed publication/distribution agreement be approved by the Grants Officer.

32. Resolution of Conflicting Conditions

Should there be any inconsistency between any special conditions contained in the grant instrument and these Grant General Conditions, F.L. 118, the special conditions in the grant instrument shall control.

In the rare event of an apparent inconsistency between these Grant General Conditions and any NSF guides, brochures, etc., cited or included by reference in the grant instrument, the matter should be referred to the NSF Grants Officer for guidance.

XC:OHR

GEORGIA TECH RESEARCH INSTITUTE
ADMINISTRATION BUILDING
GEORGIA INSTITUTE OF TECHNOLOGY
ATLANTA, GEORGIA 30332
Telex: 542507 GTRIOCAATL
Fax: (404) 894-3120
Phone: (404) 894- 4820

September 9, 1980

MEMORANDUM

TO: Dr. Joseph P. Gould, Project Director

FROM: Faith G. Costello

SUBJECT: NSF Grant No. DAR-7925722
Research Project No. E-20-684

Enclosed for your use and information is a copy of the subject grant which provides funding in the amount of $134,202 for the grant period Sept. 1, 1980 through Feb. 28, 1983 for your project entitled "Products of the Chlorination and Ozonolysis of Synthetic Dyes". The grant period includes the usual flexibility period.

A budget request form has been prepared and circulated for signatures. You will receive a copy of the form after this routing is completed. Cost-sharing in the amount of $1,390 is required during the grant period and will be accumulated in E-20-352.

Enclosed is a copy of the Research Agreement Abstract (with NSF Supplement) which contains certain important expenditure restrictions with which you should be familiar. Note particularly the restrictions on equipment and travel.

Also enclosed is a copy of the Deliverable Schedule which will assist you in the timely discharge of your obligations to the sponsor in that regard.

Individual Patent Agreements must be obtained from all persons who perform part of the work under the grant. A completed copy of any Patent Agreement should be provided for GTRI's permanent files. I am sending you a copy of a recommended Patent Agreement which you may reproduce and use.

I will be serving as grant administrator for your project. If there are any questions or problems associated with the administration of your project, please do not hesitate to contact me.

Enclosures: As stated

xc: Dr. J.E. Fitzgerald, w/cy. Enclosures
Dean W.M. Sangster
Mr. F.H. Huff, w/cy. Proposal Budget (2 pp.)
Mr. C.E. Smith w/cy. Proposal Budget (2 pp.); Grant General Conditions: Article No. 15
Mr. O.H. Rodgers, w/cy. Grant General Conditions: Articles No. 11,12, 13, and 31
Mr. J.W. Wilson, w/cy. Patent Agreement; Grant General Conditions: Article No. 17
File E-20-684
Diary

pcb

NATIONAL SCIENCE FOUNDATION
WASHINGTON, D.C. 20550

E-20-684 /Gould

AUG 5 1980

(left)

Grant No. DAR-7925722
Proposal No. DAR-7925722

Mr. E. E. Renfro
Director, Contract Administration
Georgia Tech Research Institute
Administration Building
Atlanta, GA 30332

Dear Mr. Renfro:

The National Science Foundation hereby awards a grant of $134,202 to Georgia Tech Research Institute for support of the project described in the proposal referenced above.

This project, under the direction of Joseph P. Gould, Department of Civil Engineering, is entitled:

"Products of the Chlorination and Ozonolysis of Synthetic Dyes."

This award is effective September 1, 1980 and expires February 28, 1983. A 6 month unfunded flexibility period is included in this award.

This grant is awarded pursuant to the authority of the National Science Foundation Act of 1950 (42 U.S.C. 1861 et seq.) and is subject to FL 118 Grant General Conditions (rev. Oct/79) and the following terms and conditions:

The attached clause number 73.

The attached budget indicates the amounts, by categories, on which NSF has based its support.

The cognizant NSF program official for this grant is Tapan Mukherjee (202) 357-7423. The cognizant NSF grants official is Al Rice (202) 357-9626.

Sincerely yours,

Michael L. Kenefick

Grants Officer

Enclosures

XC: Dr. Gould
Dr. Fitzgerald
Dean Langhaar
F.N. Huff
C.E. Smith
O.N. Rodgers
J.W. Wilson
(as indicated)

APPENDIX VII

NATIONAL SCIENCE FOUNDATION
Washington, D.C. 20550

FINAL PROJECT REPORT
NSF FORM 98A

PLEASE READ INSTRUCTIONS ON REVERSE BEFORE COMPLETING

PART I–PROJECT IDENTIFICATION INFORMATION

1. Institution and Address	2. NSF Program	3. NSF Award Number
Georgia Institute of Technology Atlanta, Georgia 30332	Chemistry & Chemical App'ns	DAR-7925722
	4. Award Period From 9-1-80 To 10-31-83	5. Cumulative Award Amount 134,202

6. Project Title

Products of Chlorination and Ozonalysis of Synthetic Dyes

PART II–SUMMARY OF COMPLETED PROJECT *(FOR PUBLIC USE)*

Six commercial dyes have been treated with chlorine and ozone.

Chlorination reactions were conducted at pH values of 5,7 and 9 and at hypochlorous acid to dye molar ratios ranging from 0.5 to 12. Distilled, chloride free hypochlorous acid was used in all cases and the reactions were conducted in actinic glass vessels to eliminate the effect of light on the reaction. Ultraviolet/visible spectrometry confirmed that the chlorination was associated with total loss of the initial dye color and rapid disruption of aromatic structures in all cases except two. Based on this direct visible spectrometry was used to monitor dye concentration while chlorine was analyzed by amperometric titrations. Two stilbene type dyes, studied yielded a yellow intermediate product necessitating the use of a modified analytical procedure.

All chlorination reactions were found to adhere to mixed second order kinetics. Response to pH variation was not uniform from dye to dye. Three showed substantial rate increases with increasing pH, two displayed significant decreases and one was essentially unchanged in the range of pH from 5 to 9. Chlorine consumption was clearly related to the number of reactive groups in the dye structure. Ratios as high as 11 moles of hypochlorous acid per mole of dye and as low as two moles per mole were observed. Again irratic pH dependancies were found.

The kinetics of dye ozonation measured in Semibatch heterogeneous gas flow systems were characterized by extremely high rates of dye removal and essentially total distruction of aromatic structures. Products detected were consistant with those produced or ozonation of phenols (glyoxal, glyoxylic acid, etc.). The reactions displayed the usual diffusion controlled first order kinetics commonly observed in such sysems. Rate constants were again subject to rather inconsistant trends with respect to pH. Ozone consumption values for all six dyes were in the range of 20 to 40 moles of ozone per mole of dye removed with little pH dependance observed.

PART III–TECHNICAL INFORMATION *(FOR PROGRAM MANAGEMENT USES)*

1. ITEM *(Check appropriate blocks)*	NONE	ATTACHED	PREVIOUSLY FURNISHED	TO BE FURNISHED SEPARATELY TO PROGRAM	
				Check (✓)	Approx. Date
a. Abstracts of Theses	X				
b. Publication Citations		X			
c. Data on Scientific Collaborators				X	
d. Information on Inventions	X				
e. Technical Description of Project and Results				X	11-30-84
f. Other *(specify)*					

2. Principal Investigator/Project Director Name *(Typed)*	3. Principal Investigator/Project Director Signature	4. Date
Joseph P. Gould		8-10-84

NSF Form 98A (3-83) Supersedes All Previous Editions

Form Approved OMB No. 3145-0058

ITIONAL SCIENCE FOUNDATION
Washington, D.C. 20550

FINAL PROJECT REPORT
NSF FORM 98A

PLEASE READ INSTRUCTIONS ON REVERSE BEFORE COMPLETING

PART I—PROJECT IDENTIFICATION INFORMATION

nstitution and Address	2. NSF Program	3. NSF Award Number
eorgia Institute of Technology chool of Civil Engineering tlanta, GA 30332	Physical Math & Engineering Applications	DAR-7925722
	4. Award Period From 9-1-80 To 2-28-83	5. Cumulative Award Amount $134,202

Project Title
Products and Kinetics of the Chlorination and Ozonolysis of Synthetic Dyes

PART II—SUMMARY OF COMPLETED PROJECT *(FOR PUBLIC USE)*

In order to evaluate the efficacy of chemical oxidants in destroying synthetic ganic dyes and to identify the products of these processes, a series of kinetic studies as been carried out on several purified commercial dyes using chlorine and ozone in itch and semibatch systems at controlled pH values. In addition, variations on common C/MS methods have been evaluated for identification and quantification of the dyes and eir reaction products have been investigated.

Chlorine was found to react with all dyes studied in accordance with mixed second der kinetics with consequent decolorization of all but the least reactive dye at rates ggestive of highly efficient bleaching. The relationship of the rate to pH was usually ak and not amenable to easy rationalization. No relationship between the rate and itial chlorine concentration was noted. The degree of chlorine consumption was also asured in relationship to the amount of dye destroyed. Negligible chloramine formation s observed. The kinetics and oxidant consumption for ozonationof several dyes were also udied. Again, high decolorization efficiencies were obtained.

Pyrolysis GC/MS methods were applied to several of the dyes and possible chlorination oducts. The pyrolysis patterns observed were readily rationalized and could be used to proximate the dye structure. Pyrolysis GC/MS was also capable of quantitative evaluation of synthetic dyes and when combined with simple preconcentration steps provided asurement in the part per trillion range in a waste water effluent. Doubly charged ion ss spectrometry was found very valuable in identification of pyrolysis fragments.

PART III—TECHNICAL INFORMATION *(FOR PROGRAM MANAGEMENT USES)*

ITEM *(Check appropriate blocks)*	NONE	ATTACHED	PREVIOUSLY FURNISHED	TO BE FURNISHED SEPARATELY TO PROGRAM	
				Check (✓)	Approx. Date
Abstracts of Theses	X				
Publication Citations			X	X	8-31-87
Data on Scientific Collaborators				X	8-31-87
Information on Inventions	X				
Technical Description of Project and Results		X			
Other *(specify)* None					

rincipal Investigator/Project Director Name *(Typed)*	3. Principal Investigator/Project Director Signature	4. Date
Joseph P. Gould		6-29-87

orm 98A (1-87) Supersedes All Previous Editions

Form Approved OMB No. 3145-0058

PART IV - SUMMARY DATA ON PROJECT PERSONNEL

NSF Division Applied Research/EAS

The data requested below will be used to develop a statistical profile on the personnel supported through NSF grants. The information on this part is solicited under the authority of the National Science Foundation Act of 1950, as amended. All information provided will be treated as confidential and will be safeguarded in accordance with the provisions of the Privacy Act of 1974. NSF requires that a single copy of this part be submitted with each Final Project Report (NSF Form 98A); however, submission of the requested information is not mandatory and is not a precondition of future awards. If you do not wish to submit this information, please check this box ☐

Please enter the numbers of individuals supported under this NSF grant.
Do not enter information for individuals working less than 40 hours in any calendar year.

*U.S. Citizens/ Permanent Visa	PI's/PD's		Post-doctorals		Graduate Students		Under-graduates		Precollege Teachers		Others	
	Male	Fem.	Male	Fem.	Male	Fem.	Male	Fem.	Male	Fem.	Male	Fem.
American Indian or Alaskan Native												
Asian or Pacific Islander												
Black, Not of Hispanic Origin												
Hispanic												
White, Not of Hispanic Origin	2	0			3	2	4	3			2	0
otal U.S. Citizens	2	0			3	2	4	3			2	0
lon U.S. Citizens												
otal U.S. & Non-U.S. ..	2	0			3	2	4	3			2	0
lumber of individuals who have a handicap that limits a major life activity.												

*Use the category that best describes person's ethnic/racial status. (If more than one category applies, use the one category that most closely reflects the person's recognition in the community.)

AMERICAN INDIAN OR ALASKAN NATIVE: A person having origins in any of the original peoples of North America, and who maintains cultural identification through tribal affiliation or community recognition.

ASIAN OR PACIFIC ISLANDER: A person having origins in any of the original peoples of the Far East, Southeast Asia, the Indian subcontinent, or the Pacific Islands. This area includes, for example, China, India, Japan, Korea, the Philippine Islands and Samoa.

BLACK, NOT OF HISPANIC ORIGIN: A person having origins in any of the black racial groups of Africa.

HISPANIC: A person of Mexican, Puerto Rican, Cuban, Central or South American or other Spanish culture or origin, regardless of race.

WHITE, NOT OF HISPANIC ORIGIN: A person having origins in any of the original peoples of Europe, North Africa or the Middle East.

THIS PART WILL BE PHYSICALLY SEPARATED FROM THE FINAL PROJECT REPORT AND USED AS A COMPUTER SOURCE DOCUMENT. DO NOT DUPLICATE IT ON THE REVERSE OF ANY OTHER PART OF THE FINAL REPORT.

SCEGIT-87-103

PRODUCTS AND KINETICS OF THE CHLORINATION AND OZONOLYSIS OF SYNTHETIC DYES

Final Report: NSF Grant No. DAR-7925722

by

Joseph P. Gould
School of Civil Engineering

and

Thomas F. Moran
School of Chemistry

Georgia Institute of Technology
June 1987

TABLE OF CONTENTS

LIST OF TABLES

LIST OF FIGURES

INTRODUCTION

Rationale of Investigation

Large volumes of water are used in the dyeing operations of the textile industry and upon exhaustion these dye baths are discharged into waters leading to municipal waste treatment plants. Residual synthetic organic dyes and other compounds used in the dyeing process arrive at wastewater treatment plants in relatively high concentrations. These dyes and associated compounds are resistant to the usual biological methods of wastewater treatment and significant quantities are discharged into receiving waters. Dyes and associated compounds have been found in raw city water intakes and concern has been raised about their carcinogenic activity. In addition, the chlorination of these dye laden waters can lead to formation of chlorinated organic compounds which may be more mutagenic/carcinogenic than the original compounds. Furthermore, ozone and chlorine are being considered as decolorizing reagents prior to dye bath recycle but here also the products of dye ozonolysis may present more of a public health problem than the original dye solutions, since some blow-down to treatment systems is likely even in the case of recycle.

Based on the foregoing, a program of research was initiated with two phases involved. The first phase entailed an examination of the kinetics of the reactions between the two oxidants, chlorine and ozone, and a number of synthetic organic dyes most commercial significance, a few of interest due to specific structural features. The second phase of this project entailed an exploration of methods applicable to the analysis of the dyes and their reaction products in dilute aqueous solutions. These analyses are complicated by analytical difficulties inherent in the nature of water soluble synthetic dyes. These are for the most part so totally non-volatile as to preclude separation by gas chromatographic methods and, what is worse, analysis of mass spectrometry. The second phase of the research therefore was directed toward development of a mass spectrometric method for qualitative and quantitative analysis of several sulfonic acid based azo dyes.

MATERIALS AND METHODS

Chlorination Studies

All chlorinations were run in batch systems. The reactors used were either 500 mL or 2 L containers made of actinic glass to eliminate photochemical reactions as a factor. The reactors were fitted with ground glass or teflon stoppers. The reactions were conducted in temperature controlled rooms after equilibration to ambient temperatures. Reaction temperatures were 22°C ± 1°C with an extreme range of 20°-24°C. The chlorine solution used was a chloride free hypochlorous acid solution prepared by the following procedure. Distilled water was saturated with reagent grade chlorine gas after which the pH was adjusted to 4.5-5 with sodium hydroxide. The solution was then distilled using a rotary flash evaporator at reduced pressure and a temperature of 60°C. The resulting chloride free hypochlorous acid was stored in the dark in plastic capped amber glass bottles. The solutions were stable for at least three months and had an average molarity of approximately 0.06 M with respect to HOCl.

Dye solutions were prepared in glass distilled water with a measured chlorine demand of less than 0.1 mg/L. Solution pH was controlled by use of appropriate buffer systems. At pH = 5.0 acetate was used, at pH = 7.0 the buffer was phosphate and borate was used to buffer at pH = 9.0. In each case, the total buffer concentration was 0.01 M and was able to maintain the pH during the run within 0.2 units of the desired pH. All buffer solutions were checked for chlorine demand prior to use. No 0.01 M buffer solution was used if the demand exceeded 0.15 mg/L when treated with 2.5 mg/L of chlorine in the dark for 24 hours. Demands in excess of this value were cause to reject the buffering agents involved.

Dyes Used

The synthetic dyes used in this research were subjected to a complex sequence of preparatory steps prior to use. In general, the following procedures were used although each dye had its own specific treatment scheme depending on its characteristics. This was necessitated by the non-standard nature of commercial synthetic dyes. As a rule, these dyes contained three sources of impurities. These include inorganic agents such as sodium sulfate and sodium chloride used to "salt-out" the dyes from reaction solutions and which can make up 30% or more of the weight of some commercial dyes. Organic impurities include low molecular weight dye precursors and finally, side products such as structural isomers of the dyes and other products of side reactions in the dye manufacturing process. While these impurities do not hinder the use of the dyes for commercial purposes, in studies of this type materials of much greater purity are necessary. In particular, organic contaminants must be removed before the dyes can be used. In the purification of these dyes, advantage was taken of the fact that a relatively small quantity of dye was needed to conduct these studies. Thus, significant quantities of crude dye could be wasted in the process of purification. The following procedures were used to prepare the dyes.

a) Preliminary screening: Samples of each dye selected were obtained from at least three suppliers. These dyes were analyzed for

organic carbon content and submitted to reverse phase thin layer chromatography using C-18 adsorbents (C-18 TLC) containing a fluorescent indicator (Whatman KC 18-F plates). In general, the dye showing the highest degree of purity in the C-18 TLC tests as indicated by the greatest fraction present as the desired dye was selected for further purification. In those cases in which there was more than one acceptably pure commercial dye, each was purified further but separately from the others, i.e., the samples were not pooled prior to purification.

b) Preliminary clean-up: A portion of the inorganic salts and the bulk of precursors and other low molecular weight contaminants were removed by the following procedure. The crude dyes were first dissolved in trimethyl amine, filtered, and then precipitated by addition of acetone. Following filtration, washing with acetone and drying in a vacuum dessicator, the dyes were reassayed by measurement of percent organic carbon and C-18 TLC.

c) Crystallization: Finally, the dyes were crystallized from appropriate solvents until the C-18 TLC indicated that they were essentially free of contamination by extraneous organic compounds. At this point samples of the dyes were submitted to a commercial laboratory for analysis of carbon, hydrogen, nitrogen and sulfur. Based on the results of these analyses, the dyes so prepared were judged to be of acceptable purity with respect to the stated structure although still contaminated to some degree by inorganic salts. The results of these analyses are presented in Table 1.

Analysis

In all cases save one, analysis of residual dye concentration depended on direct spectrometric analysis in the visible region of the spectrum. This was possible because of the determination early in the research that chlorination and ozonation of the dyes yielded, with the one exception, products which did not absorb to a significant degree at the visible wavelength of maximum absorption of the dye itself. It was also determined that, over the pH ranged studied (5-9), the absorption of the dyes was not dependent on pH thereby obviating any need of pH adjustment prior to analysis. The one exception to the foregoing was the dye DY-12. The structure of this dye was unusual in that it was the only one possessing an ethylenic carbon-carbon double bond (Figure 1). Furthermore, the remainder of the dye was devoid of groups which could be considered very activating with respect to the oxidants used. The early phases of reaction of this dye with both chlorine and ozone appear to have entailed reaction with this bond forming, it is believed, addition products in the former case and, by bond cleavage, carbonyl and carboxyl groups in the latter case. It can be seen on examination of this structure that attack on this double bond will leave the basic azo dye absorbing unit largely intact. In consequence, a lag was noted in the disappearance of the characteristic yellow color of this dye on treatment with the oxidants.

In order to circumvent this problem advantage was taken of the fact that the DY-12 - but not its reaction products - was converted by acidification to a sparingly soluble blue solid assumed to be the neutral

Table 1. Composition of Purified Dyes Used in Chlorine and Ozonation Studies

		C	H	O	N	S	Na	% Purity*
	Theory	50.0	2.9	20.5	9.0	10.3	7.4	-
DY-04	Analyzed	46.1	2.9	-	8.2	9.7	9.3	92.2
	Adjusted	50.0	3.1	-	8.9	10.5	-	-
	Theory	51.1	2.6	22.0	10.5	8.0	5.8	-
DO-102	Analyzed	45.7	3.0	-	9.3	7.0	8.8	89.4
	Adjusted	51.1	3.4	-	10.4	7.8	-	-
	Theory	46.6	2.8	23.0	9.3	10.6	7.6	-
DR-24	Analyzed	42.9	2.2	-	8.6	9.0	11.3	92.1
	Adjusted	46.6	3.0	-	9.3	9.8	-	-
	Theory	52.1	3.4	18.5	10.1	9.3	6.6	-
DV-09	Analyzed	45.8	3.0	-	8.5	8.7	9.3	87.9
	Adjusted	52.1	3.4	-	9.7	9.9	-	-
	Theory	43.9	2.5	21.7	8.8	13.4	9.6	-
DY-50	Analyzed	39.7	2.5	-	7.4	12.3	12.7	90.4
	Adjusted	43.9	2.8	-	8.2	13.6	-	-
	Theory	52.9	3.8	18.8	8.2	9.4	6.8	-
DY-12	Analyzed	50.9	3.8	-	8.3	9.1	7.9	96.2
	Adjusted	52.9	3.9	-	8.6	9.5	-	-

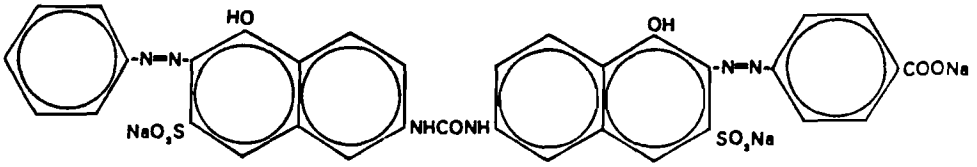

Direct Orange 102
CI 29156
Source: Fabricolor
$C_{34}H_{21}O_{11}N_6S_2Na_2$
M.W.: 799.7

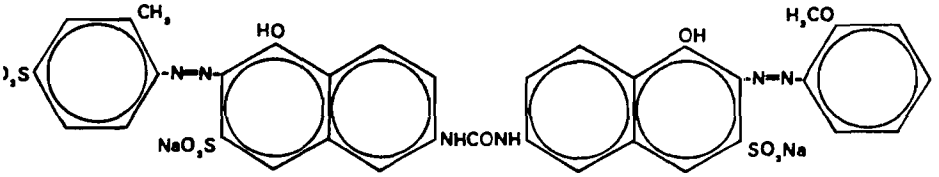

Direct Red 24
CI 29185
Source: Atlantic
$C_{35}H_{25}O_{13}N_6S_3Na_3$
M.W.: 902.8

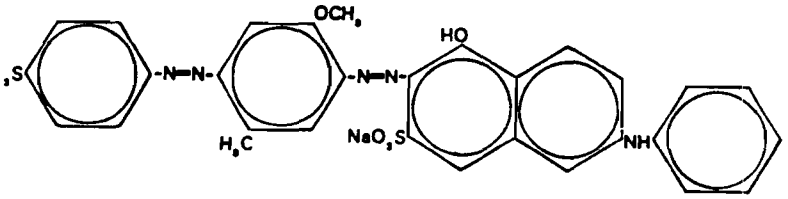

Direct Violet 9
CI 27885
Source: Atlantic
$C_{30}H_{23}O_8N_5S_2Na_2$
M.W.: 691.7

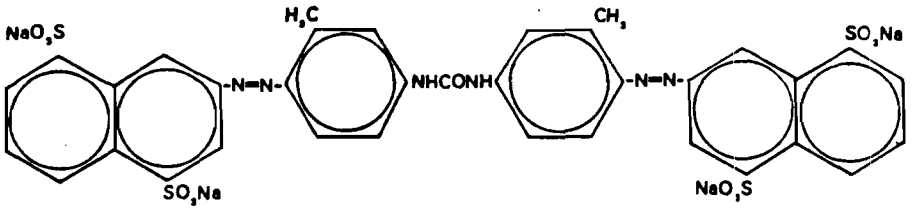

Direct Yellow 50
CI 29025
Source: Atlantic
$C_{35}H_{24}O_{13}N_6S_4Na_4$
M.W.: 956.8

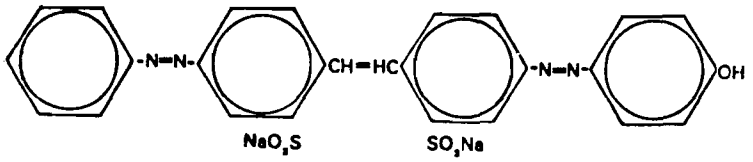

Direct Yellow 4
CI 24890
Source: Atlantic
$C_{26}H_{18}O_8N_4S_2Na_2$
M.W.: 624.6

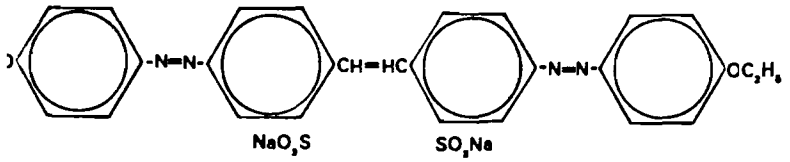

Direct Yellow 12
CI 24895
Source: Atlantic
$C_{30}H_{26}O_8N_4S_2Na_2$
M.W.: 680.7

:e: CI numbers taken from Colour Index of the Society of Dyers and Colourists.[5]

gure 1. Dyes used in chlorination and ozonation studies.

acid form of the dye. This solid could be solubilized by addition of sufficient isopropanol to bring the solution to 50% isopropanol by volume. The solution could then be analyzed at the wavelength characteristic of the neutral compound. This analysis was found to be highly sensitive and specific for unreacted DY-12. Typical calibration curves for the dyes used in these studies are presented in Figures 2 through 7.

Chlorine analysis presented a particular problem in this study. The available array of colorimetric tests could not be used in conjunction with the synthetic dyes. The only method which could be used in these systems was the Amperometric Titration method as described in Standard Methods.[1] A Fisher Chlorine Analyzer was used with phenylarsine oxide as the titrant. Chlorine stock solutions were standardized by iodometric titration using sodium thiosulfate as the titrant. The titrant was in turn standardized using potassium biiodate as the primary standard. In the case of the chlorine demand studies on the distilled water and buffer, the amperometric titrations were confirmed by means of the DPD-FAS titration method as described in Standard Methods.[1]

Ozone generation and breakthrough rates were measured by trapping the ozone in 2% sodium iodide solution in gas wash bottles followed by titration with standard sodium thiosulfate solution.

Total organic carbon analyses were carried out using a Beckman TOC analyzer. Ultraviolet and visible spectra were obtained using a Beckman Model 26 Spectrophotometer. Single sample analyses were performed using the same instrument or a Beckman DU.

Data Analysis

The chlorination kinetic data collected were analyzed on the assumption that the process was mixed second order in nature, i.e., first order with respect to the dye and first order with respect to the chlorine (Equations 1 and 2).

$$\text{Dye R(chlorine)} \longrightarrow \text{Products} \tag{1}$$

$$\frac{d\,[\text{Dye}]}{dt} = -k\,[\text{Dye}][\text{Chlorine}] \tag{2}$$

On integration, Equation 2 takes the following form (Equation 3).

$$\ln \frac{[\text{Chlorine}]}{[\text{Dye}]} = ([\text{Chlorine}]_o - R[\text{Dye}]_o)\,kt + \ln \frac{[\text{Chlorine}]_o}{[\text{Dye}]_o} \tag{3}$$

where, R is the molar ratio of chlorine consumed to dye destroyed, zero subscripted concentrations are the initial concentrations and k is the rate constant. The rate constant was then obtained from the slope of a plot of $\ln \frac{[\text{Chlorine}]}{[\text{Dye}]}$ versus time by Equation 4.

$$k = \text{Slope}/([\text{Chlorine}]_o - R\,[\text{Dye}]_o) \tag{4}$$

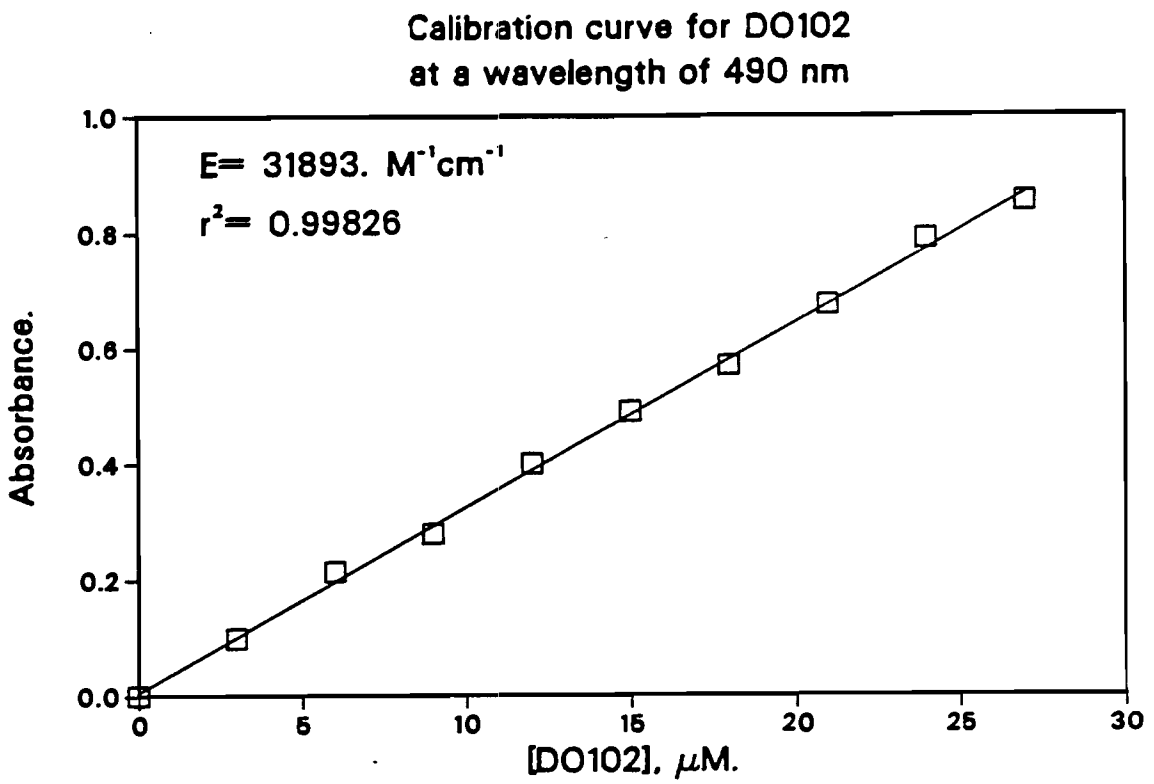

Figure 2

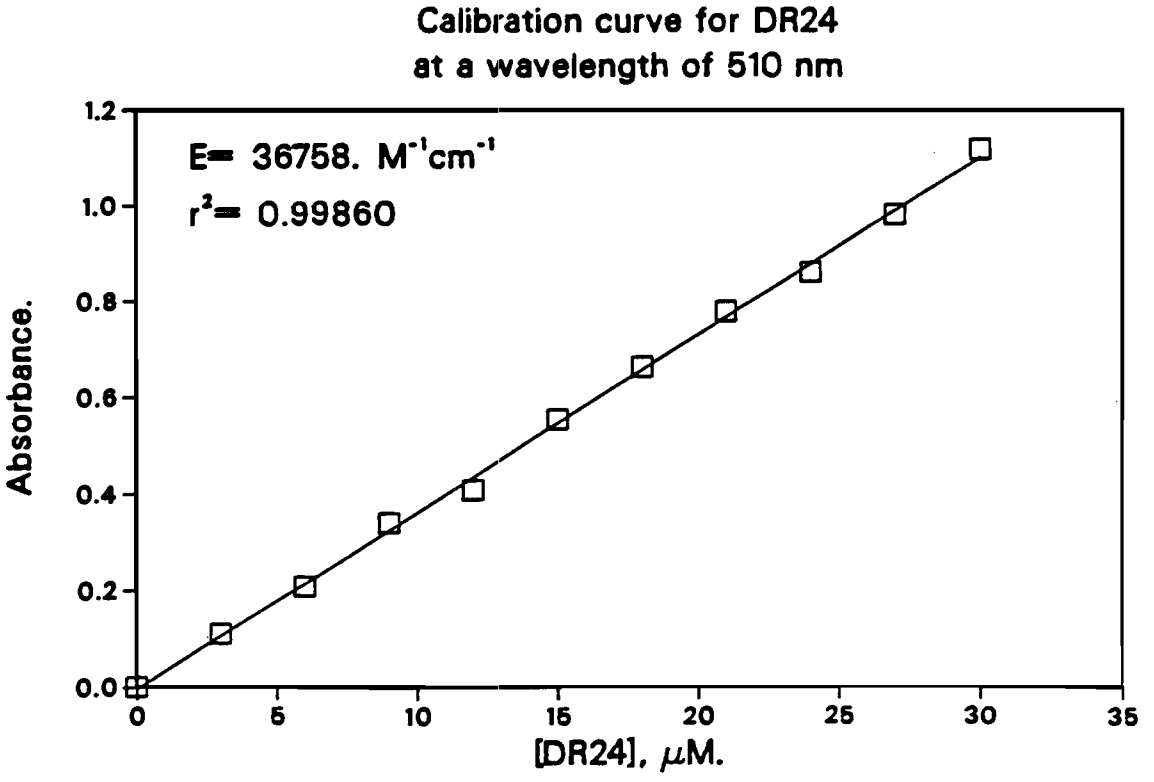

Figure 3

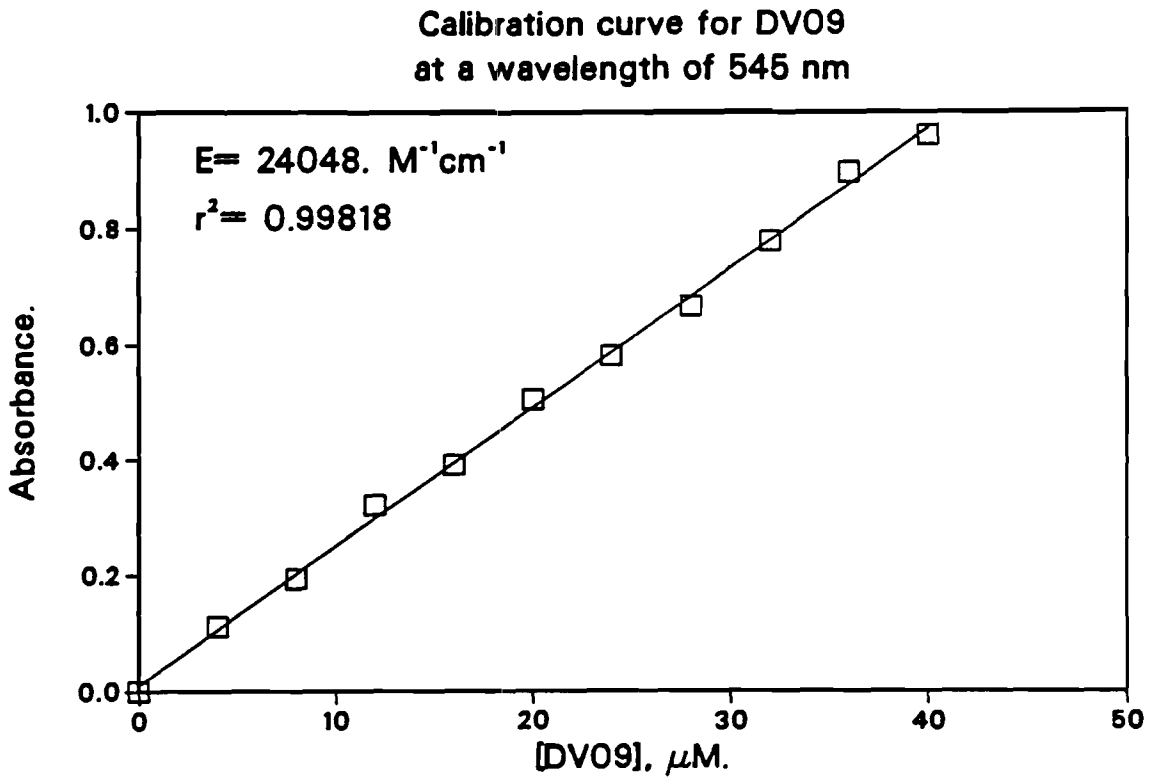

Figure 4

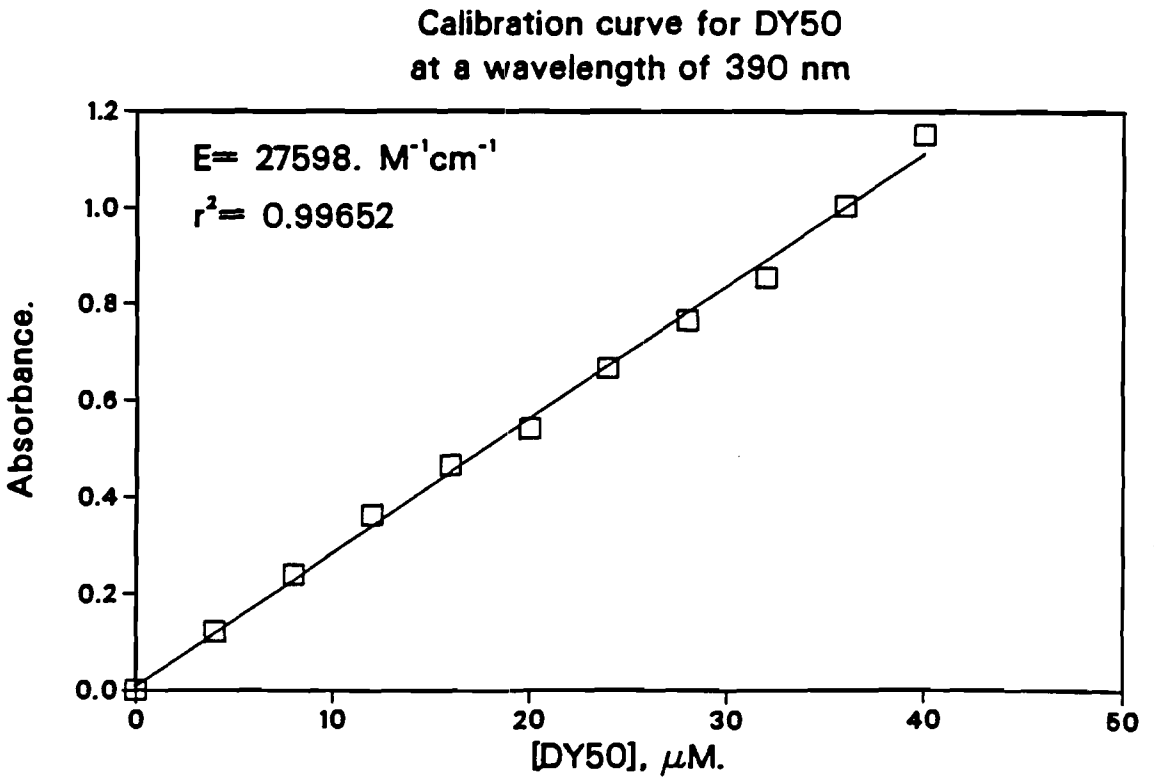

Figure 5

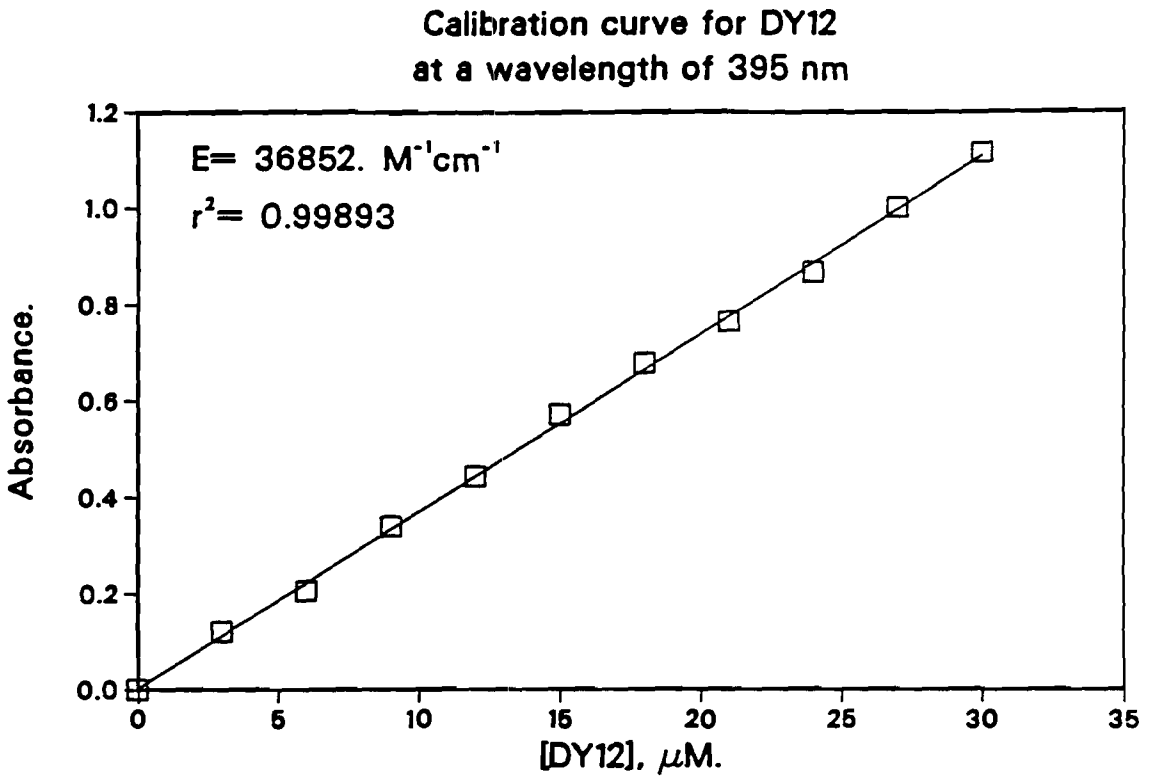

Figure 6

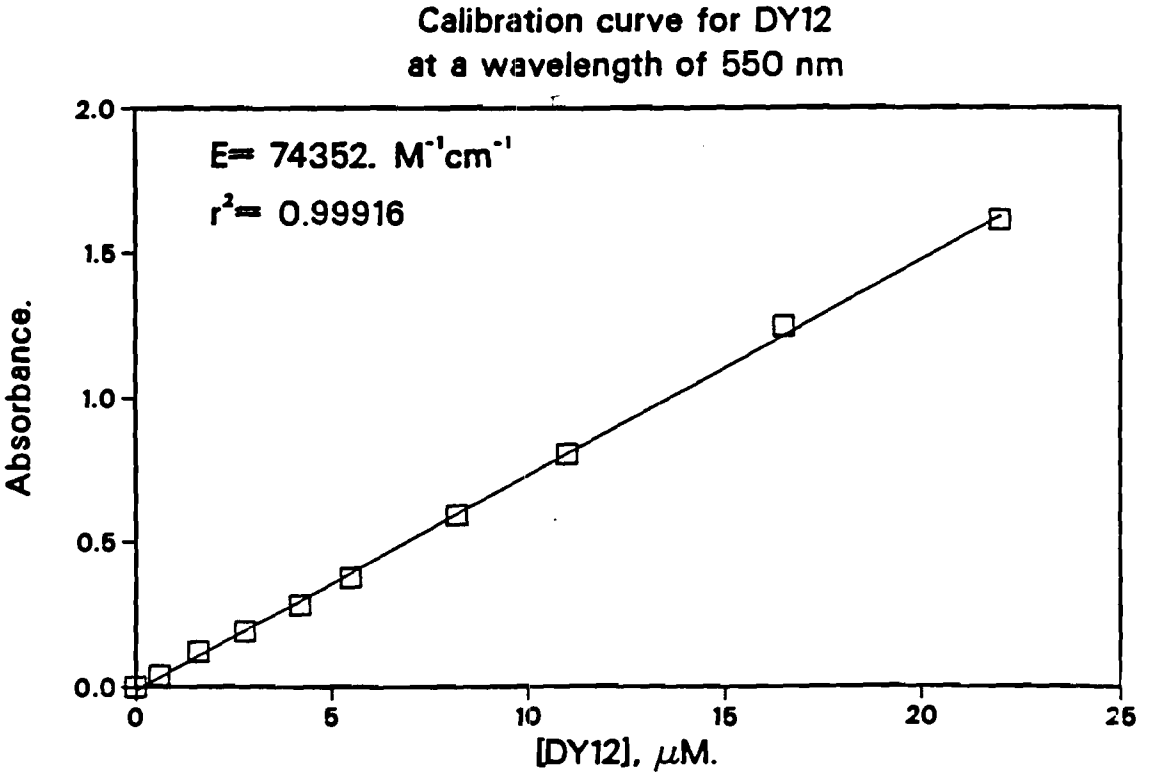

Figure 7

The foregoing analysis of mixed second order kinetics is not usable in those cases in which the ratio of initial reactant concentrations is very close to the stoichiometric or consumption ratio, R. In these cases, $\ell n \frac{[Chlorine]}{[Dye]}$ does not change with respect to time and k cannot be evaluated with any precision. To manage such systems, it need only be recognized that the kinetics in this case will mimic type one second order kinetics as shown below.

$$\frac{d\,[Dye]}{dt} = -k\,[Chlorine][Dye] = -k\,R\,[Dye]^2 \qquad (5)$$

In those cases, the data were analyzed by plotting the reciprocal of dye concentration as a function of time in accordance with the integrated form of Equation 5.

$$\frac{1}{[Dye]} = \frac{1}{[Dye]_o} + kRt \qquad (6)$$

and k is equal simply to the slope divided by the consumption ratio, R.

The consumption ratio R was measured by plotting the residual chlorine concentration as a function of residual dye concentration and evaluating the slope of the resulting plot (Equation 7).

$$\frac{d\,[Chlorine]}{d\,[Dye]} = R \qquad (7)$$

All slopes were evaluated by linear regression analysis.

The analysis of heterogeneous gas-liquid ozonation kinetics is subject to significant complication by the intrusion of physical process kinetics. Although it has been well established that the chemical interaction of ozone and ozone derived hydroxyl radicals with organic compounds of the type studied here is mixed second order, kinetic control resides in relatively slow mass transfer processes rather than the very rapid chemical reactions. As a result, the ozonation kinetics conformed to the first order kinetics reported by many investigators[2-4] (Equation 8).

$$\frac{d\,[Dye]}{dt} = -k\,D\,[Dye] \qquad (8)$$

where D is an ozone dosage parameter equal to the ozone dose in moles per liter per unit time divided by the initial dye concentration.

As indicated previously, the analysis of DY-12 was complicated considerably by the persistence of a yellow color substantially similar to that of the DY-12 but ascribed to initial reaction products. While measurement of unreacted DY-12 was possible by conversion to the blue neutral species, the residual was also monitored and plotted as a function of time. In this case, the absorbance reading for the yellow color was converted to units of concentration as DY-12 by application of the measured molar absorbtivity for DY-12 in the ionized form.

RESULTS AND DISCUSSION

Chlorination Studies

In general, the chlorination of the synthetic dyes appeared to obey assumed mixed second order kinetics. Trends with respect to pH and initial reactant concentration were not sharply defined and rather difficult to rationalize. In examining these data, it must be borne in mind that there are in fact two oxidant/chlorinating agents in action, the hypochlorite ion and hypochlorous acid. The latter is predominant at pH values below 7.6, while the former predominates at pH values in excess of 7.6 (Equation 9).

$$HOCl \rightleftharpoons H^+ + OCl^- \qquad pK_a = 7.6 \qquad (9)$$

Thus, at the pH values used in this research, the percent compositions of the solutions with respect to HOCl and OCl^- are given in Table 2.

Table 2. Mole Percent Distribution of HOCl and OCl^- at pH Values Used in Study

	Mole % of	
pH	HOCl	OCl^-
5	99.75	0.25
7	79.9	20.1
9	2.5	97.5

While, as will be seen further on, there does appear to be a tendency toward pH dependence of the rate constants, it does not ever attain a magnitude consistent with the 10,000 fold range of hydrogen ion concentrations involved in these studies (pH values from 5 to 9). For each dye studied, the possibility that the reaction rate will be first order with respect to [HOCl] specifically rather than total chlorine ([HOCl] + [OCl^-]) will be examined by correcting the average rate constants for each pH with respect to the portion of total chlorine present as HOCl.

DO:102: There was conducted a total of 18 studies involving the dye Direct Orange 102 in reaction with chlorine. A typical set of concentration versus time, kinetic and chlorine plots is presented in Figure 8. All plots for this dye are shown in Appendix 1. Initial reaction conditions and significant resulting data are presented in Table 3.

Rate constants for this system were found to range from 0.041 $M^{-1}s^{-1}$ to 13.6 $M^{-1}s^{-1}$. The rate data were grouped according to pH and range of initial chlorine concentration in Table 4. Taking an average of the data grouped by pH and by initial chlorine concentration, it is apparent that there is no discernible relationship between k and initial chlorine concentration. There is, however, a clear relationship between pH and the value of k with the average value of k ranging from 0.15 $M^{-1}s^{-1}$ at a pH of 5 to

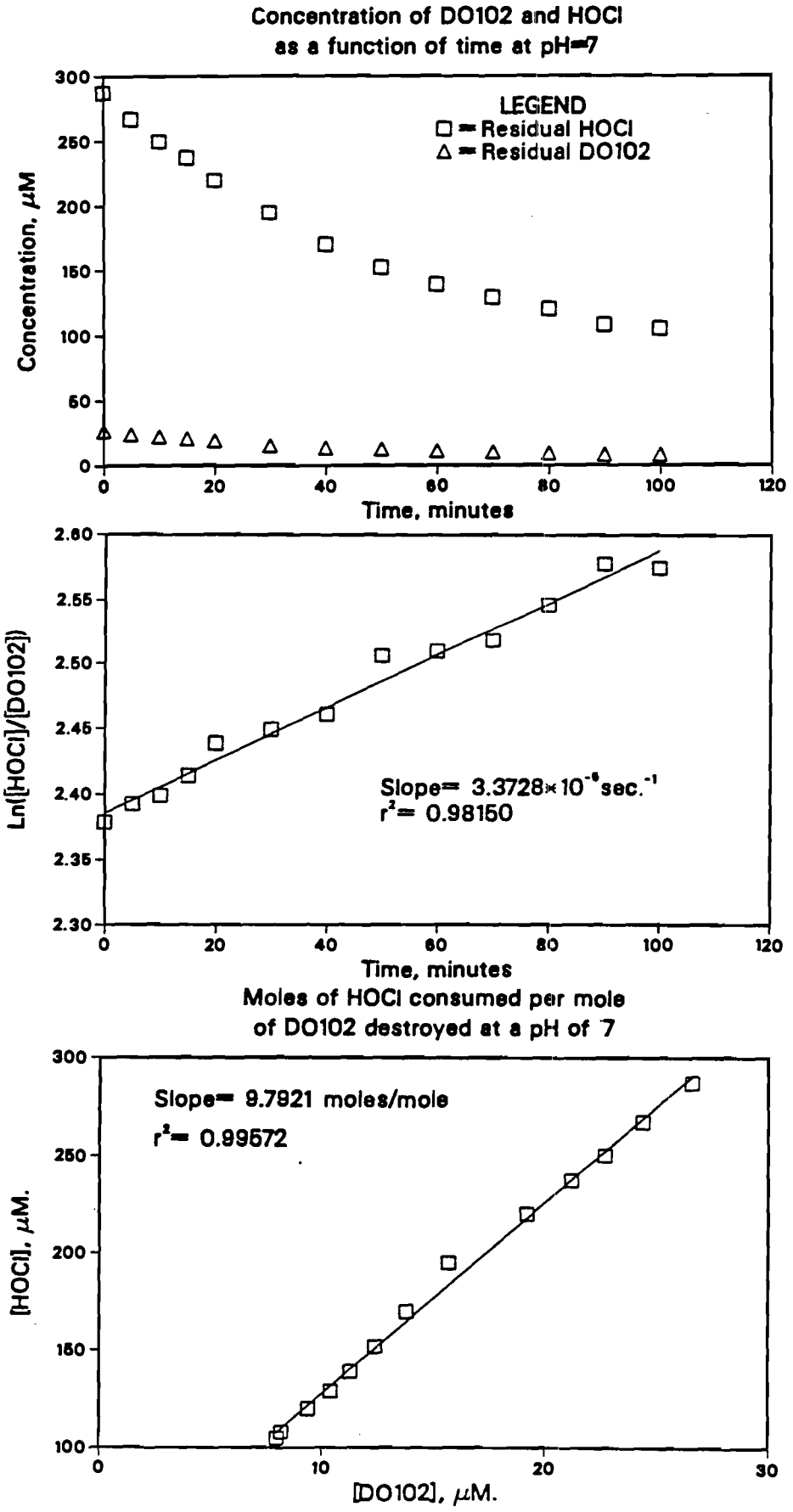

Figure 8. Typical data plots for DO-102.

Table 3. Kinetic Data for DO-102 Chlorination

	Chlorine	DO-102	pH	*Slope x 10^4, s^{-1}	R	k, $M^{-1}s^{-1}$
1	393	26.6	5	0.0509	10.124	0.0412
2	356	26.6	7	2.405	8.984	2.055
3	355	27.8	9	3.345	10.258	3.215
4	95	27.4	5	-0.262	11.173	0.124
5	93	28.9	7	-2.015	7.259	1.725
6	89	27.9	9	-3.862	4.862	8.279
7	355	29.0	9	5.332	7.730	4.076
8	276	27.0	5	0.0373	8.954	0.109
9	287	26.6	7	0.337	9.792	1.271
10	379	27.1	9	1.106	13.148	3.750
11	21	26.2	5	-0.851	13.423	0.257
12	25	28.9	7	-4.128	7.220	2.248
13	16	26.6	9	-3.923	2.785	6.697
14	43	28.0	5	-0.316	7.115	0.202
15	41	29.2	7	-2.260	4.805	2.276
16	43	29.8	9	-5.244	3.782	7.567
17	149	20.1	9	-3.183	8.580	13.569
18	202	28.3	7	(121.0)	6.855	1.765

*Numbers in parenthesis slopes of reciprocal plots ($mM^{-1}s^{-1}$) x 10^4.

Table 4. Rate Constants and Consumption Ratios for Chlorination of DO-102 Grouped According to pH and Initial Chlorine Concentrations

Initial Chlorine, µM	k vs pH			R vs pH		
	5	7	9	5	7	9
375-400	0.0412		3.750	10.12		13.15
350-360		2.055	3.215		8.98	10.26
			4.076			7.73
275-300	0.109	1.271		8.95	9.79	
202		1.765			6.86	
149			13.569			8.58
85-95	0.124	1.725	8.279	11.17	7.26	4.86
40-45	0.202	2.276	7.567	7.12	4.80	3.78
15-25	0.257	2.248	6.697	13.42	7.22	2.78
Average	0.147	1.89	6.72	10.16	7.48	7.31

6.74 $M^{-1}s^{-1}$ at a pH of 9. This behavior is difficult to explain. The 45 fold range of values while substantial is too small to be associated directly with the 10^4 fold range of hydrogen ion concentrations represented by the four unit range of pH values. The behavior observed is not consistent with pH determined changes in HOCl speciation, since the rate is greatest at pH values at which hypochlorite ion is the dominant species. Assuming attack on the dyes by the chlorine to be electrophilic in nature, the OCl^- would be expected to yield the slower kinetics. While pH induced changes in the structure of the DY-102 might be responsible for the observed behavior, no evidence for such changes was obtained during preliminary studies on the variations in dye spectra arising from pH changes over the range of 5 to 9. At best, the evidence of these data suggests that a pH based change in the reaction mechanism occurs in this pH range. Beyond that no conclusions may be drawn.

Chlorine consumption roughly parallels the behavior of the rate constants although trending in the opposite direction. Examination of R values grouped according to pH and initial chlorine concentrations (Table 4) shows that, while there is no apparent relationship between initial chlorine concentration and R, a clear trend toward decreasing R with increasing pH is detected. The R value was 10.2 moles of chlorine per mole of dye on average at a pH of 5 and 6.0 moles/mole at a pH of 9. Again, there is no obvious rationalization available for this behavior. These data are also supportive of a change in reaction mechanism. The nature of this change, however, remains to be elucidated.

DR-24: The chlorination of the Direct Red 24 (Figure 9 and Appendix 2) was, with regards to kinetics similar to that of DO-102 in that the lowest average k value (0.43 $M^{-1}s^{-1}$) was observed at a pH value of 5 while the highest (2.29 $M^{-1}s^{-1}$) was obtained for runs at a pH of 9 (Tables 5 and 6). By contrast, however, this range of k values spanned a factor of only about 5 as opposed to the 45 fold range observed for DO-102. Again, neither pH, chlorine speciation nor observed dye behavior could be invoked to rationalize the variations in the rate constant. Also, as in the case of DO-102, the initial chlorine concentration had no obvious impact on the value of the rate constants.

Trends in chlorine consumption ratio, R, as shown in Tables 5 and 6 showed a weak dependence on pH increasing from 3.6 moles per mole at a pH of 5 to 6.9 moles per mole at a pH of 7 with no change as the pH increased thereafter to 9. This trend was the opposite of that observed for DO-102. Again, there was no relationship between initial chlorine concentration and R.

DV-09: The kinetics of the reactions between Direct Violet-9 and chlorine were found to respond to pH in a fashion the opposite in nature to that observed for DO-102 or DR-24 (Figure 10 and Appendix 3). As can be seen in Tables 7 and 8, k decreased from an average of 13.3 $M^{-1}s^{-1}$ at a pH of 5 to 1.8 $M^{-1}s^{-1}$ at a pH of 9. The trend in these values very roughly parallels the trend in HOCl levels in the chlorine mixture. However, the values adjusted for the levels of HOCl in the mixture at pH equal to 9 are substantially higher than those of pH 5 and 7. It is interesting to note however that, on adjustment to a basis of the concentration of HOCl, the measured k values averaged 17.3 ± 5.9 $M^{-1}s^{-1}$ with no obvious relationship

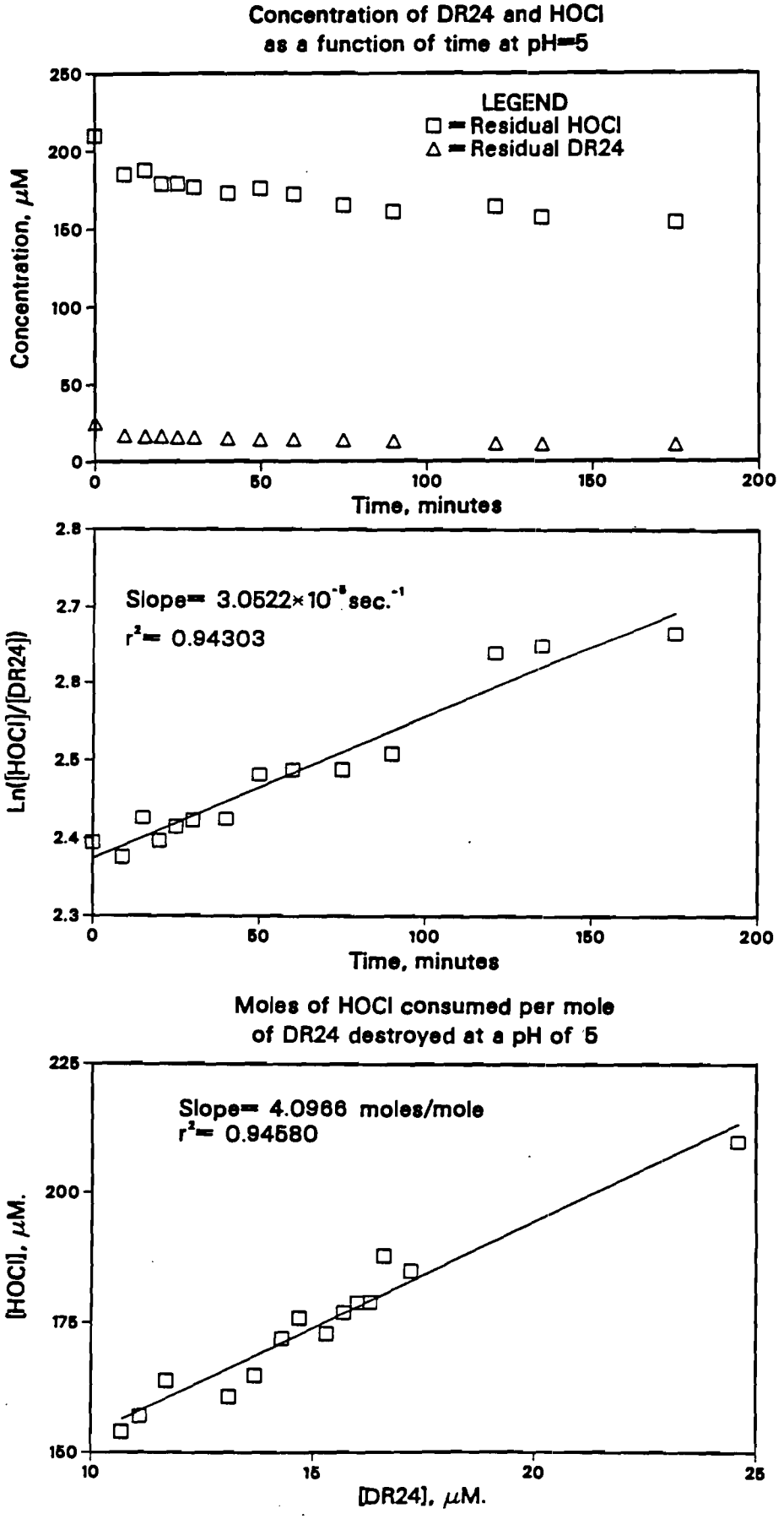

Figure 9. Typical data plots for DR-24.

Table 5. Kinetic Data for DR-24 Chlorination

	Chlorine	DR-24	pH	*Slope x 10^4, s^{-1}	R	k, $M^{-1}s^{-1}$
1	300	20.0	5	1.142	3.176	0.483
2	300	20.0	7	0.268	8.326	0.200
3	300	20.0	9	4.618	5.418	2.410
4	53	22.0	5	-0.103	3.736	0.352
5	47	22.2	7	-0.781	7.182	0.702
6	48	22.3	9	-2.330	4.849	3.875
7	210	24.6	5	0.305	4.097	0.279
8	210	24.9	7	(191.3)	8.272	2.312
9	208	24.8	9	(186.3)	8.382	2.223
10	25	19.1	5	-0.251	3.858	0.516
11	25	19.1	7	-0.803	4.999	1.139
12	26	18.5	9	-1.294	7.092	1.230
13	102	24.3	5	0.173	2.846	0.527
14	103	24.6	7	-0.402	5.892	0.958
15	106	25.0	9	-1.376	7.422	1.730

*Numbers in parenthesis slopes of reciprocal plots ($mM^{-1}s^{-1}$) x 10^4.

Table 6. Rate Constants and Consumption Ratios for Chlorination of DR-24 Grouped According to pH and Initial Chlorine Concentrations

Initial Chlorine, μM	k vs pH			R vs pH		
	5	7	9	5	7	9
300	0.483	0.200	2.410	3.18	8.33	5.42
210	0.279	2.312	2.223	4.10	8.27	8.38
105	0.527	0.958	1.730	2.85	5.89	7.42
50	0.352	0.702	3.875	3.74	7.18	4.85
25	0.516	1.139	11.230	3.86	5.00	7.09
Average	0.431	1.06	2.29	3.55	6.93	6.63

between k and pH. Thus, it might be tentatively taken that the rate equation for DV-09 is expressed by Equation 10 to a reasonable degree of precision.

$$\frac{d\,[DV\text{-}09]}{dt} = -17.3\,[DV\text{-}09][HOCl] \qquad (10)$$

The chlorine consumption behavior is also complicated by the presence in the pH = 9 studies of two apparent outliers (Tables 7 and 8). Omission of these outliers yields results indicative of an absence of dependence of R on both pH and initial chlorine concentration. On omission of the outliers, an average value of R of 4.6 ± 1.4 moles of chlorine per mole of DV-09 is obtained.

DY-50: The rate constant for the reaction of Direct Yellow 50 with chlorine showed a weak positive relationship with pH between values of 7 and 9 (Figure 11 and Appendix 4). The k value was unaffected by pH at values below 7 (Tables 9 and 10). The rate constant ranged from an average value of 5.3 $M^{-1}s^{-1}$ at a pH of 9 to an average of 2.2 $M^{-1}s^{-1}$ between 5 and 7. The chlorine consumption ratio R was at the lowest value of 2.3 moles per mole. There was little evidence of a pH dependence at the higher pH values with R equal to approximately 6.6 at those levels (Tables 9 and 10). The initial chlorine concentration appeared to have no influence on either k or R.

DY-12: The relationship between pH and k for Direct Yellow 12 chlorination (Figure 12 and Appendix 5)is strongly indicative of primary dependence on HOCl as the reactive entity (Tables 11 and 12). The average value of k when adjusted for [HOCl] for these reactions was 0.87 $M^{-1}s^{-1}$ with no clear dependence on either initial chlorine concentration or pH value. Based on this the kinetic expression for the reaction between chlorine and DY-12 is:

$$\frac{d\,[DY\text{-}12]}{dt} = -0.87\,[DY\text{-}12][HOCl] \qquad (11)$$

Likewise, in the case of DY-12, no dependence could be unambiguously documented between the chlorine consumption ratio R and either the pH or the initial chlorine concentration with an average R of 2.9 moles/mole. In the case of DY-12, it can be postulated that the primary reaction involved is addition of HOCl to the ethylenic carbon-carbon double bond. This is consistent in large measure with all observed properties of this reaction. Only later in the reaction do more radical processes such as ring cleavage and nitrogen-nitrogen double breaking reactions both complicate the overall process and lead to increased chlorine consumption.

Overview of Dye Chlorination Kinetics

The results of these studies are indicative of the complexity of behavior of such complicated systems as represented by these dyes. With the sole exception of the DY-12 which is dominated in its behavior by the ethylenic double bond, even very similar dyes (DO-102, DR-24, DY-50) in structure showed somewhat divergent behavior on chlorination, although in general, all three dyes showed increases in k as the pH increased. In the case of DV-09 and DY-12 pH dependence was suggestive of dominance by HOCl as the reactive chlorine species.

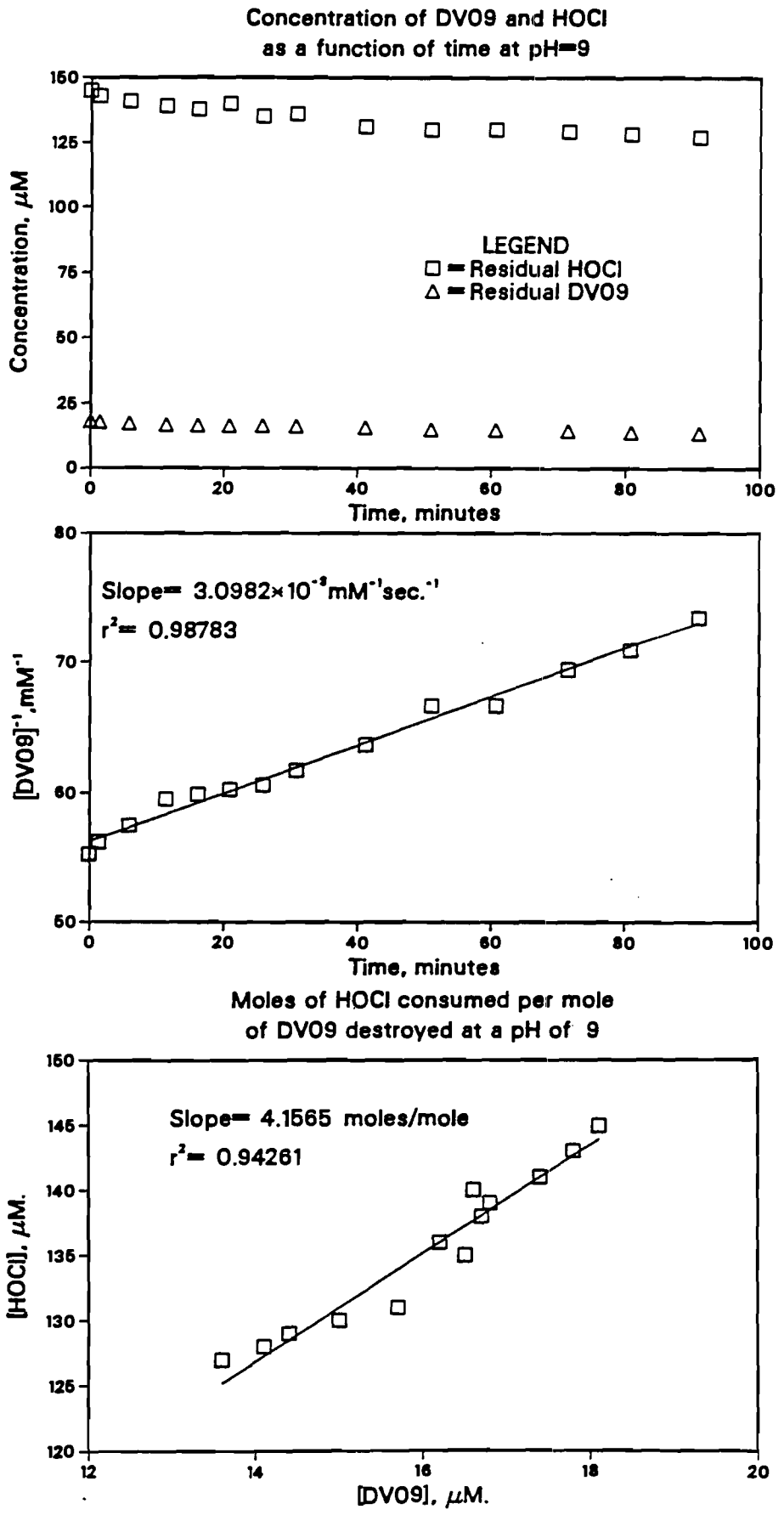

Figure 10. Typical data plots for DV-09.

Table 7. Kinetic Data for DV-09 Chlorination

	Chlorine	DV-09	pH	*Slope x 10^4, s^{-1}	R	k, $M^{-1}s^{-1}$
1	76	18.9	5	3.372	2.492	11.67
2	96	18.4	7	2.640	3.050	6.62
3	186	18.1	9	(30.98)	4.156	0.745
4	12	19.2	5	-7.995	3.175	16.20
5	45	20.1	7	-0.697	3.540	2.64
6	44	19.7	9	-3.542	22.72	0.878
7	83	19.1	9	(34.37)	28.98	0.667
8	171	19.9	5	(602.2)	6.049	9.96
9	157	19.9	7	(163.8)	3.613	4.66
10	45	9.4	5	-2.445	6.901	12.31
11	150	46.0	7	-0.722	5.867	6.02
12	20	20.4	5	-5.700	2.714	16.35
13	71	16.8	9	(74.74)	6.143	1.22

*Numbers in parenthesis slopes of reciprocal plots ($mM^{-1}s^{-1}$) x 10^4.

Table 8. Rate Constants and Consumption Ratios for Chlorination of DV-09 Grouped According to pH and Initial Chlorine Concentrations

Initial Chlorine,	k vs pH			R vs pH		
μM	5	7	9	5	7	9
150-190	9.96	4.66	0.745	6.05	3.63	4.16
		6.02			5.87	
96		6.62			3.05	
83			0.667			28.98*
70-50	11.67		1.22	2.49		6.14
45	12.31	2.64	0.878	6.90	3.54	22.72*
10-20	16.20				3.18	
	16.35				2.71	
Average	13.30	4.99	0.878	4.27	4.02	5.15

*Suspect values omitted from computation of average.

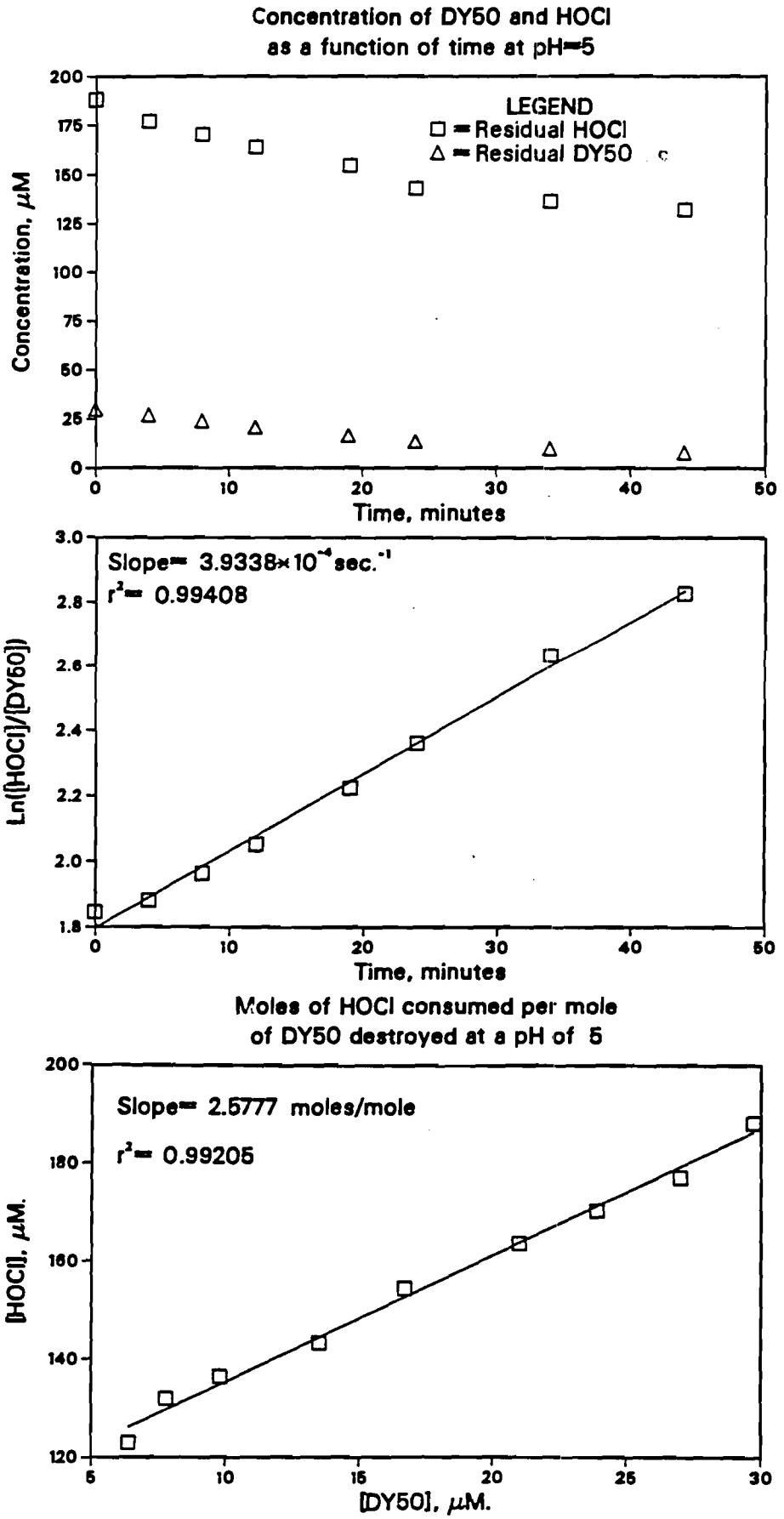

Figure 11. Typical data plots for DY-50.

Table 9. Kinetic Data for DY-50 Chlorination

	Chlorine	DY-50	pH	*Slope x 10^4, s^{-1}	R	k, $M^{-1}s^{-1}$
1	260	25.2	9	10.52	3.110	8.27
2	300	25.6	5	4.620	3.130	2.10
3	301	26.2	7	2.626	4.990	1.54
4	282	26.7	9	2.437	8.479	4.38
5	189	25.7	7	3.441	3.990	3.98
6	188	29.7	5	3.934	2.578	3.53
7	100	28.8	9	(153.8)	3.762	4.09
8	99	25.3	7	-1.114	5.888	2.23
9	100	30.6	5	0.660	2.083	1.82
10	52	25.8	9	-3.597	4.482	5.65
11	47	26.7	7	-2.605	13.152	0.895
12	47	30.7	5	-0.355	2.489	1.21
13	25	27.5	7	-4.337	10.727	1.61
14	25	27.5	9	-7.018	7.799	3.71
15	26	29.9	5	-0.454	1.406	2.83

*Numbers in parenthesis slopes of reciprocal plots ($mM^{-1}s^{-1}$) x 10^4.

Table 10. Rate Constants and Consumption Ratios for Chlorination of DY-50 Grouped According to pH and Initial Chlorine Concentrations

Initial Chlorine, μM	k vs pH			R vs pH		
	5	7	9	5	7	9
300	2.10	1.54		3.11	4.99	
282			4.38			8.48
260			8.27			3.11
190	3.53	3.98		2.58	3.99	
100	1.82	2.23	4.09	2.08	5.89	3.76
50	1.21	0.895	5.65	2.49	13.15	4.48
25	2.83	1.61	3.71	1.41	10.73	7.80
Average	2.30	2.05	5.22	2.33	7.75	5.53

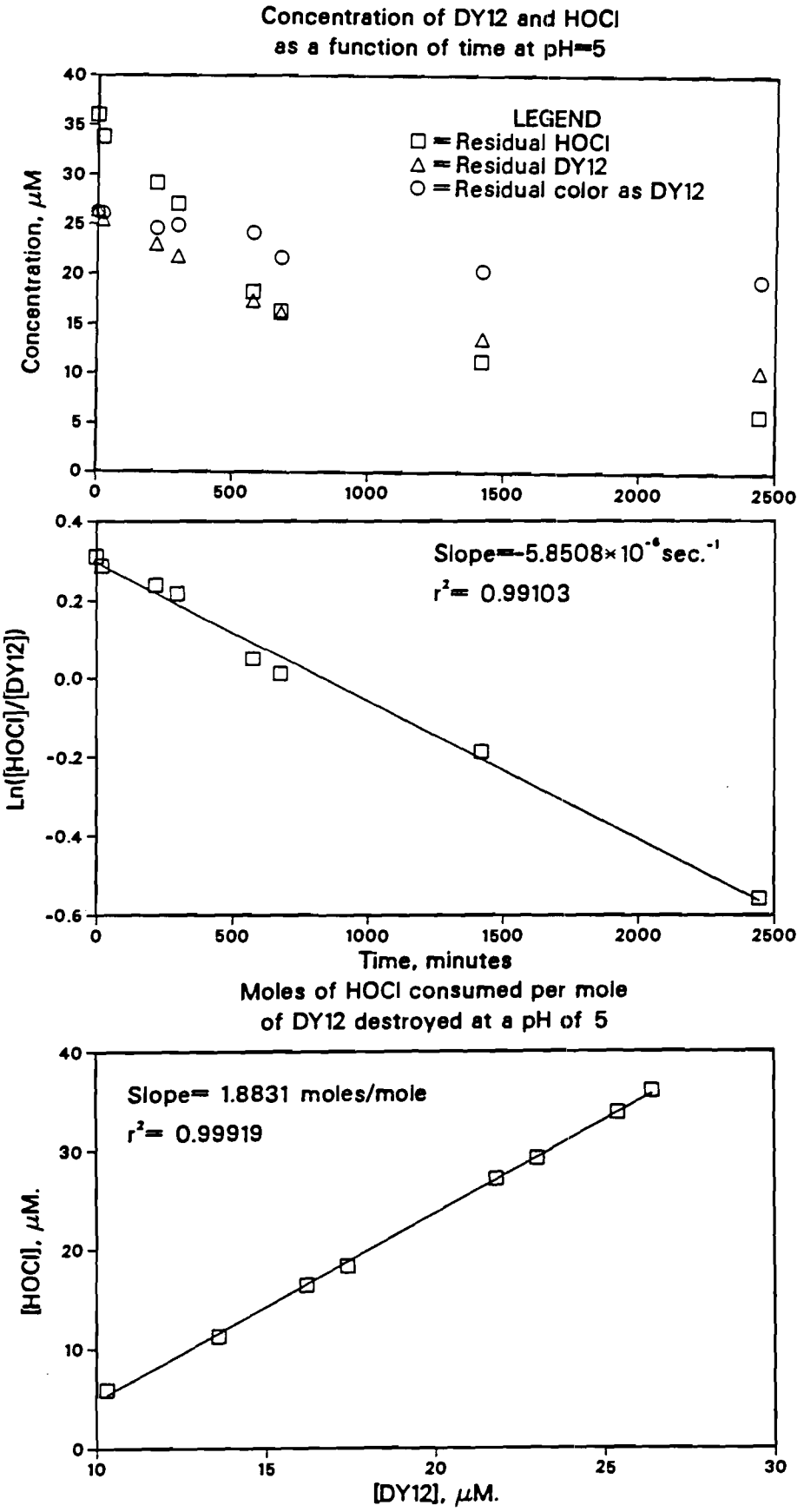

Figure 12. Typical data plots for DY-12.

Table 11. Kinetic Data for DY-12 Chlorination

	Chlorine	DY-12	pH	*Slope x 10^6, s^{-1}	R	k, $M^{-1}s^{-1}$
1	307	28.3	9	47.18	1.974	0.181
2	301	28.0	5	616.2	1.388	2.351
3	177	25.9	9	2.956	2.420	0.0259
4	183	25.9	7	11.16	2.695	0.0986
5	190	25.5	5	71.23	1.728	0.488
6	100	30.6	9	(25.39)	3.727	0.00681
7	100	25.9	7	(144.4)	3.574	0.0404
8	39	27.9	9	-1.720	3.691	0.0270
9	50	24.1	7	(345.6)	2.002	0.173
10	36	26.4	5	-5.851	1.883	0.427
11	29	27.2	9	-6.717	5.103	0.0613
12	31	27.6	7	-2.848	2.267	0.0908
13	32	27.3	5	-13.47	3.596	0.205
14	306	32.9	7	19.33	3.788	0.106
15	100	32.5	5	(8763.)	4.229	2.072

*Numbers in parenthesis slopes of reciprocal plots ($mM^{-1}s^{-1}$) x 10^6.

Table 12. Rate Constants and Consumption Ratios for Chlorination of DY-12 Grouped According to pH and Initial Chlorine Concentrations

Initial Chlorine, μM	k vs pH			R vs pH		
	5	7	9	5	7	9
305	2.351	0.106	0.181	1.39	3.79	1.97
175-190	0.488	0.0986	0.0259	1.73	2.70	2.42
100	2.072	0.0404	0.00681	4.23	3.57	3.73
35-50	0.427	0.173	0.0270	1.88	2.00	3.69
31	0.205	0.0908	0.0613	3.60	2.27	5.10
Average	1.109	0.102	0.0604	2.57	2.87	3.38

One interesting feature of the chlorination of these dyes relates to the formation of combined chlorine. In none of these studies was a significant (>5%) fraction of measured chlorine present as combined chlorine. This suggests that the nature of the dye structures was such that either no combined chlorine was formed or that it was of such a labile nature as to appear in the free fraction during analysis. There was no indication of the formation of stabile chloramines.

From an applied standpoint it is clear that the rates of dye removal measured are such that decolorization of exhausted dye baths prior to recycle is an entirely practical process. Given the hundred fold or higher excesses of chlorine likely to be used in such processes, pseudofirst order rates would prevail with reaction half lives of much less than one second.

Dye Ozonation Studies

The dyes were ozonated in heterogeneous gas flow semi-batch systems using ozone generated by means of a Welsbach T816 Benchtop ozone generator and extra dry oxygen as a feed gas. All runs were conducted in gas wash bottles of one liter capacity fitted with coarse sintered glass diffusors. Solution volumes were 0.5 ℓ. The reactor train included wash bottles containing 2% sodium iodide solution so placed as to permit analysis of both feed and effluent ozone levels in the gas streams. The solutions were buffered using 0.01 M total concentration phosphate buffers. Measured pH changes over the course of each run were used to estimate hydrogen ion generation during ozonation.

Direct Yellow 12 was chosen to receive the most detailed examination of the six dyes studied. The experimental conditions used and values of k' and ozone consumption for this dye are given in Table 13. The interaction of this dye with ozone was strongly dependent on the somewhat unusual nature of its structure as shown in Figure 1. It was found that at initial pH values

Table 13. Summary of Results for DY-12

Co, μM	pH	k', M^{-1}	$\Delta O_3/\Delta$Dye	$\Delta[H^+]/\Delta$Dye
998	7.1	432	6.8	3.6
797	7.1	478	6.6	3.5
501	7.1	467	7.0	4.4
365	7.1	404	9.9	4.5
228	7.1	429	13.8	4.5
100	7.1	435	23.0	3.3
1,070	5.1	768*-244	2.6*-19.2	-
810	5.1	998*-191	3.6*-25.4	-
616	5.0	1,112*-260	3.6*-18.2	-
454	5.0	1,908*-249	1.8*-22.7	-
1,010	9.1	598	5.4	-
844	9.0	620	4.7	-
676	9.2	576	8.6	-

*From zero to two minutes.

of 7 and 9, the ozonation kinetics of DY-12 adhered well to Equation 8. Presented in Figure 13 are the results obtained at all initial concentrations at pH values of 7 and 9, plotted as ℓn(Co/C) versus Dt. As can be seen, these data conformed excellently to the expected behavior with the rate constant at an initial pH of 9 being approximately 35% higher than that observed at a pH of 7. The kinetics at a pH of 5 were markedly different from those at the higher pH values. At this pH, the kinetics were characterized by a break which occurred in all cases, at approximately two minutes into the run. A typical run is illustrated in Figure 14. The two portions of these curves were analyzed separately.

That portion of the runs which occurred after the break at two minutes was found to have a k' which was essentially independent of the initial dye concentration and, in agreement with the trend observed between a pH of 7 and a pH of 9, was only about 54% of the value obtained at a pH of 7. The initial portion of these runs had rates which were clearly dependent on the initial dye concentrations. Since such a dependence often suggests that the assumed reaction order with respect to the specific substrate is incorrect, the data were analyzed by the Van't Hoff differential method. This analysis indicated (Fig. 15) that the assumed reaction order was high by one unit and that, over the initial two minutes of the run the reaction was, in fact, zero order with respect to dye. It is also interesting to note that, during

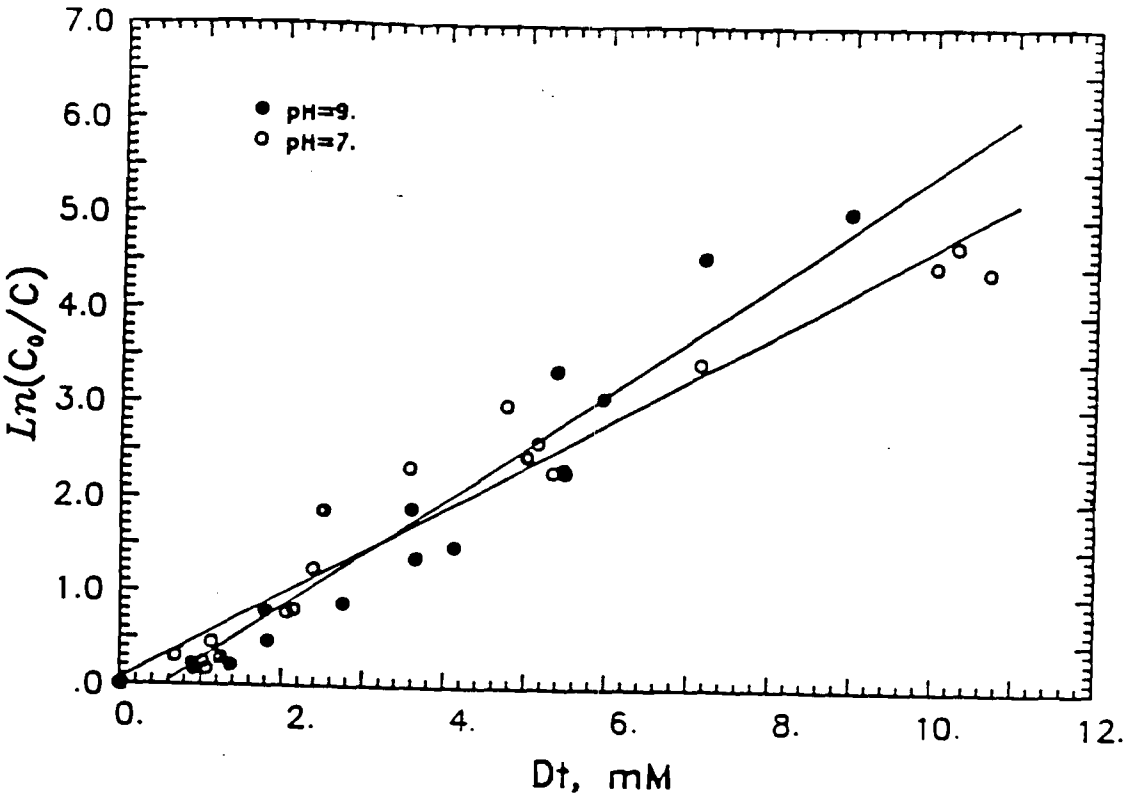

Figure 13. Kinetic plots for the ozonation of DY-12.

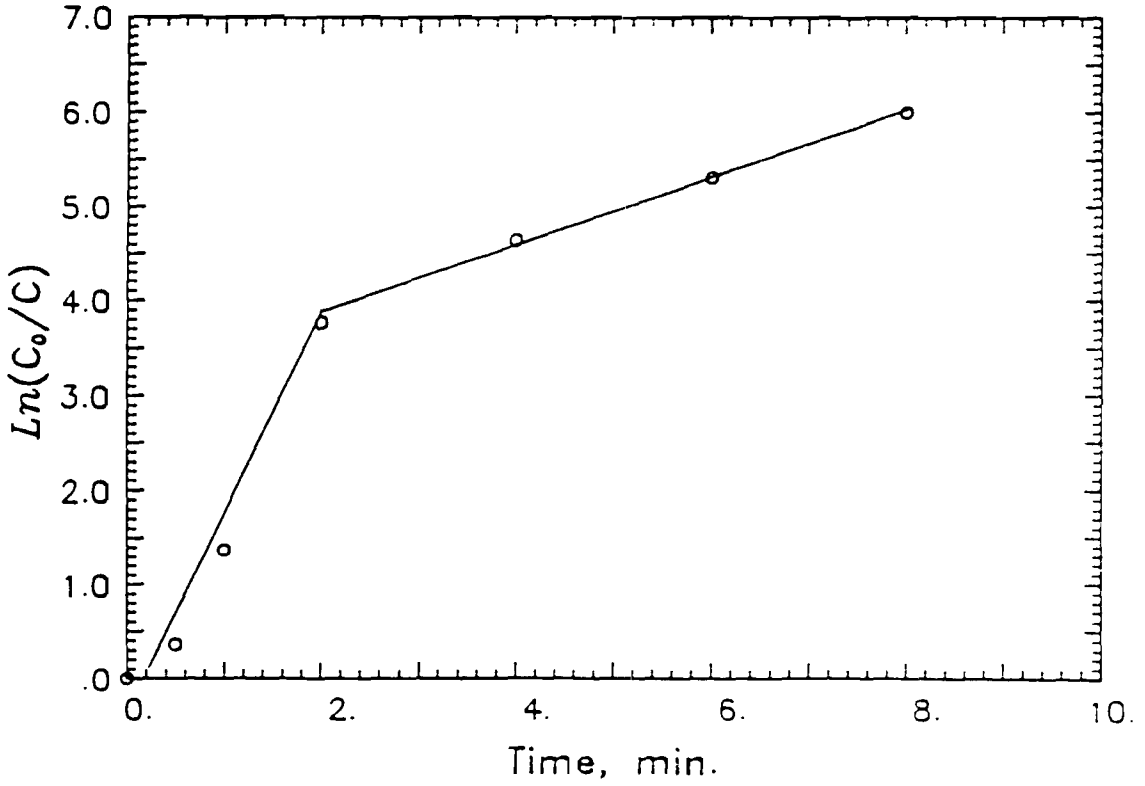

Figure 14. Kinetic plot [illegible] DY-12 at pH = 5. $[DY\text{-}12]_0$ = 1,0 [illegible] µM.

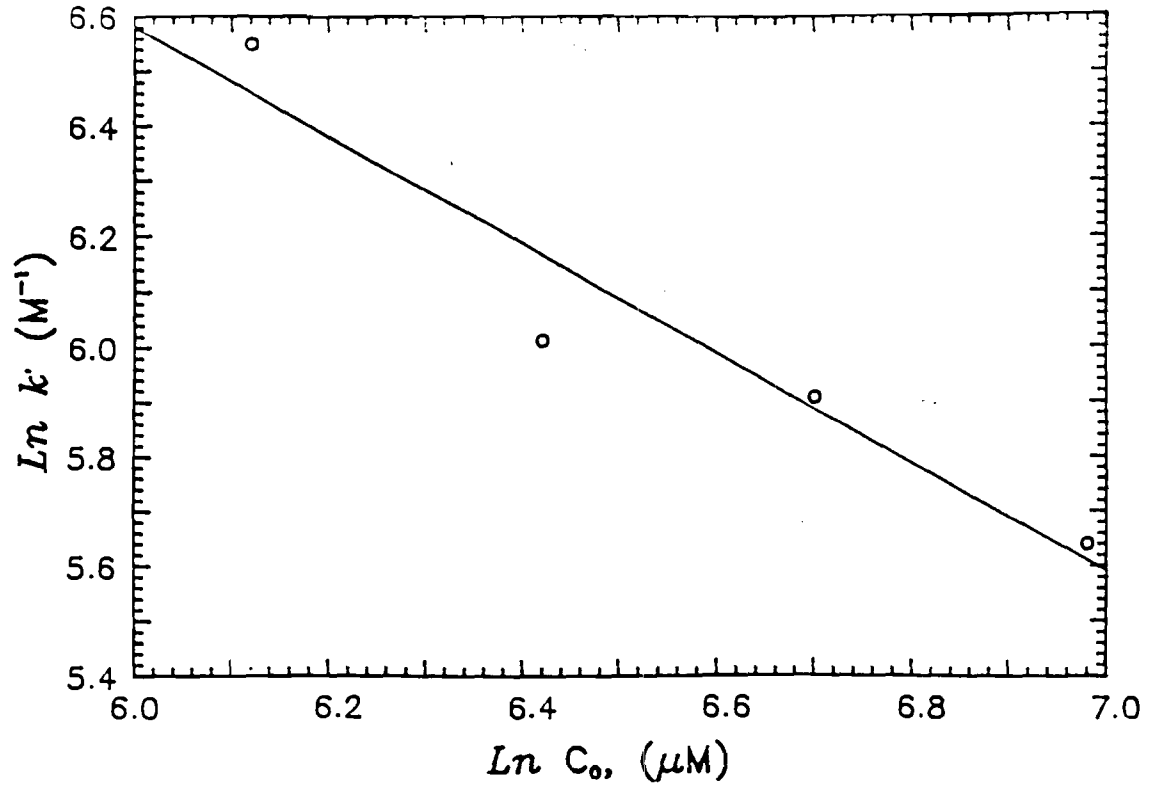

Figure 15. Differential plot for the initial phase of the pH = 5 ozonation of DY-12.

this phase of the runs, the ozone consumption was only about three moles per mole of dye removed, a value not too far removed from that expected for cleavage of a carbon-carbon double bond with carbonyl formation. It is probable that, at this relatively low pH, enough ozone remains as O_3 to favor the early selective attack of the ozone on the ethylenic carbon-carbon double bond of the dye. As the reaction proceeds, increased ozone hydrolysis and a decrease in the available ethylenic carbon carbon double bonds causes the reaction to shift in favor of the non-selective hydroxyl radical attack on the dye with a corresponding change in reaction rate and order as well as an increase in relative ozone consumption. The fact that this transition occurred at approximately two minutes into the run regardless of the initial dye concentration suggests that it may have been a function of the time dependent accumulation of ozone derived free radicals rather than the reduction in the concentration of the initial dye.

With the exception of the initial phase of the pH equals five runs, the consumption of ozone in these runs was well in excess of the two moles per mole of dye consumed expected for a simple attack on the single ethylenic double bond. This clearly reflected the nonselective attack on the molecule by hydroxyl and other free radicals produced by ozone consumption ratio increased markedly (Fig. 16) as the initial dye concentration decreased

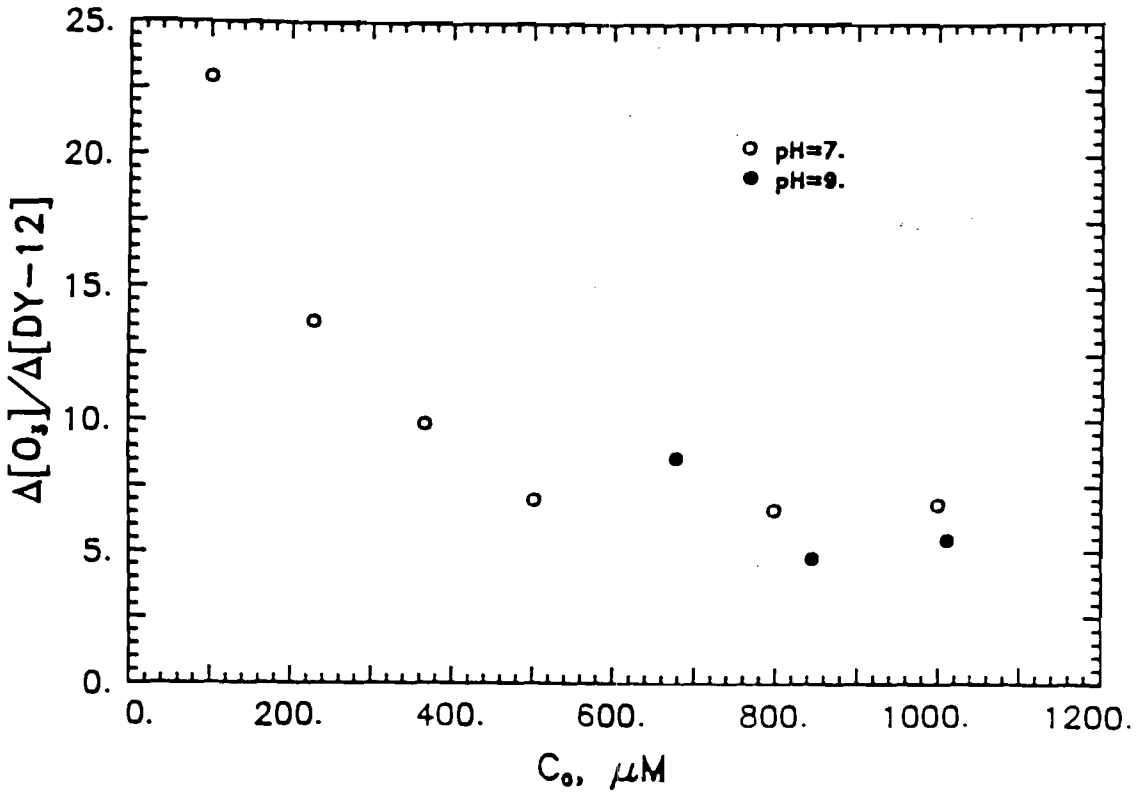

Figure 16. Ozone consumption versus the initial concentration of DY-12.

suggesting that diversion of ozone into the nonselective reaction pathways tended to increase as the availability of the DY-12 decreased. While it is impossible to rationalize the relationship between ozone consumption and initial DY-12 concentration by any fundamental considerations at this time, it was found empirically that an excellent correlation between the log of the ozone consumption ratio and the log of the initial dye concentration existed (Fig. 17) at pH values of 7 and 9. pH control in these systems was complicated by the rapid consumption of hydroxide ions coincident with the dye ozonation. Shown in Figure 18 is the variation of pH as a function of time during the runs at an initial pH of 7. Since the phosphate total concentration used to buffer these solutions was 15 mM in all cases - a minimum buffer to dye molar ratio of 15 to one - the variations shown in Figure 18 were considerable. Analysis of these data indicated that approximately four moles of hydrogen ions were being generated per mole of dye consumed up to the point at which 90% of the DY-12 had been consumed. This value was not unusual as compared with the other dyes studied.

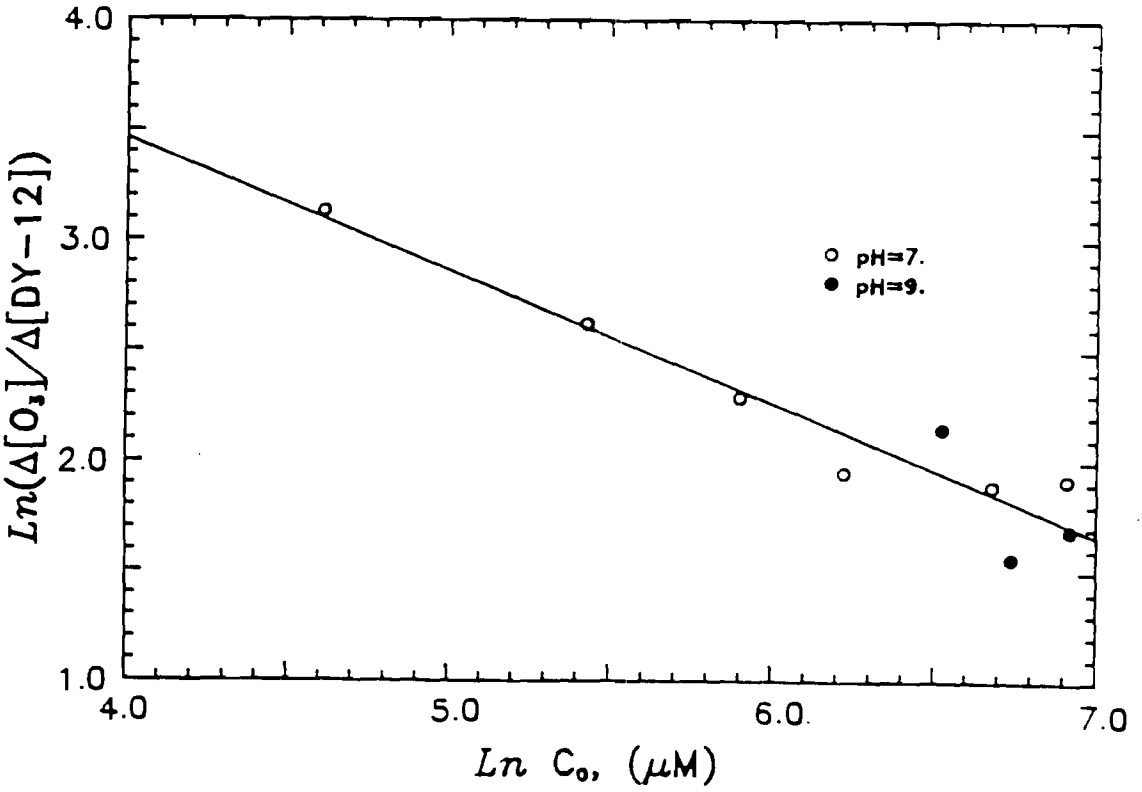

Figure 17. Log-log plot of ozone consumption versus the initial concentration of DY-12.

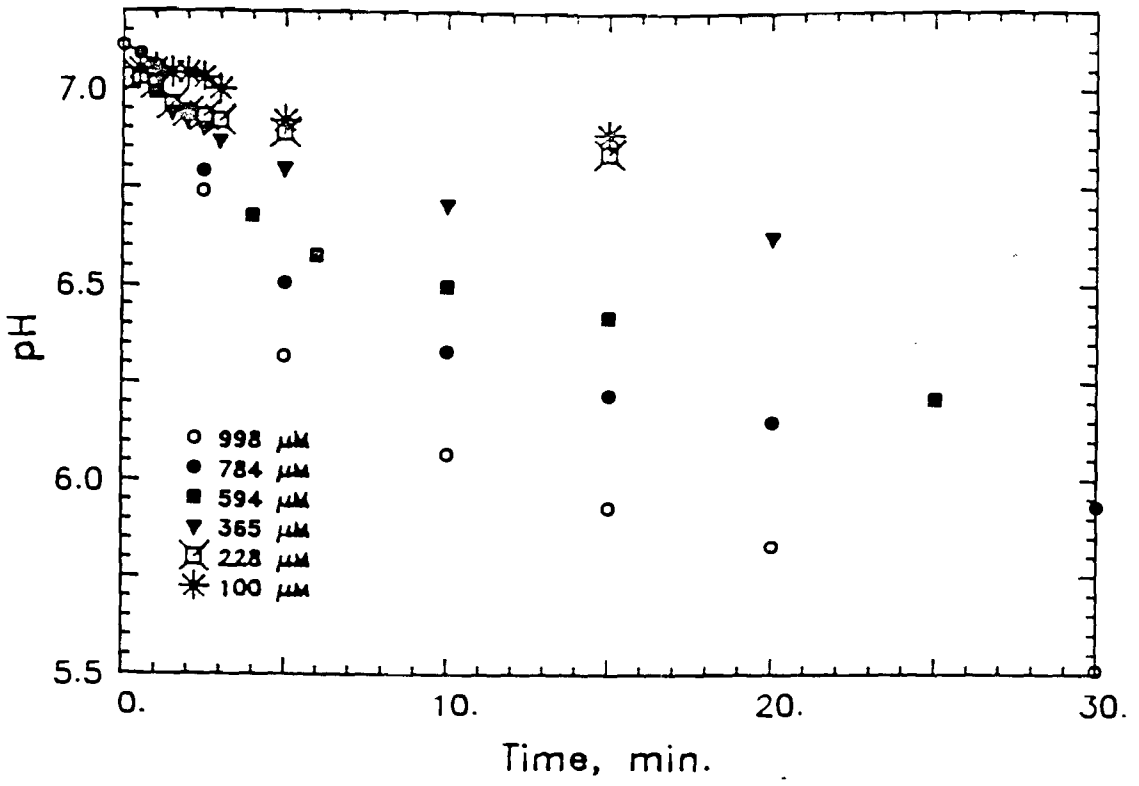

Figure 18. pH as a function of ozonation time at various initial concentrations of DY-12.

Other Dyes

Ozonation studies of the other dyes selected (Fig. 1) were conducted at pH values of 5, 7 and 9 and initial dye concentrations of ≈100 μM. All dyes followed the first order behavior as formulated in Equation 8. The kinetic constants, ozone consumption ratios and hydrogen ion generation ratios are presented in Table 14. These dyes are quite rich in polar functional groups and did not display any two phase behavior such as was observed for DY-12 at a pH of 5. There was little evidence of selectivity of attack in these ozonation reactions. Kinetic constant dependence on pH was limited, irratic and not amenable to any rational mechanistic interpretation on the basis of the data at hand. Ozone consumption and hydrogen ion generation ratios appeared to be independent of pH in all cases and are presented in Table 14 as averages for all runs of each dye studied. Ozone consumption ratios ranged from 19 moles O_3 per mole DY-50 to 36 moles O_3 per mole DR-24. Hydrogen ion generation ranged from 4.0 moles per mole of DY-12 to 10.8 moles per mole of DV-9.

The loss of organic carbon in these systems is slow (Fig. 19). This is in accord with the findings of other researchers[5,6] who have found that, while ozone attacks many organic structures rapaciously, the ultimate conversion of these compounds to CO_2 and water is not favored.

Table 14. Summary of Ozonation for All Dyes

Dye	$\Delta O_3/\Delta$Dye	$\Delta[H^+]/\Delta$Dye	pH	k', M^{-1}	1n2/k', mM
DY-12	23.0	4.0	5	236	2.94
			7	441	1.57
			9	598	1.16
DV-9	24.4	10.8	5	523	1.32
			7	482	1.43
			9	418	1.66
DR-24	36.4	5.5	5	274	2.53
			7	276	2.51
			9	317	2.18
DY-50	19.0	8.8	5	320	2.17
			7	282	2.46
			9	274	2.53
DO-102	21.6	8.3	5	202	3.43
			7	303	2.29
			9	401	1.73
DY-4	23.1	4.7	5	402	1.73
			7	398	1.74
			9	408	1.70

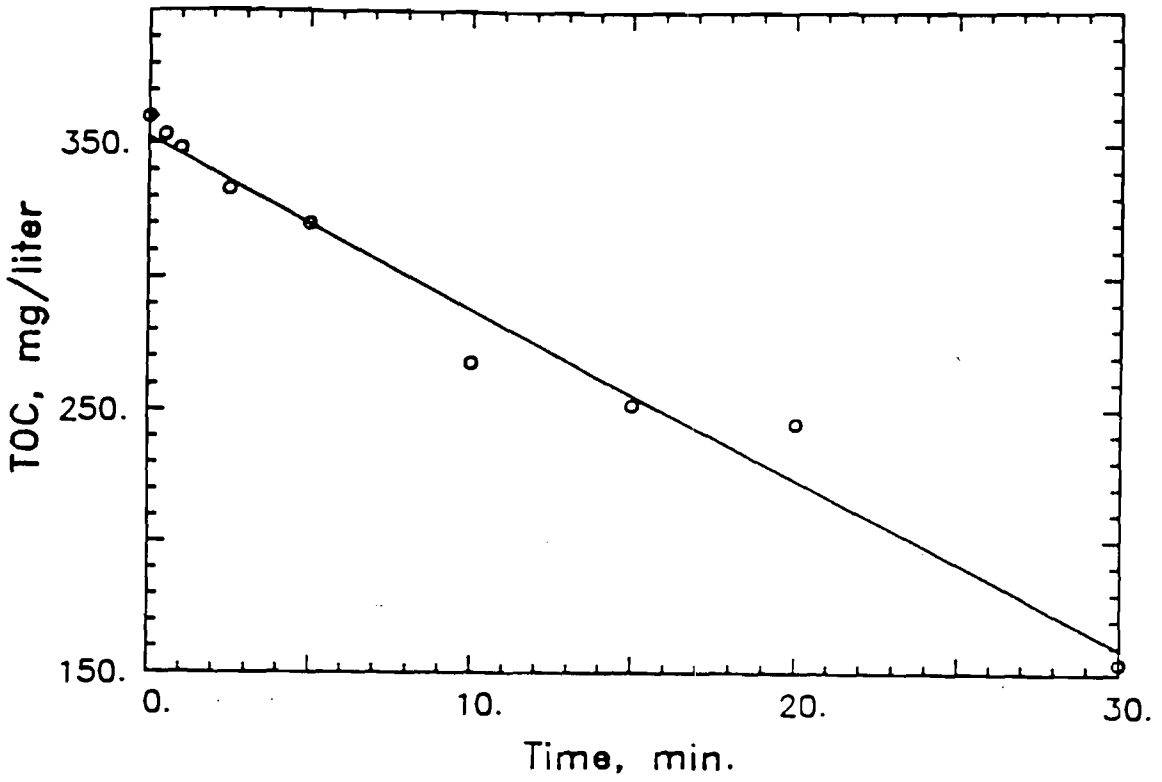

Figure 19. Total organic carbon produced during ozonation of DY-12. pH = 7, $[DY\text{-}12]_0$ = 998 μM.

Dyes Chosen for Investigation of Mass Spectrometric Studies

The azo dyes chosen for this phase of the study are, as in the previous work, representative of the major class of water soluble dyes currently used for industrial dyeing processes. Certain dyes have been added for investigation based on their structural properties however which are not used commercially for dyeing. These azo dyes are water soluble sulfonit acid type molecules with known structures. Eight of the dyes studied in this phase of the research are listed in Figure 20.

Of the dyes studied, four--methyl orange, methyl red, direct yellow 4 and direct yellow 12--were obtained from commercial sources and purified as described previously. Dye purity was confirmed by thin layer chromatography.

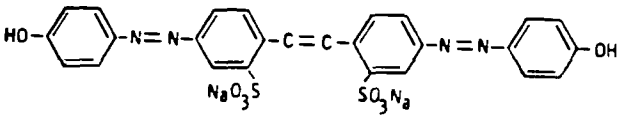

Direct Yellow 4

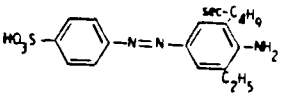

ESBA

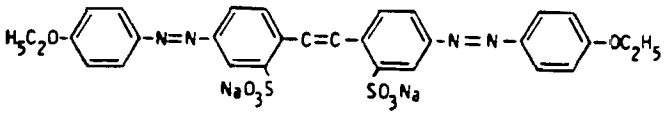

Direct Yellow 12

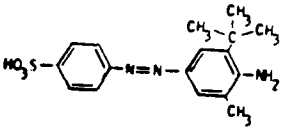

MTBA

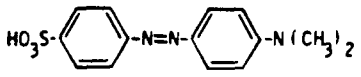

Methyl Orange

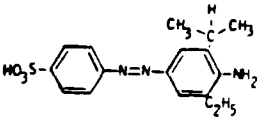

EIPA

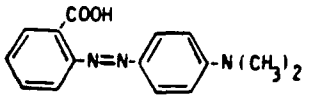

Methyl Red

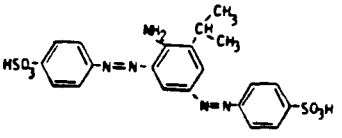

OIPA

Figure 20. Dye structures and designations for mass spectrometric studies.

The other dyes were synthesized by the classical method in which the appropriate compound wascoupled with a small excess of diazotized sulfanilic acid at a pH favorable for the reaction. The names assigned to the synthesized dyes represent abbreviations of the names of the compounds coupled with diazotized sulfanilic acid to produce the respective dyes. Thus, the dye designated by "ESBA" was prepared using 2-ethyl-6-sec-butylaniline as a starting material. The crude dyes were precipitated as the free acids at low pH, dried and purified as described previously.

Involatile Sample Analysis

With the addition of highly efficient coupling of capillary chromatographic columns to the available mass spectrometer system, there is possessed an extremely precise method to separate a mixture into its volatile components and analyze the separate components using highly sensitive mass spectrometric techniques (GC-MS). Each of the aforementioned dyes used in this investigation are however involatile and for this reason they present severe problems with respect to analysis by GC-MS techniques. It has been found that it is possible to take advantage of already developed state-of-the-art GC-MS techniques for analysis of these involatile compunds by adding a pyrolysis stage at the inlet of the gas chromatograph.

By the use of modern pyrolysis instrumentation it is possible to heat a sample in an inert atmosphere under carefully controlled conditions and do so in a very reproducible manner. Pyrolysis was carried out with a Chemical Data Systems Pyroprobe 100 unit linked by a heated interface to the inlet system of a microprocessor controlled Varian 3700 gas chromatograph. Samples were placed in thin-walled micro-sized quartz boats and inserted into a platinum filament coil. The samples were heated to 800°C in a millisecond and the involatile compounds decomposed to thermodynamically stable, volatile molecular subunits. These degradation products are immediately swept into a high resolution capillary column of a gas-liquid chromatograph for compound by compound separation and detection. The spectrum of molecular products provides a chemical "fingerprint" of the original starting material.

In addition, n-octanol has been used to extract aniline based dyes and compounds from dilute aqueous environmental samples. Aqueous samples to be examined were adjusted to a pH below 2 using hydrochloric acid. A 250 cc portion of the sample was then extracted with two successive 5 cc volumes of reagent grade n-octanol and the octanol fractions were combined. A 1 cc sample of the n-octanol extract was then placed on a 5 x 50 mm column of 60/200 mesh chromatographic grade of active alumina. After complete absorption of the octanol, the column was washed with 25 mL of reagent grade ethyl acetate to remove the bulk of the octanol. The dyes being studied were retained on the upper 5 mm of the alumina. The column was then dried by passing a stream of nitrogen gas through it and a sample of the dye laden alumina placed in the quartz micro-container for pyrolysis/analysis. Solvents retained on the alumina during the separation process are effectively evolved when the alumina is placed in the pyrolysis interface at 200°C. Once these solvents have cleared the column, the pyrolysis at 800°C was initiated.

The gas chromatographic column used in this analysis was a surface coated open tubular (SCOT) column coated with Carbowax 20M. The SCOT column was 40 meters long with an inside diameter of 0.5 mm. The column was connected to the chromatograph using a capillary column system and mass spectrometer interface (Midwest Analytical Consultants, Champaign, IL). An inlet split ratio of 10:1 was maintained. Temperatures of the system were as follows: pyrolysis probe, 801°C, a 12 ms rise time to final temperature and held for 10 s duration; pyrolysis interface, 200°C; injector heater, 230°C; detector heater, 230°C; mass spectrometer interface, 240°C; ion source, 250°C; column, initially 65°C (held for 240 s) then programmed linearly to 165°C at 1°C/10 s rate and held at 165°C for one hour. The carrier gas flow was 1 mL/min.

The Varian-MAT 112S double focusing mass spectrometer was interfaced with a SS 200 data system. Mass spectra were obtained using an ion kinetic energy of 820 eV, an electron energy of 80 eV, electron emission current of 0.7 mA and an electron multiplier with a 1000 Hz filter. The mass spectrometer was operated at a resolution of 700 andspectra were obtained at an exponential scanning rate of 0.7 s/mass decade in the mass range m/z 20 to 350. Products from the pyrolysis were identified from their mass spectra. A Biemann search routine was used to scan the 34,000 compounds in our NIH/EPA MSDC data file on disc in our data system. Once tentative identifications were made, the authentic compounds were obtained, injected directly into the chromatograph and both the retention times and mass spectra determined to confirm the compound identification. Since the mass spectra of several of the pyrolysis product materials are not listed in our data base, this procedure of comparing retention times and reference spectra of the products with authentic compounds was useful for identification purposes.

The pyrolysis-GC-mass spectrometry of direct yellow 12 and direct yellow 4 are illustrated in Figure 21. In this figure the total ion intensity recorded by the mass spectrometer is presented as a function of time (as given by the number of mass spectrometer scans. The zero of time is taken to be the time when pyrolysis is initiated. As shown in Figure 21. The dominant products are complete subunits of the respective dye molecules. Thus, the products from the pyrolysis yield considerable information regarding the structure of the original involatile dye molecule, since these products result from relatively simple elimination processes at high temperatures.

Similar presentations of pyrolysis-GC-mass spectrometry "fingerprints" of methyl orange and methyl red dyes are shown in Figure 22. Aniline and substituted anilines from direct thermal cleavages of the respective dye molecules dominate the spectra in Figure 22. The same type of simple bond cleavages are observed in the data of Figures 23 and 24 for the synthesized azo based dyes. The formulas above each of the ion peaks give the structures of the respective pyrolysis products. Aniline and 2-ethyl-6-sec-butylaniline are the dominant products from the azo dye composed of these subunits. Likewise, aniline and 2-ethyl-isopropylaniline ion peaks provide a chemical "fingerpring" of the starting sulfonic acid dye molecule composed of these two molecules coupled through an N=N bond.

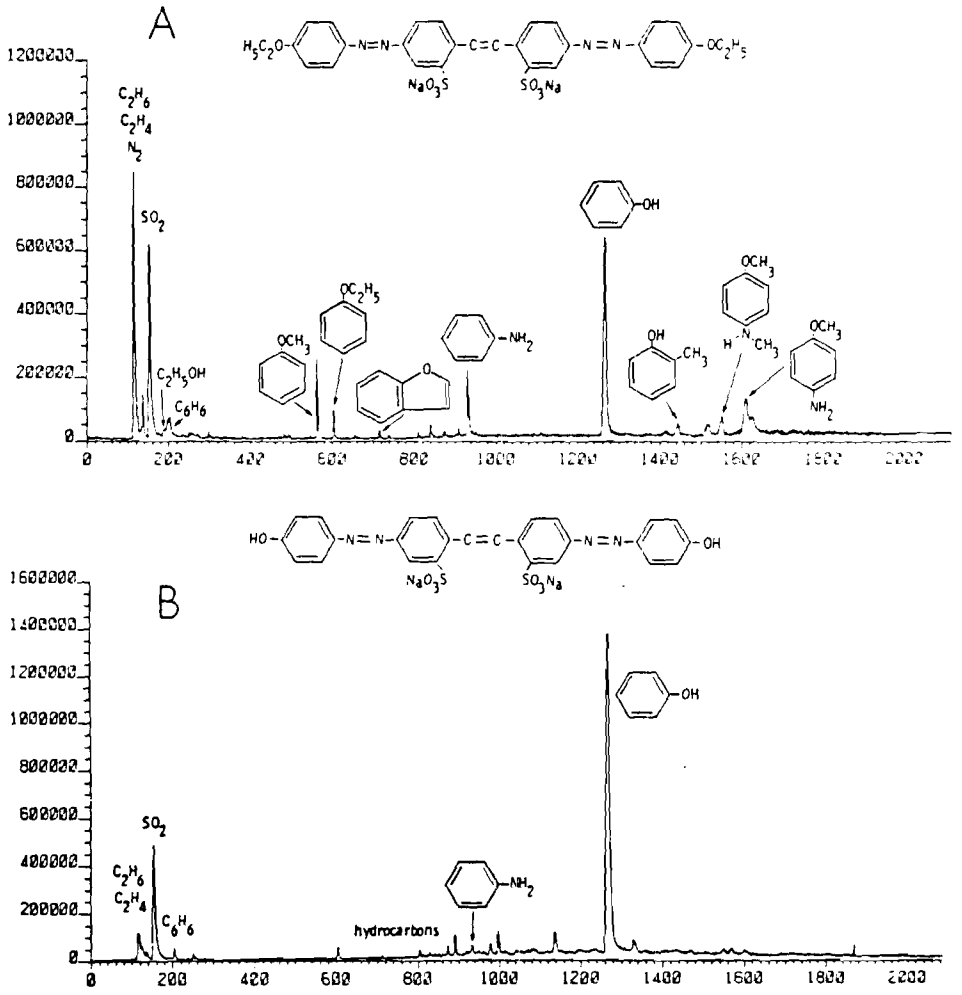

Figure 21. Pyrolysis-GC-Mass Spectrometry of: A, direct yellow 12 and B, direct yellow 4. Total ion intensity as a function of number of mass spectrometer scans (time).

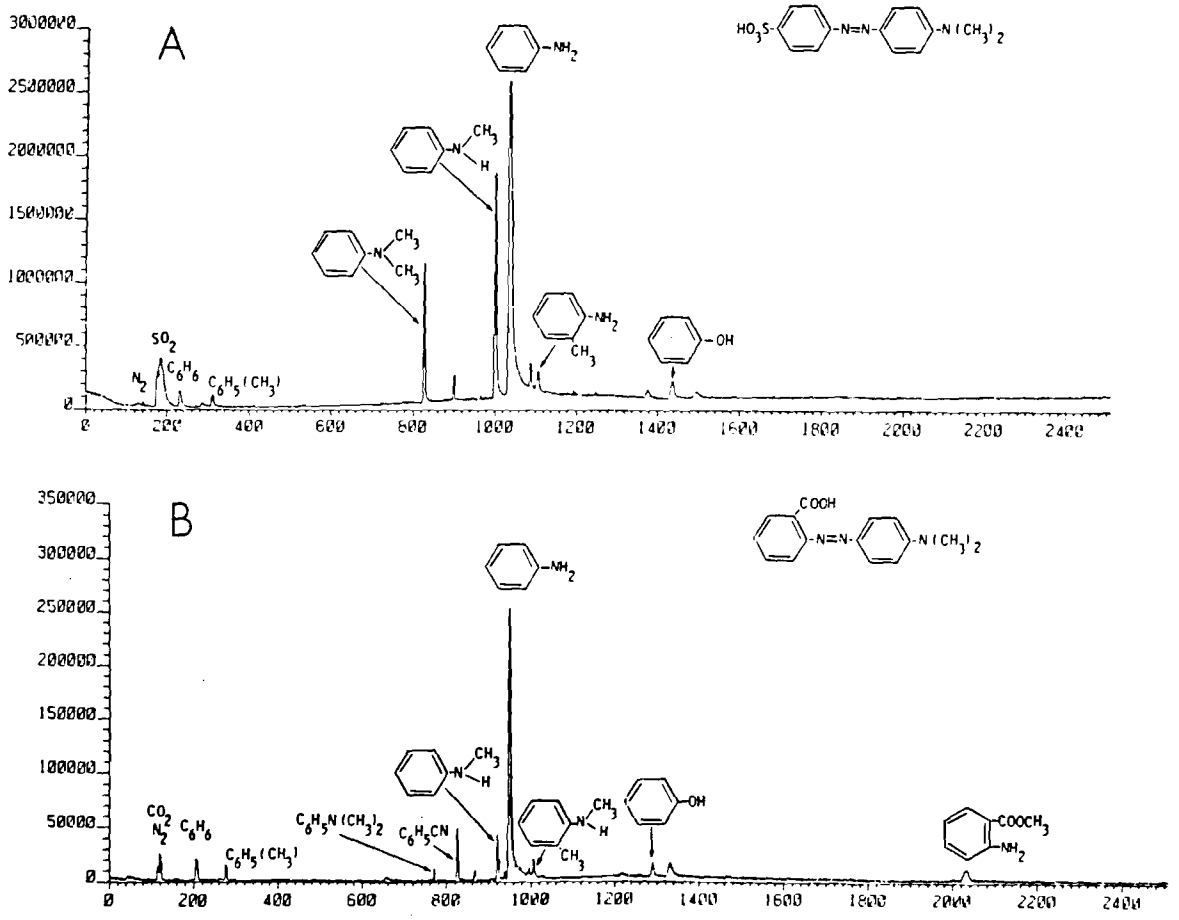

Figure 22. Pyrolysis-GC-Mass Spectrometry of: A, methyl orange and B, methyl red. Total ion intensity as a function of number of mass spectrometer scans (time).

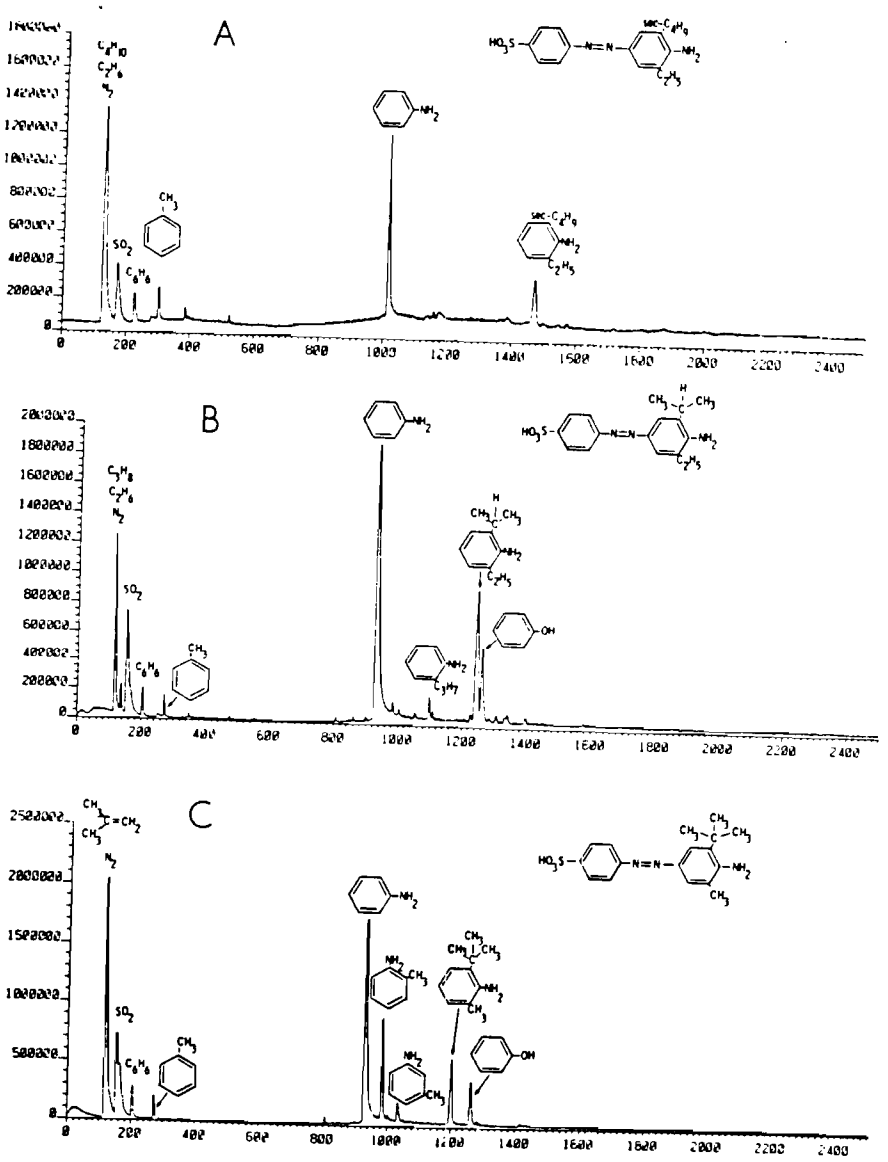

Figure 23. Pyrolysis-GC-Mass Spectrometry of: A, ESBA; B, EIPA; C, MTBA. Total ion intensity as a function of mass spectrometer scans.

Pyrolysis of the chlorinated dye having a dichlorophenol subunit is shown in Figure 25. The aniline and dichlorophenol pyrolysis products are the largest peaks in the pyrochromatogram.

One of the most significant results of these investigations is the common appearance of entire structural subunits of the starting dye molecules. Pyrolysis can in some cases result in small amounts of slightly modified fragments of those structural units. In general, these minor products result from relatively simple rearrangement reactions. For example, on pyrolysis, both methyl orange and methyl red yield N,N dimethylaniline, the basic structural unit, and N methylaniline, a slightly fragmented but logical pyrolysis product of this unit. It is also noted that minor quantities of the rearrangement of the N,N dimethylaniline such as 2,N dimethylaniline and 2-methylaniline are also formed. In general, however, the dominant products are consistent with the unimoleculr decomposition which lead to intact subunits of the starting dye molecule. Similar fragmentation processes are also observed in the case of dialkyl-aniline dyes shown in Figure 23 as well as the dichlorophenol based dye illustrated in Figure 25. The Figures 21 to 25 show that aniline is a consistent product from the pyrolysis of aniline based, azo dyes. Even in the examples shown in Figure 21, where aniline would be expected and found to be a minor product, the presence of aniline has been established unequivocally. In the pyrolysis of all the other dyes, aniline is the most abundant fragmentation product. Thus, the presence of aniline serves as a reliable indicator of these dyes.

In addition to using the pyrolysis technique as a qualitative method for dye identification, it is possible to quantify the amount of dye pyrolyzed. Samples weighed on an electronic micro-balance have been pyrolyzed and total product ion currents, in units of 10^{-10} amps, have been measured. Typical results are presented in Figure 26 for the dye ESBA (Fig. 20) in the range of 0.4 to 60 x 10^{-6} g. As shown in this figure, the total ion current is a linear function of sample weight. A linear regression analysis of the data gives a solid line passing through the points which has a slope of 0.306 x 10^{-10} amps/microgram with a 0.999 correlation coefficient. We find that this linear behavior tends to fall off for sample weights below 100 picograms. This lack of pyrolysis product volatility may be a result of inefficient energy transfer due to physical adsorption of this small amount of dye to the quartz boats. For dye quantities in the picogram range, it is our procedure to add a microdrop of methanol-dye solution to the quartz sample holder. Capillary action tends to spread this drop which gives a large liquid-solid interface and thus maximizes dye-quartz interaction as the methanol evaporates. This fall-off from linearity notwithstanding, it is clear from the data in Figure 26 that it is possible to use pyrolysis techniques to monitor dye quantities in the low microgram to high picogram range.

Samples of a carbon-methanol extract from a wastewater treatment plant downstream from the textile dyeing plants of Dalton, Georgia have been analyzed using the pyrolysis-GC-mass spectrometry method. In a typical example a carbon-methanol extract corresponding to 20 liters of wastewater was processed and the dyes concentrated in the top 119.3 mg portion of the alumina column. A 1.937 mg fraction of this material was removed and pyrolyzed. The pyrolysis-GC chromatogram obtained is shown in the top of

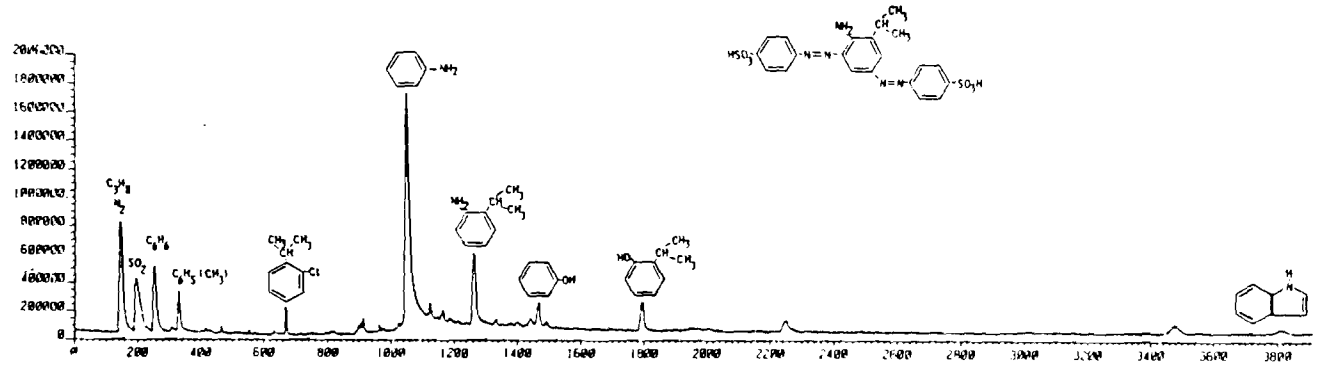

24. Pyrolysis-GC-Mass Spectrometry of OIPA. Total ion intensity as a function of mass spectrometer scans.

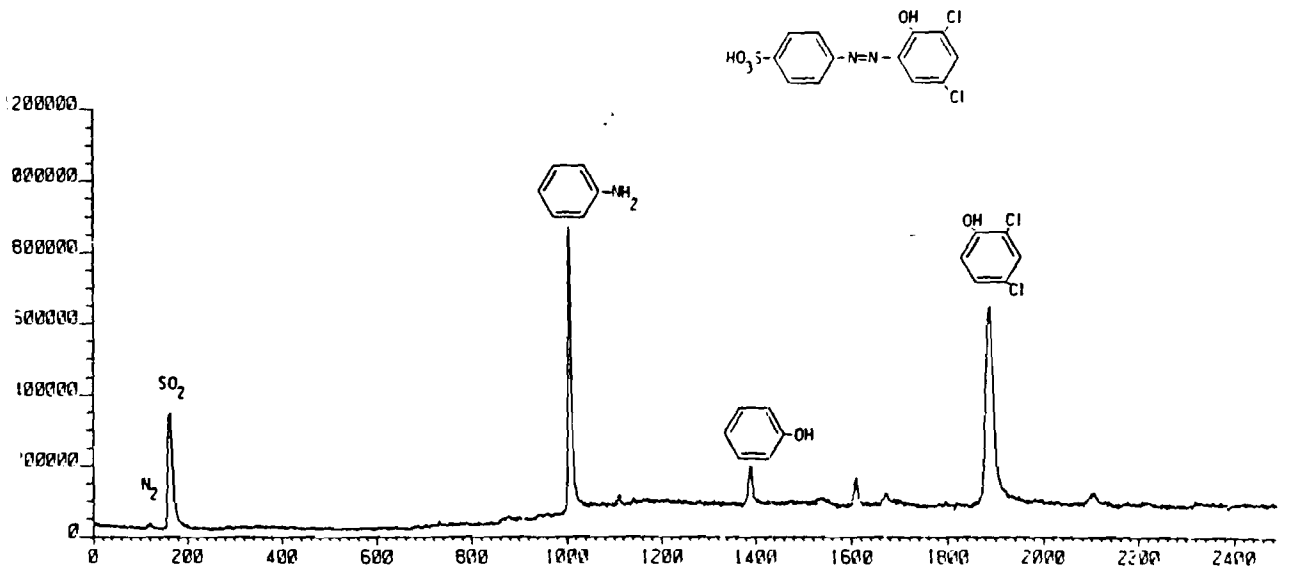

25. Pyrolysis-GC-Mass Spectrometry of DCP. Total ion intensity as a function of mass spectrometer scans.

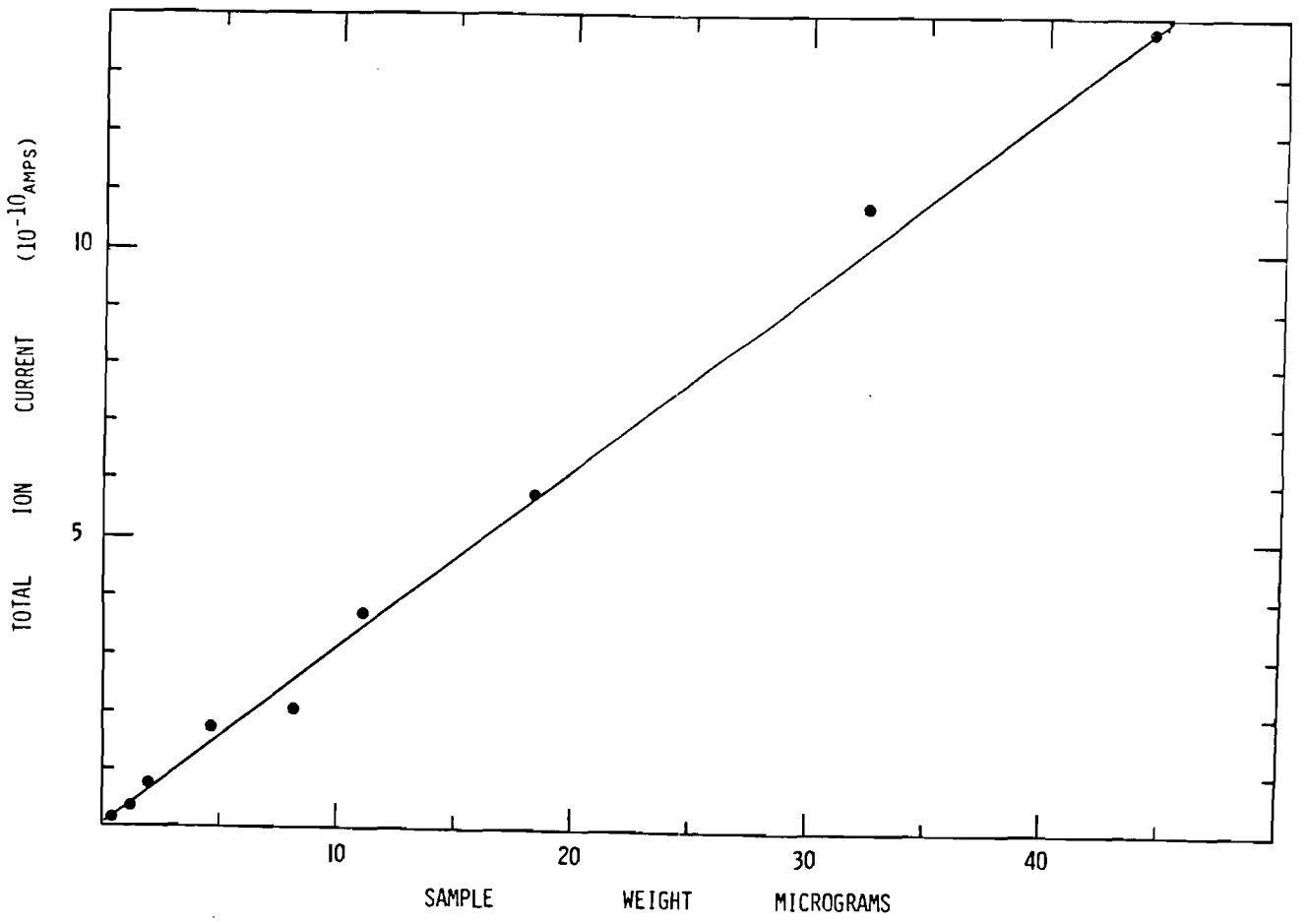

Figure 26. Total ion current, in units of 10^{-10} A plotted as a function of dye sample weight in micrograms.

Figure 27. A blank sample was processed in an identical manner and the pyrolysis data for a 1.945 mg of this alumina blank is shown in the bottom portion of Figure 27. From the data in Figure 26 we can estimate that approximately 1.5×10^{-6} g of aniline based dye, expressed on the basis of the aniline from ESBA pyrolysis, was adsorbed on 1.937 mg of alumina and that 92.4 µg of dye was present in the total carbon-methanol extract sample. Our separation procedure is thus concentrating dye compounds which are present as 5 ppb. Furthermore, based on the system sensitivity it is now possible to detect as little as 0.08 ppb of dye in the aquatic environment using carbon concentration and pyrolysis-gas chromatography.

The sensitivity of the complete pyrolysis-GC-interface system has been continuously upgraded by careful choice of pyrolysis temperature and time of pyrolysis, elimination of as much "dead volume" as possible in the system. Once the most efficient configuration of the GC column/mass spectrometer interface was established a newly proposal analytical method, doubly charged ion mass spectrometry, was applied to this problem. This is a method of detecting with high selectivity the pyrolytic molecules from azo dye products. Much of the development work was performed on the double focusing Hitachi spectrometer and then the technique applied to the Varian-MAT 1125 mass spectrometer. The doubly charged ion technique detects aromatic and substituted aromatics such as aniline, chlorinated benzenes, phenols, chlorinated anilines, etc. with high selectivity. Both singly and doubly charged ions are formed by electron impact ionization. However, the two different classes of ions are difficult to distinguish from one another, since doubly charged ions of even mass (M^{2+}) appear at the same mass-to-charge ratio as singly charged ($M^+/2$) ions. In the technique as applied here, all ions are accelerated and then reacted with a neutral target gas and the singly charged products passed through an electrostatic energy analysis sector for detection. Doubly charged ions M^{2+} react very efficiently to form singly charged M^+ product ions which possess the same velocity as the M^{2+} reactants. For example, when benzene is ionized both single charged ions $C_6H_6^+$ at M/Z 78 are formed as well as $C_6H_6^{2+}$ at M/Z 39. After acceleration, the $C_6H_6^{2+}$ ions have twice the kinetic energy of the $C_6H_6^+$ ions and when an electrostatic sector is set pass the singly charged $C_6H_6^+$ products, from reactions of the type $C_6H_6^{2+}$ + T (target gas), <u>all</u> other singly charged ions are rejected by the sector. This has the advantage of eliminating "chemical noise" usually inherent in the operation of a working mass spectrometer. Background signals due to sample retention in the ion, source, GC carrier gas, column bleed, etc. are eliminated in this mode of operation. The high signal-to-noise advantage of the doubly charged ion mode of operation is particularly useful when dealing with sub-microgram quantities of material.

The previously mentioned pyrolysis-GC-mass spectrometric studies of azo based dye molecules using the normal mass spectral has served as the benchmark technique with which to improve the analytical procedure. The doubly charged ion mass spectrum of aniline is particularly simple with the molecular ion the largest peak. Other product ion peaks are less than 13% of the largest peak but they do furnish a fingerprint spectrum from which molecular identification is readily made. The doubly charged ion mass spectra of chlorinated anilines, phenols and chlorinated phenols have doubly charged ion mass spectra similar in the respect that the molecular ion is very intense with the smaller fragment ion peaks providing structural

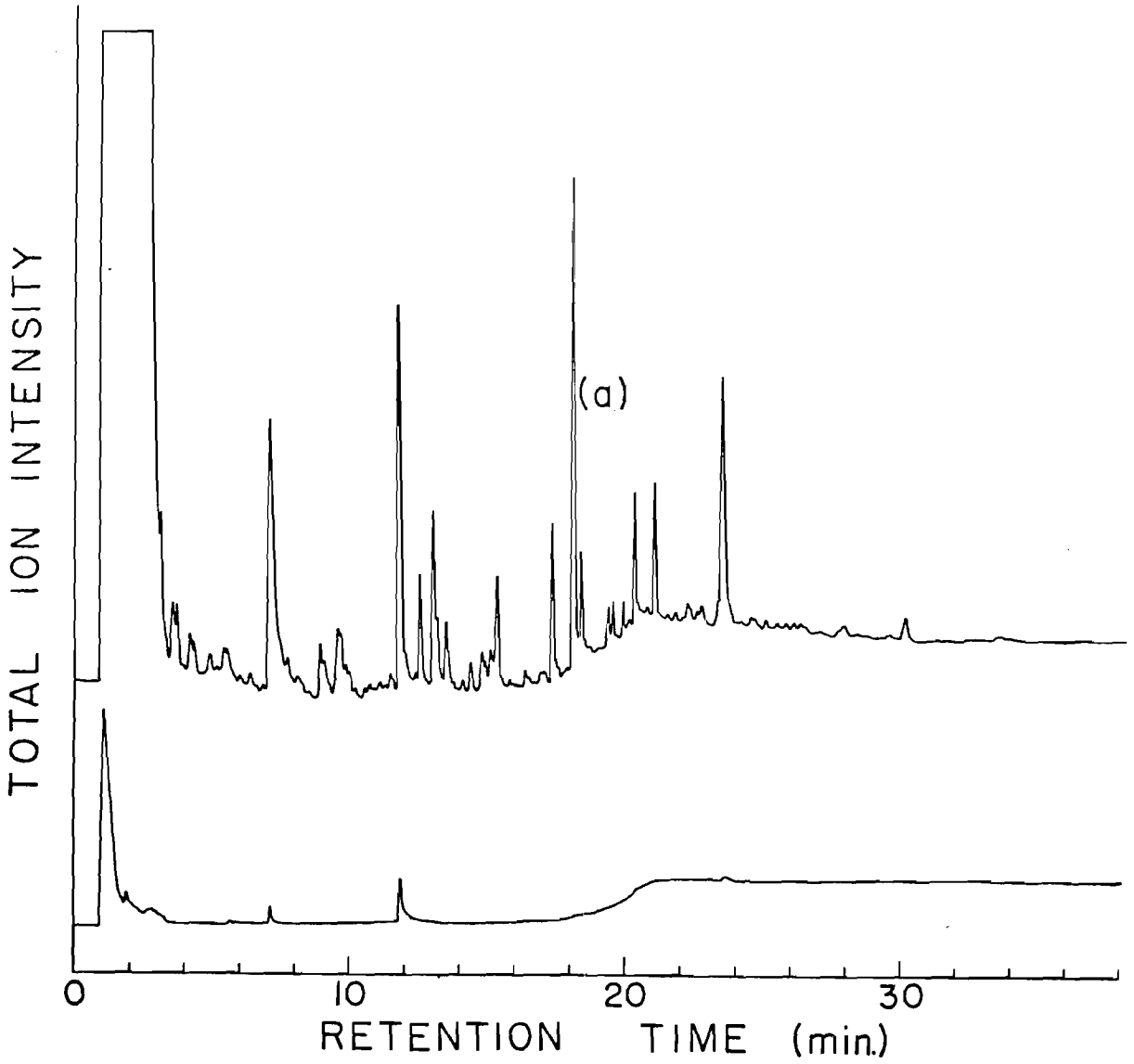

Figure 27. Pyrolysis-GC chromatograms giving ion intensity as a function of time in minutes. The upper trace is the pyrolysis of carbon-methanol extract of the wastewater treatment plant effluent. The peak labeled (a) is aniline and is characteristic of the dyes concentrated by our method. The lower trace is that of a blank alumina run.

information on the starting molecule. The doubly charged ion mass spectra of chlorinated alkanes, aliphatic amines and oxygenated alkanes were not known and the prior to inception of this research attached papers at the end of this report summarizes our investigations of these compounds. While these compounds are not the major products from dye product pyrolysis they do appear and their spectra, were previously unknown, and presented an obstacle to the full implementation of mass spectrometry in the work.

CONCLUSIONS

Both chlorination and ozonation proved capable of removing synthetic dyes from aqueous solutions with associated destruction of the color of the dyes rapidly and with high efficiency. Relationships between the fundamental parameters of pH and initial reactant concentrations and the rates and reactant consumption ratios were difficult to systematize, although the initial reactant concentration appeared to be of negligible importance in both cases. Production of stable chloramines was not a significant factor in the chlorination process. The behavior of DY-12 was dominated to a great extent in chlorination and to a lesser degree in ozonation by the ethylenic bond in its structure. The low reactivity of the dye was apparent in its reaction kinetics with both oxidants.

The low volatility of the dyes and their reaction products rendered their analysis by conventional GC-MS techniques impossible. Two innovative techniques, pyrolysis GC-MS and a doubly charged ion technique, were investigated and showed significant promise in providing specific analytical data on these dyes in natural aqueous matrices. Considerable structural information was available and high quantitative sensitivity attained when these methods were applied in conjunction with simple preconcentration methods.

REFERENCES

1. APHA-AWWA-WPCF. Standard Methods for the Examination of Water and Wastewater, 15th Ed. (1980).

2. Gould, J. P. and Weber, W. J., Jr. "Oxidation of Phenols by Ozone." J. Water Poll. Cont. Fed., 48, 47 (1976).

3. Eisenhauer, H. R. "Ozonation of PHenolic Wastes." J. Water Poll. Cont. Fed., 40, 187 (1968).

4. Saunders, F. M., Gould, J. P. and Southerland, C. R. "The Effect of Solute Competition on Ozonolysis of Industrial Dyes." Water Res., 17, 1407 (1983).

5. Society of Dyers and Colourists. Colour Index Published in Bradford, England, 3rd Ed. (1971).

APPENDIX 1

DATA PLOTS FOR DIRECT ORANGE 102

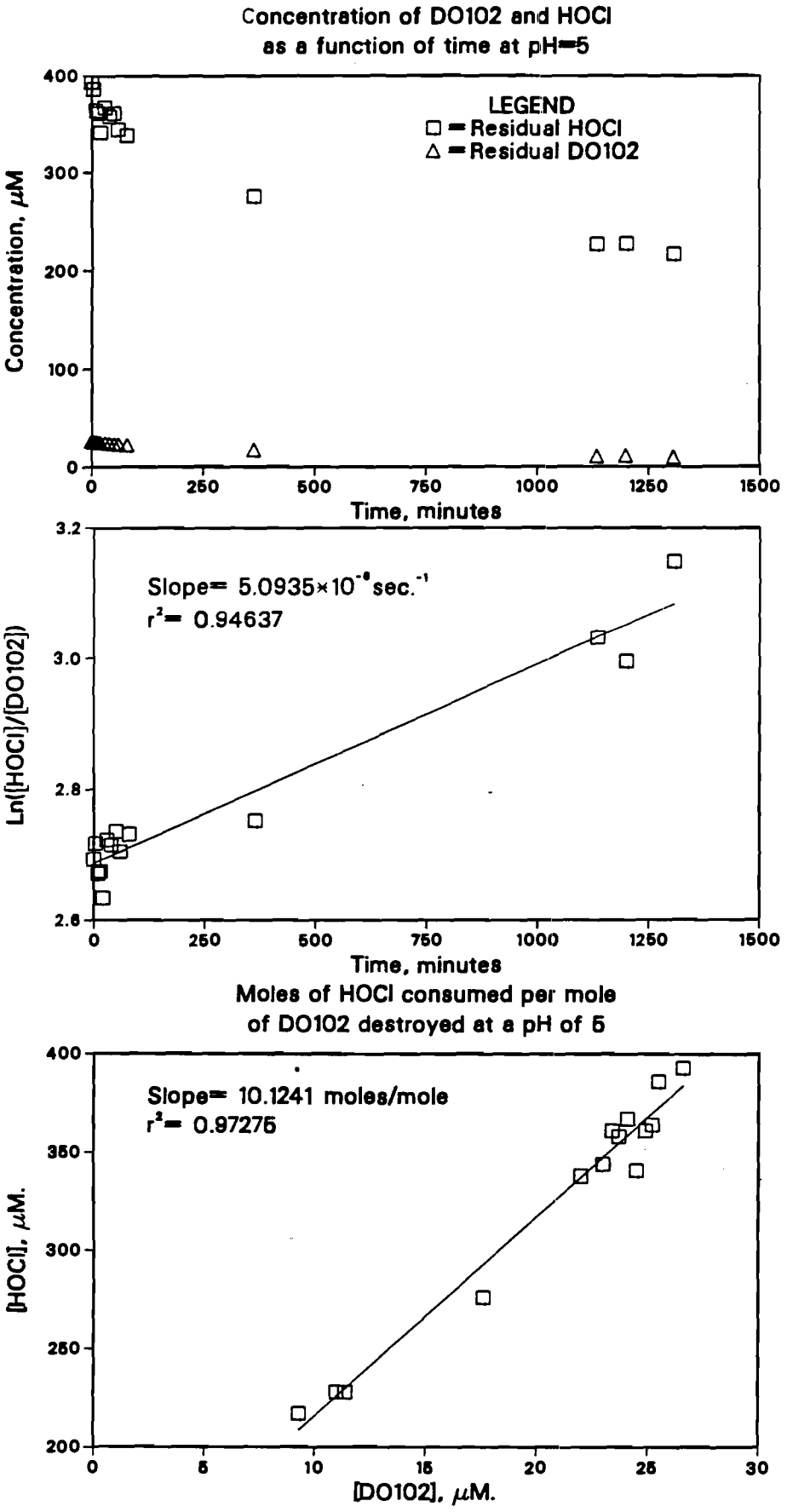
Concentration of DO102 and HOCl
as a function of time at pH=5
LEGEND
□ = Residual HOCl
△ = Residual DO102
Concentration, μM
Time, minutes
Slope= 5.0935×10⁻⁶sec.⁻¹
r²= 0.94637
Ln([HOCl]/[DO102])
Time, minutes
Moles of HOCl consumed per mole
of DO102 destroyed at a pH of 5
Slope= 10.1241 moles/mole
r²= 0.97275
[HOCl], μM.
[DO102], μM.

Figure A1.1

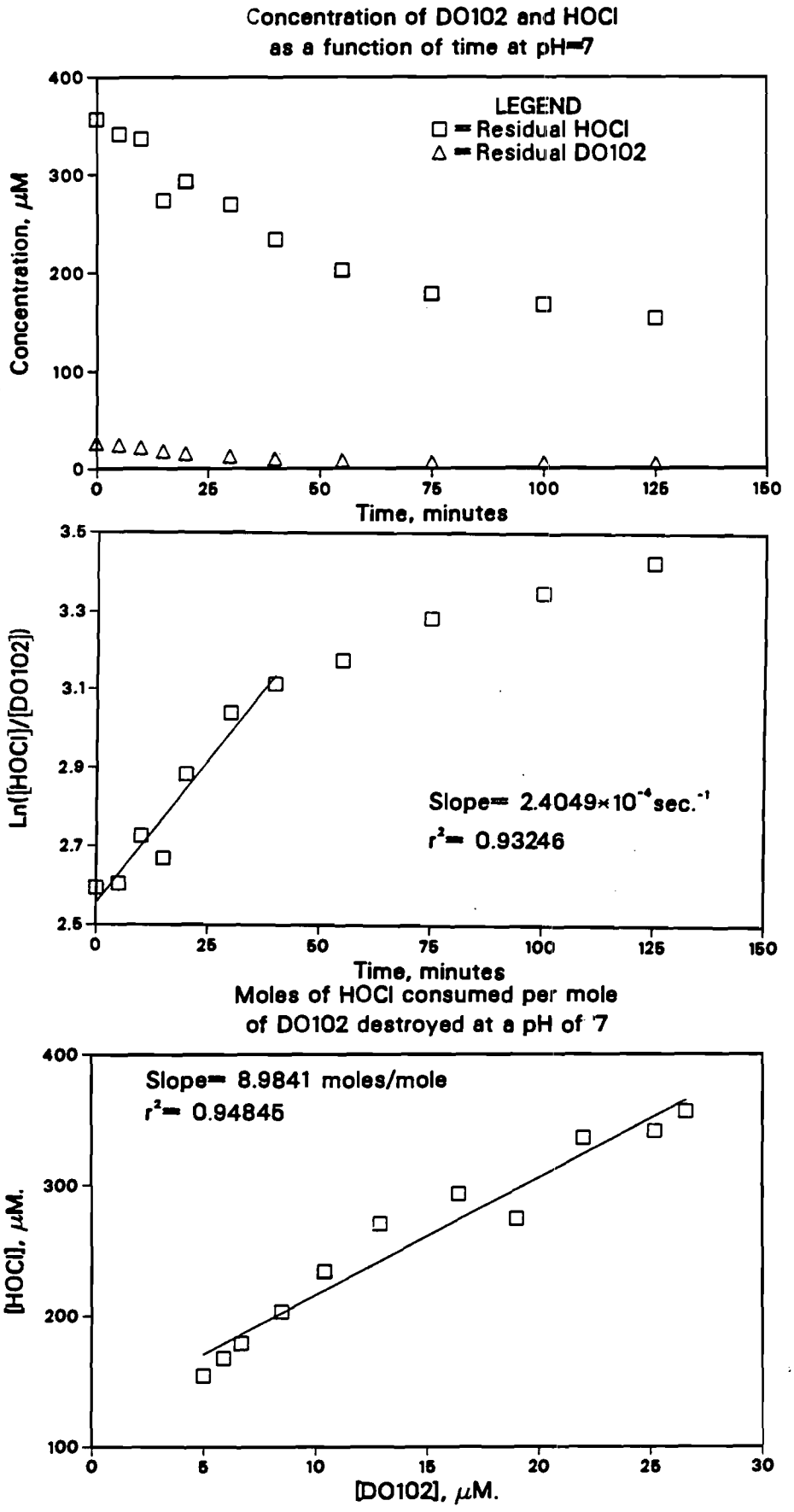
Concentration of DO102 and HOCl
as a function of time at pH=7
LEGEND
□ = Residual HOCl
△ = Residual DO102
Concentration, μM
Time, minutes
Ln([HOCl]/[DO102])
Slope= 2.4049×10⁻⁴sec.⁻¹
r²= 0.93246
Time, minutes
Moles of HOCl consumed per mole
of DO102 destroyed at a pH of 7
Slope= 8.9841 moles/mole
r²= 0.94845
[HOCl], μM.
[DO102], μM.

Figure A1.2

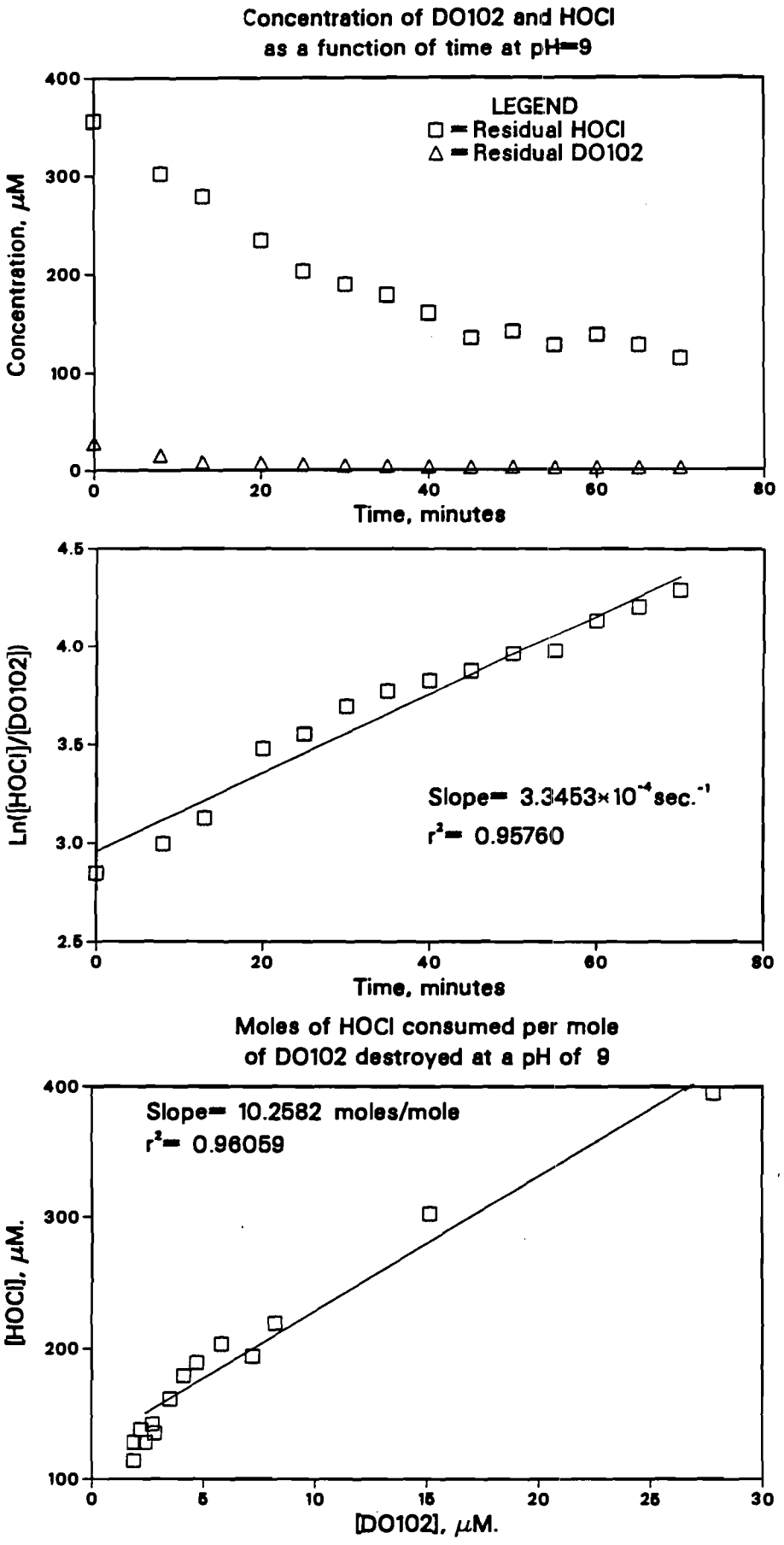
Concentration of DO102 and HOCl
as a function of time at pH=9
LEGEND
□ = Residual HOCl
△ = Residual DO102
Concentration, μM
Time, minutes
Ln([HOCl]/[DO102])
Slope= 3.3453×10⁻⁴sec.⁻¹
r²= 0.95760
Time, minutes
Moles of HOCl consumed per mole
of DO102 destroyed at a pH of 9
Slope= 10.2582 moles/mole
r²= 0.96059
[HOCl], μM.
[DO102], μM.

Figure A1.3

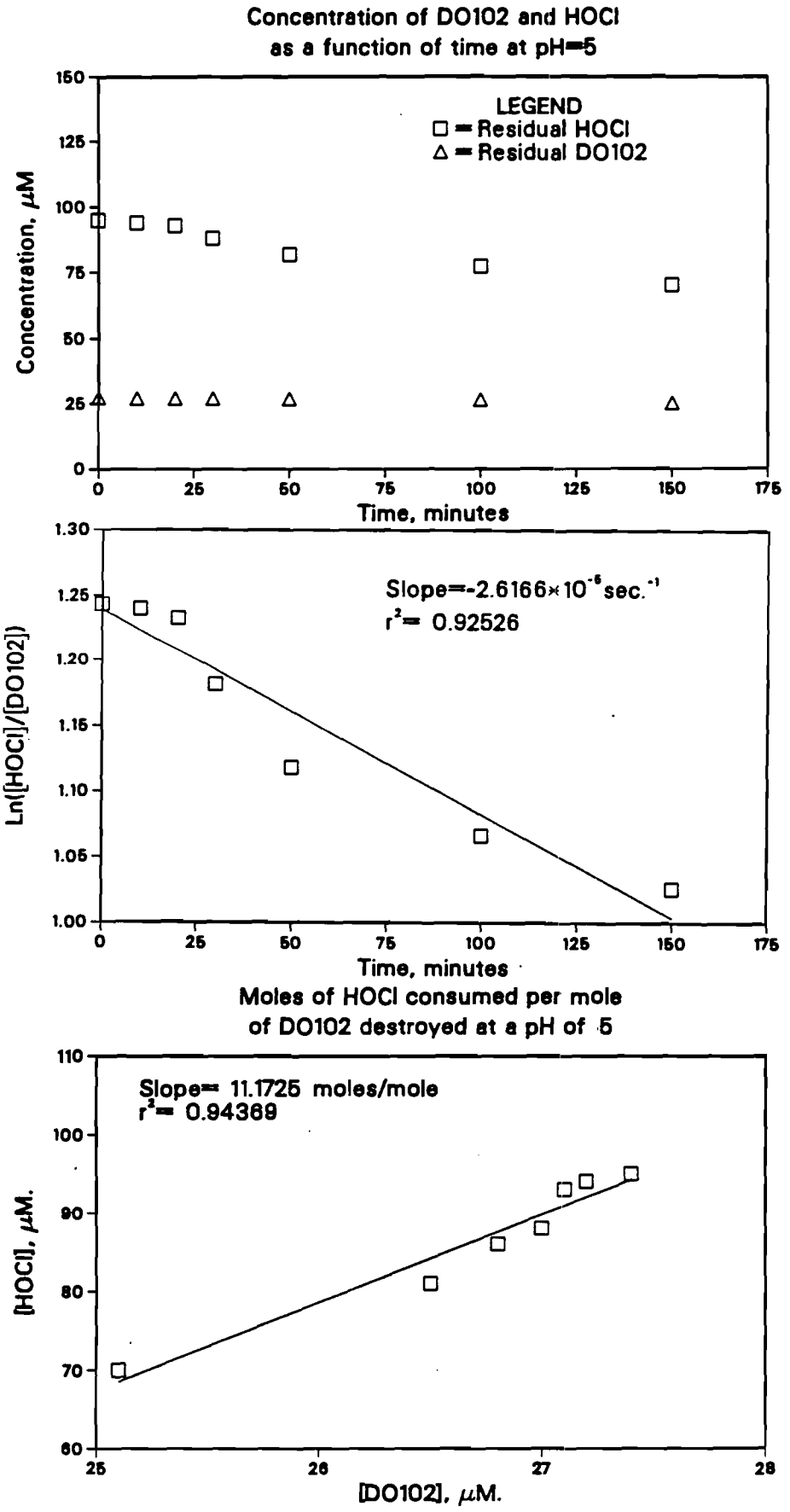
Concentration of DO102 and HOCl
as a function of time at pH=5
LEGEND
□ = Residual HOCl
△ = Residual DO102
Concentration, μM
Time, minutes
Slope=-2.6166×10⁻⁵ sec.⁻¹
r²= 0.92526
Ln([HOCl]/[DO102])
Time, minutes
Moles of HOCl consumed per mole
of DO102 destroyed at a pH of 5
Slope= 11.1725 moles/mole
r²= 0.94369
[HOCl], μM.
[DO102], μM.

Figure A1.4

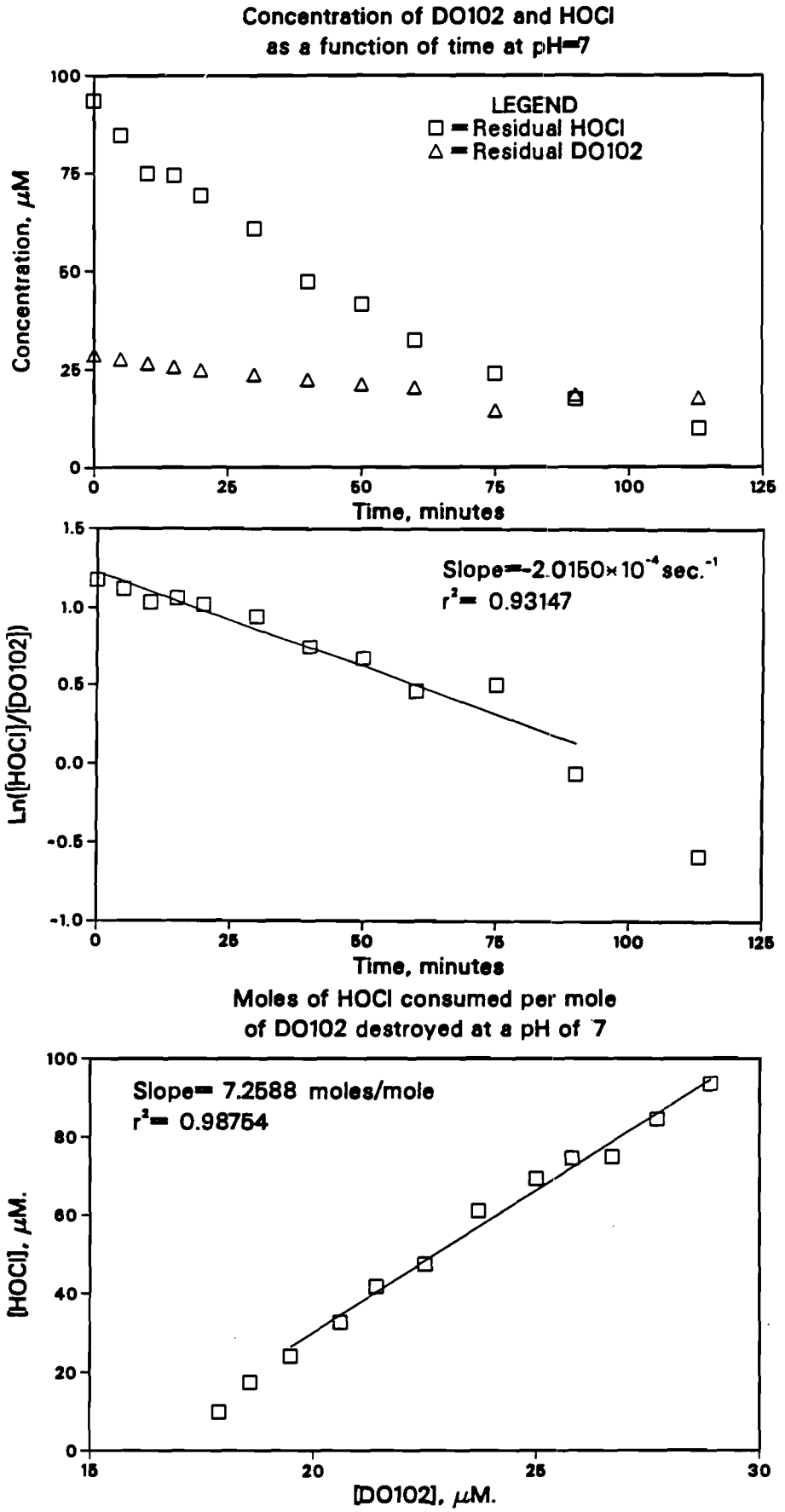
Concentration of DO102 and HOCl
as a function of time at pH=7
LEGEND
□ = Residual HOCl
△ = Residual DO102
Concentration, μM
Time, minutes
Slope=-2.0150×10⁻⁴ sec.⁻¹
r²= 0.93147
Ln([HOCl]/[DO102])
Time, minutes
Moles of HOCl consumed per mole
of DO102 destroyed at a pH of 7
Slope= 7.2588 moles/mole
r²= 0.98754
[HOCl], μM.
[DO102], μM.

Figure A1.5

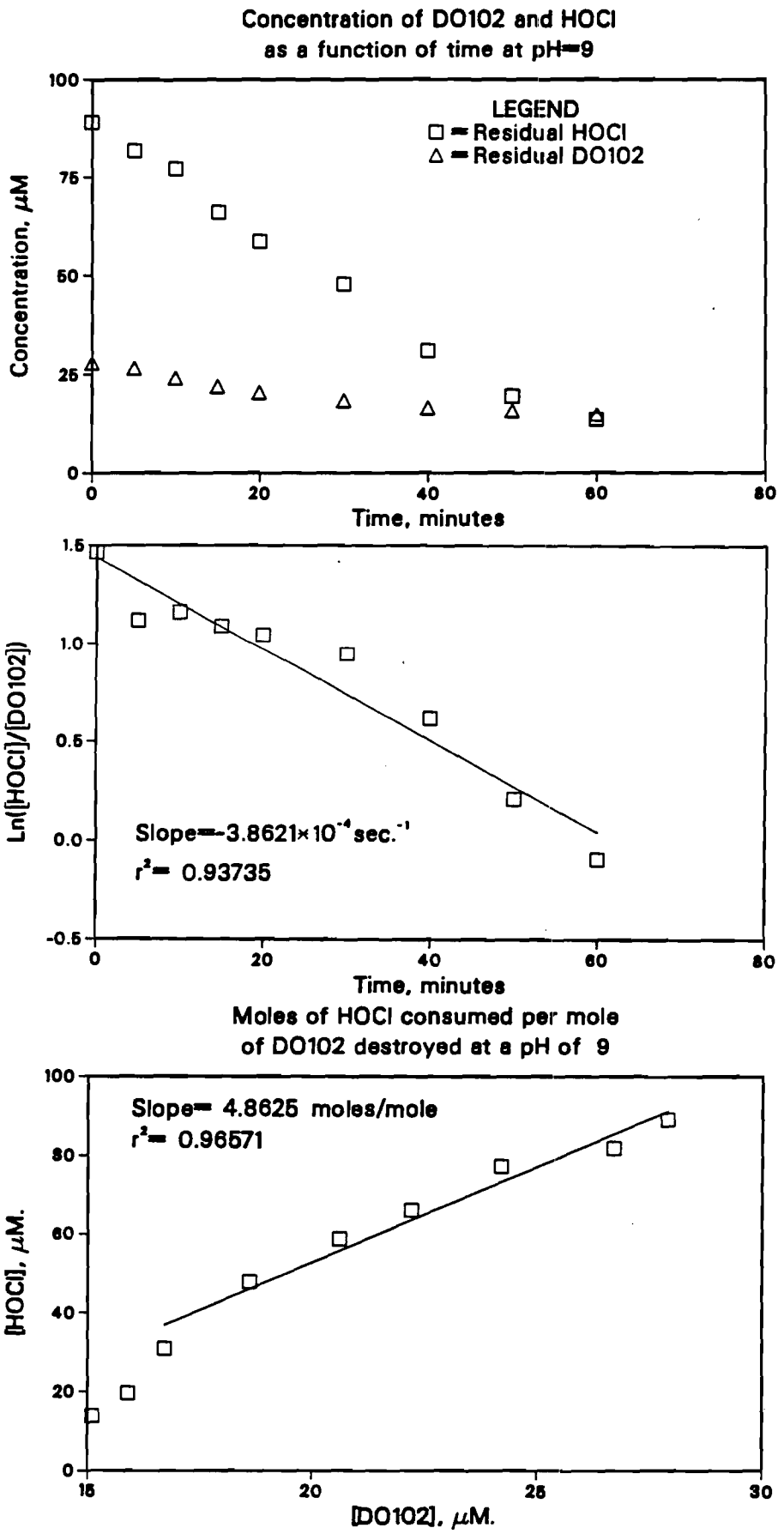
Concentration of DO102 and HOCl
as a function of time at pH=9
LEGEND
□ = Residual HOCl
△ = Residual DO102
Concentration, μM
Time, minutes
Ln([HOCl]/[DO102])
Slope=-3.8621×10⁻⁴ sec.⁻¹
r²= 0.93735
Time, minutes
Moles of HOCl consumed per mole
of DO102 destroyed at a pH of 9
Slope= 4.8625 moles/mole
r²= 0.96571
[HOCl], μM.
[DO102], μM.

Figure A1.6

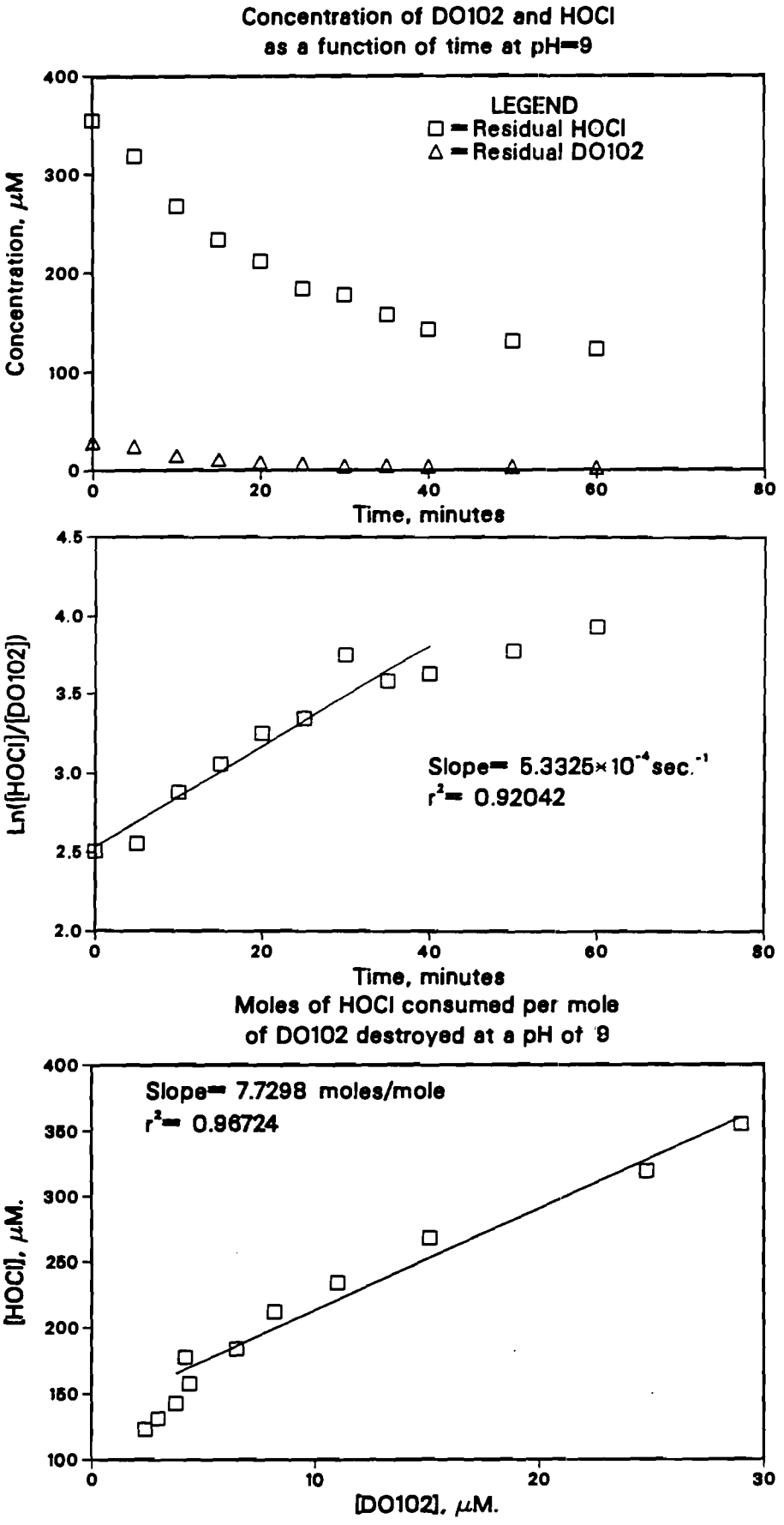
Concentration of DO102 and HOCl
as a function of time at pH=9
LEGEND
□ = Residual HOCl
△ = Residual DO102
Concentration, μM
Time, minutes
Ln([HOCl]/[DO102])
Slope= 5.3325×10⁻⁴sec.⁻¹
r²= 0.92042
Time, minutes
Moles of HOCl consumed per mole
of DO102 destroyed at a pH of 9
Slope= 7.7298 moles/mole
r²= 0.96724
[HOCl], μM.
[DO102], μM.

Figure A1.7

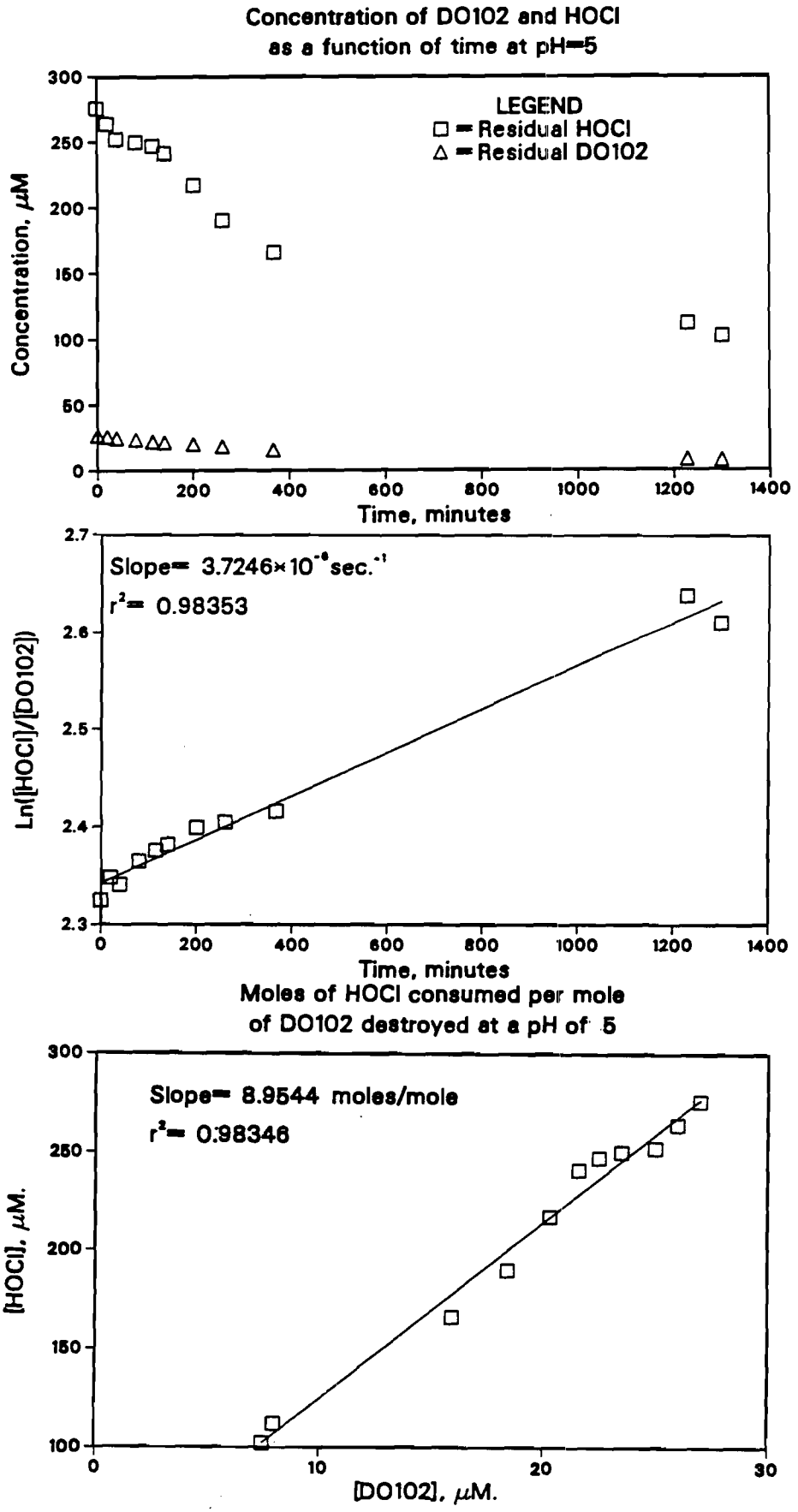
Concentration of DO102 and HOCl
as a function of time at pH=5
LEGEND
□ = Residual HOCl
△ = Residual DO102
Concentration, μM
Time, minutes
Slope= 3.7246×10⁻⁶sec.⁻¹
r²= 0.98353
Ln([HOCl]/[DO102])
Time, minutes
Moles of HOCl consumed per mole
of DO102 destroyed at a pH of 5
Slope= 8.9544 moles/mole
r²= 0.98346
[HOCl], μM.
[DO102], μM.

Figure A1.8

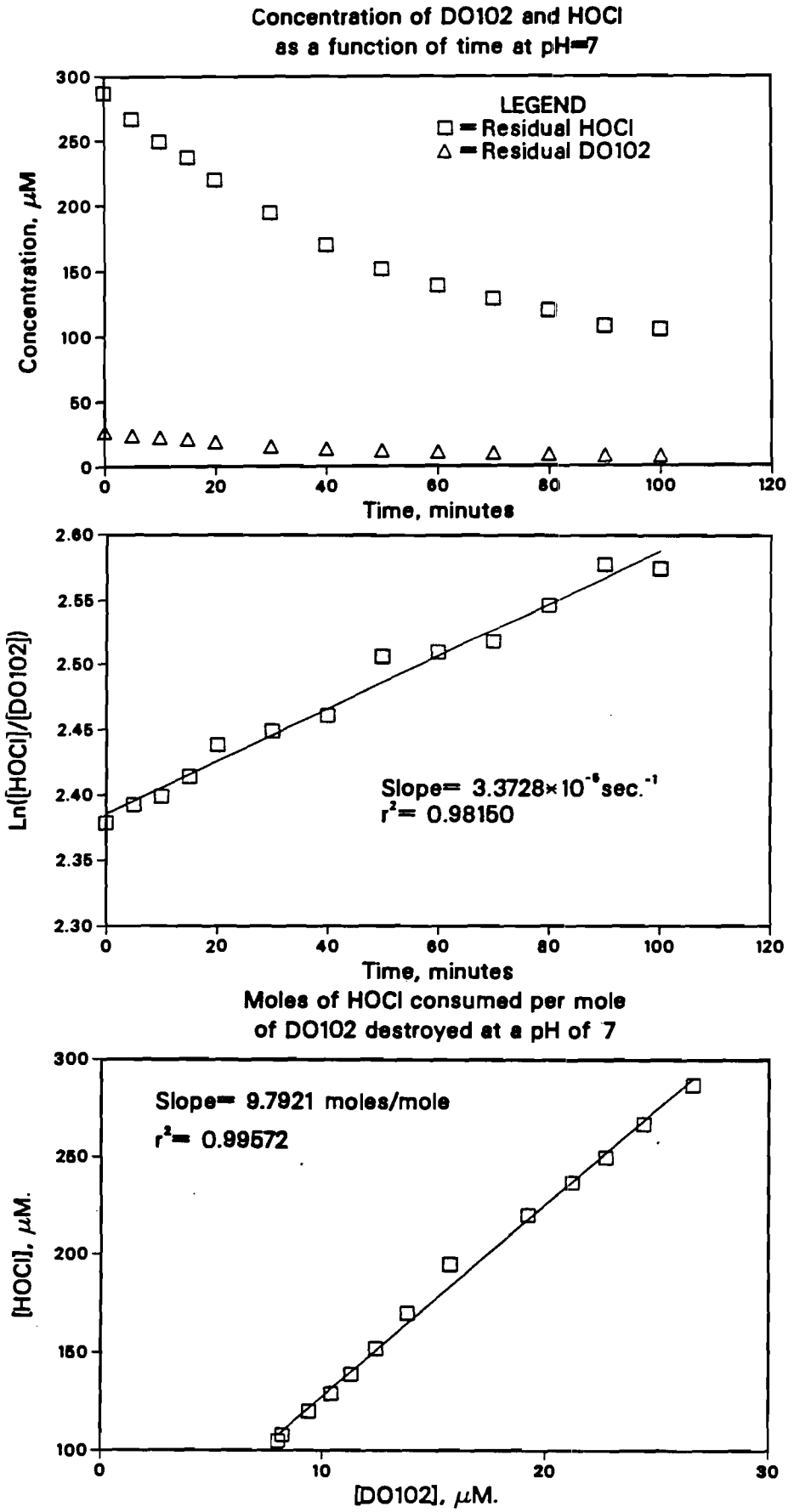
Concentration of DO102 and HOCl
as a function of time at pH=7
LEGEND
□ = Residual HOCl
△ = Residual DO102
Concentration, μM
Time, minutes
Ln([HOCl]/[DO102])
Slope= 3.3728×10⁻⁵sec.⁻¹
r²= 0.98150
Time, minutes
Moles of HOCl consumed per mole
of DO102 destroyed at a pH of 7
Slope= 9.7921 moles/mole
r²= 0.99572
[HOCl], μM.
[DO102], μM.

Figure A1.9

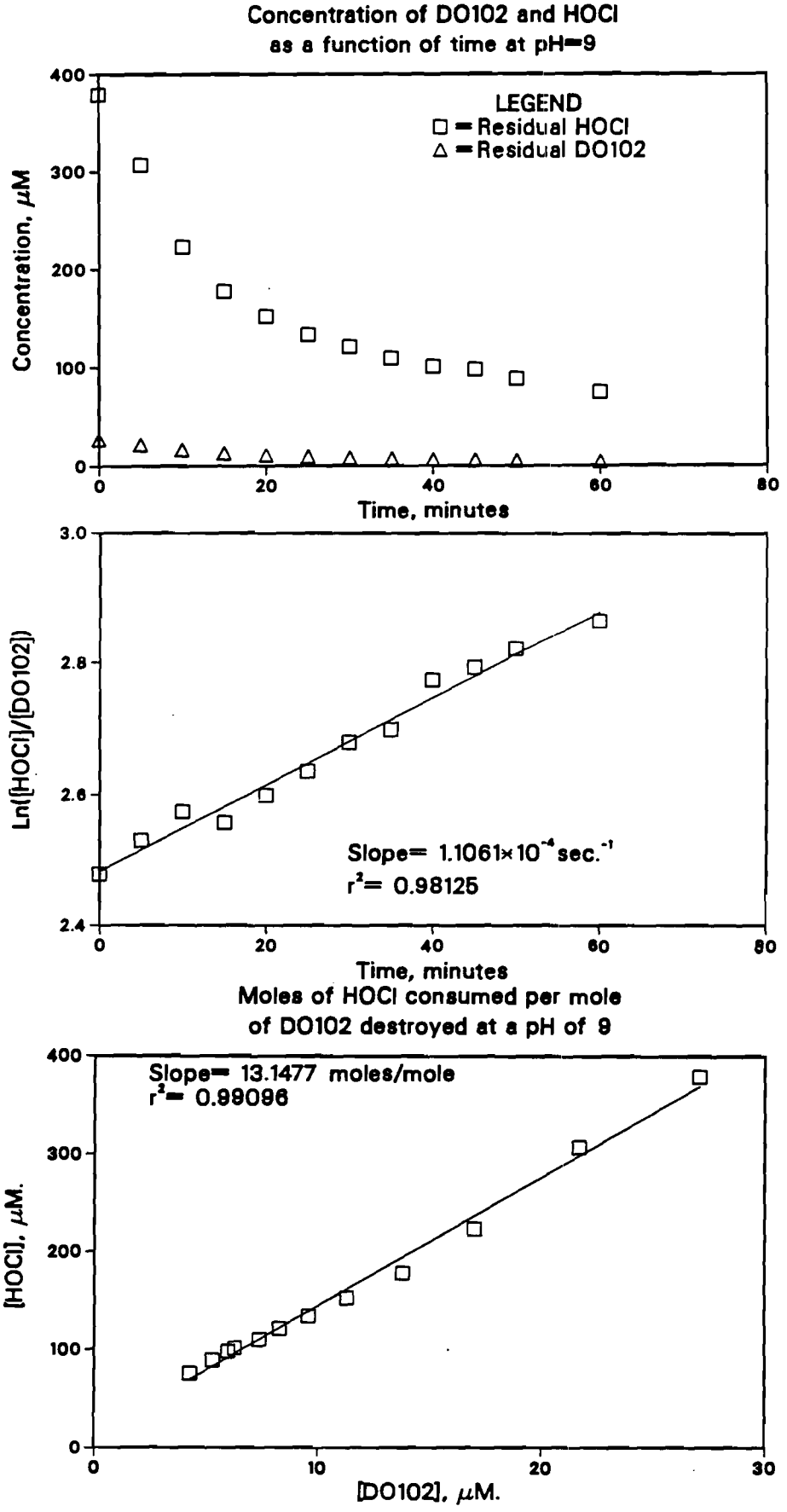
Concentration of DO102 and HOCl
as a function of time at pH=9
LEGEND
□ = Residual HOCl
△ = Residual DO102
Concentration, μM
Time, minutes
Ln([HOCl]/[DO102])
Slope= 1.1061×10⁻⁴ sec.⁻¹
r²= 0.98125
Time, minutes
Moles of HOCl consumed per mole
of DO102 destroyed at a pH of 9
Slope= 13.1477 moles/mole
r²= 0.99096
[HOCl], μM.
[DO102], μM.

Figure A1.10

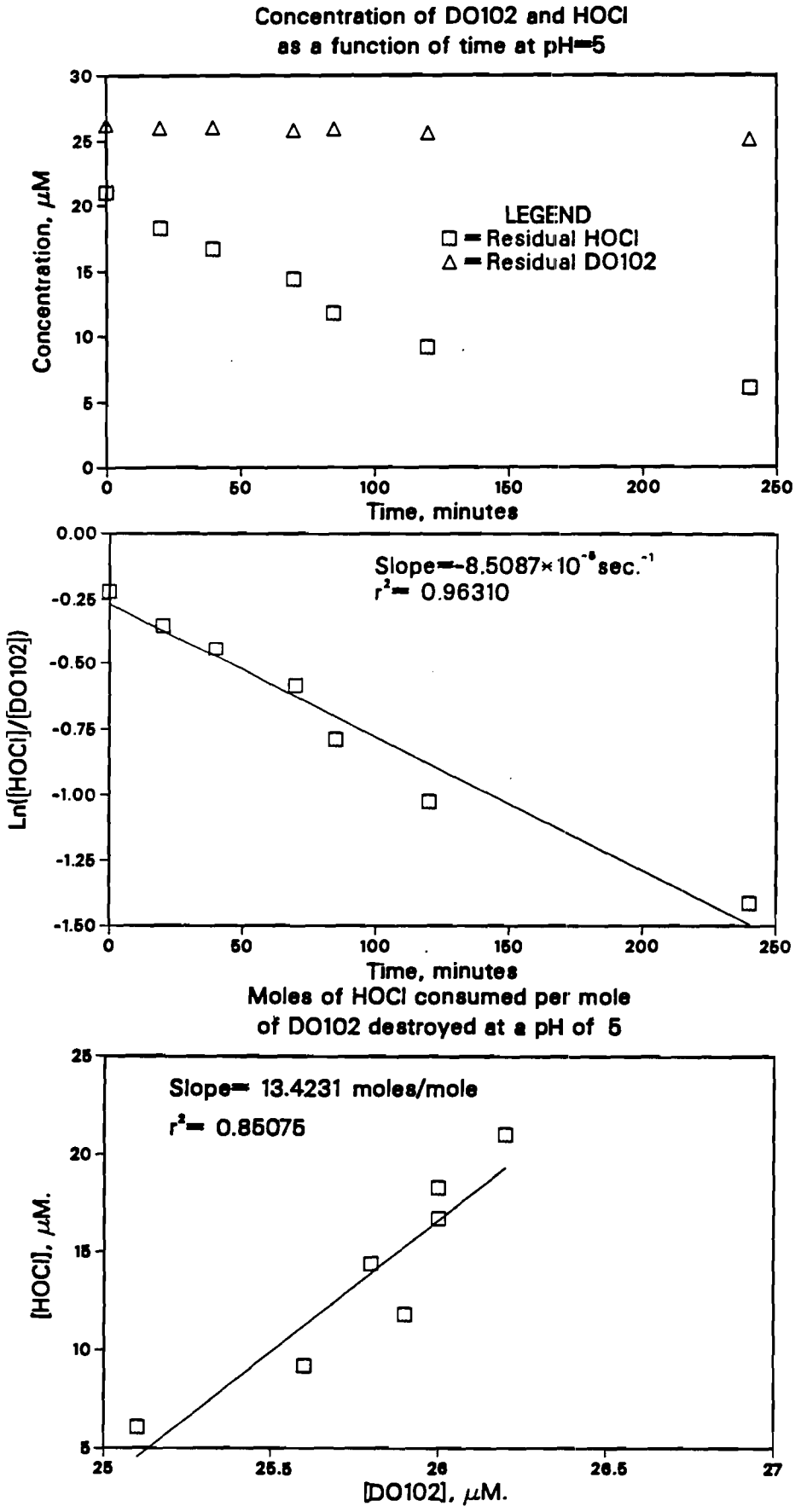
Concentration of DO102 and HOCl
as a function of time at pH=5
Concentration, μM
Time, minutes
LEGEND
□ = Residual HOCl
△ = Residual DO102
Ln([HOCl]/[DO102])
Slope=-8.5087×10⁻⁵sec.⁻¹
r²= 0.96310
Time, minutes
Moles of HOCl consumed per mole
of DO102 destroyed at a pH of 5
Slope= 13.4231 moles/mole
r²= 0.85075
[HOCl], μM.
[DO102], μM.

Figure A1.11

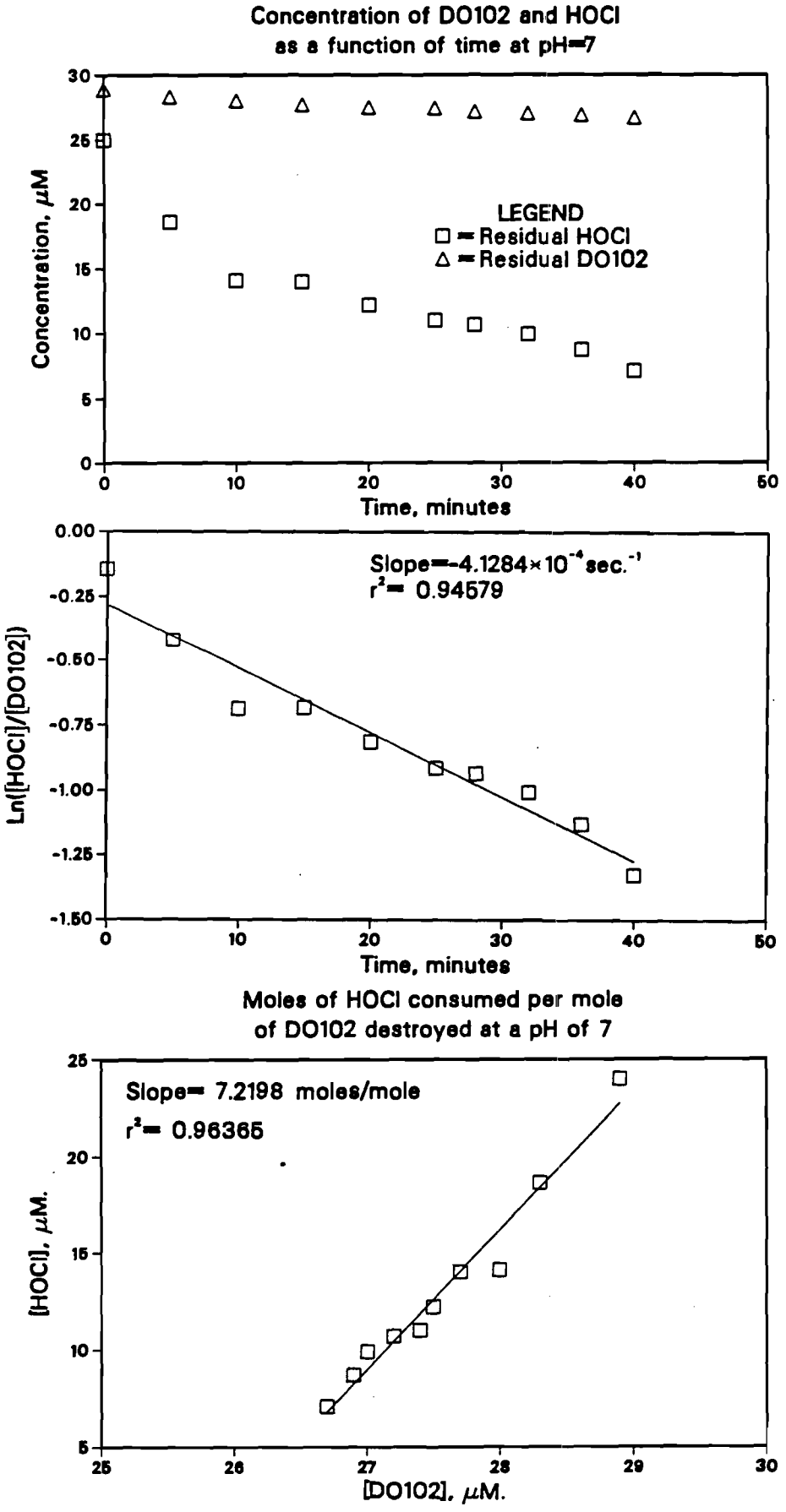
Concentration of DO102 and HOCl
as a function of time at pH=7
Concentration, μM
Time, minutes
LEGEND
□ = Residual HOCl
△ = Residual DO102
Ln([HOCl]/[DO102])
Slope=-4.1284×10⁻⁴ sec.⁻¹
r²= 0.94579
Time, minutes
Moles of HOCl consumed per mole
of DO102 destroyed at a pH of 7
Slope= 7.2198 moles/mole
r²= 0.96365
[HOCl], μM.
[DO102], μM.

Figure A1.12

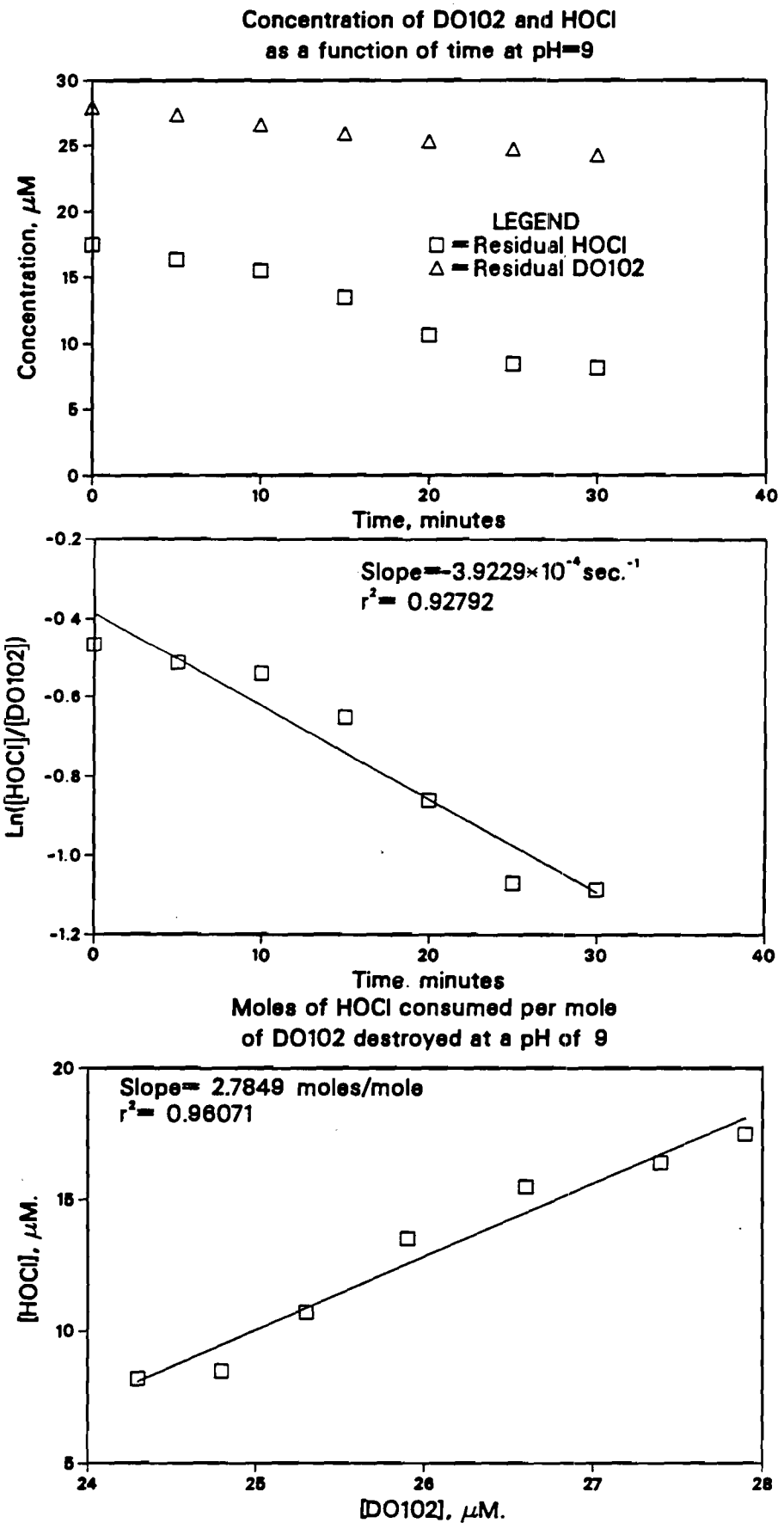
Concentration of DO102 and HOCl
as a function of time at pH=9
Concentration, μM
Time, minutes
LEGEND
□ = Residual HOCl
△ = Residual DO102
Ln([HOCl]/[DO102])
Slope=-3.9229×10⁻⁴sec.⁻¹
r²= 0.92792
Time. minutes
Moles of HOCl consumed per mole
of DO102 destroyed at a pH of 9
Slope= 2.7849 moles/mole
r²= 0.96071
[HOCl], μM.
[DO102], μM.

Figure A1.13

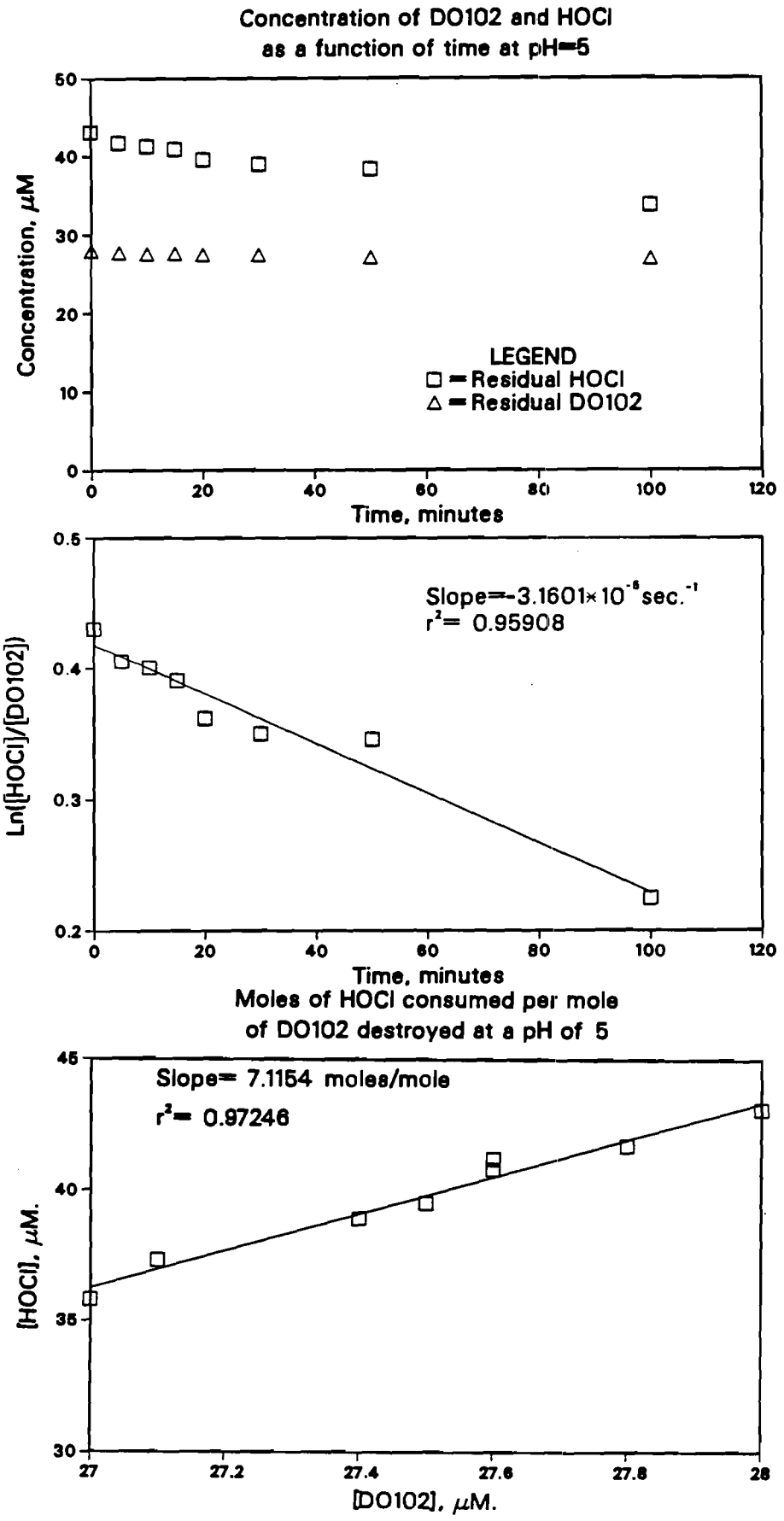
Concentration of DO102 and HOCl
as a function of time at pH=5
Concentration, μM
Time, minutes
LEGEND
□ = Residual HOCl
△ = Residual DO102
Ln([HOCl]/[DO102])
Slope=-3.1601×10⁻⁵sec.⁻¹
r²= 0.95908
Time, minutes
Moles of HOCl consumed per mole
of DO102 destroyed at a pH of 5
Slope= 7.1154 moles/mole
r²= 0.97246
[HOCl], μM.
[DO102], μM.

Figure A1.14

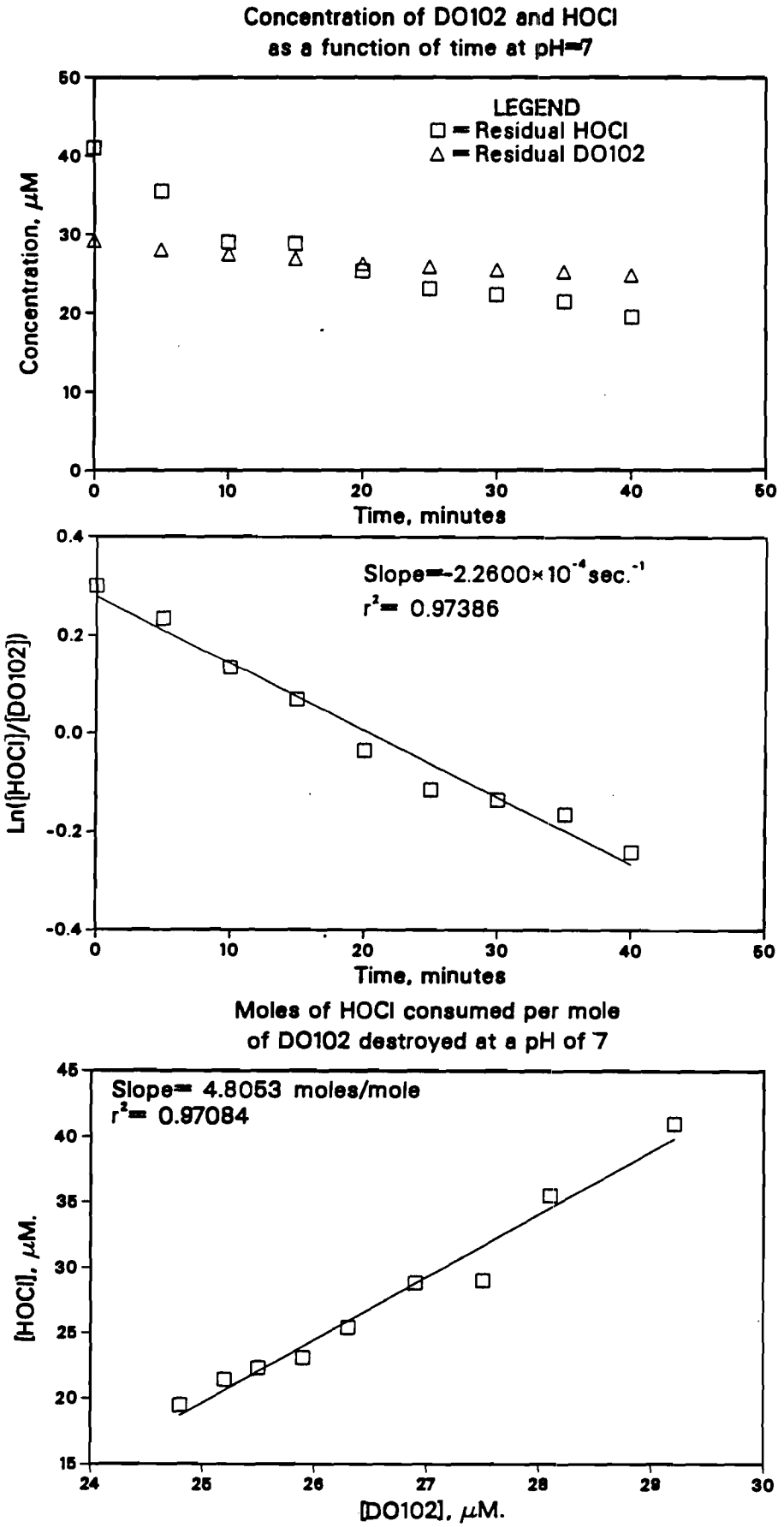
Concentration of DO102 and HOCl
as a function of time at pH=7
LEGEND
□ = Residual HOCl
△ = Residual DO102
Concentration, μM
Time, minutes
Slope=-2.2600×10⁻⁴sec.⁻¹
r²= 0.97386
Ln([HOCl]/[DO102])
Time, minutes
Moles of HOCl consumed per mole
of DO102 destroyed at a pH of 7
Slope= 4.8053 moles/mole
r²= 0.97084
[HOCl], μM.
[DO102], μM.

Figure A1.15

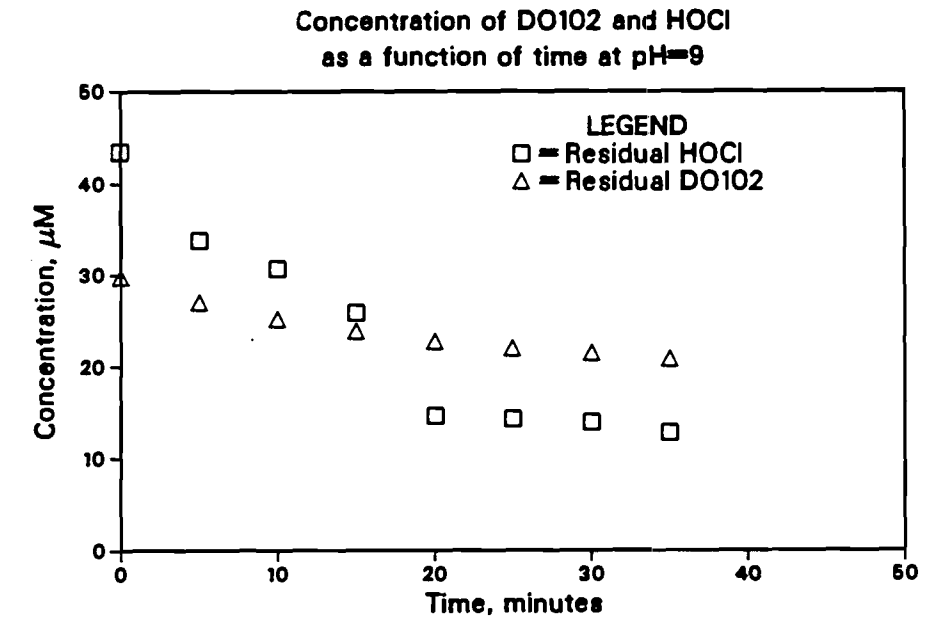
Concentration of DO102 and HOCl
as a function of time at pH=9
LEGEND
□ = Residual HOCl
△ = Residual DO102
Concentration, μM
Time, minutes

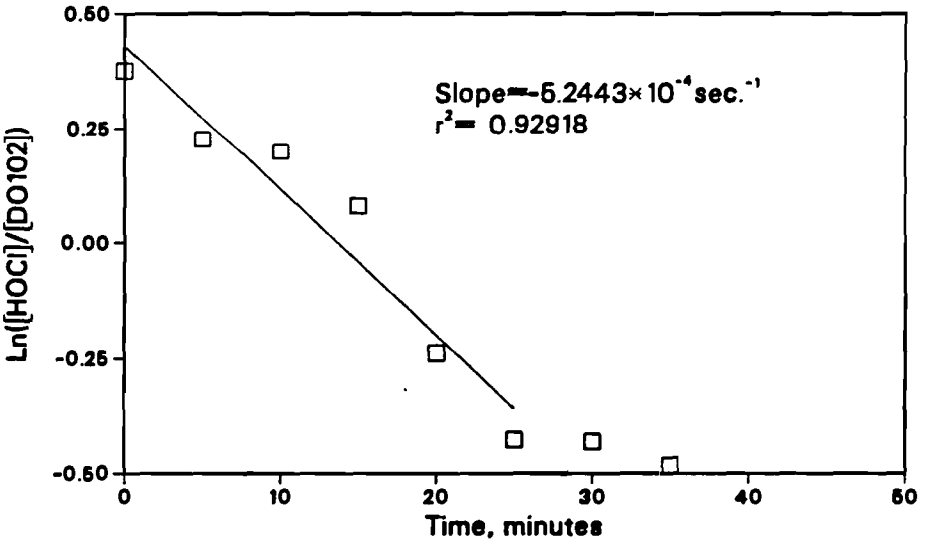
Slope=-5.2443×10⁻⁴ sec.⁻¹
r² = 0.92918
Ln([HOCl]/[DO102])
Time, minutes

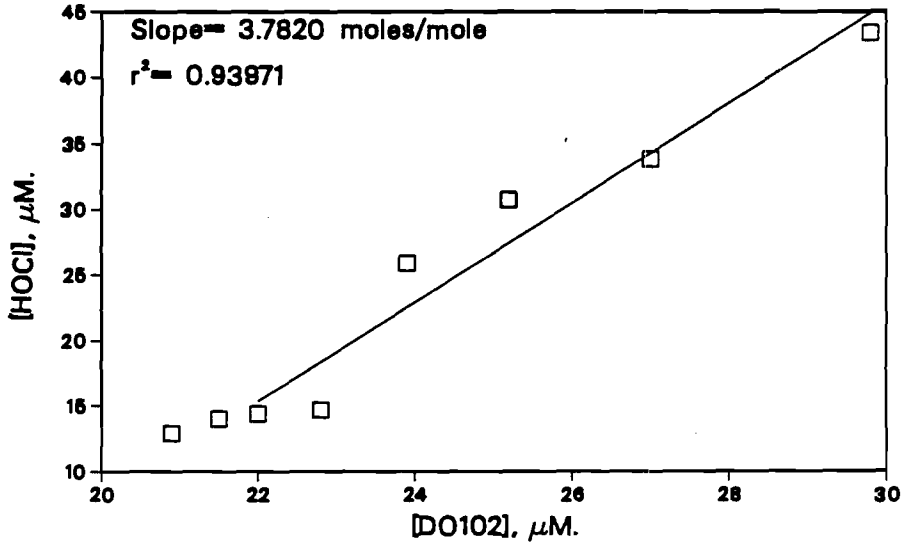
Moles of HOCl consumed per mole
of DO102 destroyed at a pH of 9
Slope= 3.7820 moles/mole
r² = 0.93971
[HOCl], μM.
[DO102], μM.

Figure A1.16

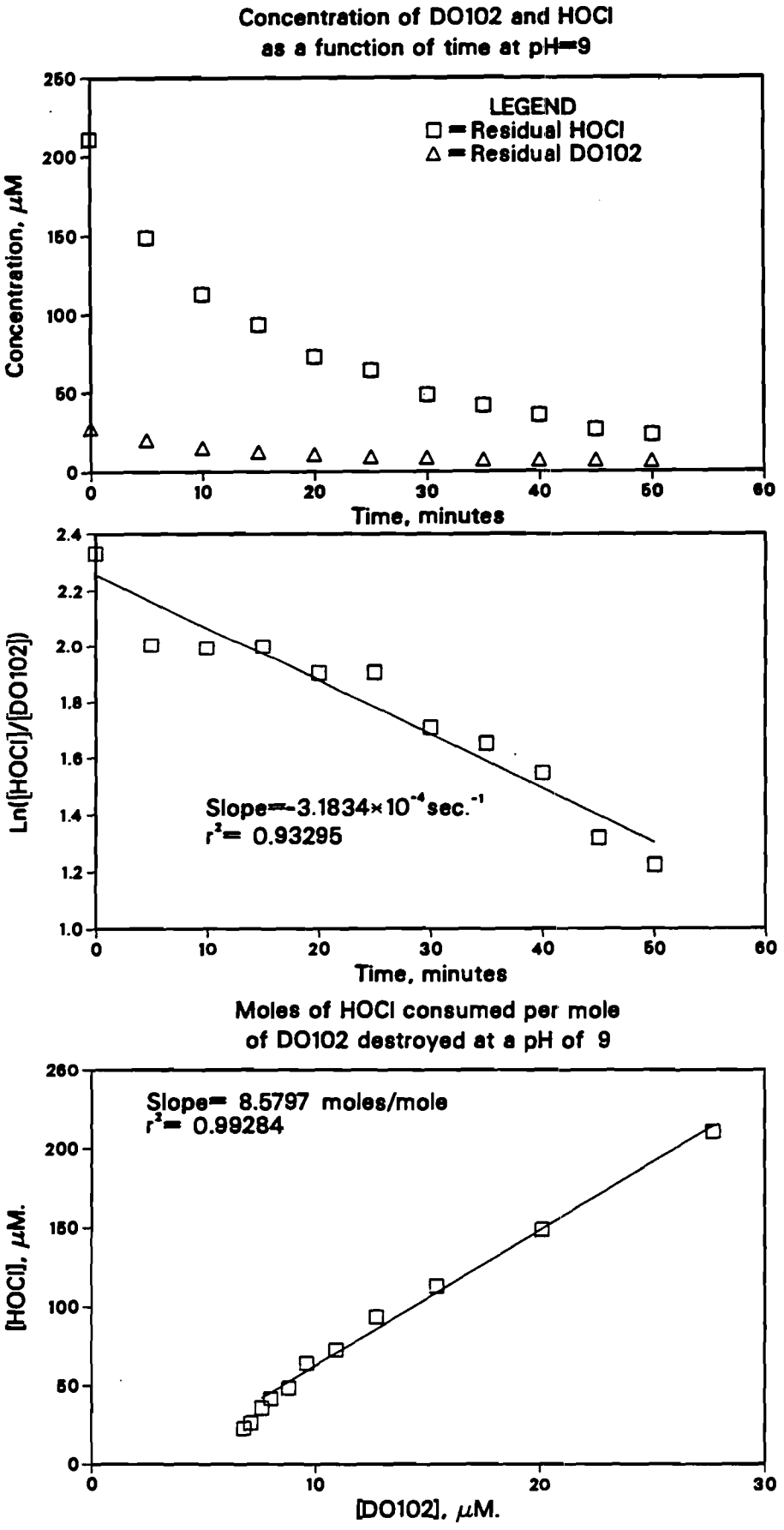
Concentration of DO102 and HOCl
as a function of time at pH=9
LEGEND
□ = Residual HOCl
△ = Residual DO102
Concentration, μM
Time, minutes
Ln([HOCl]/[DO102])
Slope=-3.1834×10⁻⁴sec.⁻¹
r²= 0.93295
Time, minutes
Moles of HOCl consumed per mole
of DO102 destroyed at a pH of 9
Slope= 8.5797 moles/mole
r²= 0.99284
[HOCl], μM.
[DO102], μM.

Figure A1.17

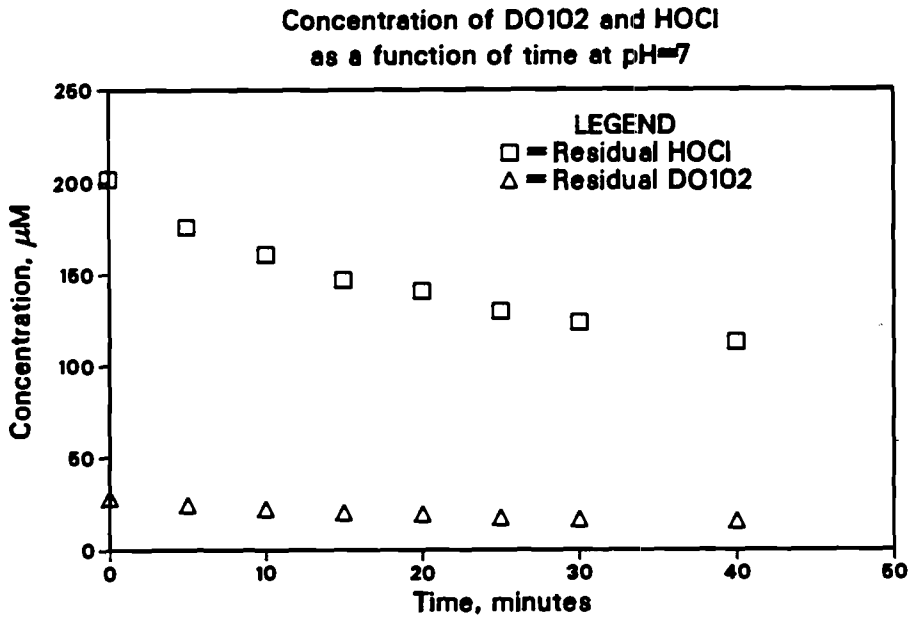
Concentration of DO102 and HOCl
as a function of time at pH=7
LEGEND
□ = Residual HOCl
△ = Residual DO102
Concentration, μM
Time, minutes

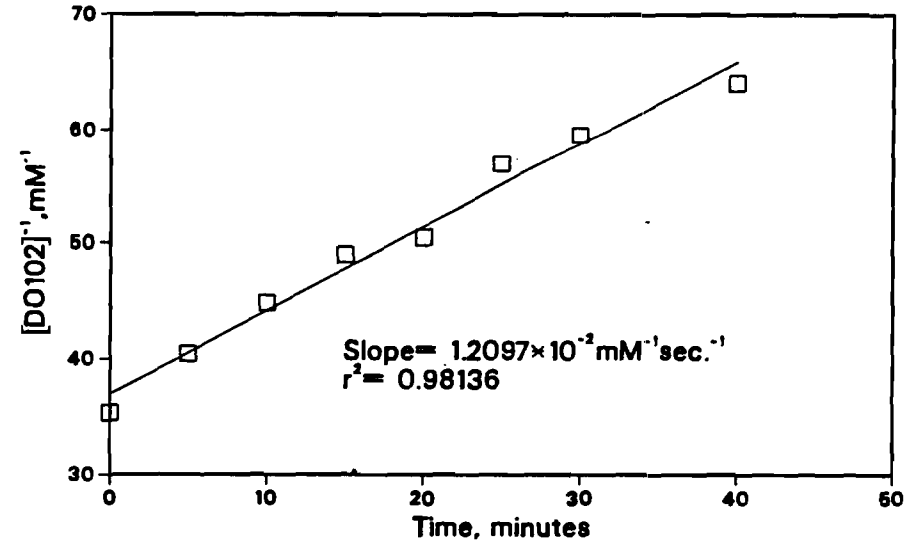
[DO102]⁻¹, mM⁻¹
Slope= 1.2097×10⁻²mM⁻¹sec.⁻¹
r²= 0.98136
Time, minutes

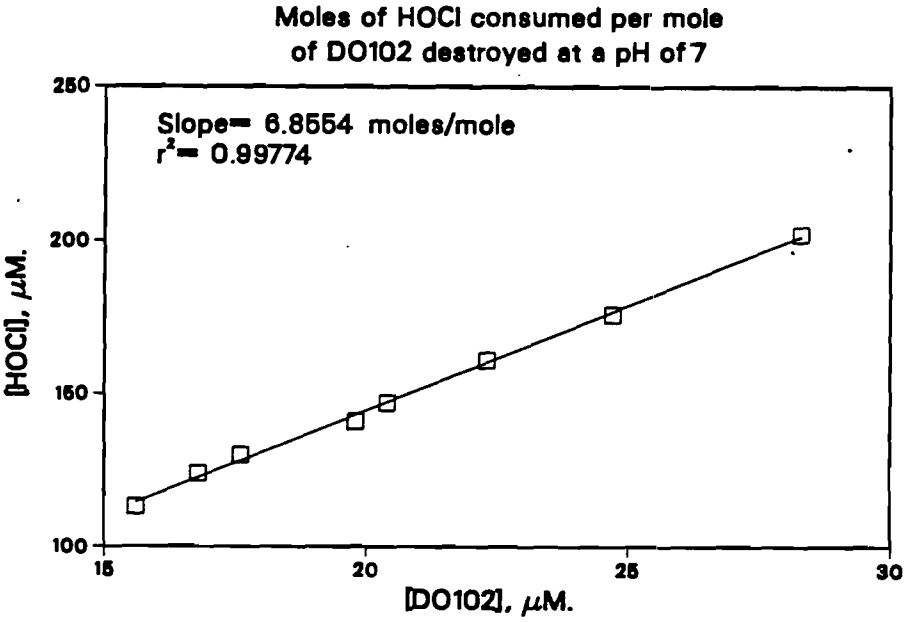
Moles of HOCl consumed per mole
of DO102 destroyed at a pH of 7
Slope= 6.8554 moles/mole
r²= 0.99774
[HOCl], μM.
[DO102], μM.

Figure A1.18

APPENDIX 2

DATA PLOTS FOR DIRECT RED 24

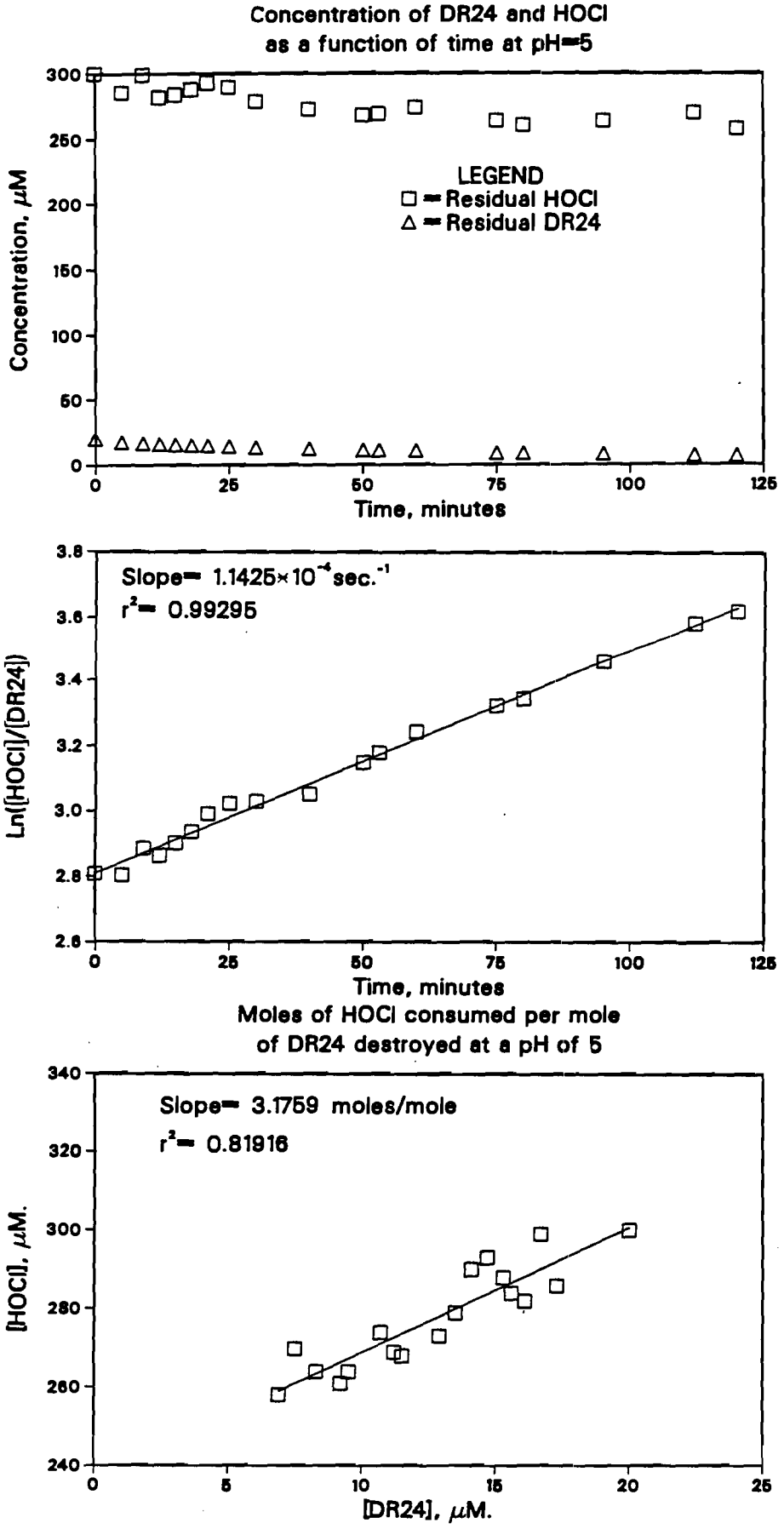
Concentration of DR24 and HOCl
as a function of time at pH=5
Concentration, μM
300
250
200
150
100
50
0
LEGEND
□ = Residual HOCl
△ = Residual DR24
0
25
50
75
100
125
Time, minutes
Ln([HOCl]/[DR24])
3.8
3.6
3.4
3.2
3.0
2.8
2.6
Slope= 1.1425×10⁻⁴sec.⁻¹
r²= 0.99295
0
25
50
75
100
125
Time, minutes
Moles of HOCl consumed per mole
of DR24 destroyed at a pH of 5
[HOCl], μM.
340
320
300
280
260
240
Slope= 3.1759 moles/mole
r²= 0.81916
0
5
10
15
20
25
[DR24], μM.

Figure A2.1

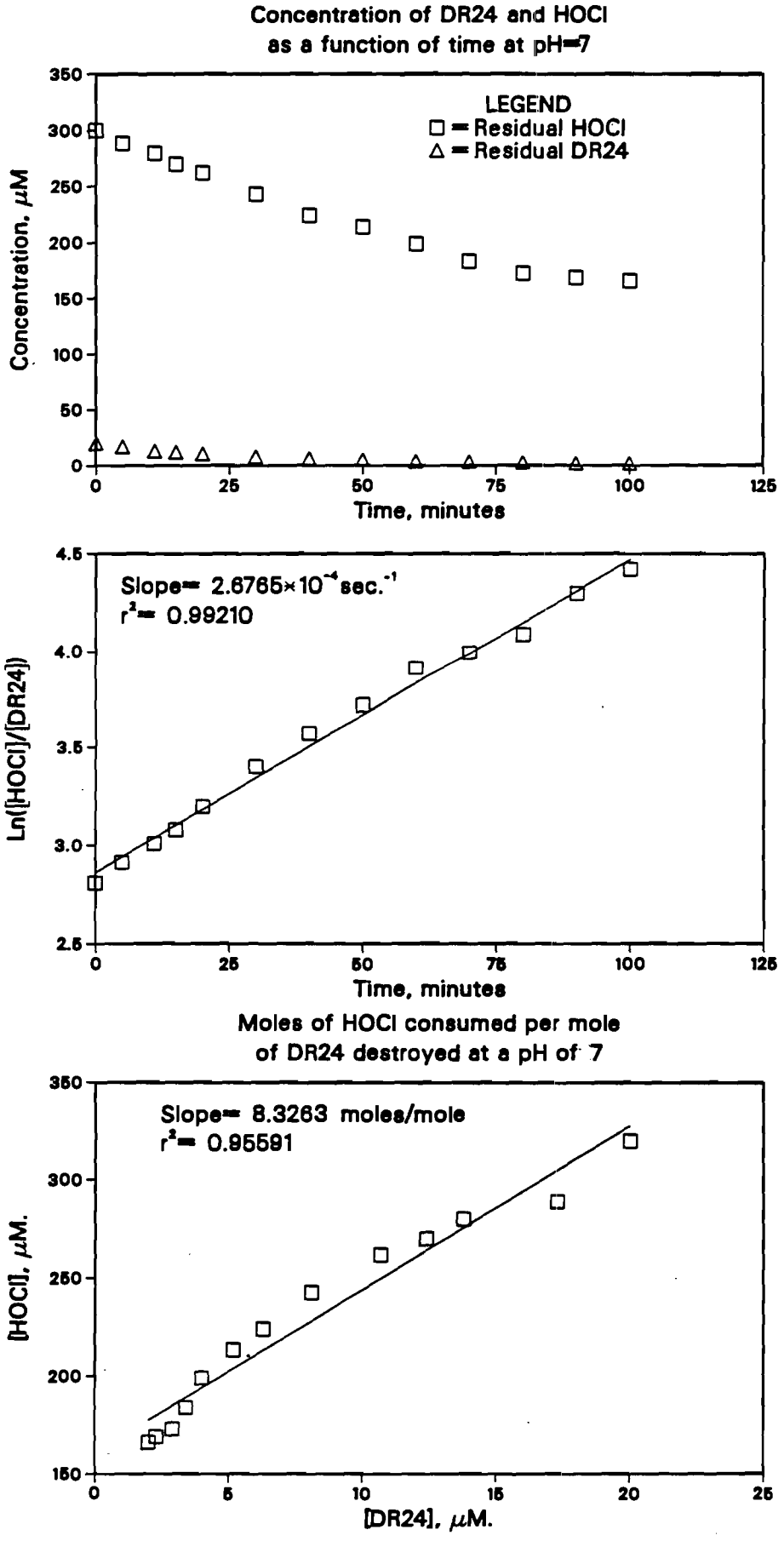
Concentration of DR24 and HOCl
as a function of time at pH=7
LEGEND
□ = Residual HOCl
△ = Residual DR24
Concentration, μM
Time, minutes
Slope= 2.6765×10⁻⁴ sec.⁻¹
r²= 0.99210
Ln([HOCl]/[DR24])
Time, minutes
Moles of HOCl consumed per mole
of DR24 destroyed at a pH of 7
Slope= 8.3263 moles/mole
r²= 0.95591
[HOCl], μM.
[DR24], μM.

Figure A2.2

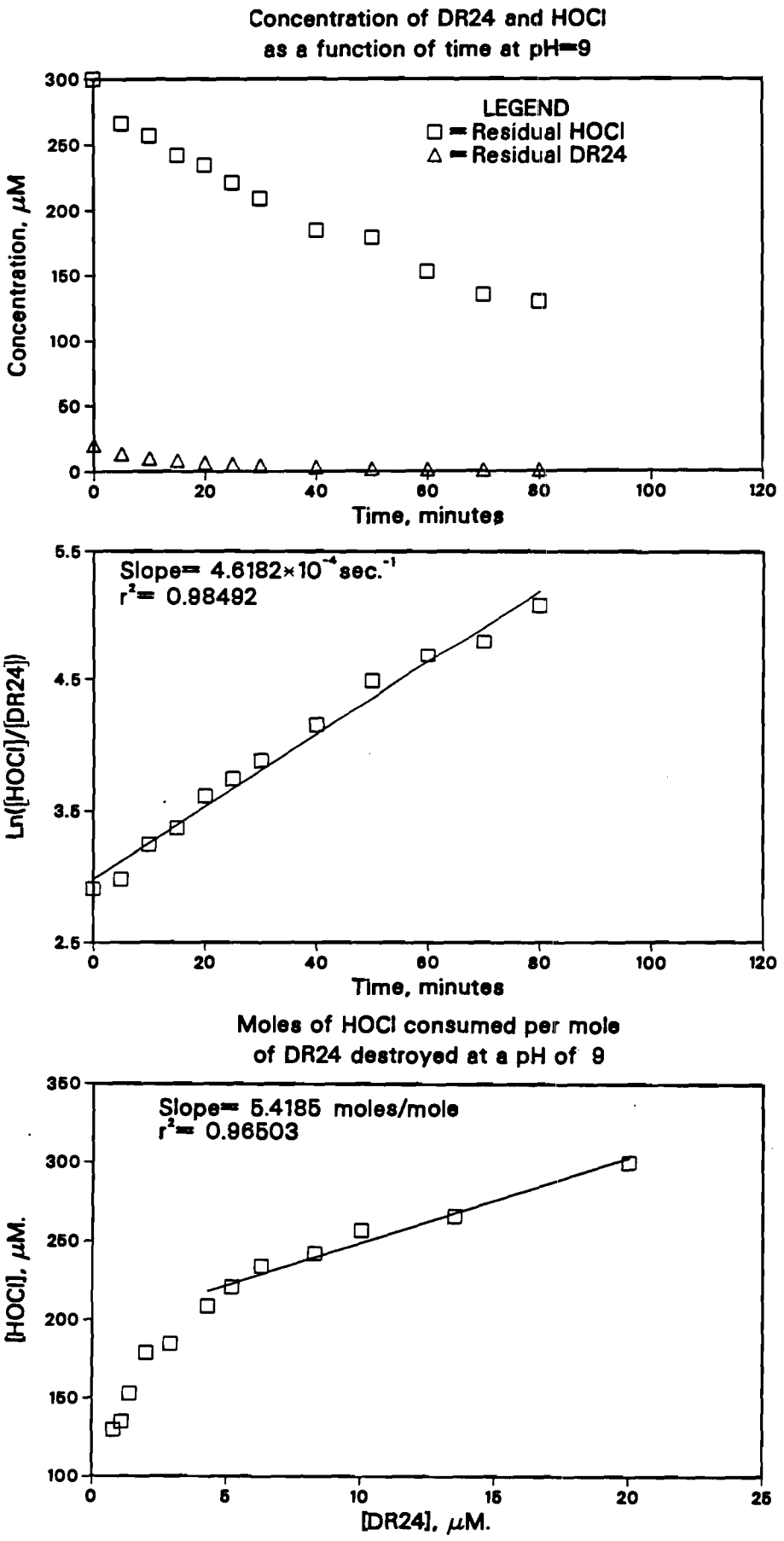
Concentration of DR24 and HOCl
as a function of time at pH=9
LEGEND
□ = Residual HOCl
△ = Residual DR24
Concentration, μM
Time, minutes
Slope= 4.6182×10⁻⁴ sec.⁻¹
r²= 0.98492
Ln([HOCl]/[DR24])
Time, minutes
Moles of HOCl consumed per mole
of DR24 destroyed at a pH of 9
Slope= 5.4185 moles/mole
r²= 0.96503
[HOCl], μM.
[DR24], μM.

Figure A2.3

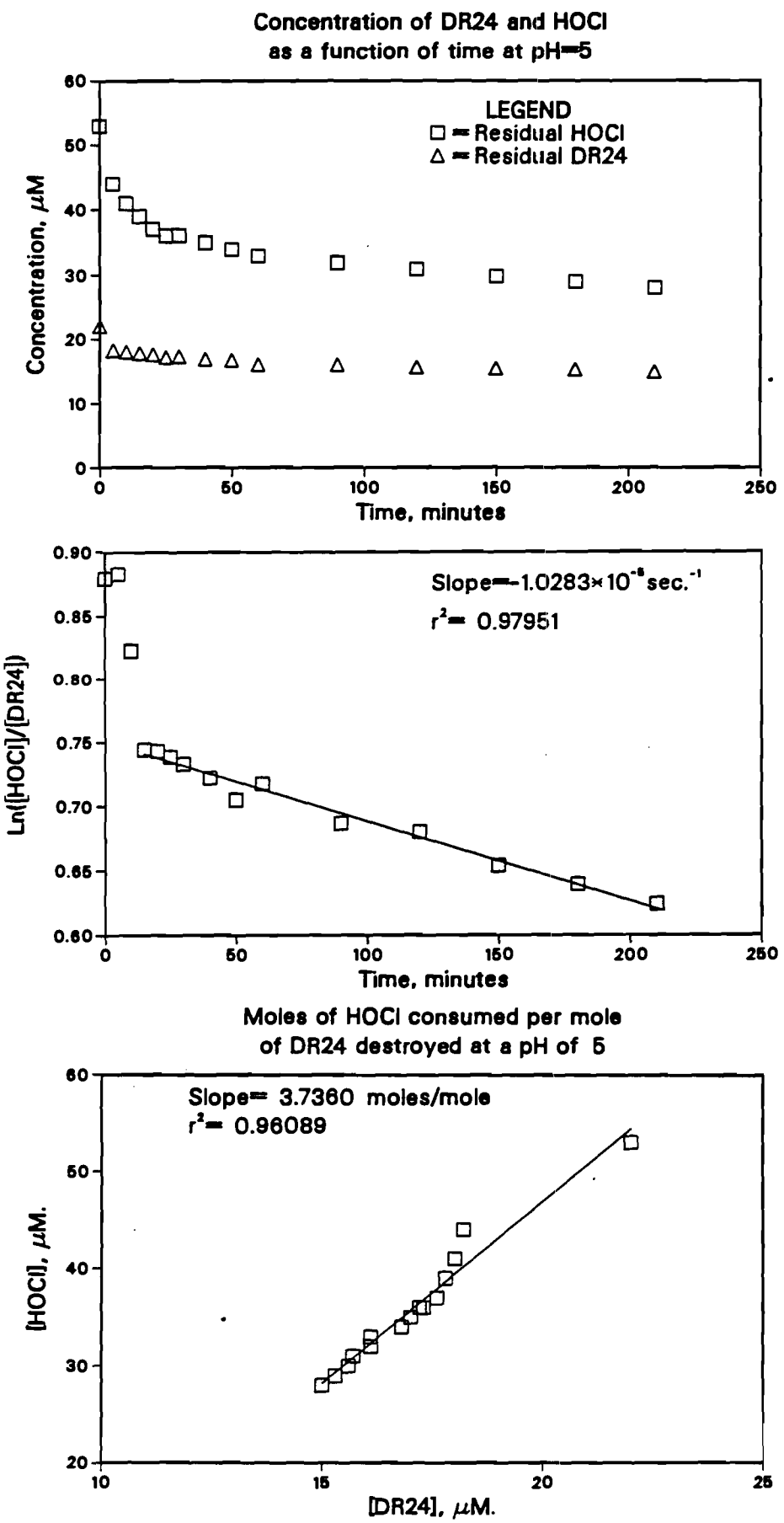
Concentration of DR24 and HOCl
as a function of time at pH=5
LEGEND
□ = Residual HOCl
△ = Residual DR24
Concentration, μM
Time, minutes
Slope=-1.0283×10⁻⁶sec.⁻¹
r²= 0.97951
Ln([HOCl]/[DR24])
Time, minutes
Moles of HOCl consumed per mole
of DR24 destroyed at a pH of 5
Slope= 3.7360 moles/mole
r²= 0.96089
[HOCl], μM.
[DR24], μM.

Figure A2.4

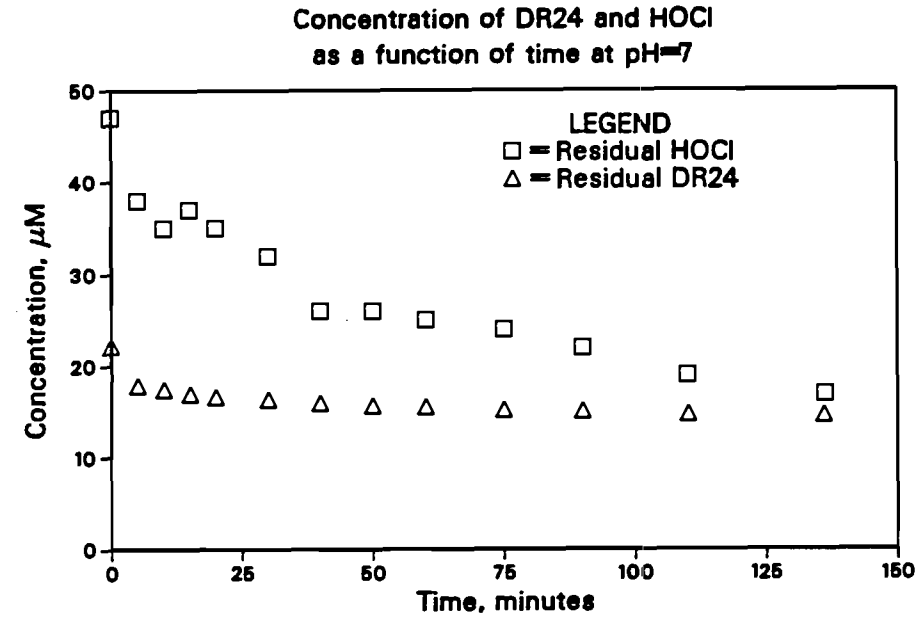
Concentration of DR24 and HOCl
as a function of time at pH=7
LEGEND
□ = Residual HOCl
△ = Residual DR24
Concentration, μM
Time, minutes

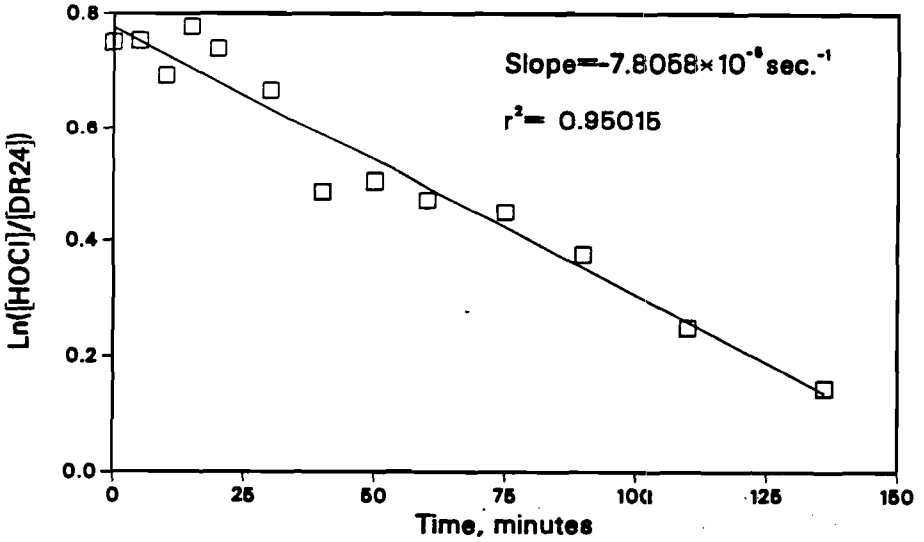
Slope=-7.8058×10⁻⁵ sec.⁻¹
r²= 0.95015
Ln([HOCl]/[DR24])
Time, minutes

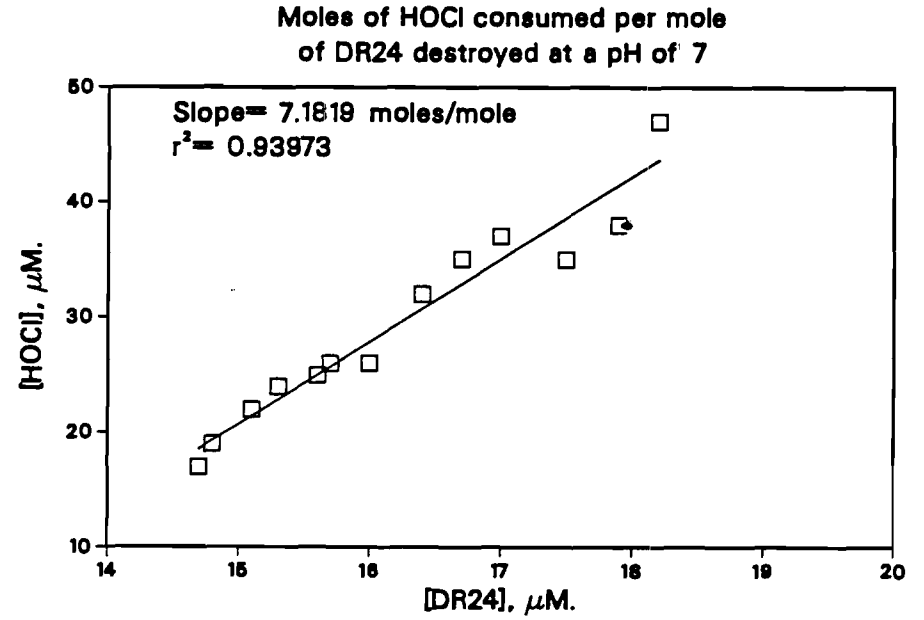
Moles of HOCl consumed per mole
of DR24 destroyed at a pH of 7
Slope= 7.1819 moles/mole
r²= 0.93973
[HOCl], μM.
[DR24], μM.

Figure A2.5

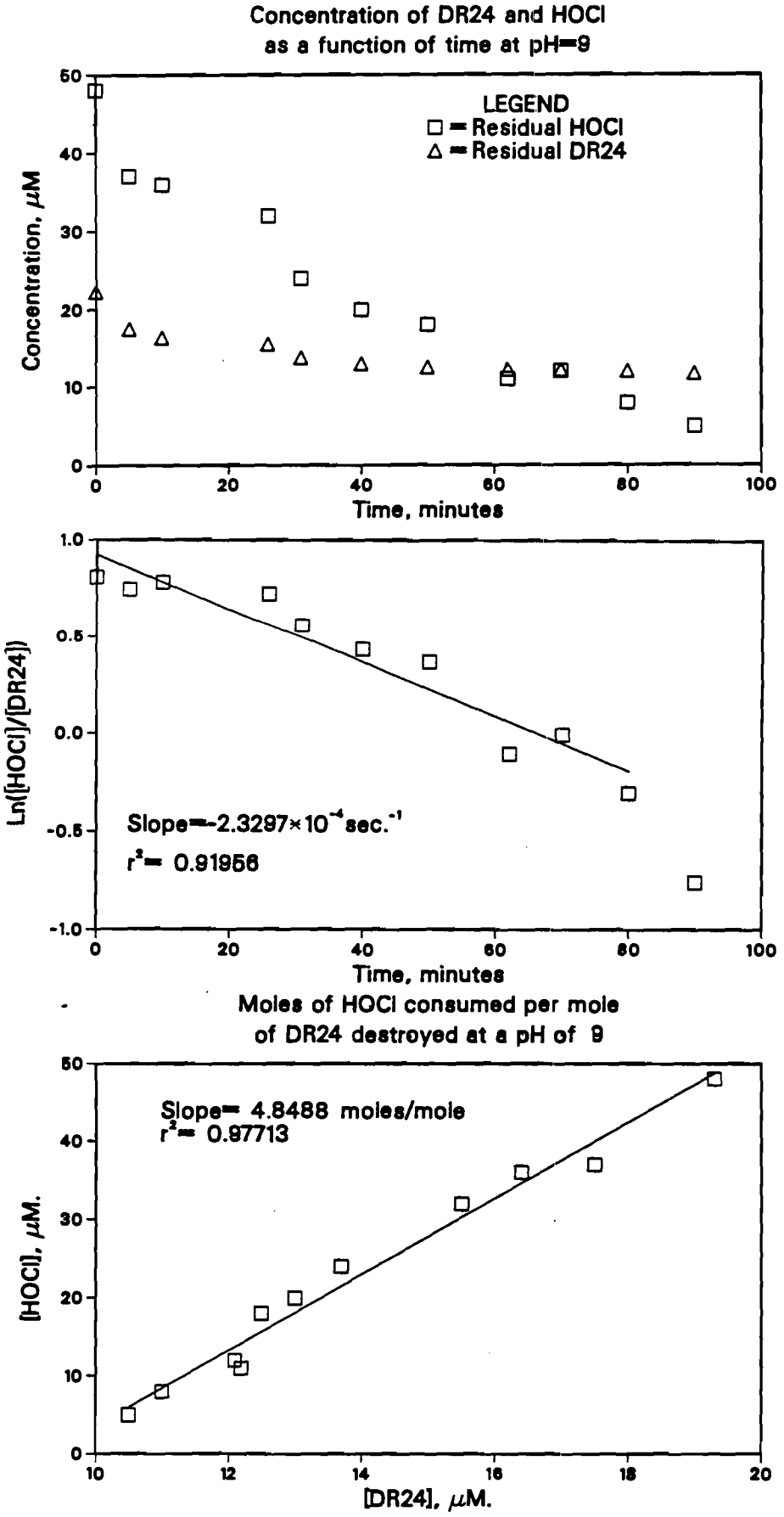
Concentration of DR24 and HOCl
as a function of time at pH=9
LEGEND
□ = Residual HOCl
△ = Residual DR24
Concentration, μM
Time, minutes
Ln([HOCl]/[DR24])
Slope=-2.3297×10⁻⁴sec.⁻¹
r²= 0.91956
Time, minutes
Moles of HOCl consumed per mole
of DR24 destroyed at a pH of 9
Slope= 4.8488 moles/mole
r²= 0.97713
[HOCl], μM.
[DR24], μM.

Figure A2.6

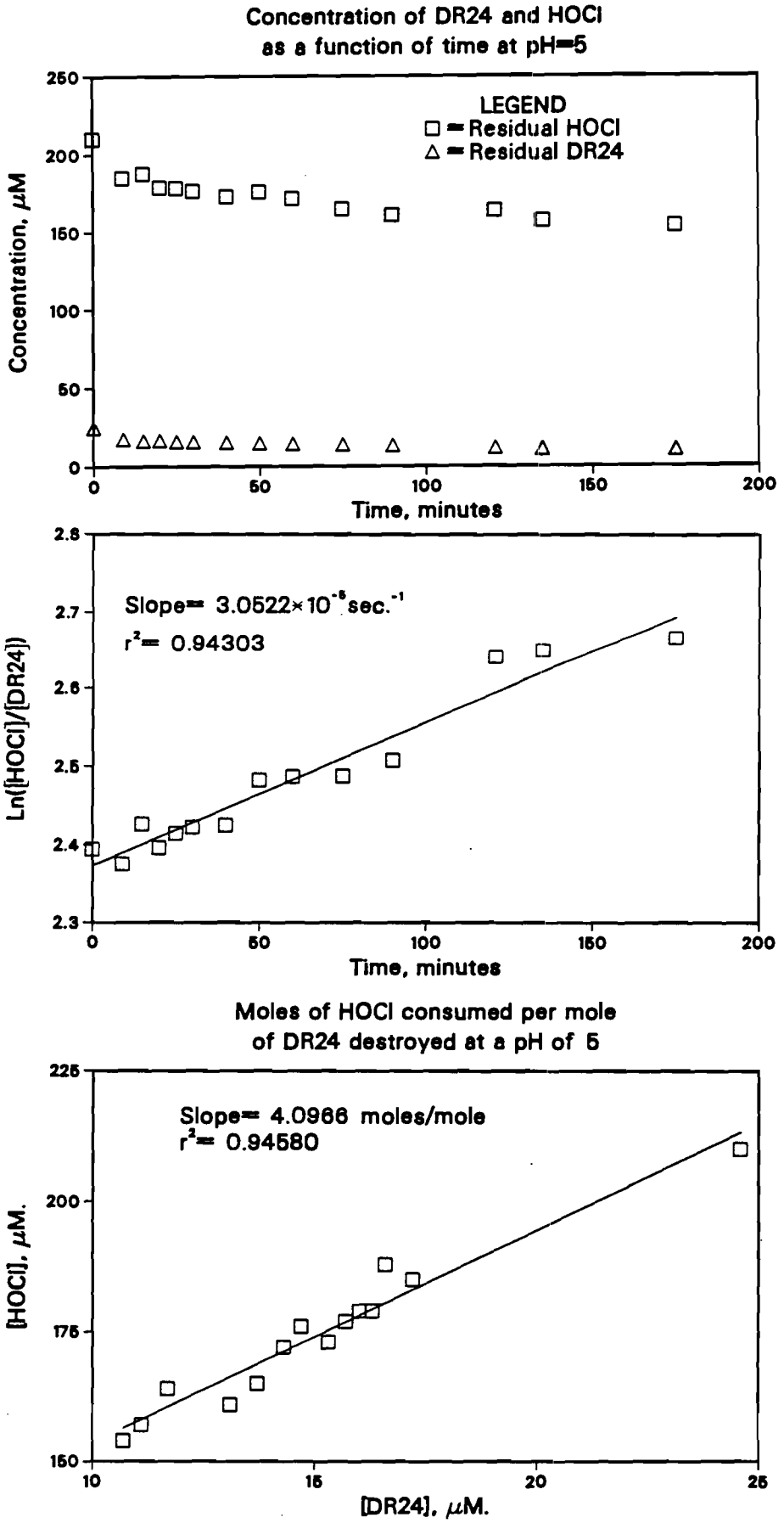
Concentration of DR24 and HOCl
as a function of time at pH=5
LEGEND
□ = Residual HOCl
△ = Residual DR24
Concentration, μM
Time, minutes
Slope= 3.0522×10⁻⁵ sec.⁻¹
r²= 0.94303
Ln([HOCl]/[DR24])
Time, minutes
Moles of HOCl consumed per mole
of DR24 destroyed at a pH of 5
Slope= 4.0966 moles/mole
r²= 0.94580
[HOCl], μM.
[DR24], μM.

Figure A2.7

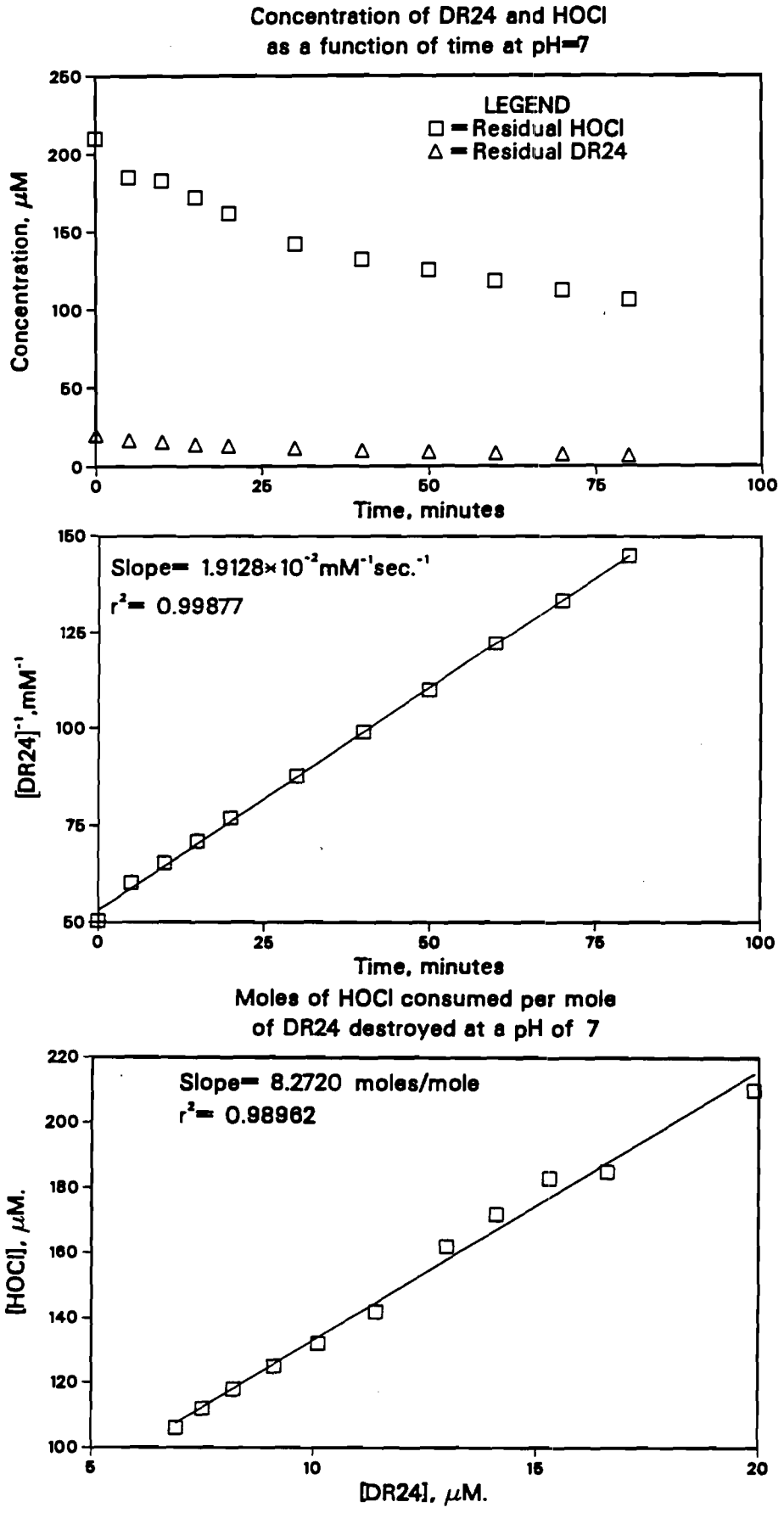
Concentration of DR24 and HOCl
as a function of time at pH=7
LEGEND
□ = Residual HOCl
△ = Residual DR24
Concentration, μM
Time, minutes
Slope= 1.9128×10⁻²mM⁻¹sec.⁻¹
r²= 0.99877
[DR24]⁻¹,mM⁻¹
Time, minutes
Moles of HOCl consumed per mole
of DR24 destroyed at a pH of 7
Slope= 8.2720 moles/mole
r²= 0.98962
[HOCl], μM.
[DR24], μM.

Figure A2.8

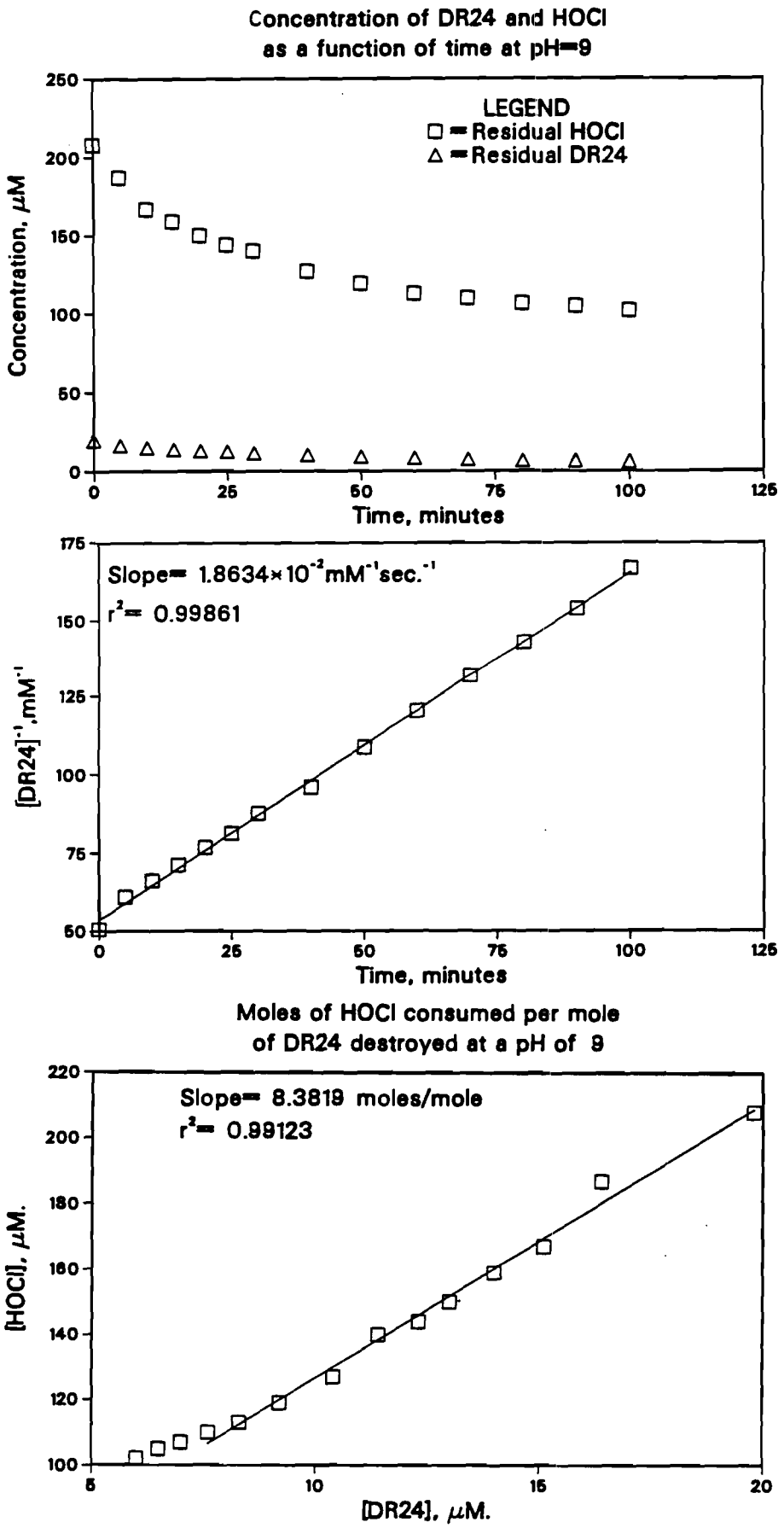
Concentration of DR24 and HOCl
as a function of time at pH=9
LEGEND
□ = Residual HOCl
△ = Residual DR24
Concentration, μM
Time, minutes
Slope= 1.8634×10⁻²mM⁻¹sec.⁻¹
r²= 0.99861
[DR24]⁻¹,mM⁻¹
Time, minutes
Moles of HOCl consumed per mole
of DR24 destroyed at a pH of 9
Slope= 8.3819 moles/mole
r²= 0.99123
[HOCl], μM.
[DR24], μM.

Figure A2.9

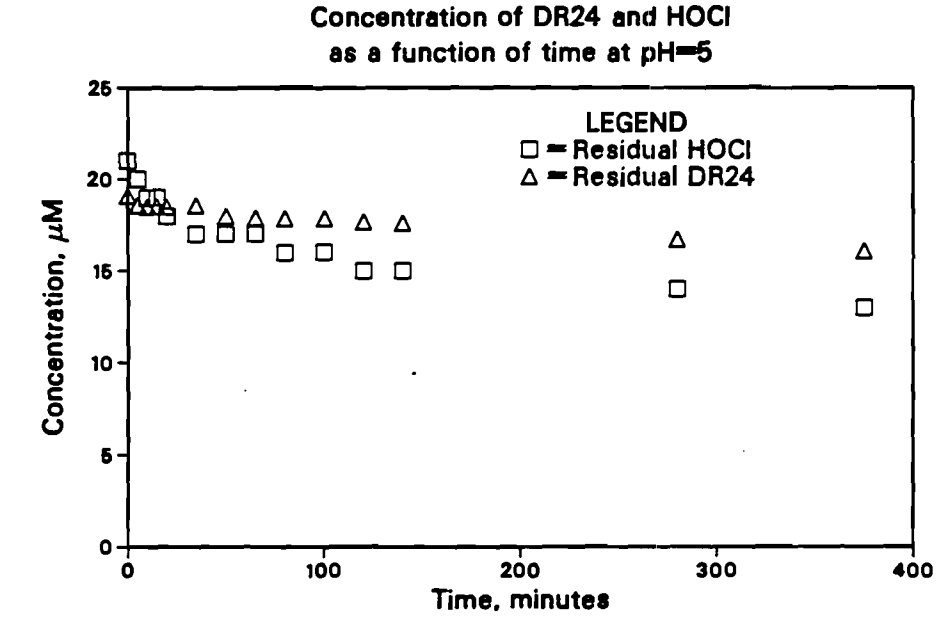
Concentration of DR24 and HOCl
as a function of time at pH=5
LEGEND
□ = Residual HOCl
△ = Residual DR24
Concentration, μM
Time, minutes

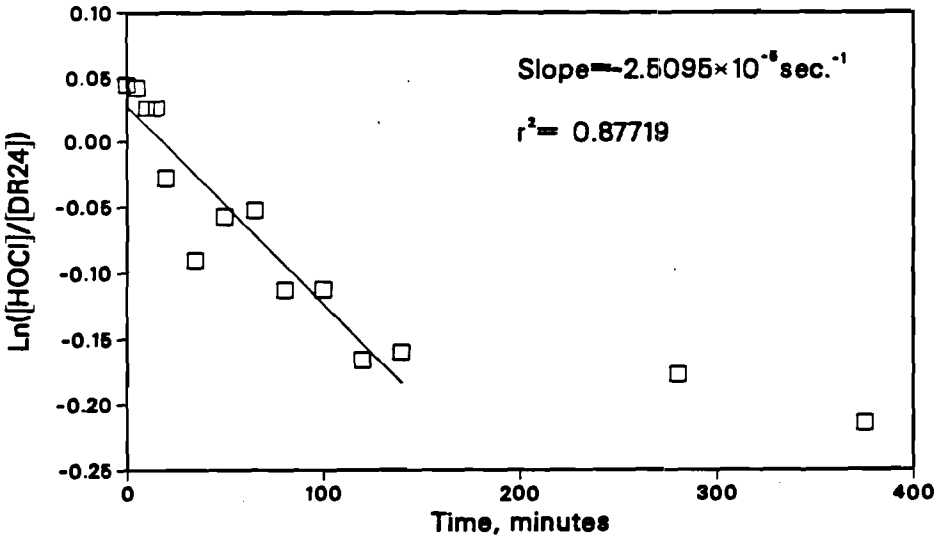
Slope=-2.5095×10⁻⁵sec.⁻¹
r²= 0.87719
Ln([HOCl]/[DR24])
Time, minutes

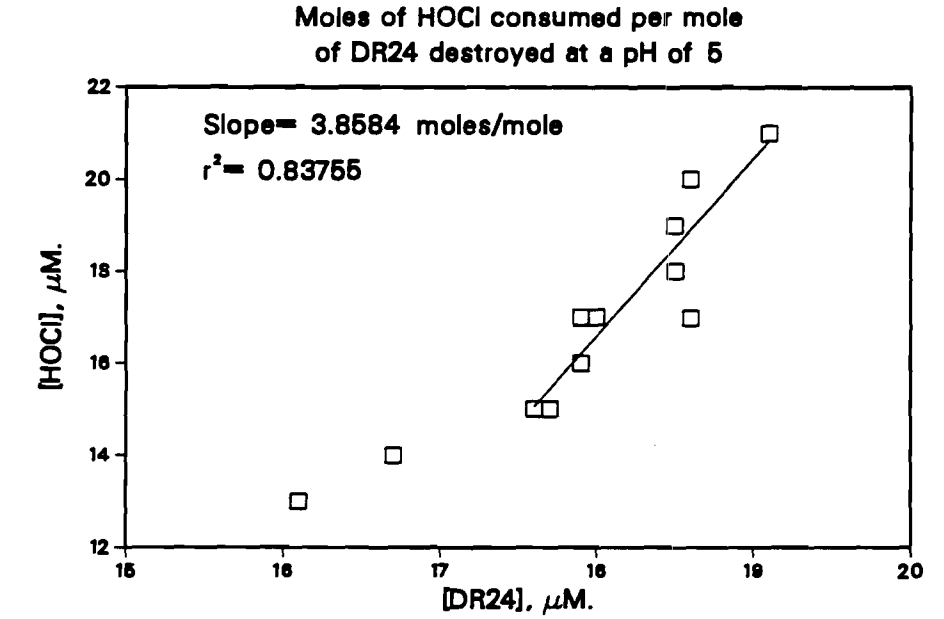
Moles of HOCl consumed per mole
of DR24 destroyed at a pH of 5
Slope= 3.8584 moles/mole
r²= 0.83755
[HOCl], μM.
[DR24], μM.

Figure A2.10

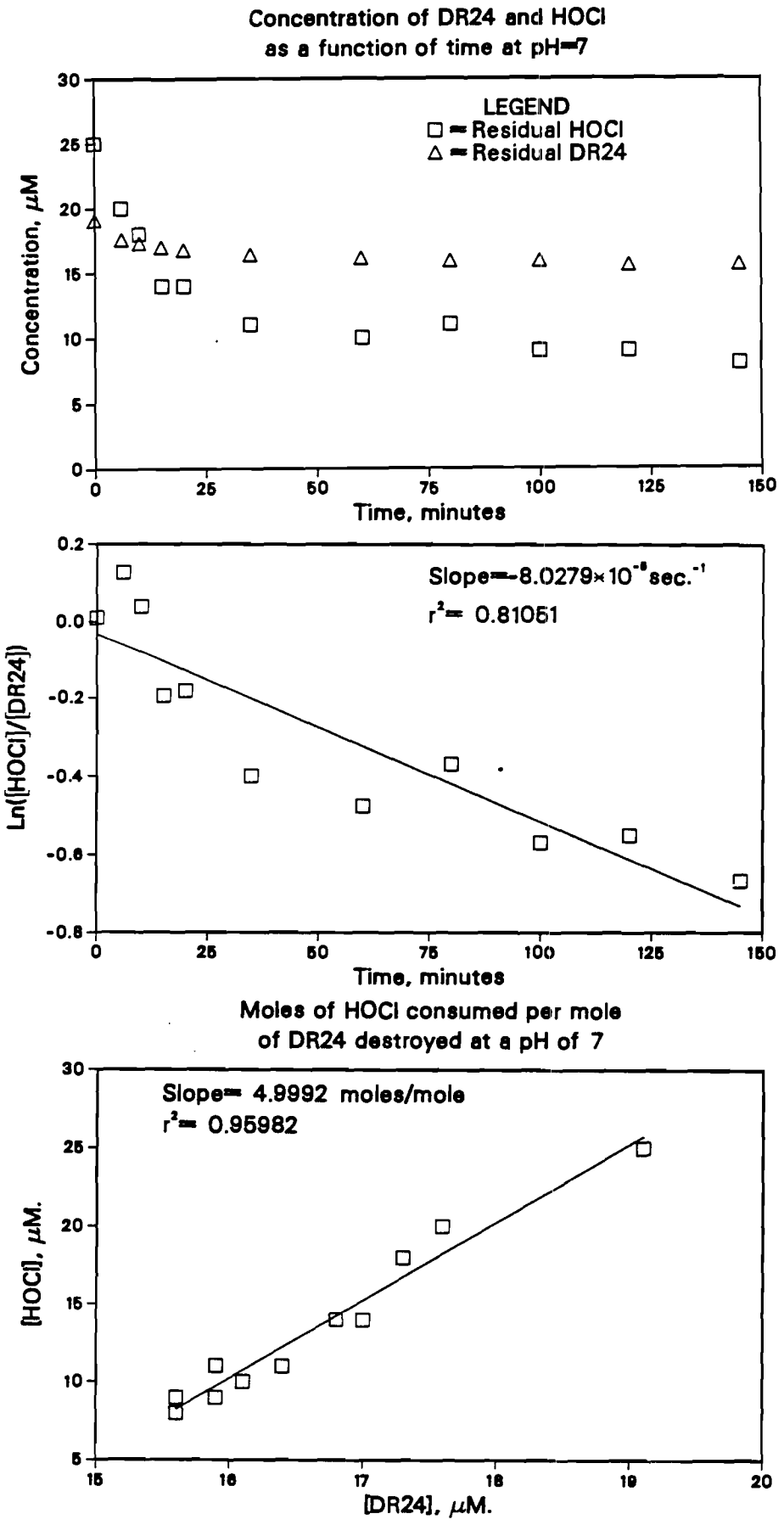
Concentration of DR24 and HOCl
as a function of time at pH=7
LEGEND
□ = Residual HOCl
△ = Residual DR24
Concentration, μM
Time, minutes
Slope=-8.0279×10⁻⁴ sec.⁻¹
r²= 0.81051
Ln([HOCl]/[DR24])
Time, minutes
Moles of HOCl consumed per mole
of DR24 destroyed at a pH of 7
Slope= 4.9992 moles/mole
r²= 0.95982
[HOCl], μM.
[DR24], μM.

Figure A2.11

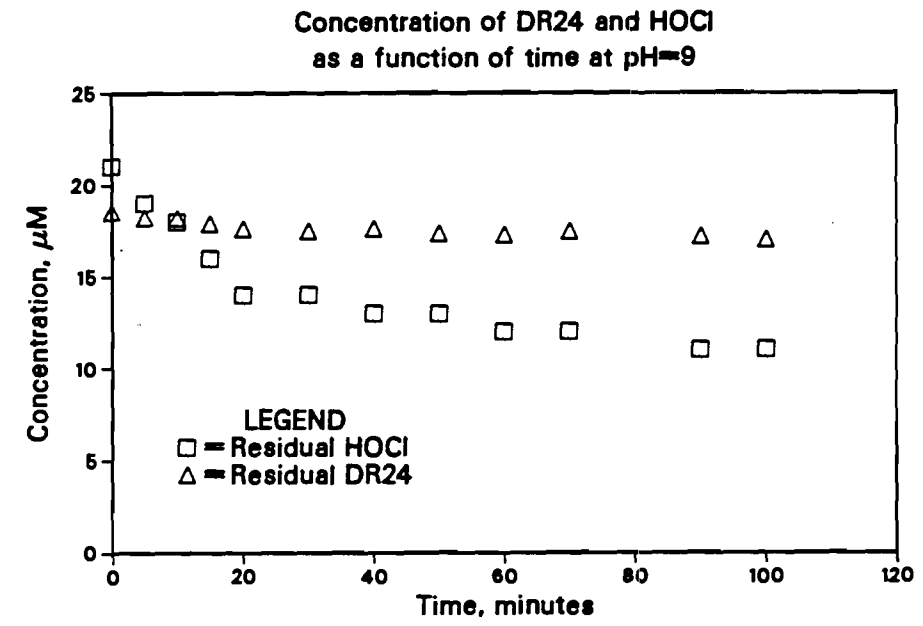
Concentration of DR24 and HOCl
as a function of time at pH=9
Concentration, μM
Time, minutes
LEGEND
□ = Residual HOCl
△ = Residual DR24

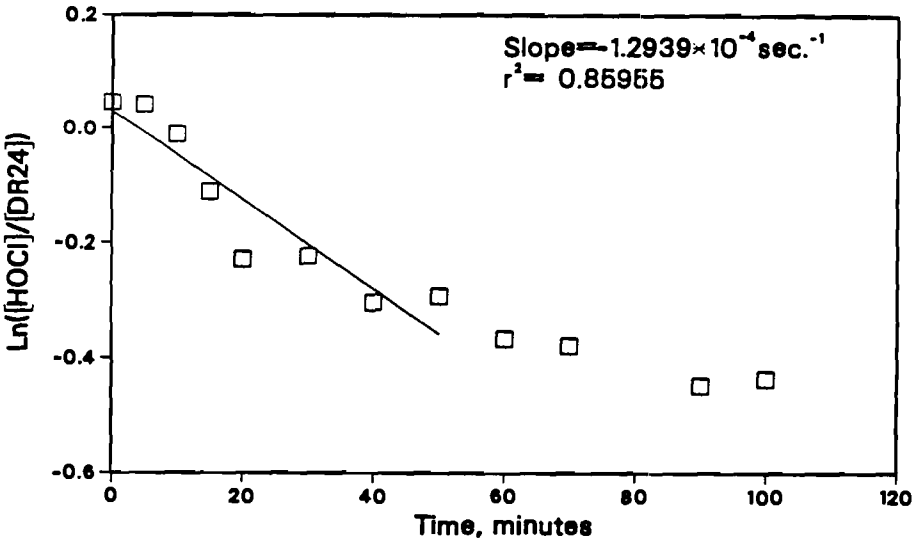
Slope=-1.2939×10⁻⁴sec.⁻¹
r²= 0.85955
Ln([HOCl]/[DR24])
Time, minutes

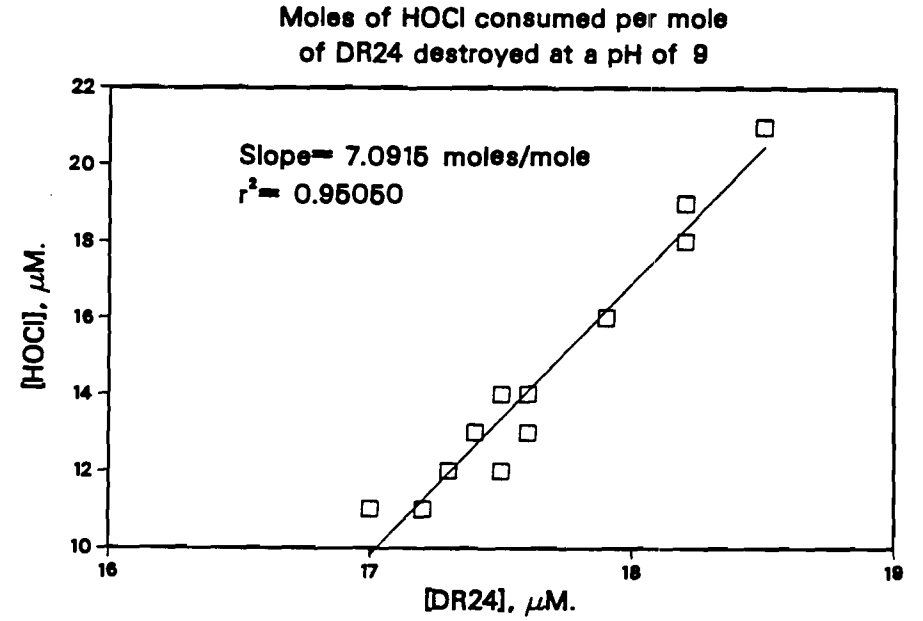
Moles of HOCl consumed per mole
of DR24 destroyed at a pH of 9
Slope= 7.0915 moles/mole
r²= 0.95050
[HOCl], μM.
[DR24], μM.

Figure A2.12

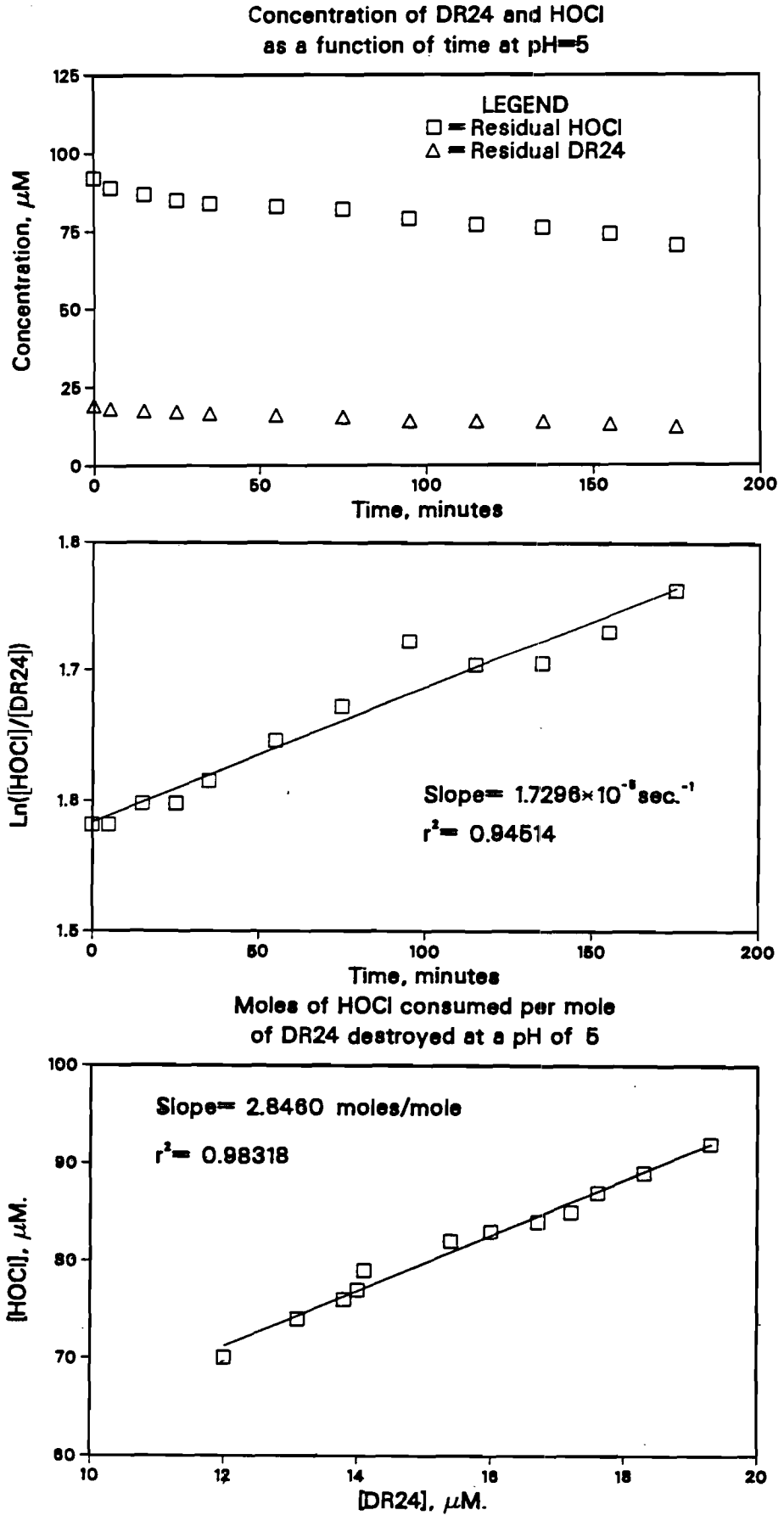
Concentration of DR24 and HOCl
as a function of time at pH=5
LEGEND
□ = Residual HOCl
△ = Residual DR24
Concentration, μM
Time, minutes
Ln([HOCl]/[DR24])
Slope= 1.7296×10⁻⁴ sec.⁻¹
r²= 0.94514
Time, minutes
Moles of HOCl consumed per mole
of DR24 destroyed at a pH of 5
Slope= 2.8460 moles/mole
r²= 0.98318
[HOCl], μM.
[DR24], μM.

Figure A2.13

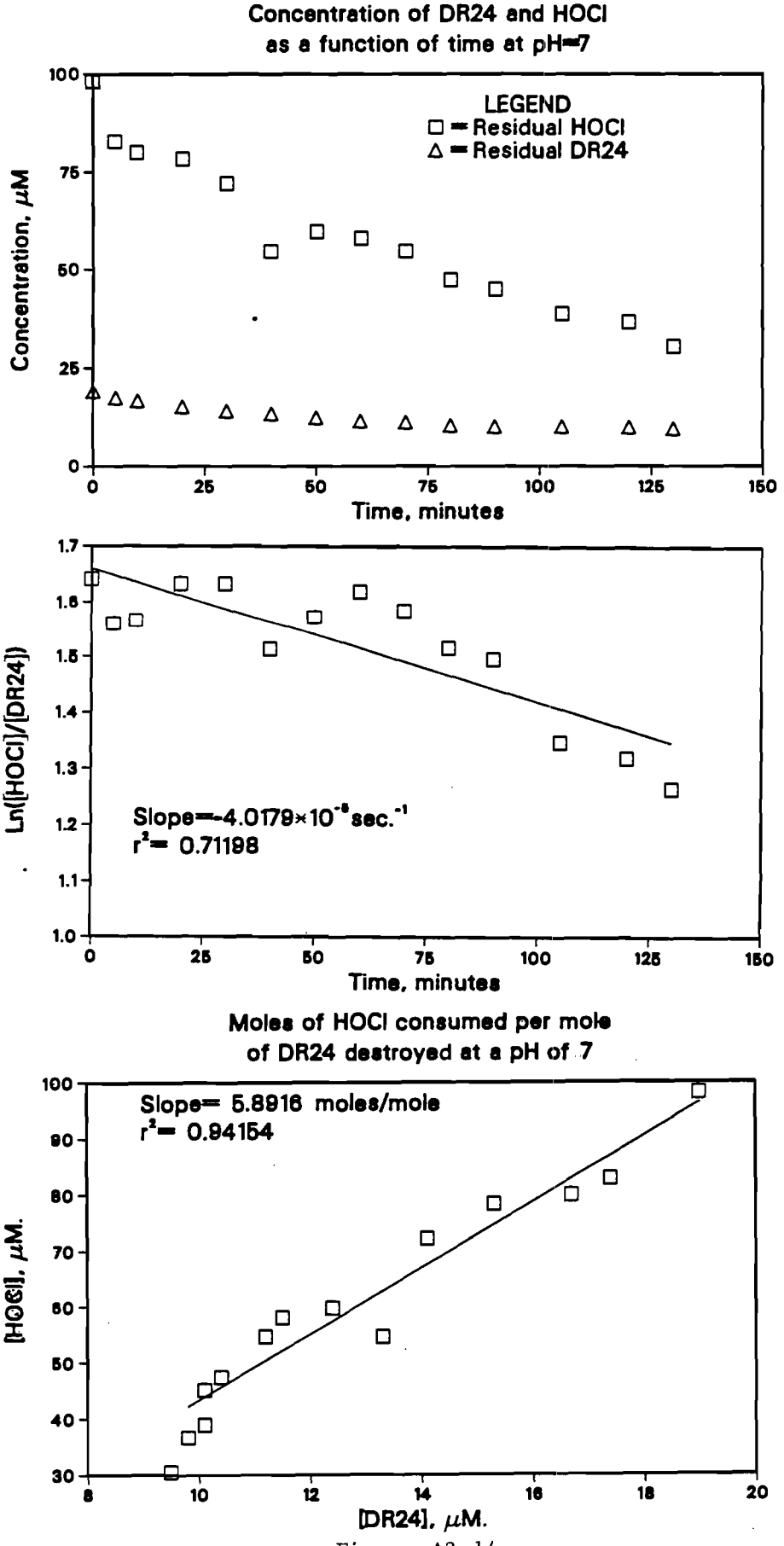
Concentration of DR24 and HOCl
as a function of time at pH=7
LEGEND
□ = Residual HOCl
△ = Residual DR24
Concentration, μM
Time, minutes
Ln([HOCl]/[DR24])
Slope=-4.0179×10⁻⁵ sec.⁻¹
r²= 0.71198
Time, minutes
Moles of HOCl consumed per mole
of DR24 destroyed at a pH of 7
Slope= 5.8916 moles/mole
r²= 0.94154
[HOCl], μM.
[DR24], μM.

Figure A2.14

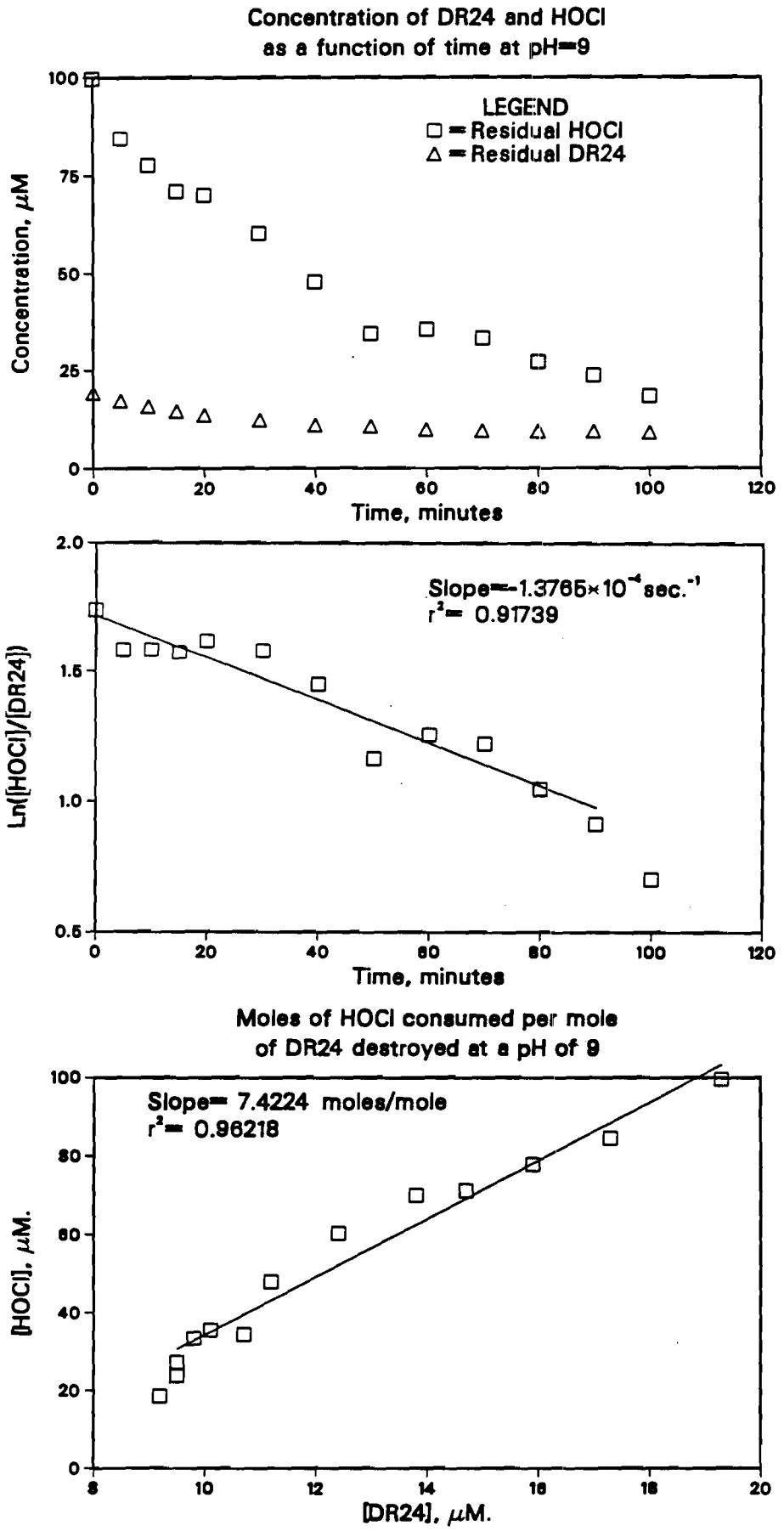
Concentration of DR24 and HOCl
as a function of time at pH=9
LEGEND
□ = Residual HOCl
△ = Residual DR24
Concentration, μM
Time, minutes
Slope=-1.3765×10⁻⁴ sec.⁻¹
r²= 0.91739
Ln([HOCl]/[DR24])
Time, minutes
Moles of HOCl consumed per mole
of DR24 destroyed at a pH of 9
Slope= 7.4224 moles/mole
r²= 0.96218
[HOCl], μM.
[DR24], μM.

Figure A2.15

APPENDIX 3

DATA PLOTS FOR DIRECT VIOLET 09

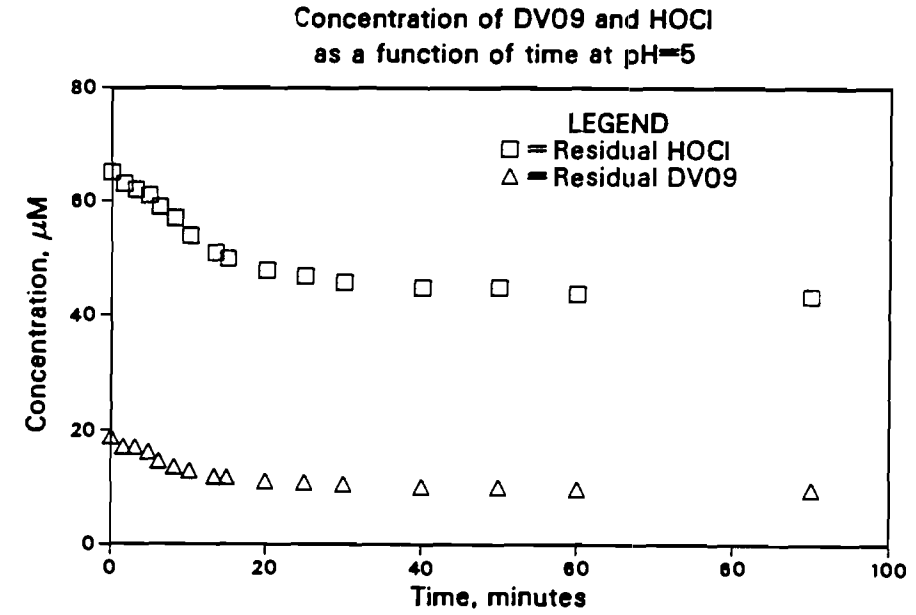
Concentration of DV09 and HOCl
as a function of time at pH=5
LEGEND
□ = Residual HOCl
△ = Residual DV09
Concentration, μM
Time, minutes

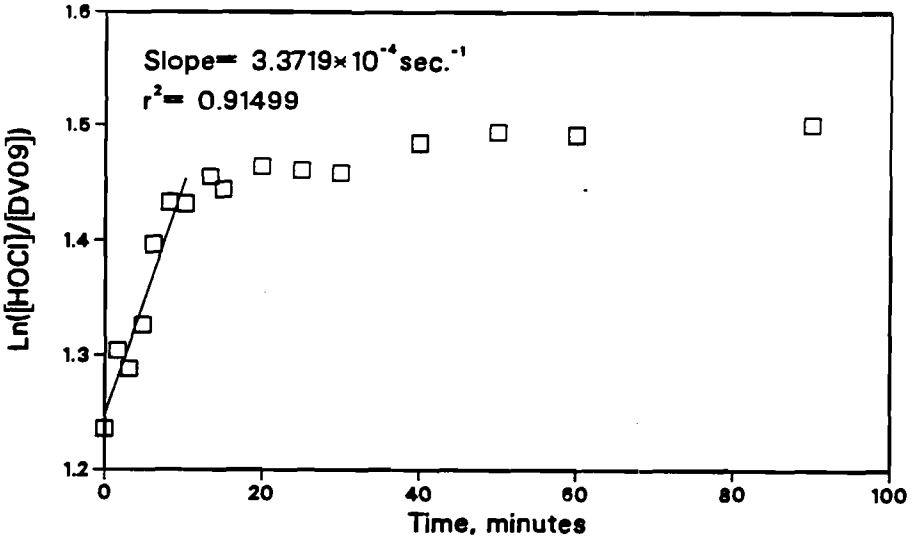
Slope= 3.3719×10⁻⁴ sec.⁻¹
r²= 0.91499
Ln([HOCl]/[DV09])
Time, minutes

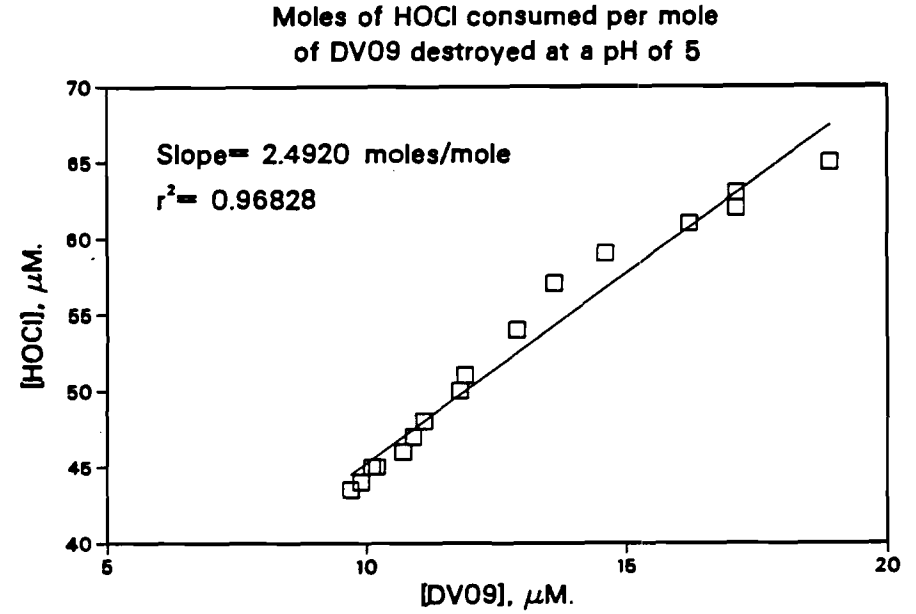
Moles of HOCl consumed per mole
of DV09 destroyed at a pH of 5
Slope= 2.4920 moles/mole
r²= 0.96828
[HOCl], μM.
[DV09], μM.

Figure A3.1

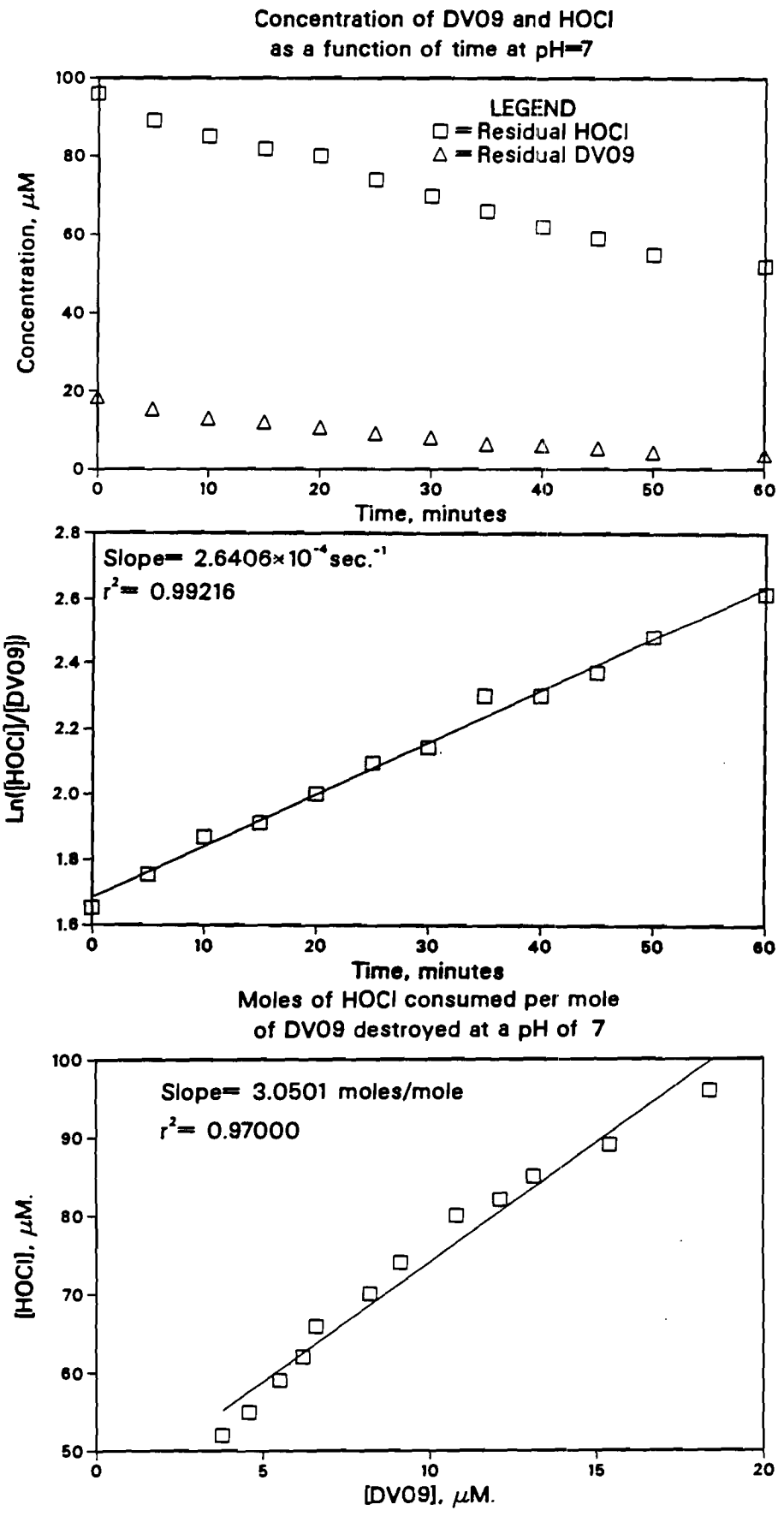
Concentration of DV09 and HOCl
as a function of time at pH=7
LEGEND
□ = Residual HOCl
△ = Residual DV09
Concentration, μM
Time, minutes
Slope= 2.6406×10⁻⁴sec.⁻¹
r²= 0.99216
Ln([HOCl]/[DV09])
Time, minutes
Moles of HOCl consumed per mole
of DV09 destroyed at a pH of 7
Slope= 3.0501 moles/mole
r²= 0.97000
[HOCl], μM.
[DV09], μM.

Figure A3.2

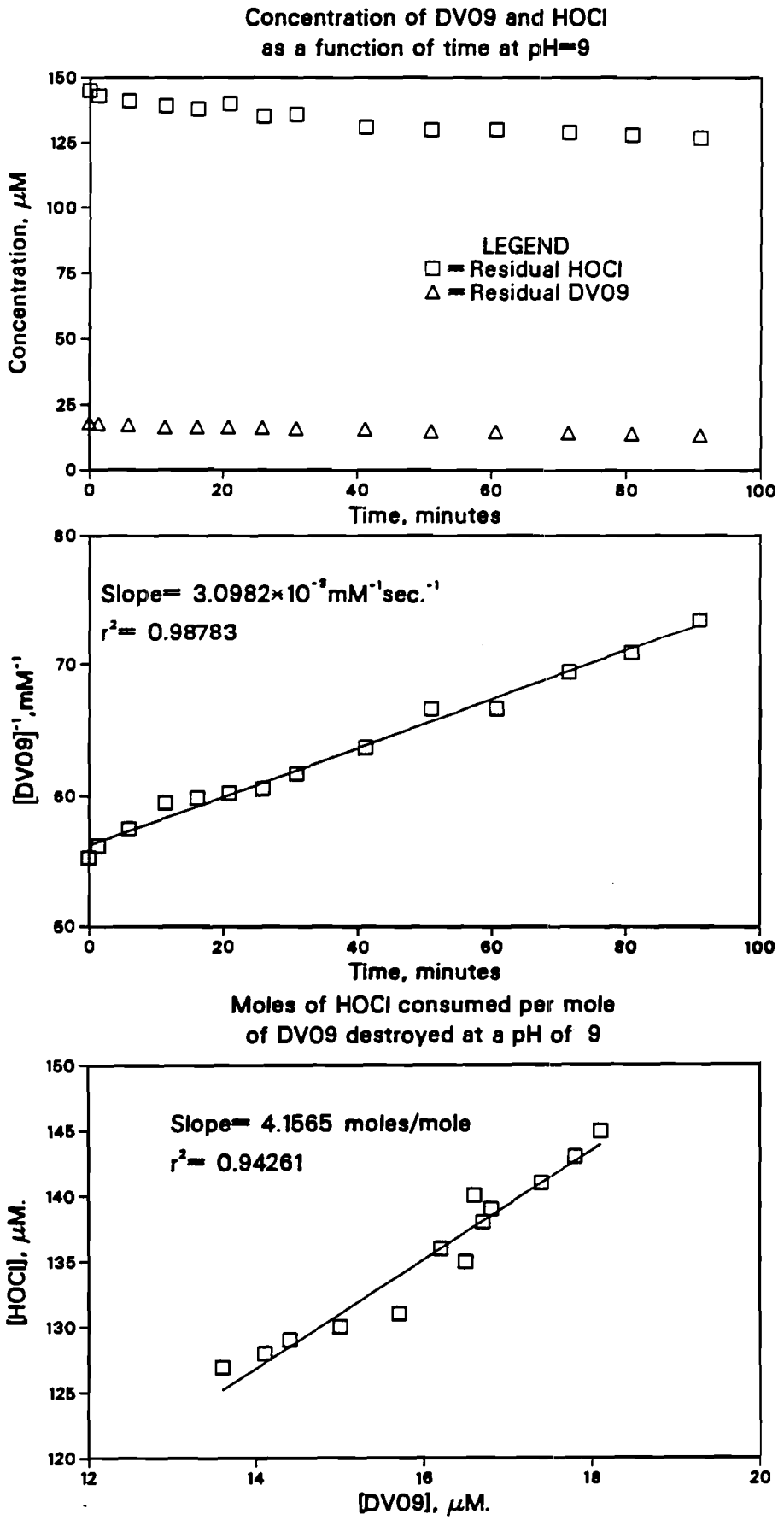
Concentration of DV09 and HOCl
as a function of time at pH=9
Concentration, μM
Time, minutes
LEGEND
□ = Residual HOCl
△ = Residual DV09
[DV09]⁻¹, mM⁻¹
Slope= 3.0982×10⁻³mM⁻¹sec.⁻¹
r²= 0.98783
Time, minutes
Moles of HOCl consumed per mole
of DV09 destroyed at a pH of 9
[HOCl], μM.
Slope= 4.1565 moles/mole
r²= 0.94261
[DV09], μM.

Figure A3.3

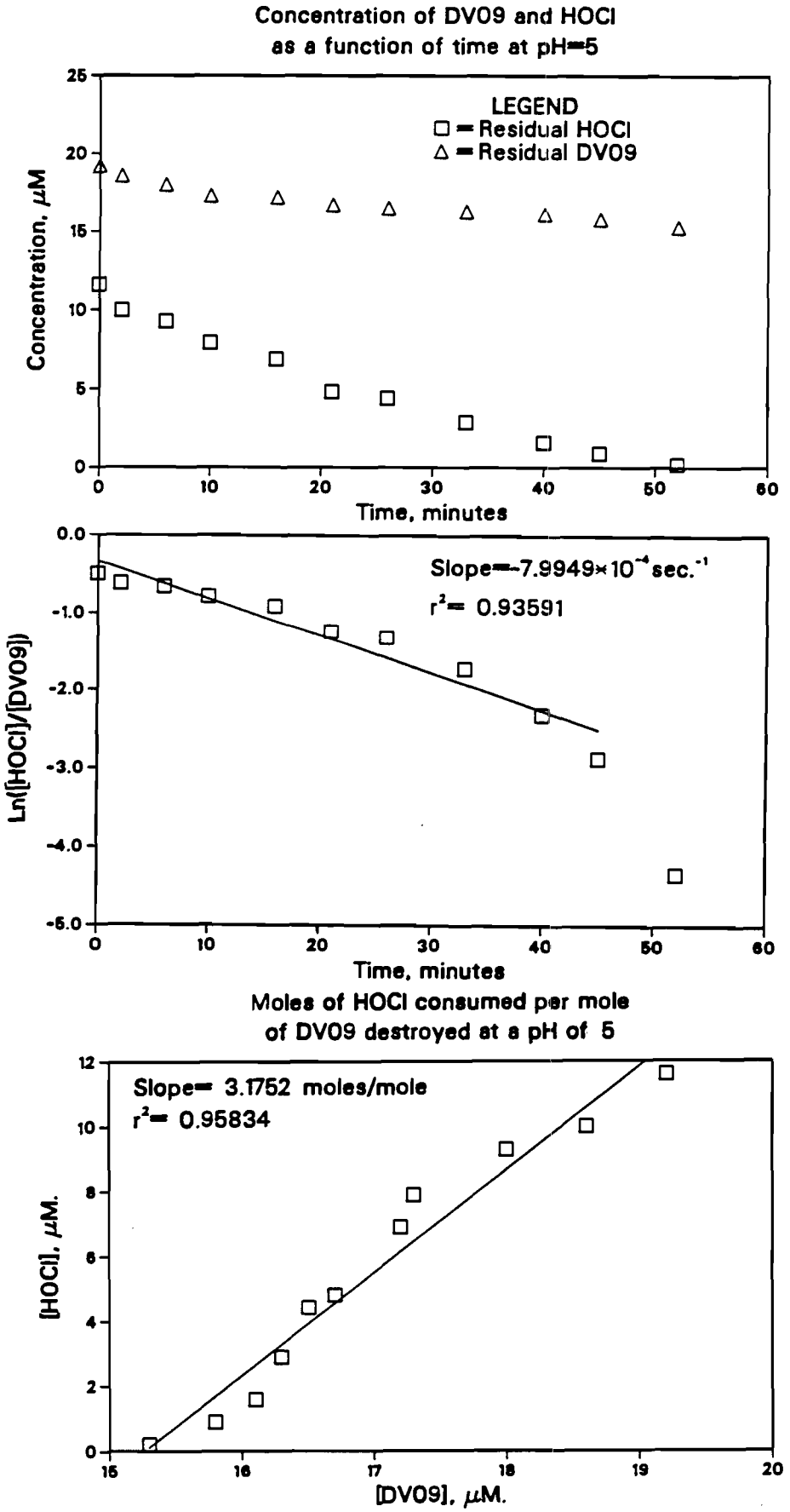
Concentration of DV09 and HOCl
as a function of time at pH=5
LEGEND
□ = Residual HOCl
△ = Residual DV09
Concentration, μM
Time, minutes
Slope=-7.9949×10⁻⁴ sec.⁻¹
r²= 0.93591
Ln([HOCl]/[DV09])
Time, minutes
Moles of HOCl consumed per mole
of DV09 destroyed at a pH of 5
Slope= 3.1752 moles/mole
r²= 0.95834
[HOCl], μM.
[DV09], μM.

Figure A3.4

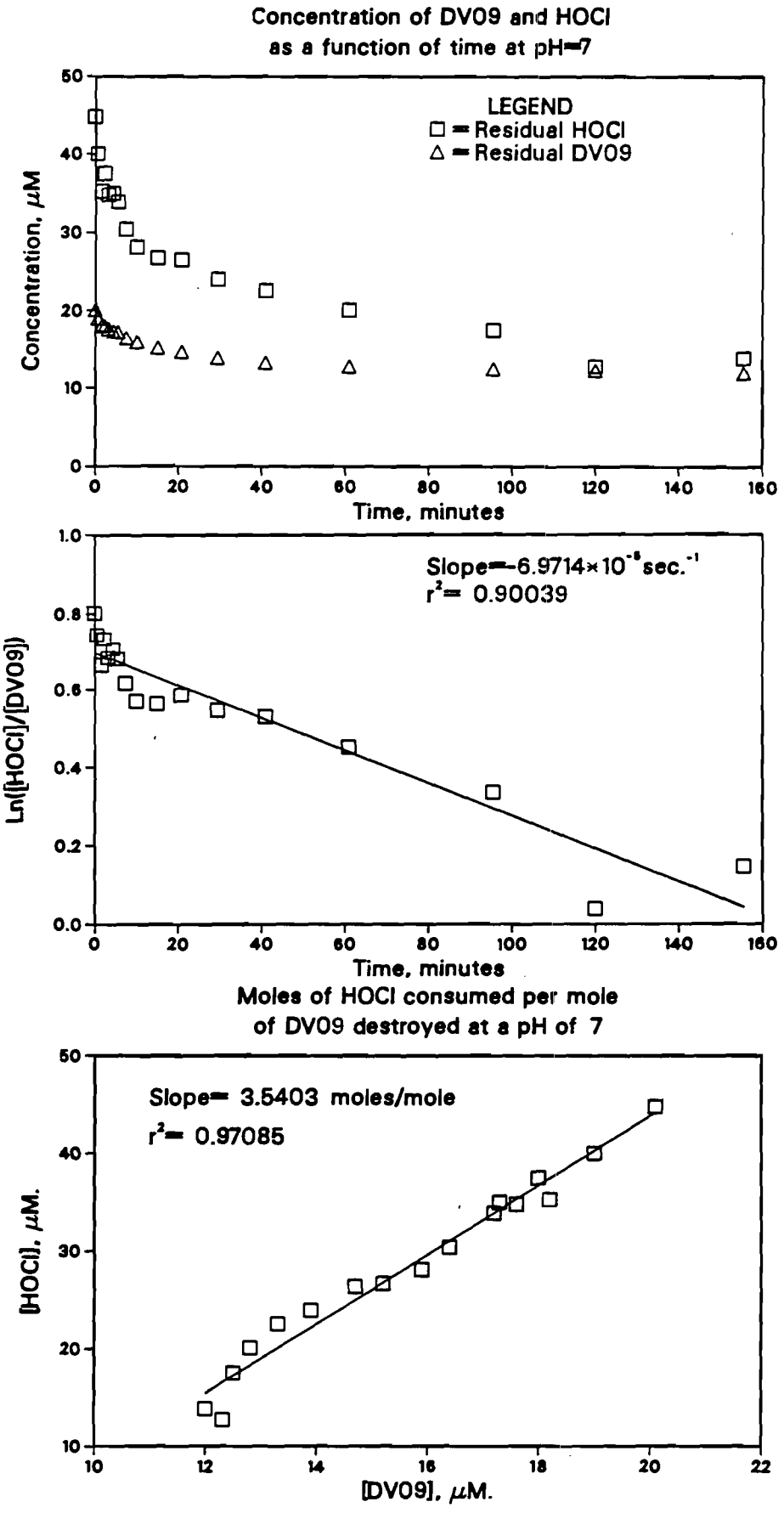
Concentration of DV09 and HOCl
as a function of time at pH=7
LEGEND
□ = Residual HOCl
△ = Residual DV09
Concentration, μM
Time, minutes
Slope=-6.9714×10⁻⁵sec.⁻¹
r²= 0.90039
Ln([HOCl]/[DV09])
Time, minutes
Moles of HOCl consumed per mole
of DV09 destroyed at a pH of 7
Slope= 3.5403 moles/mole
r²= 0.97085
[HOCl], μM.
[DV09], μM.

Figure A3.5

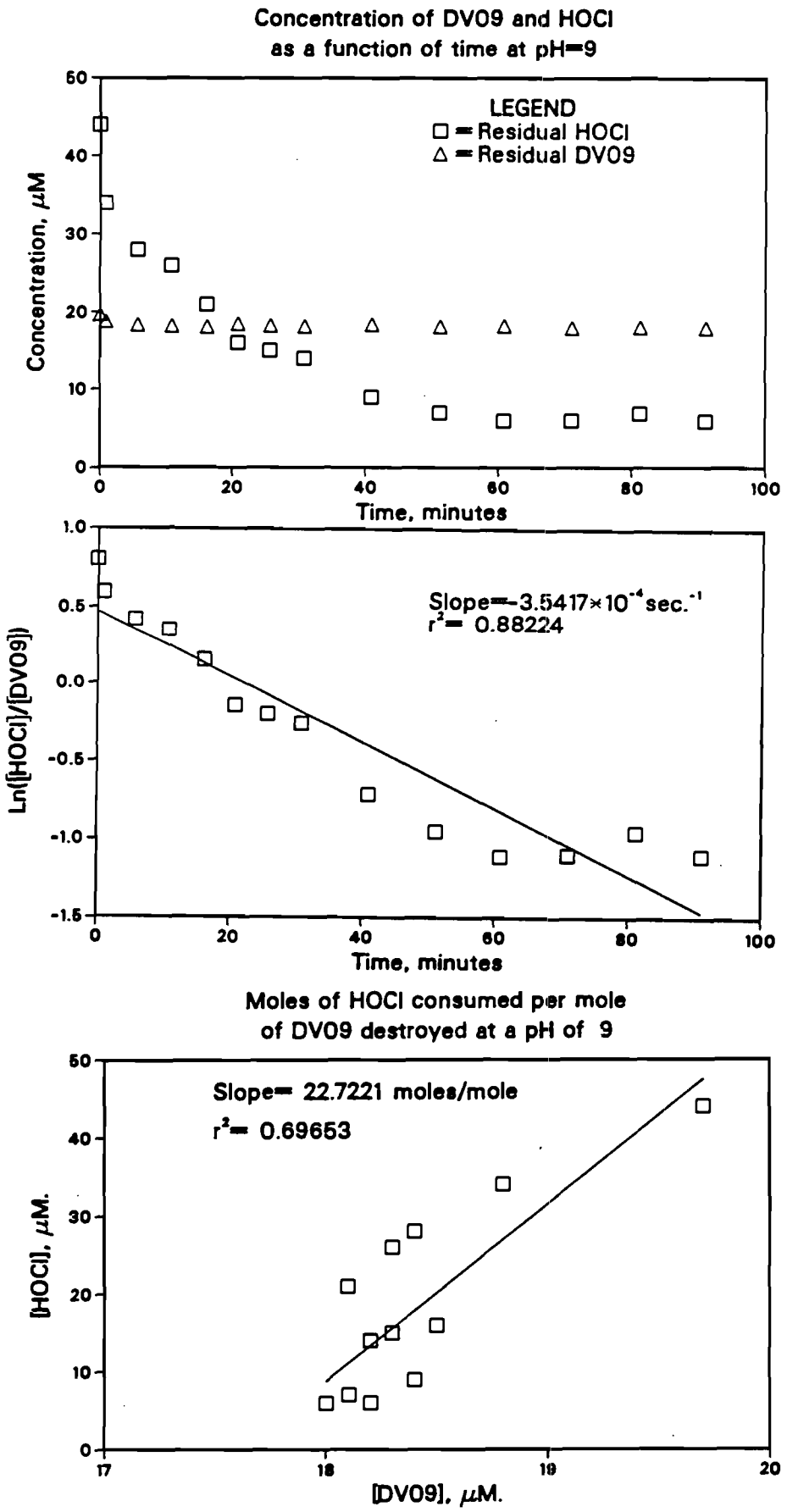
Concentration of DV09 and HOCl
as a function of time at pH=9
LEGEND
□ = Residual HOCl
△ = Residual DV09
Concentration, μM
Time, minutes
Slope=-3.5417×10⁻⁴ sec.⁻¹
r²= 0.88224
Ln([HOCl]/[DV09])
Time, minutes
Moles of HOCl consumed per mole
of DV09 destroyed at a pH of 9
Slope= 22.7221 moles/mole
r²= 0.69653
[HOCl], μM.
[DV09], μM.

Figure A3.6

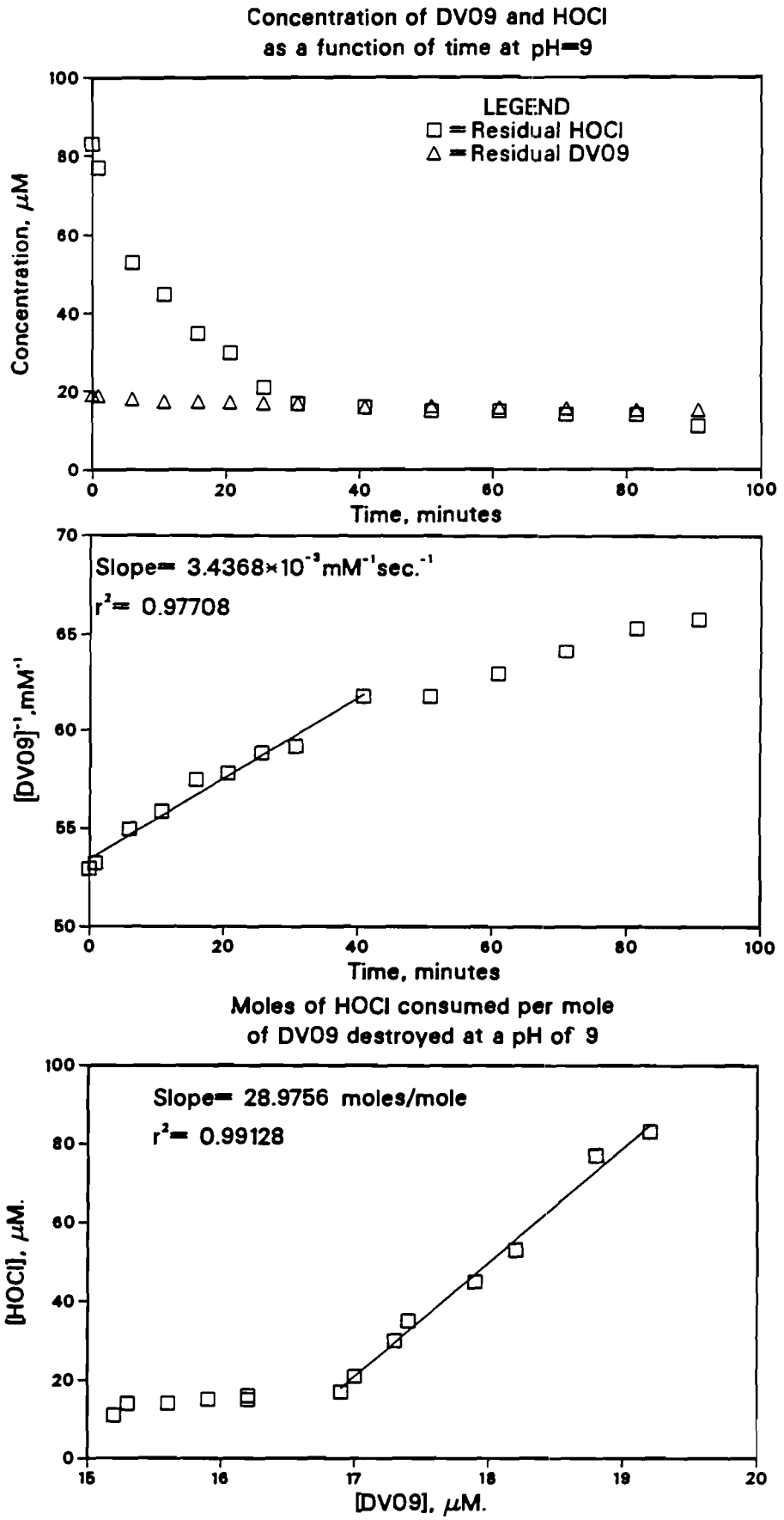
Concentration of DV09 and HOCl
as a function of time at pH=9
LEGEND
□ = Residual HOCl
△ = Residual DV09
Concentration, μM
Time, minutes
Slope= 3.4368×10⁻³mM⁻¹sec.⁻¹
r²= 0.97708
[DV09]⁻¹, mM⁻¹
Time, minutes
Moles of HOCl consumed per mole
of DV09 destroyed at a pH of 9
Slope= 28.9756 moles/mole
r²= 0.99128
[HOCl], μM.
[DV09], μM.

Figure A3.7

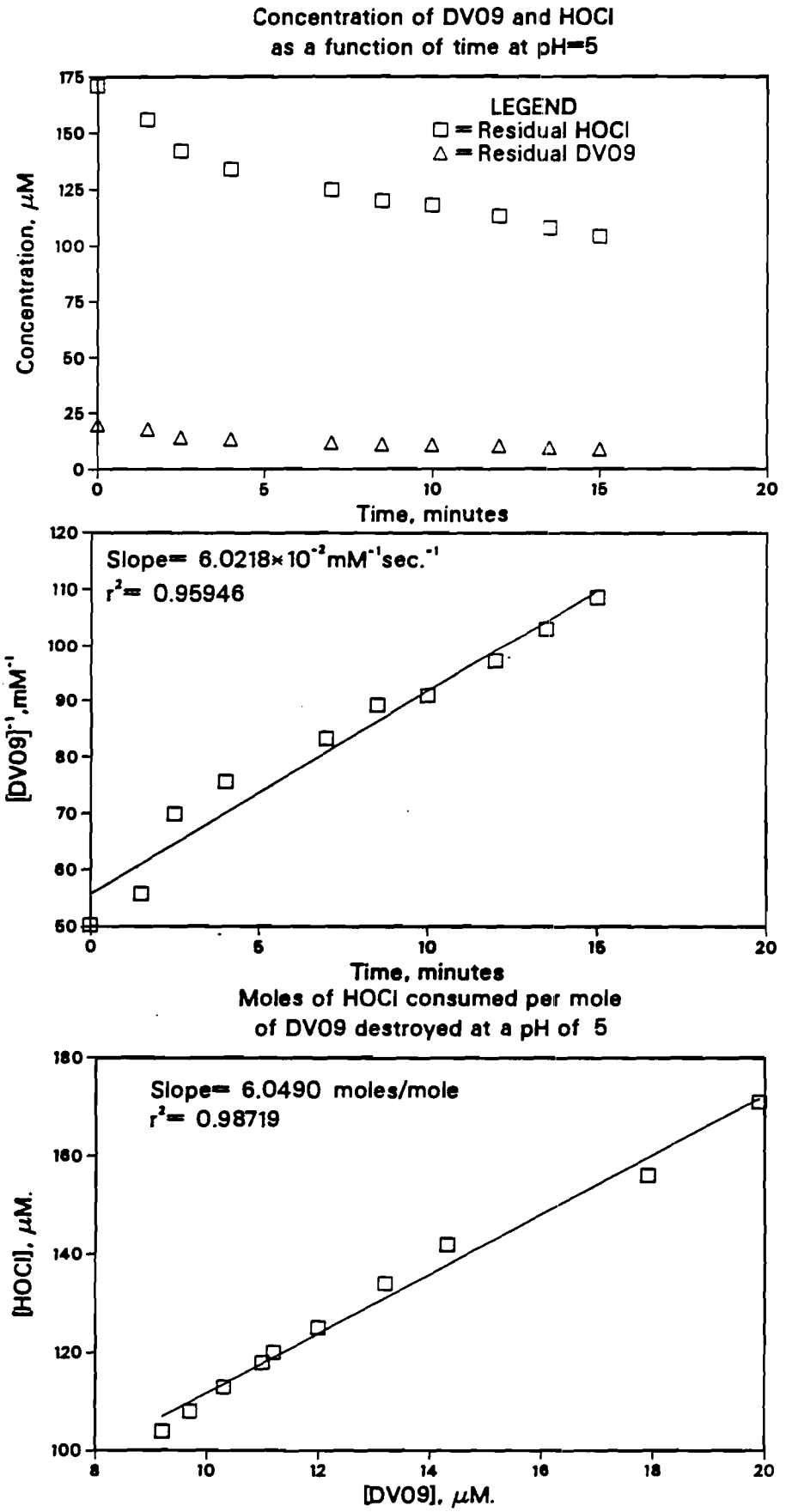
Concentration of DV09 and HOCl
as a function of time at pH=5
LEGEND
□ = Residual HOCl
△ = Residual DV09
Concentration, μM
Time, minutes
Slope= 6.0218×10⁻²mM⁻¹sec.⁻¹
r²= 0.95946
[DV09]⁻¹, mM⁻¹
Time, minutes
Moles of HOCl consumed per mole
of DV09 destroyed at a pH of 5
Slope= 6.0490 moles/mole
r²= 0.98719
[HOCl], μM.
[DV09], μM.

Figure A3.8

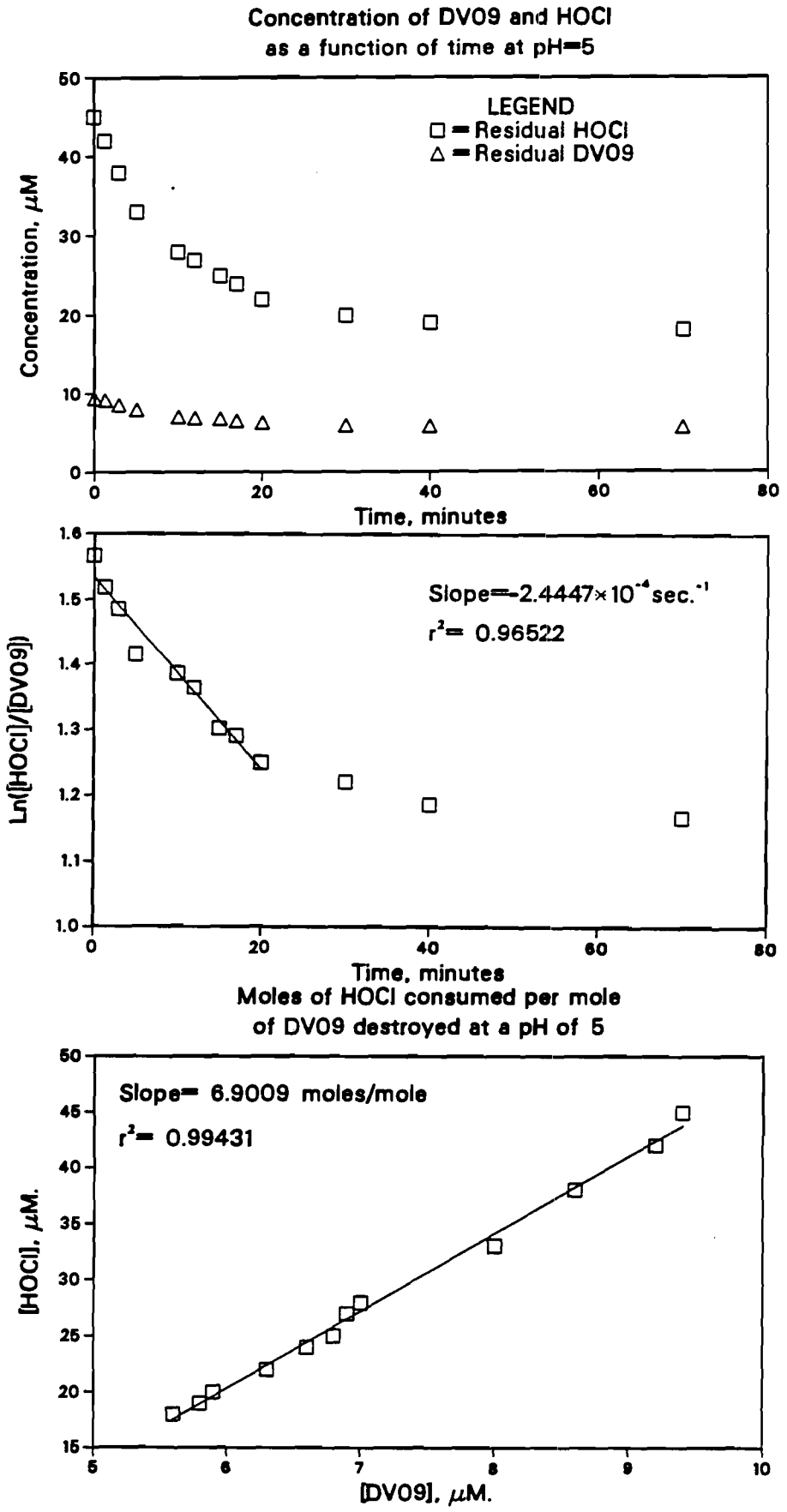
Concentration of DV09 and HOCl
as a function of time at pH=5
LEGEND
□ = Residual HOCl
△ = Residual DV09
Concentration, μM
Time, minutes
Slope=-2.4447×10⁻⁴ sec.⁻¹
r²= 0.96522
Ln([HOCl]/[DV09])
Time, minutes
Moles of HOCl consumed per mole
of DV09 destroyed at a pH of 5
Slope= 6.9009 moles/mole
r²= 0.99431
[HOCl], μM.
[DV09], μM.

Figure A3.9

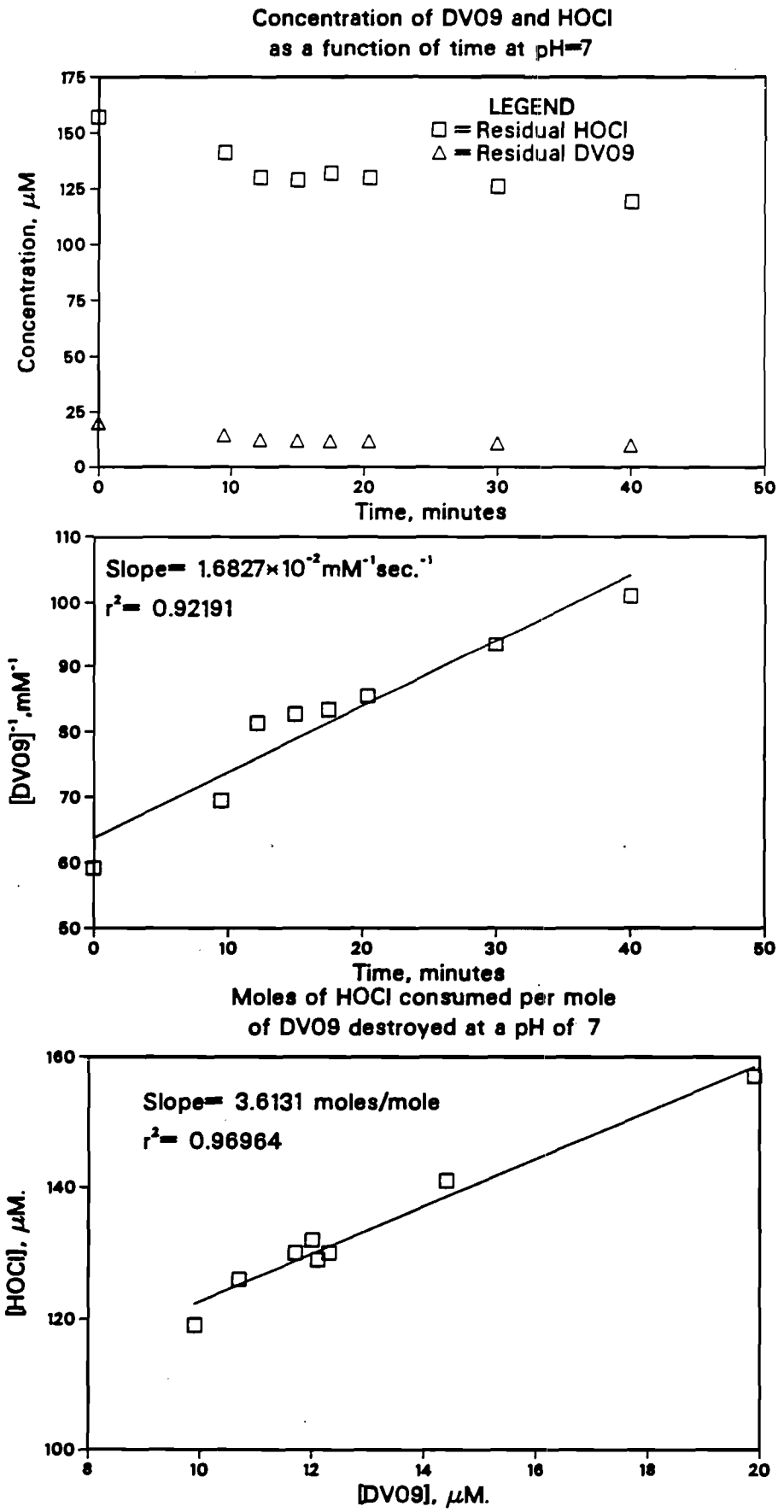
Concentration of DV09 and HOCl
as a function of time at pH=7
LEGEND
□ = Residual HOCl
△ = Residual DV09
Concentration, μM
Time, minutes
Slope= 1.6827×10⁻²mM⁻¹sec.⁻¹
r²= 0.92191
[DV09]⁻¹,mM⁻¹
Time, minutes
Moles of HOCl consumed per mole
of DV09 destroyed at a pH of 7
Slope= 3.6131 moles/mole
r²= 0.96964
[HOCl], μM.
[DV09], μM.

Figure A3.10

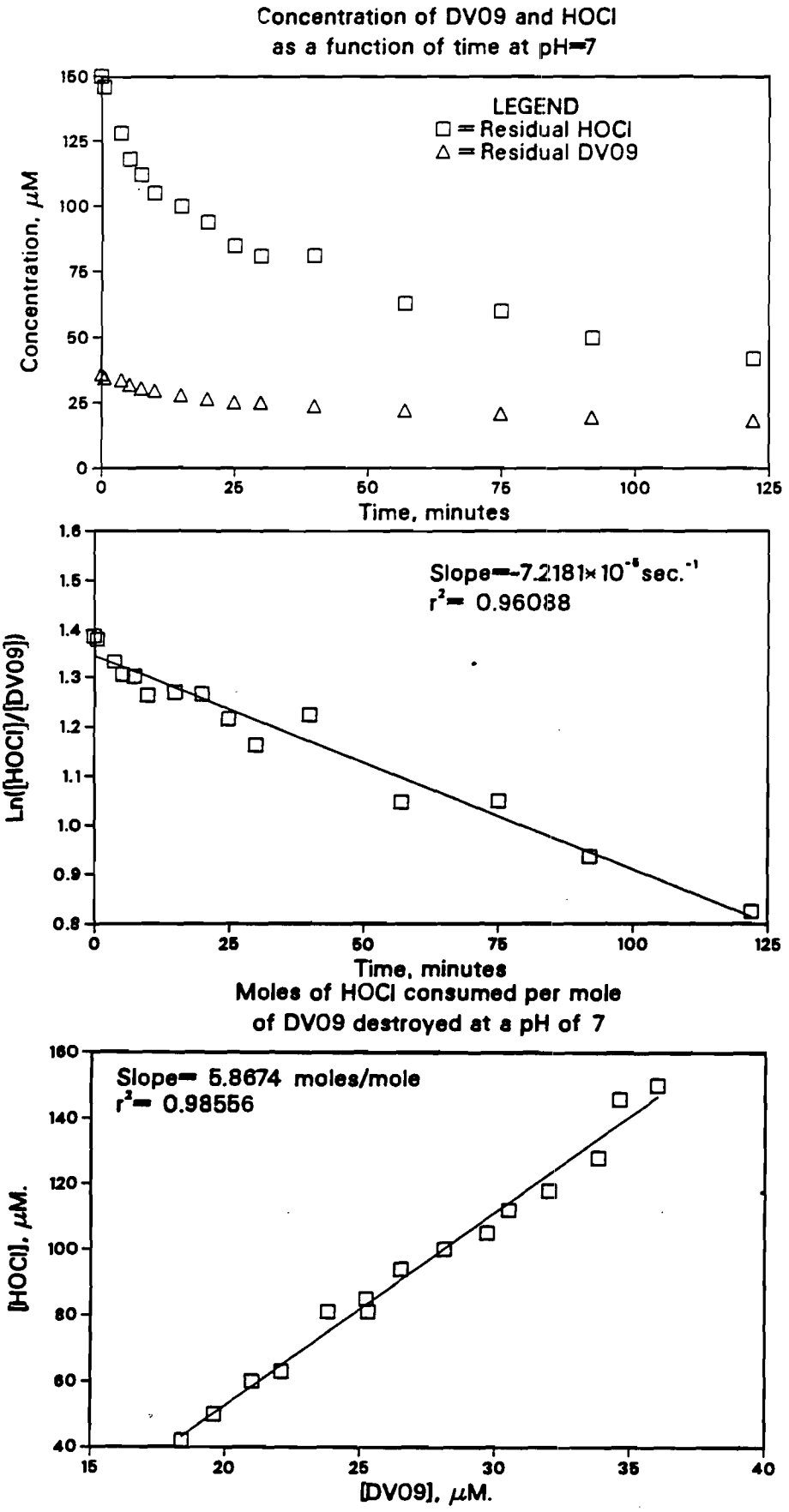
Concentration of DV09 and HOCl
as a function of time at pH=7
LEGEND
□ = Residual HOCl
△ = Residual DV09
Concentration, μM
Time, minutes
Slope=-7.2181×10⁻⁴ sec.⁻¹
r²= 0.96088
Ln([HOCl]/[DV09])
Time, minutes
Moles of HOCl consumed per mole
of DV09 destroyed at a pH of 7
Slope= 5.8674 moles/mole
r²= 0.98556
[HOCl], μM.
[DV09], μM.

Figure A3.11

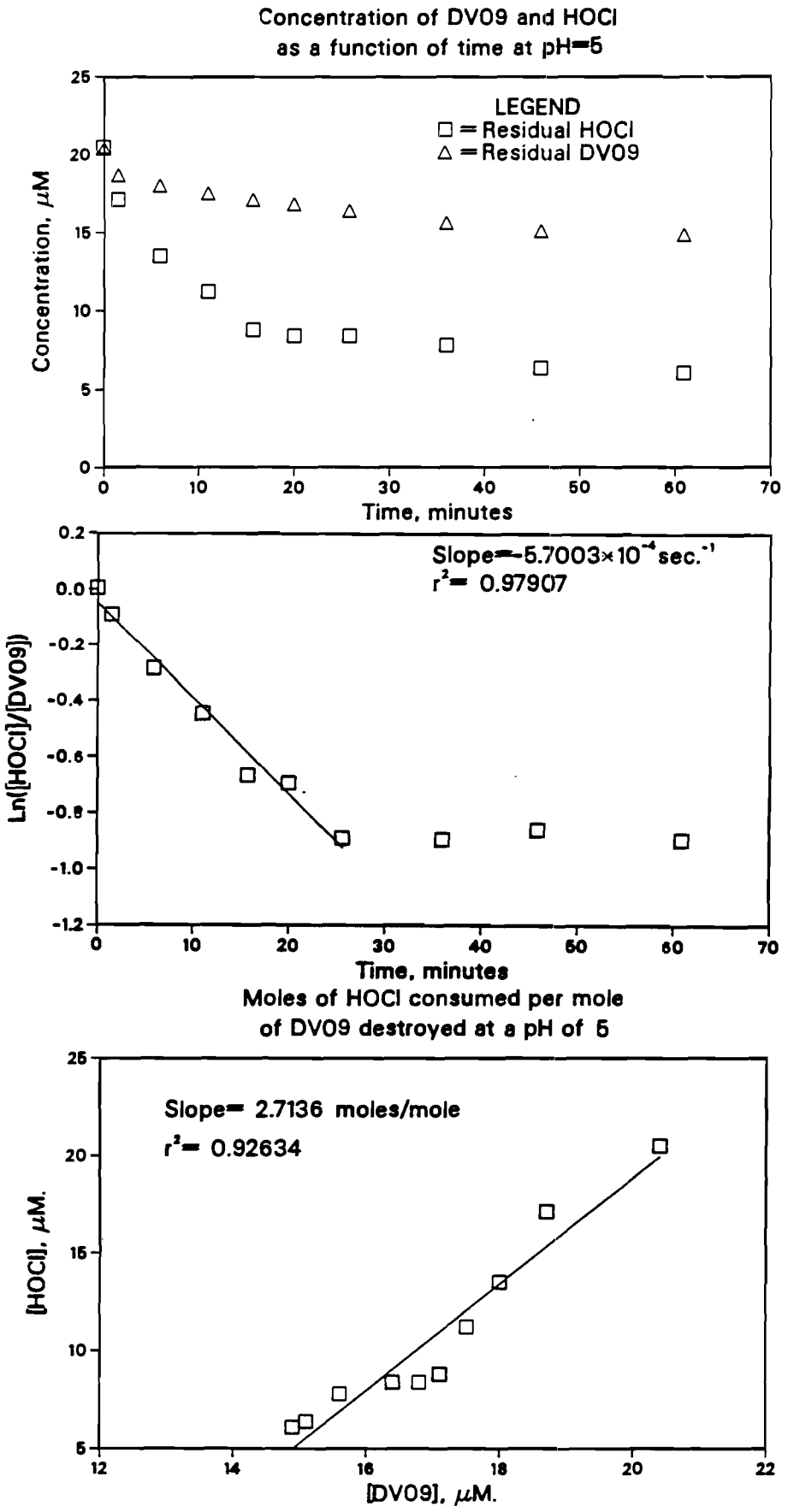
Concentration of DV09 and HOCl
as a function of time at pH=5
LEGEND
□ = Residual HOCl
△ = Residual DV09
Concentration, μM
Time, minutes
Slope=-5.7003×10⁻⁴ sec.⁻¹
r²= 0.97907
Ln([HOCl]/[DV09])
Time, minutes
Moles of HOCl consumed per mole
of DV09 destroyed at a pH of 5
Slope= 2.7136 moles/mole
r²= 0.92634
[HOCl], μM.
[DV09], μM.

Figure A3.12

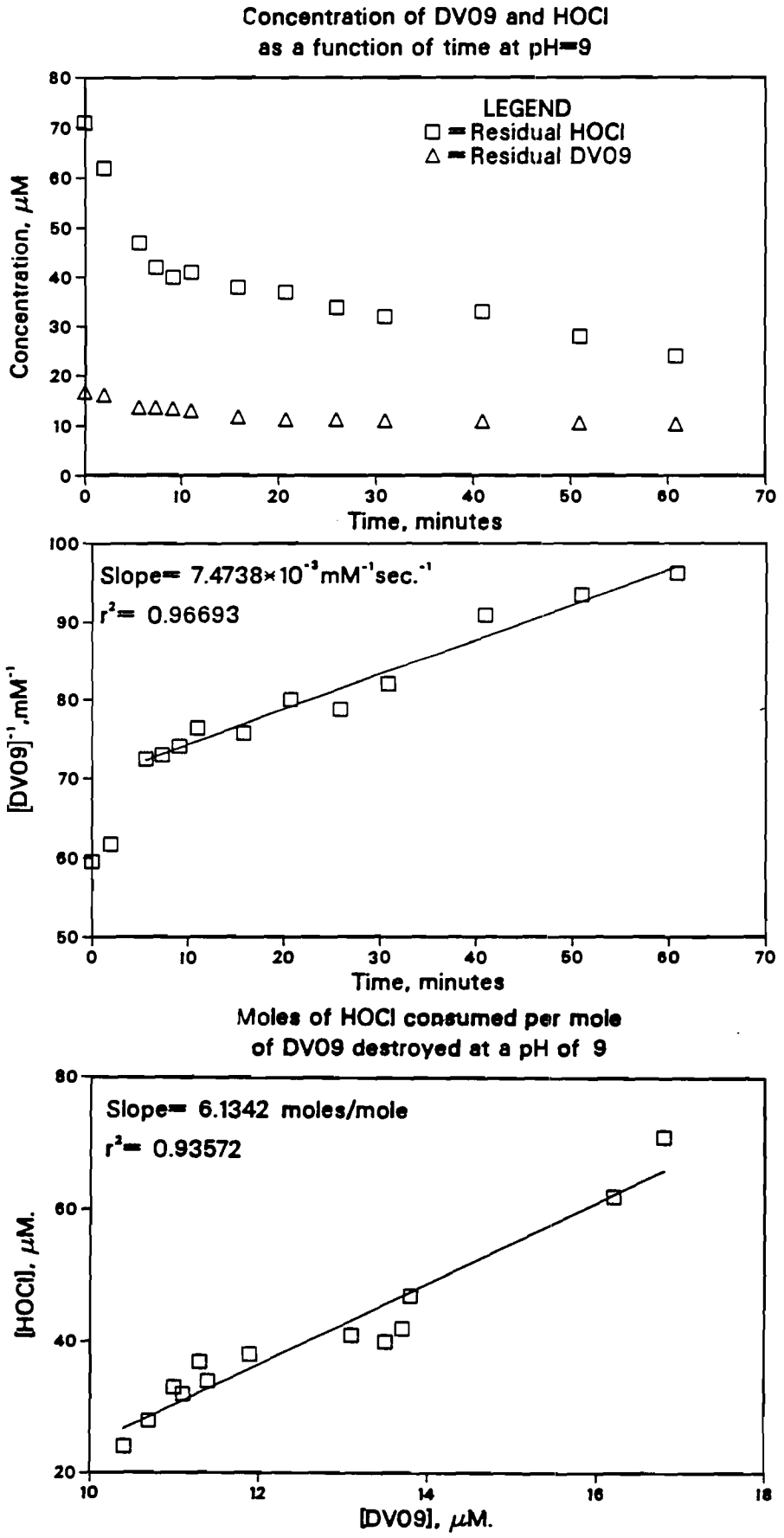
Concentration of DV09 and HOCl
as a function of time at pH=9
LEGEND
□ = Residual HOCl
△ = Residual DV09
Concentration, μM
Time, minutes
Slope= 7.4738×10⁻³mM⁻¹sec.⁻¹
r²= 0.96693
[DV09]⁻¹,mM⁻¹
Time, minutes
Moles of HOCl consumed per mole
of DV09 destroyed at a pH of 9
Slope= 6.1342 moles/mole
r²= 0.93572
[HOCl], μM.
[DV09], μM.

Figure A3.13

APPENDIX 4

DATA PLOTS FOR DIRECT YELLOW 50

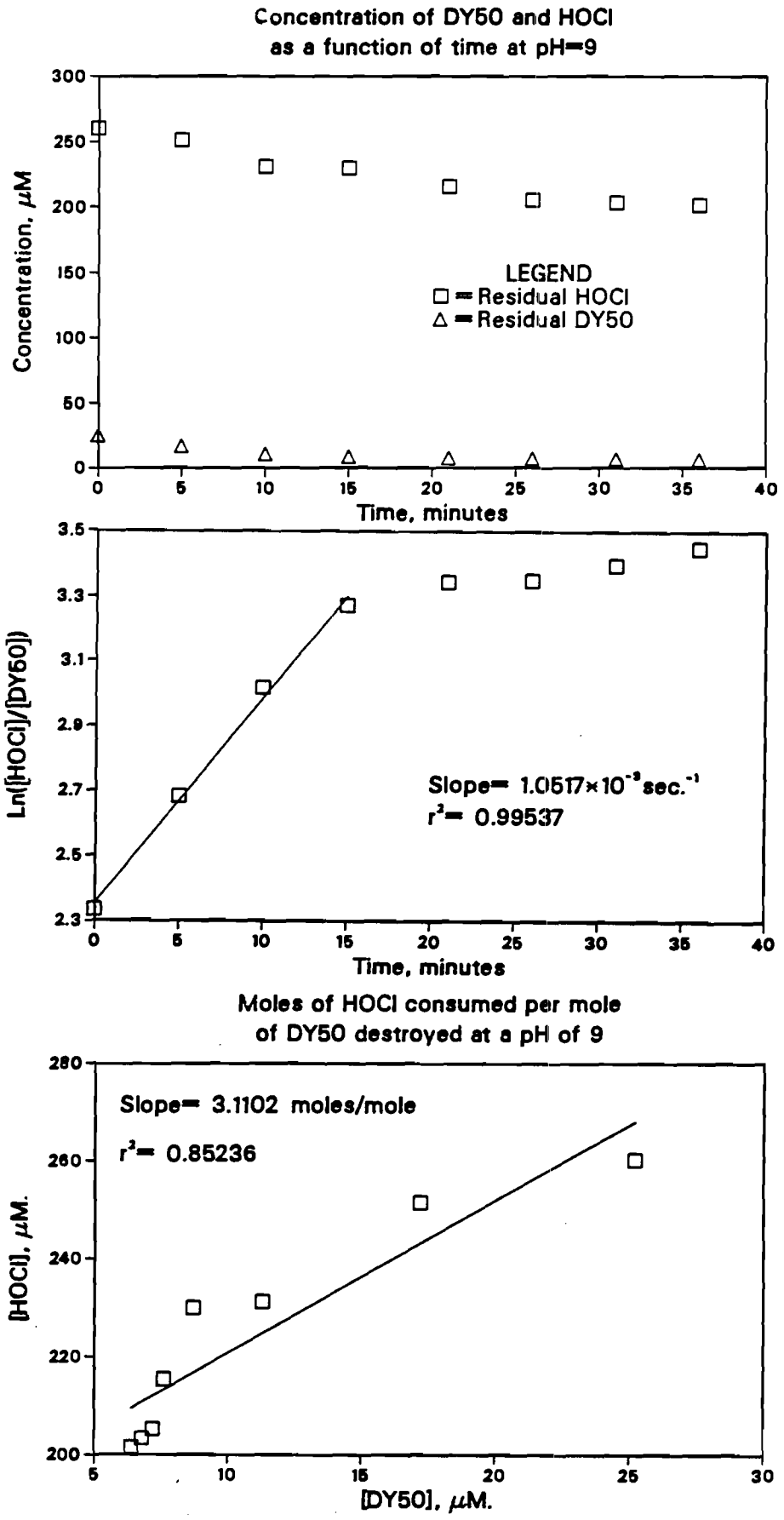
Concentration of DY50 and HOCl
as a function of time at pH=9
Concentration, μM
Time, minutes
LEGEND
□ = Residual HOCl
△ = Residual DY50
Ln([HOCl]/[DY60])
Slope= 1.0517×10⁻³sec.⁻¹
r²= 0.99537
Moles of HOCl consumed per mole
of DY50 destroyed at a pH of 9
Slope= 3.1102 moles/mole
r²= 0.85236
[HOCl], μM.
[DY50], μM.

Figure A4.1

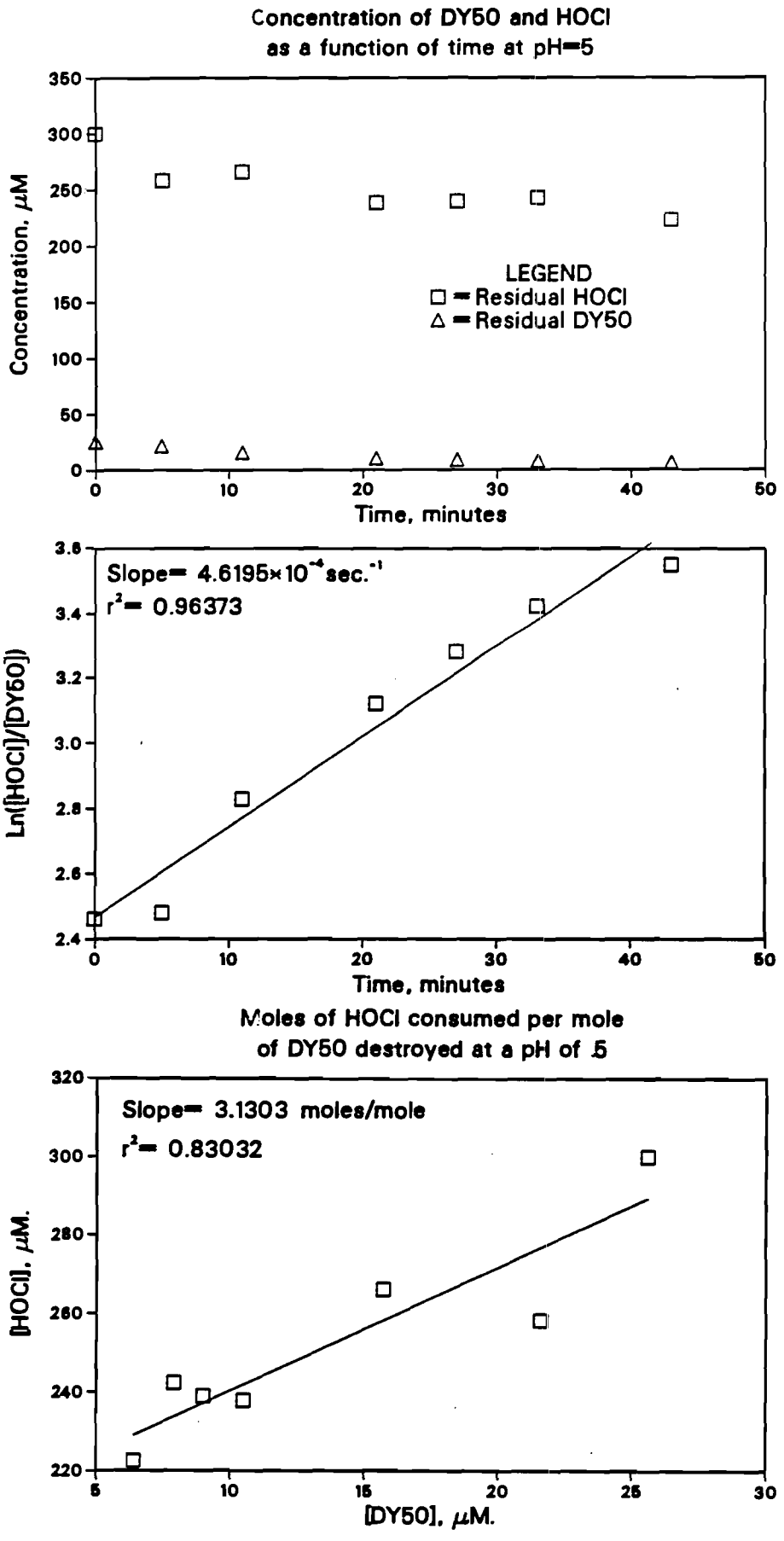
Concentration of DY50 and HOCl
as a function of time at pH=5
Concentration, μM
Time, minutes
LEGEND
□ = Residual HOCl
△ = Residual DY50
Ln([HOCl]/[DY60])
Slope= 4.6195×10⁻⁴ sec.⁻¹
r²= 0.96373
Time, minutes
Moles of HOCl consumed per mole
of DY50 destroyed at a pH of 5
[HOCl], μM.
Slope= 3.1303 moles/mole
r²= 0.83032
[DY50], μM.

Figure A4.2

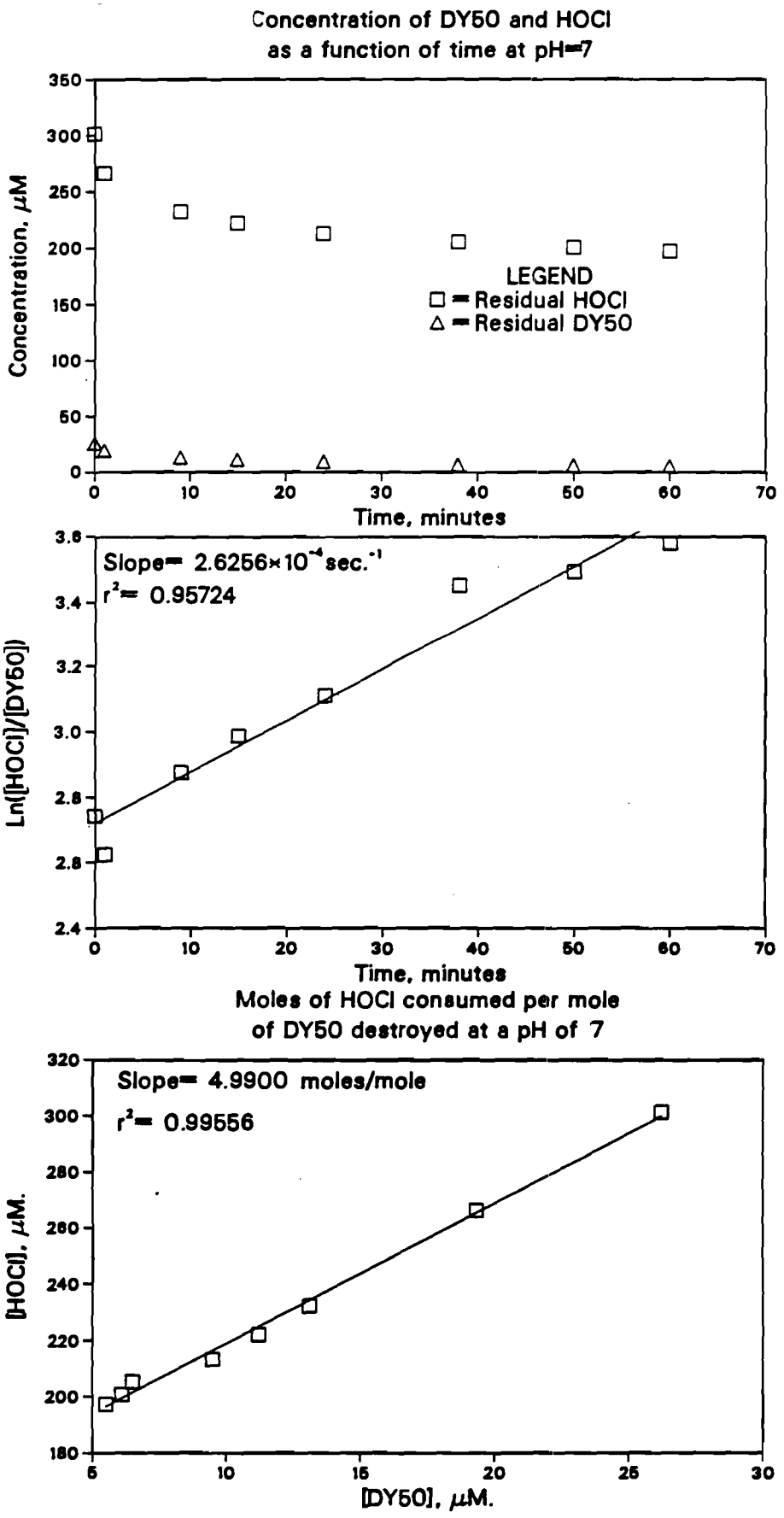
Concentration of DY50 and HOCl
as a function of time at pH=7
Concentration, μM
Time, minutes
LEGEND
□ = Residual HOCl
△ = Residual DY50
Ln([HOCl]/[DY50])
Slope= 2.6256×10⁻⁴ sec.⁻¹
r²= 0.95724
Time, minutes
Moles of HOCl consumed per mole
of DY50 destroyed at a pH of 7
[HOCl], μM.
Slope= 4.9900 moles/mole
r²= 0.99556
[DY50], μM.

Figure A4.3

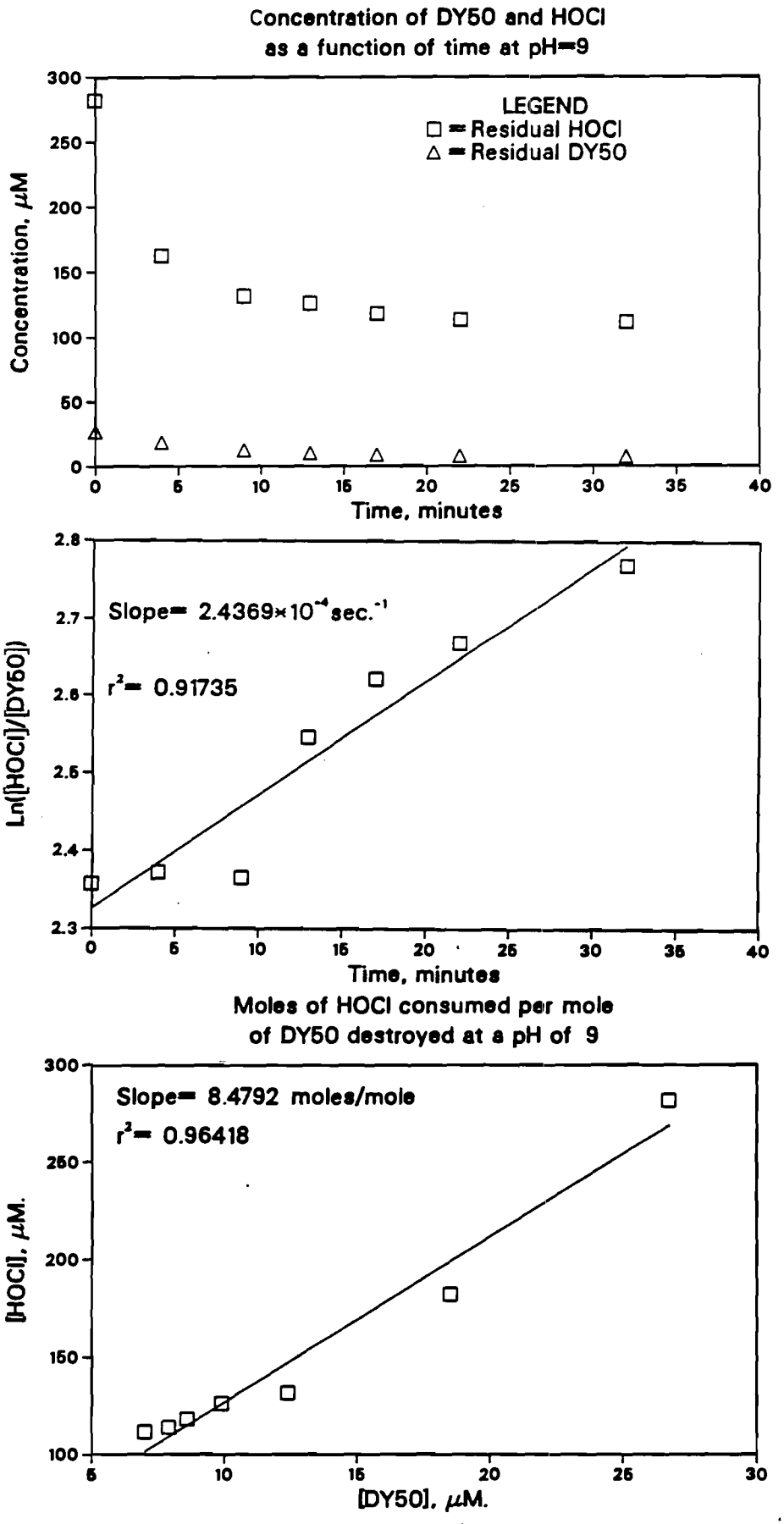
Concentration of DY50 and HOCl
as a function of time at pH=9
LEGEND
□ = Residual HOCl
△ = Residual DY50
Concentration, μM
Time, minutes
Slope= 2.4369×10⁻⁴sec.⁻¹
r²= 0.91735
Ln([HOCl]/[DY50])
Time, minutes
Moles of HOCl consumed per mole
of DY50 destroyed at a pH of 9
Slope= 8.4792 moles/mole
r²= 0.96418
[HOCl], μM.
[DY50], μM.

Figure A4.4

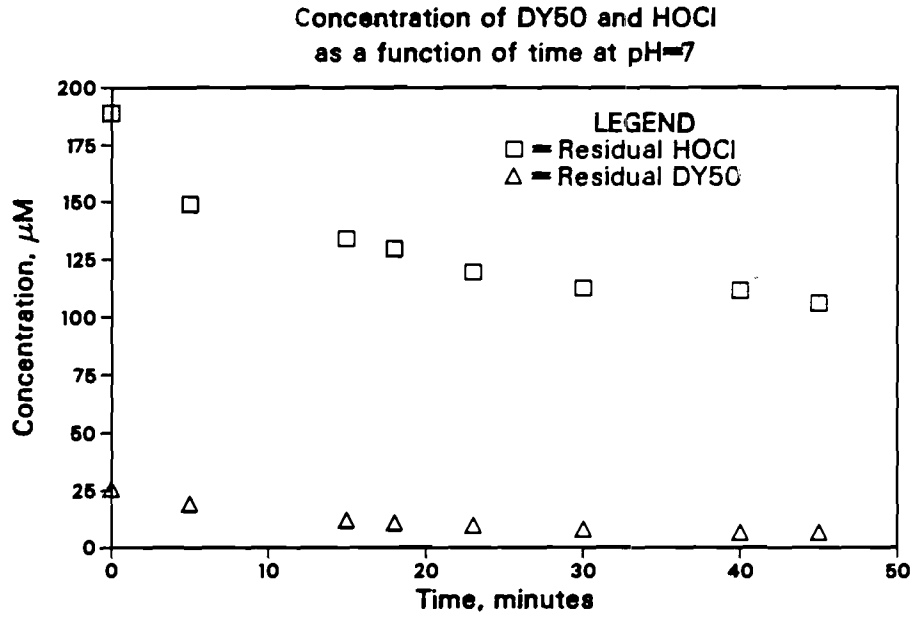
Concentration of DY50 and HOCl
as a function of time at pH=7
LEGEND
□ = Residual HOCl
△ = Residual DY50
Concentration, μM
Time, minutes

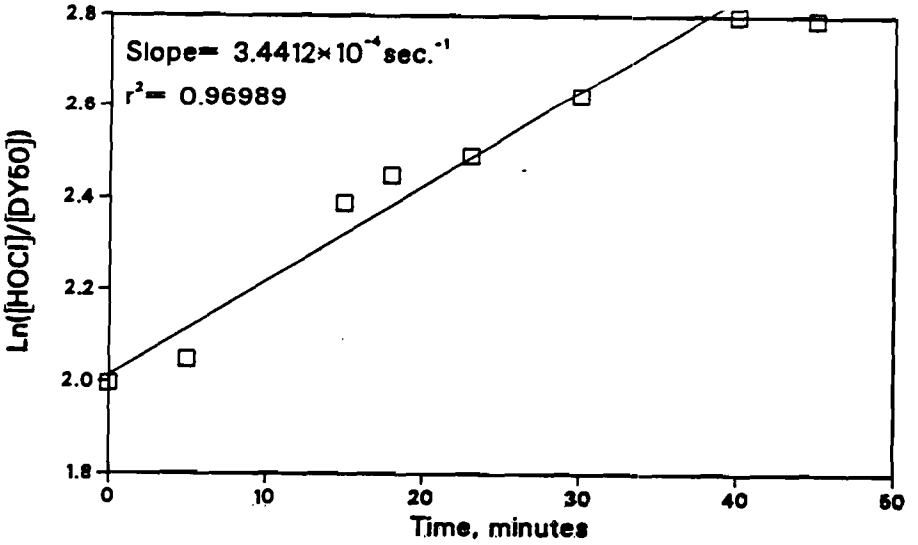
Slope= 3.4412×10⁻⁴ sec.⁻¹
r²= 0.96989
Ln([HOCl]/[DY60])
Time, minutes

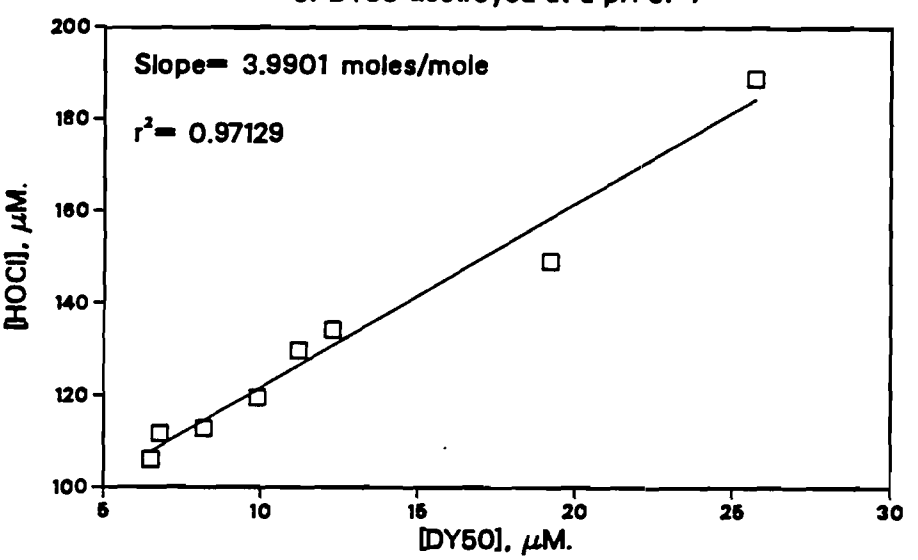
Moles of HOCl consumed per mole
of DY50 destroyed at a pH of 7
Slope= 3.9901 moles/mole
r²= 0.97129
[HOCl], μM.
[DY50], μM.

Figure A4.5

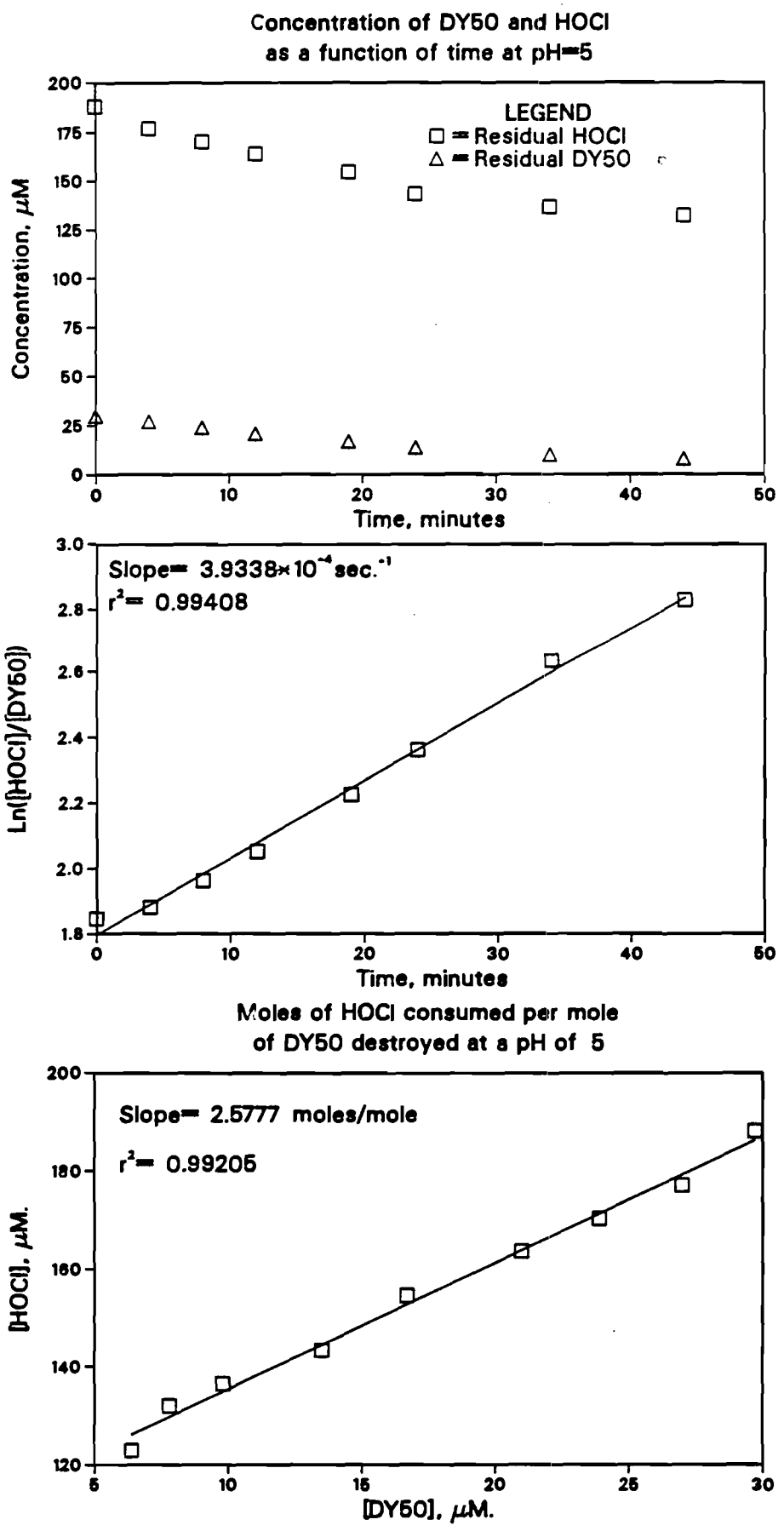
Concentration of DY50 and HOCl
as a function of time at pH=5
LEGEND
□ = Residual HOCl
△ = Residual DY50
Concentration, μM
Time, minutes
Slope= 3.9338×10⁻⁴ sec.⁻¹
r²= 0.99408
Ln([HOCl]/[DY50])
Time, minutes
Moles of HOCl consumed per mole
of DY50 destroyed at a pH of 5
Slope= 2.5777 moles/mole
r²= 0.99205
[HOCl], μM.
[DY50], μM.

Figure A4.6

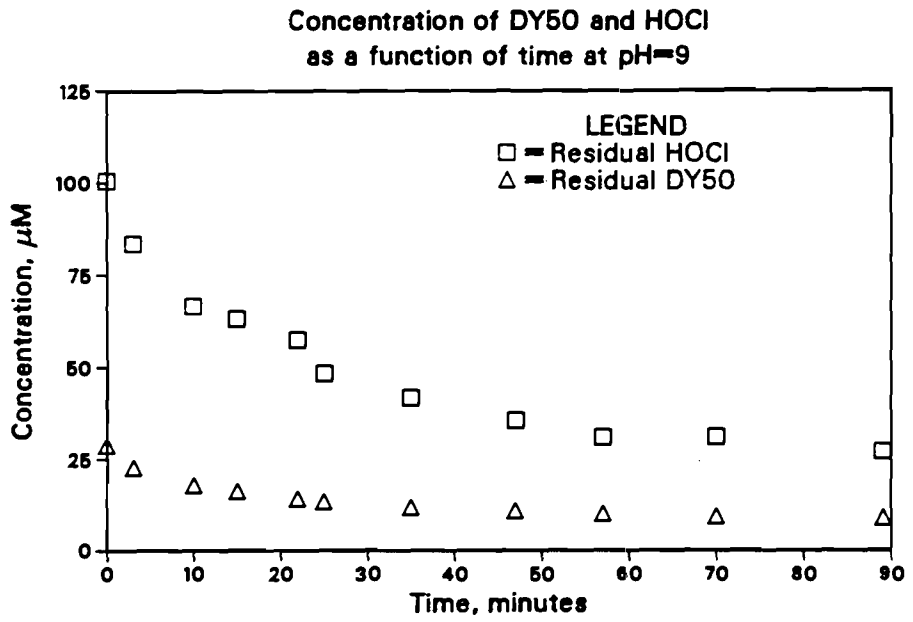
Concentration of DY50 and HOCl
as a function of time at pH=9
LEGEND
□ = Residual HOCl
△ = Residual DY50
Concentration, μM
Time, minutes

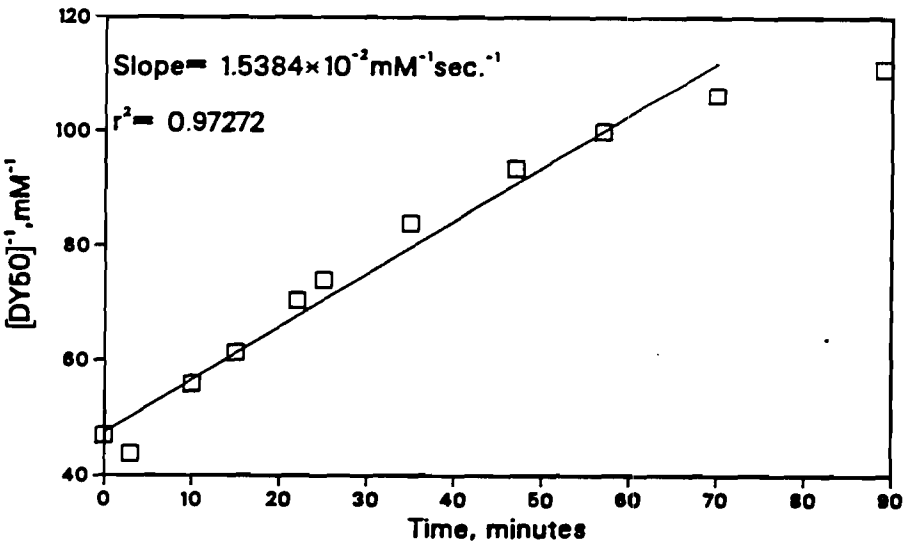
Slope= 1.5384×10⁻²mM⁻¹sec.⁻¹
r²= 0.97272
[DY50]⁻¹,mM⁻¹
Time, minutes

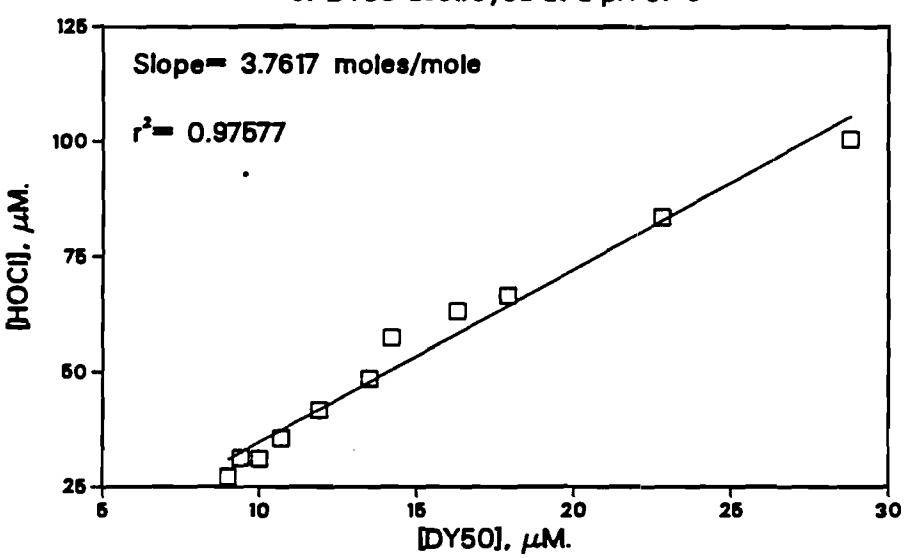
Moles of HOCl consumed per mole
of DY50 destroyed at a pH of 9
Slope= 3.7617 moles/mole
r²= 0.97577
[HOCl], μM.
[DY50], μM.

Figure A4.7

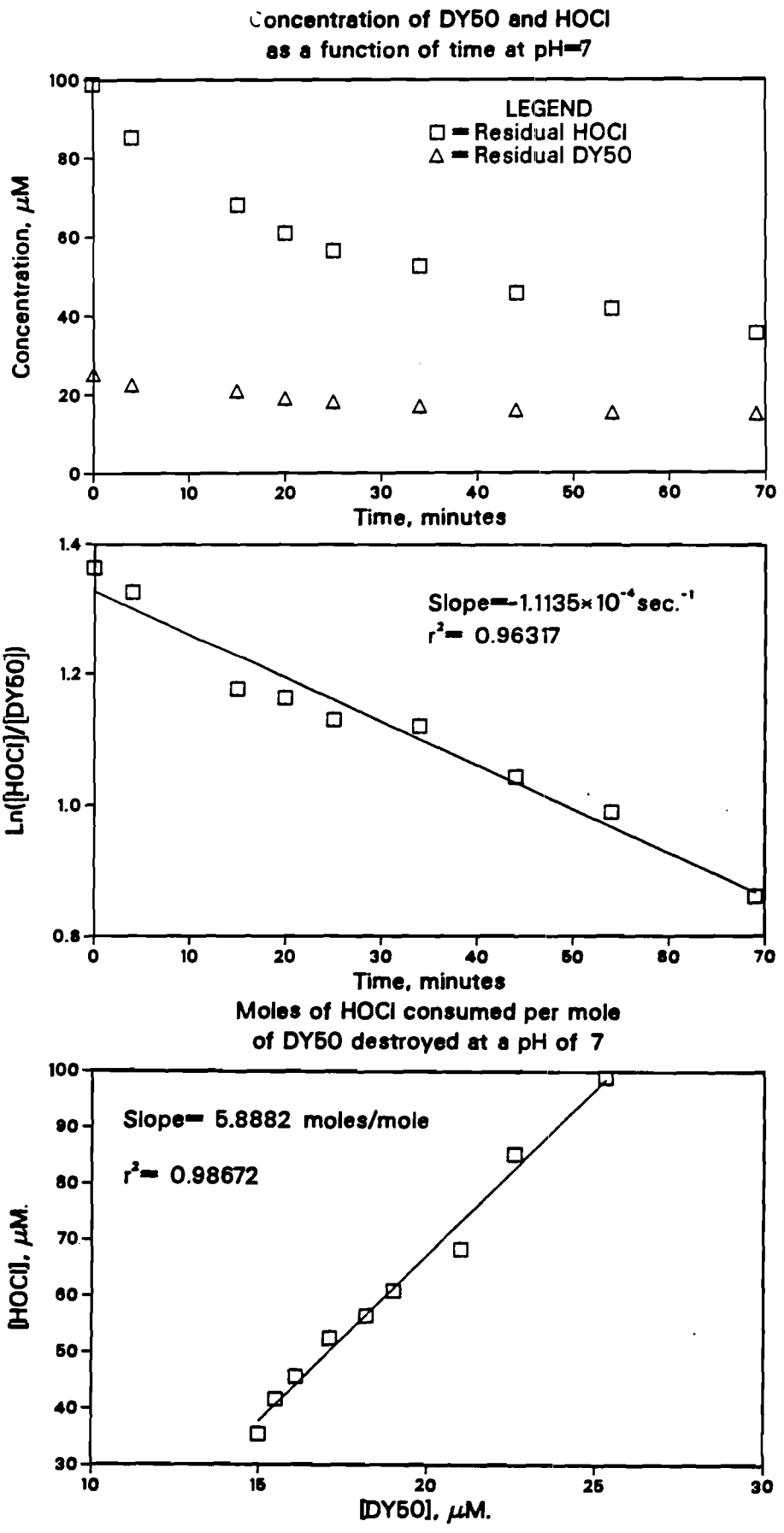
Concentration of DY50 and HOCl
as a function of time at pH=7
LEGEND
□ = Residual HOCl
△ = Residual DY50
Concentration, μM
Time, minutes
Slope=-1.1135×10⁻⁴sec.⁻¹
r²= 0.96317
Ln([HOCl]/[DY60])
Time, minutes
Moles of HOCl consumed per mole
of DY50 destroyed at a pH of 7
Slope= 5.8882 moles/mole
r²= 0.98672
[HOCl], μM.
[DY50], μM.

Figure A4.8

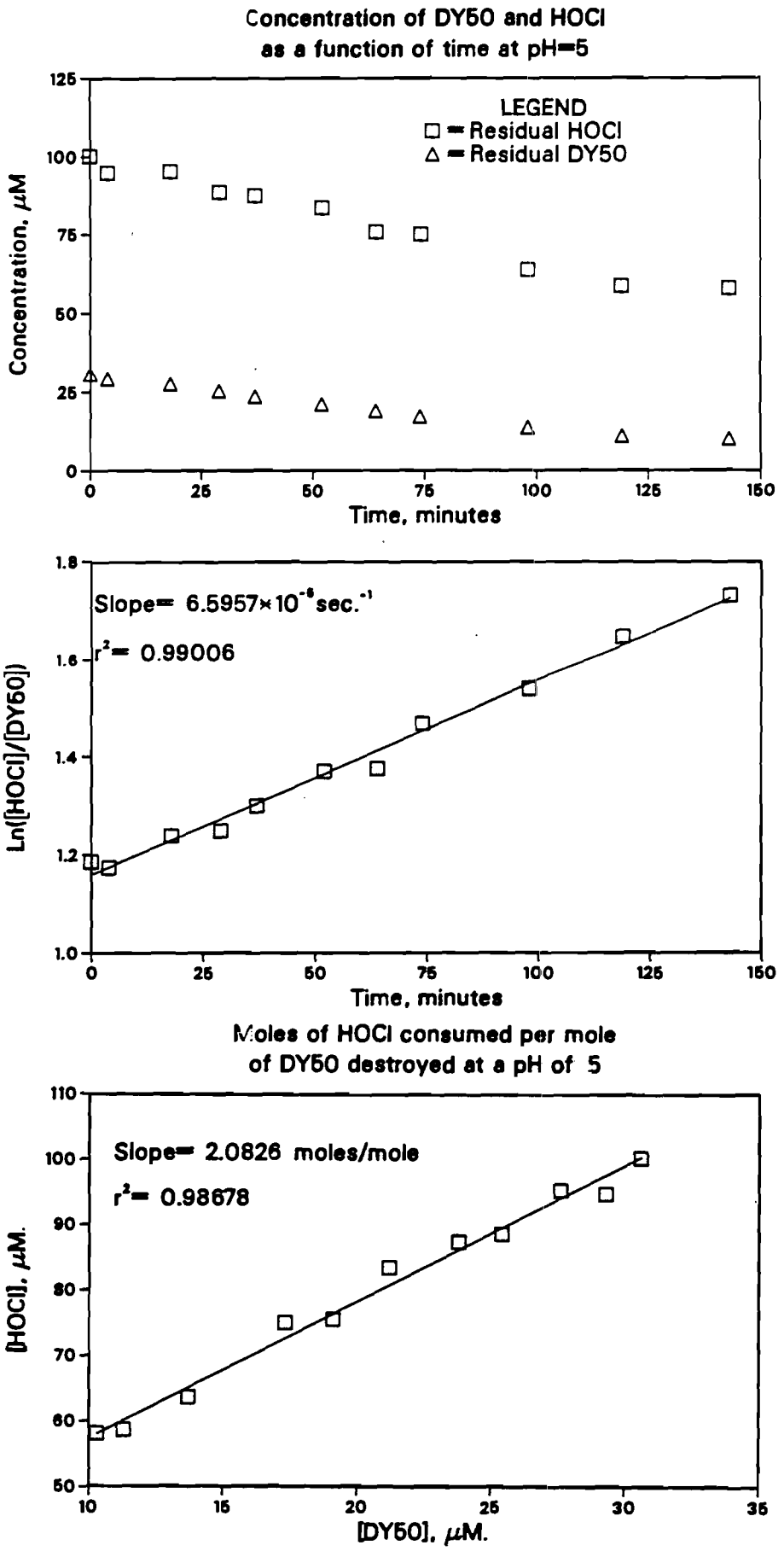
Concentration of DY50 and HOCl
as a function of time at pH=5
LEGEND
□ = Residual HOCl
△ = Residual DY50
Concentration, μM
Time, minutes
Slope= 6.5957×10⁻⁶ sec.⁻¹
r²= 0.99006
Ln([HOCl]/[DY60])
Time, minutes
Moles of HOCl consumed per mole
of DY50 destroyed at a pH of 5
Slope= 2.0826 moles/mole
r²= 0.98678
[HOCl], μM.
[DY50], μM.

Figure A4.9

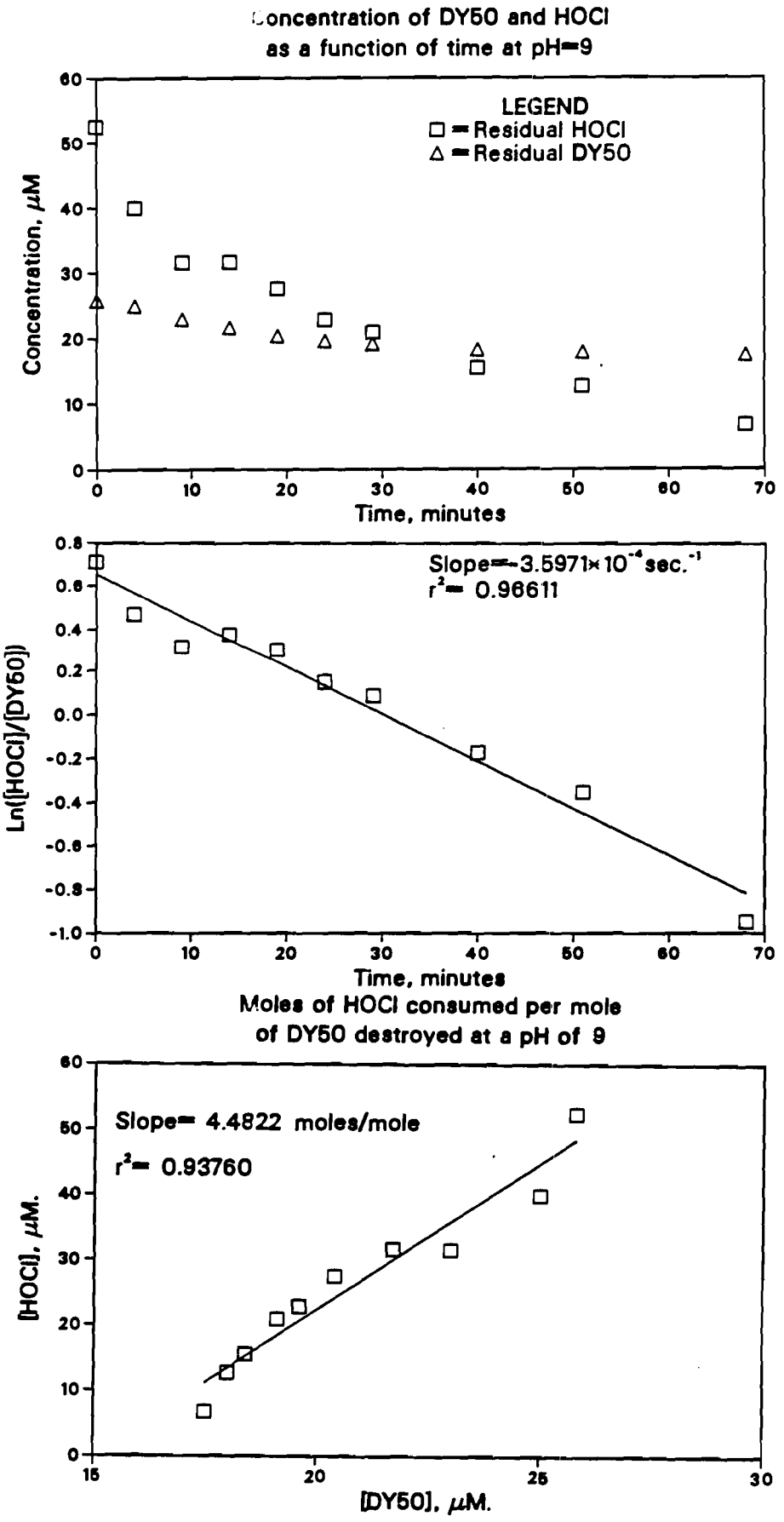
Concentration of DY50 and HOCl
as a function of time at pH=9
LEGEND
□ = Residual HOCl
△ = Residual DY50
Concentration, μM
Time, minutes
Slope=-3.5971×10⁻⁴ sec.⁻¹
r²= 0.96611
Ln([HOCl]/[DY50])
Time, minutes
Moles of HOCl consumed per mole
of DY50 destroyed at a pH of 9
Slope= 4.4822 moles/mole
r²= 0.93760
[HOCl], μM.
[DY50], μM.

Figure A4.10

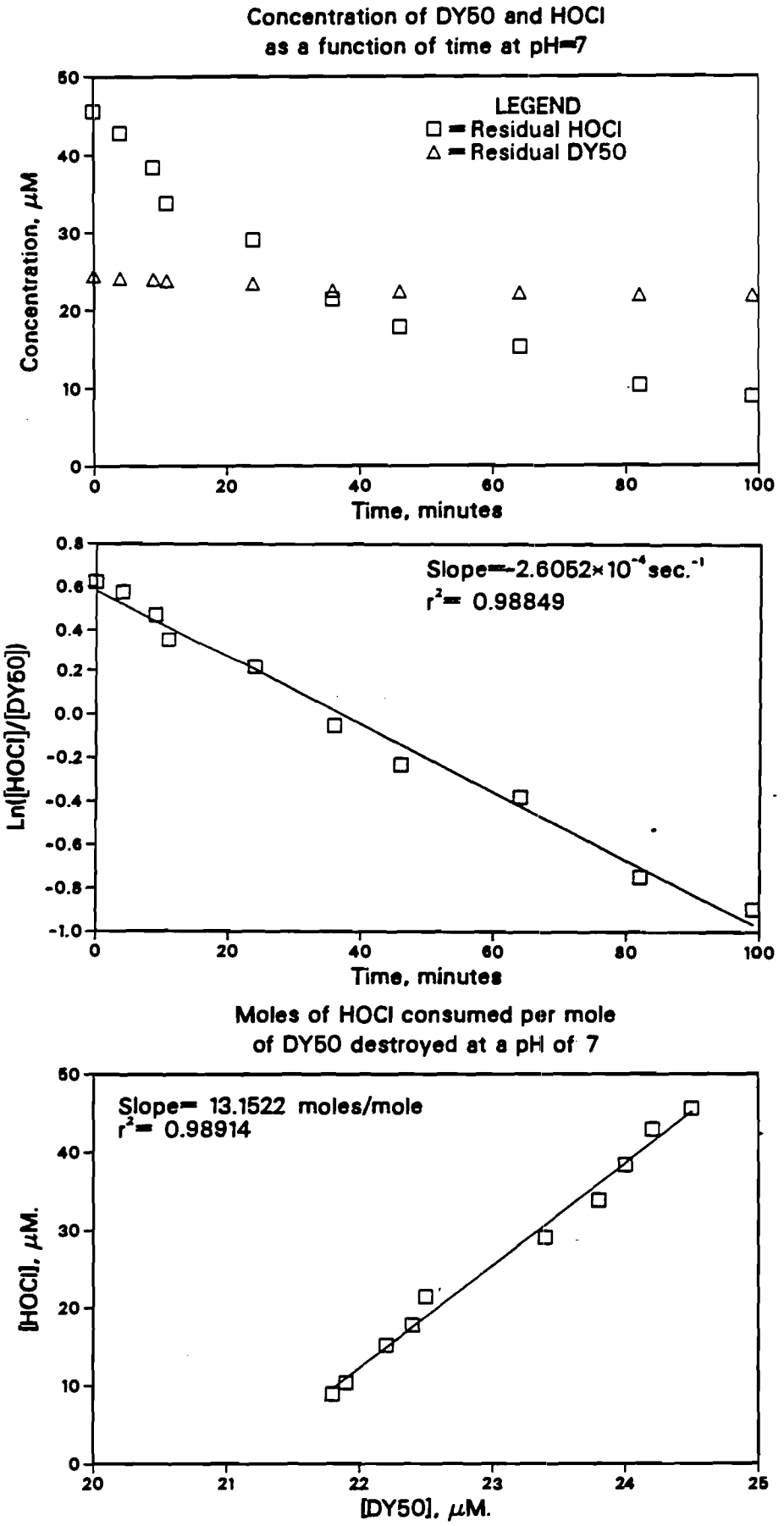
Concentration of DY50 and HOCl
as a function of time at pH=7
LEGEND
□ = Residual HOCl
△ = Residual DY50
Concentration, μM
Time, minutes
Slope=-2.6052×10⁻⁴ sec.⁻¹
r²= 0.98849
Ln([HOCl]/[DY60])
Time, minutes
Moles of HOCl consumed per mole
of DY50 destroyed at a pH of 7
Slope= 13.1522 moles/mole
r²= 0.98914
[HOCl], μM.
[DY50], μM.

Figure A4.11

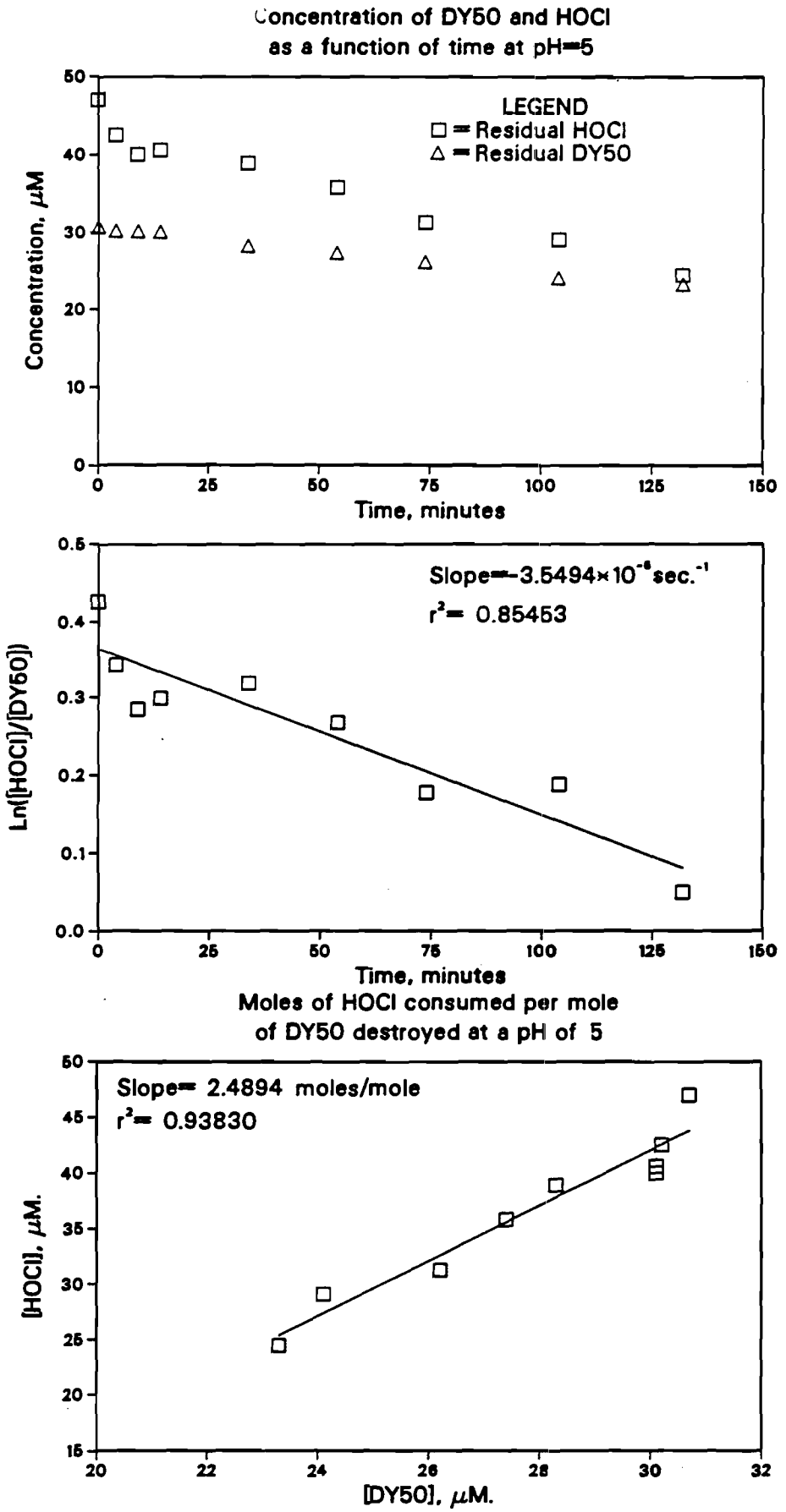
Concentration of DY50 and HOCl
as a function of time at pH=5
LEGEND
□ = Residual HOCl
△ = Residual DY50
Concentration, μM
Time, minutes
Slope=-3.5494×10⁻⁶sec.⁻¹
r²= 0.85453
Ln([HOCl]/[DY50])
Time, minutes
Moles of HOCl consumed per mole
of DY50 destroyed at a pH of 5
Slope= 2.4894 moles/mole
r²= 0.93830
[HOCl], μM.
[DY50], μM.

Figure A4.12

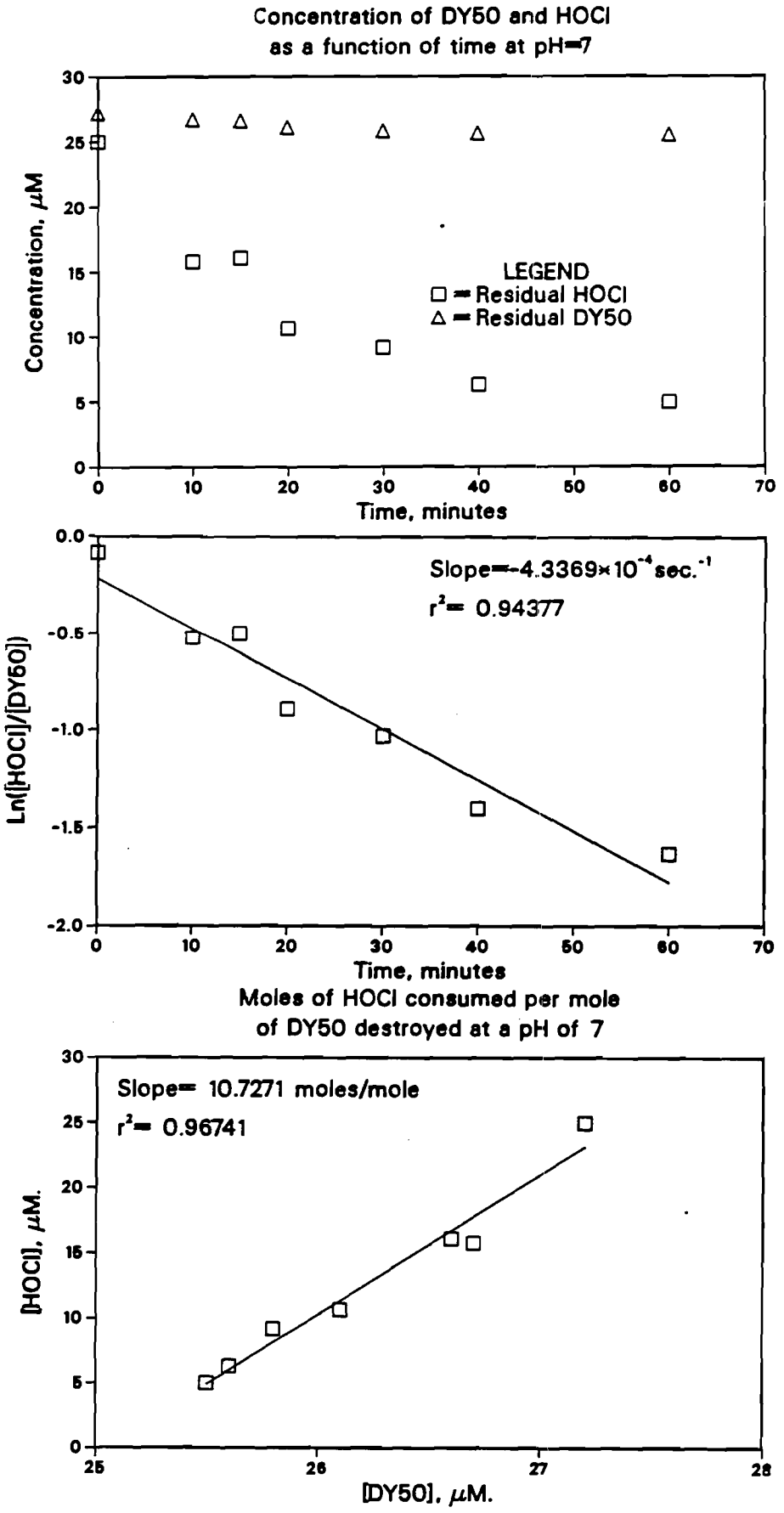
Concentration of DY50 and HOCl
as a function of time at pH=7
Concentration, μM
Time, minutes
LEGEND
□ = Residual HOCl
△ = Residual DY50
Ln([HOCl]/[DY60])
Slope=-4.3369×10⁻⁴sec.⁻¹
r²= 0.94377
Time, minutes
Moles of HOCl consumed per mole
of DY50 destroyed at a pH of 7
Slope= 10.7271 moles/mole
r²= 0.96741
[HOCl], μM.
[DY50], μM.

Figure A4.13

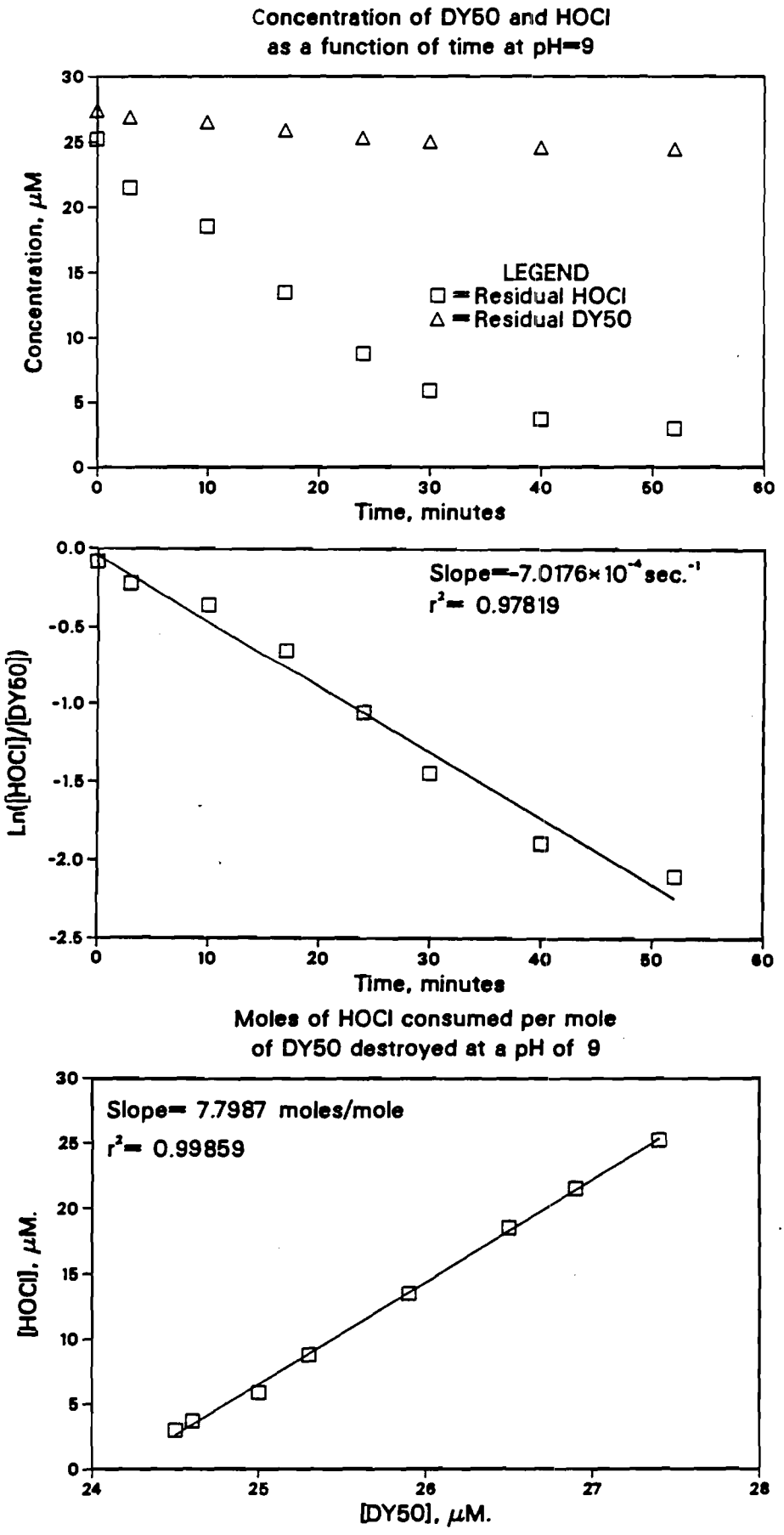
Concentration of DY50 and HOCl
as a function of time at pH=9
Concentration, μM
Time, minutes
LEGEND
□ = Residual HOCl
△ = Residual DY50
Ln([HOCl]/[DY60])
Slope=-7.0176×10⁻⁴ sec.⁻¹
r²= 0.97819
Time, minutes
Moles of HOCl consumed per mole
of DY50 destroyed at a pH of 9
Slope= 7.7987 moles/mole
r²= 0.99859
[HOCl], μM.
[DY50], μM.

Figure A4.14

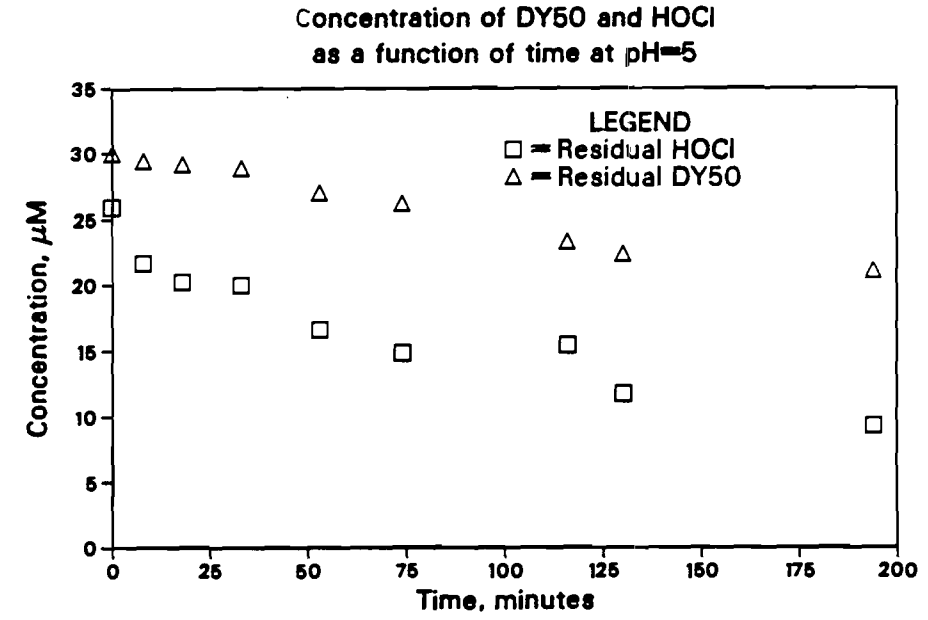
Concentration of DY50 and HOCl
as a function of time at pH=5
LEGEND
□ = Residual HOCl
△ = Residual DY50
Concentration, μM
Time, minutes

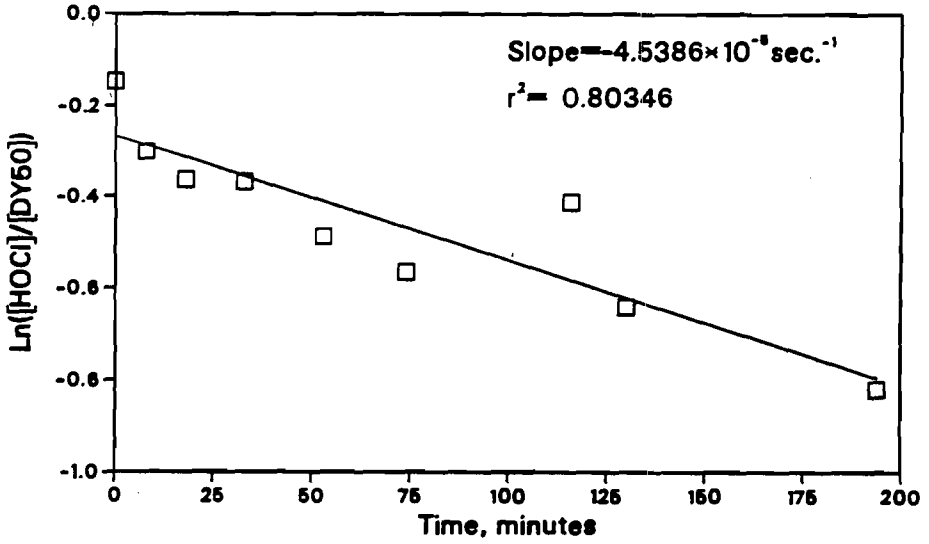
Slope=-4.5386×10⁻⁵sec.⁻¹
r²= 0.80346
Ln([HOCl]/[DY50])
Time, minutes

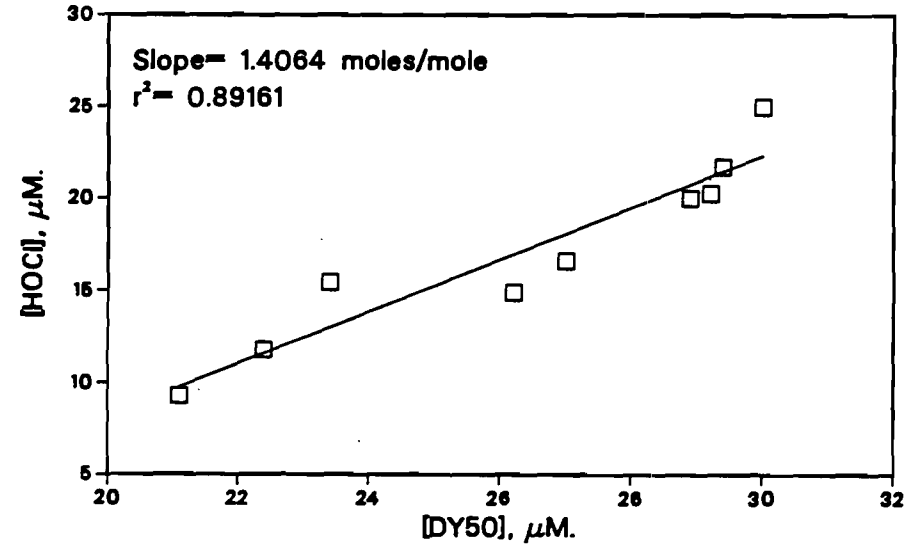
Moles of HOCl consumed per mole
of DY50 destroyed at a pH of 5
Slope= 1.4064 moles/mole
r²= 0.89161
[HOCl], μM.
[DY50], μM.

Figure A4.15

APPENDIX 5

DATA PLOTS FOR DIRECT YELLOW 12

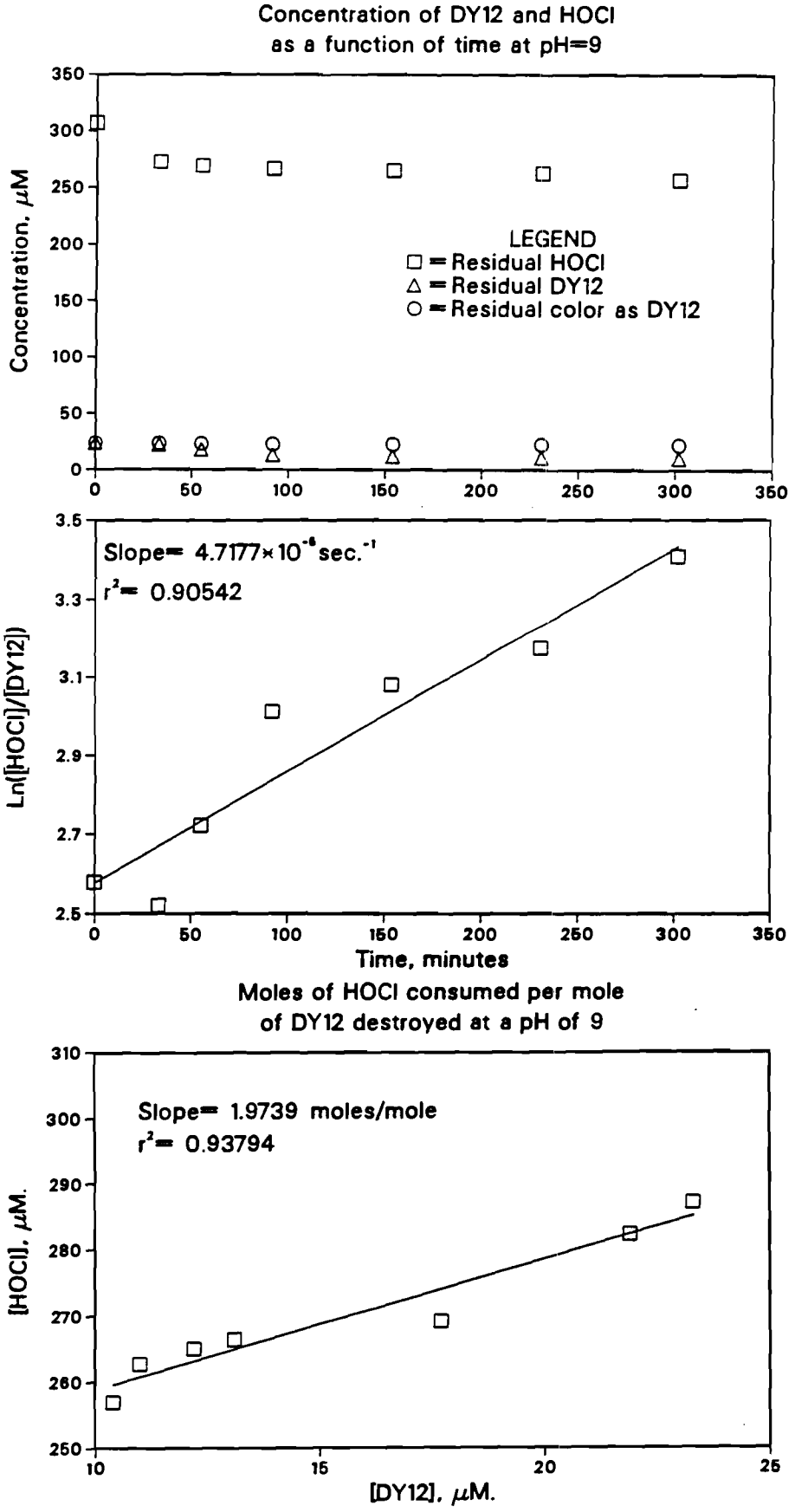
Concentration of DY12 and HOCl
as a function of time at pH=9
Concentration, μM
LEGEND
□ = Residual HOCl
△ = Residual DY12
○ = Residual color as DY12
Slope= 4.7177×10⁻⁶ sec.⁻¹
r²= 0.90542
Ln([HOCl]/[DY12])
Time, minutes
Moles of HOCl consumed per mole
of DY12 destroyed at a pH of 9
Slope= 1.9739 moles/mole
r²= 0.93794
[HOCl], μM.
[DY12], μM.

Figure A5.1

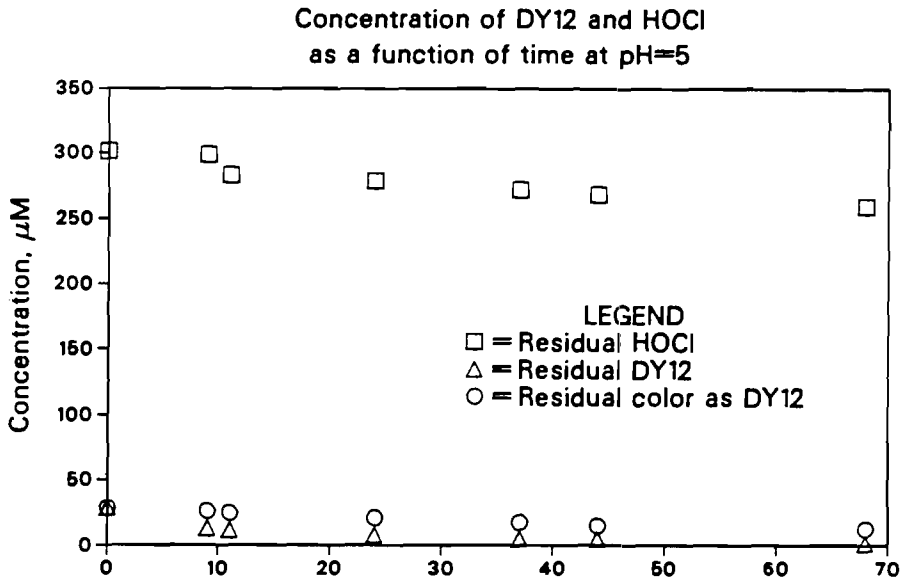
Concentration of DY12 and HOCl
as a function of time at pH=5
Concentration, μM
LEGEND
□ = Residual HOCl
△ = Residual DY12
○ = Residual color as DY12

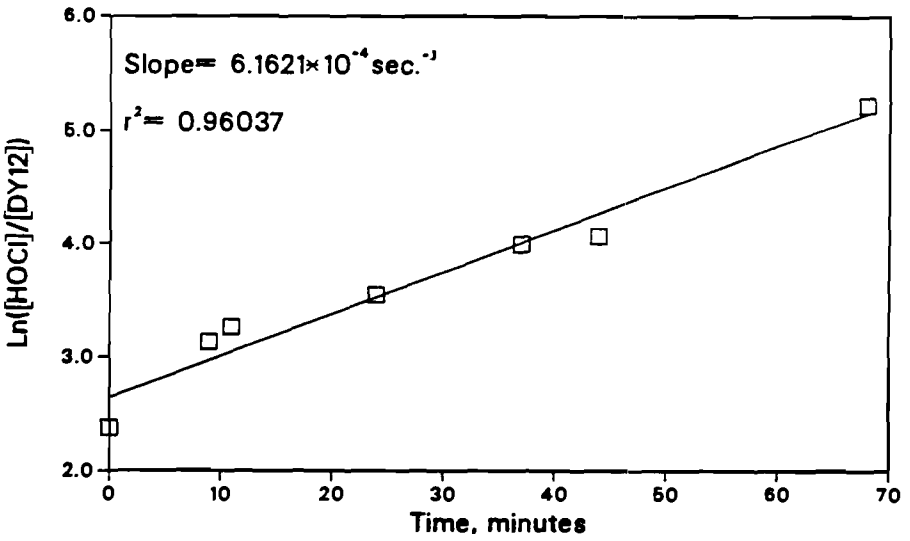
Slope= 6.1621×10⁻⁴ sec.⁻¹
r² = 0.96037
Ln([HOCl]/[DY12])
Time, minutes

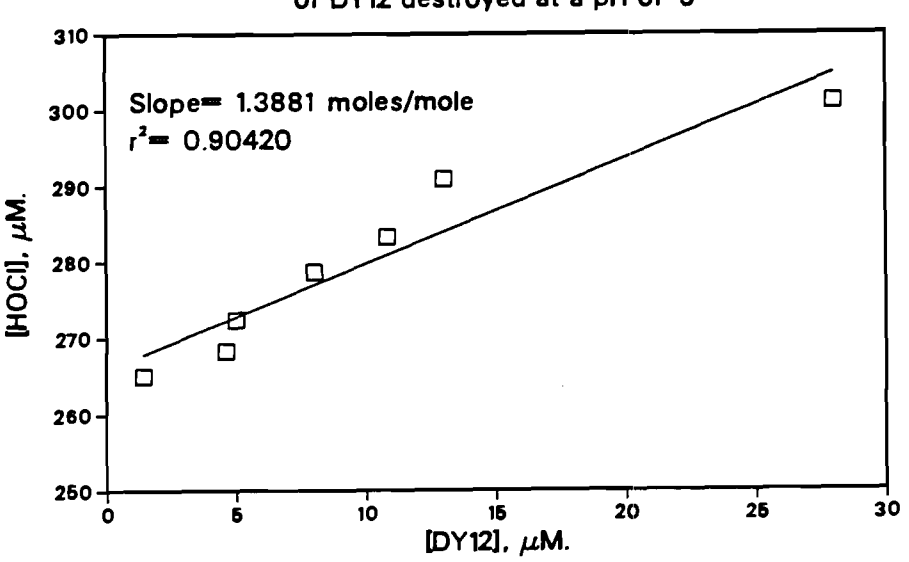
Moles of HOCl consumed per mole
of DY12 destroyed at a pH of 5
Slope= 1.3881 moles/mole
r² = 0.90420
[HOCl], μM.
[DY12], μM.

Figure A5.2

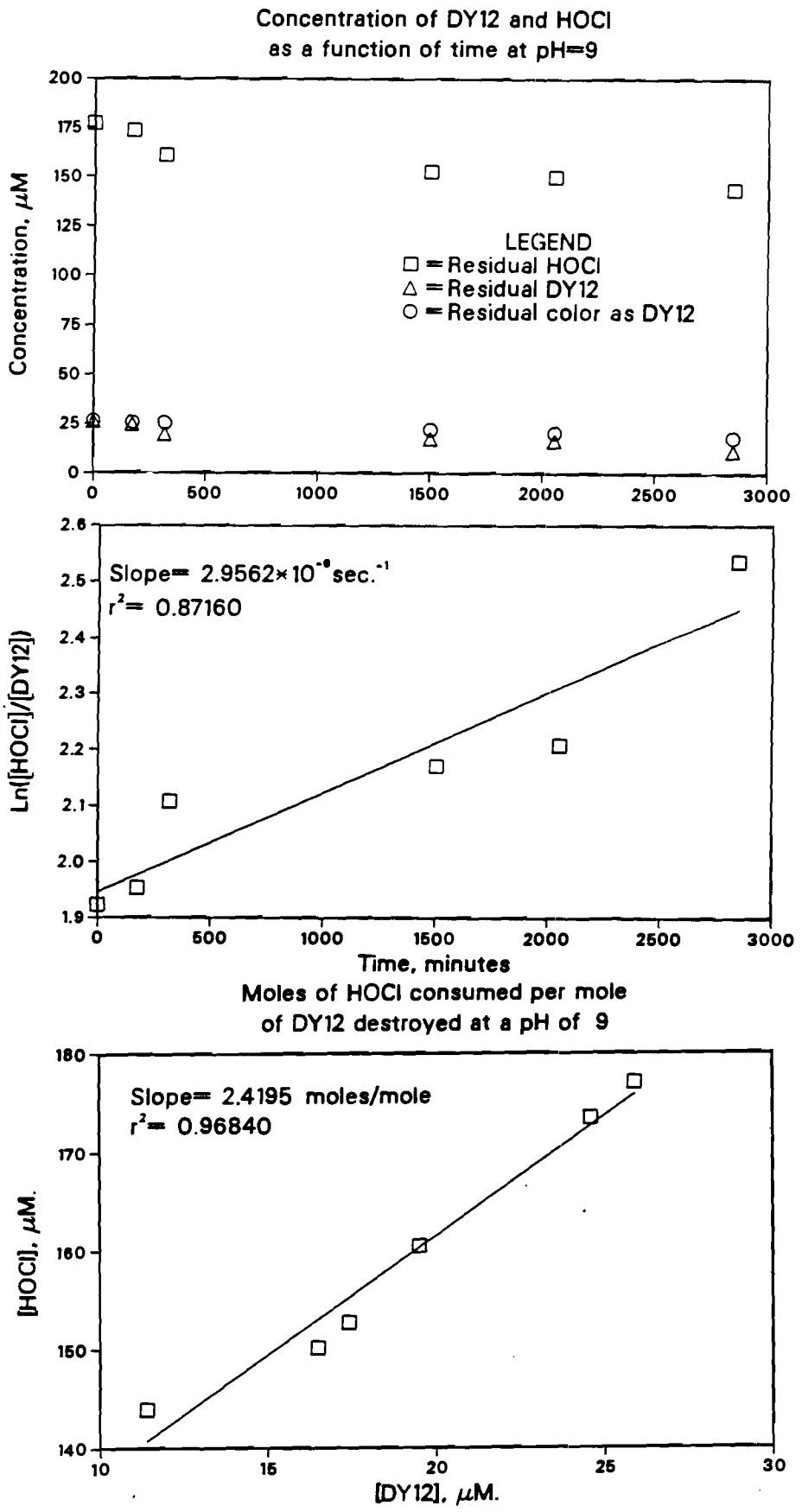
Concentration of DY12 and HOCl
as a function of time at pH=9
Concentration, μM
LEGEND
□ = Residual HOCl
△ = Residual DY12
○ = Residual color as DY12
Ln([HOCl]/[DY12])
Slope= 2.9562×10⁻⁶ sec.⁻¹
r²= 0.87160
Time, minutes
Moles of HOCl consumed per mole
of DY12 destroyed at a pH of 9
Slope= 2.4195 moles/mole
r²= 0.96840
[HOCl], μM.
[DY12], μM.

Figure A5.3

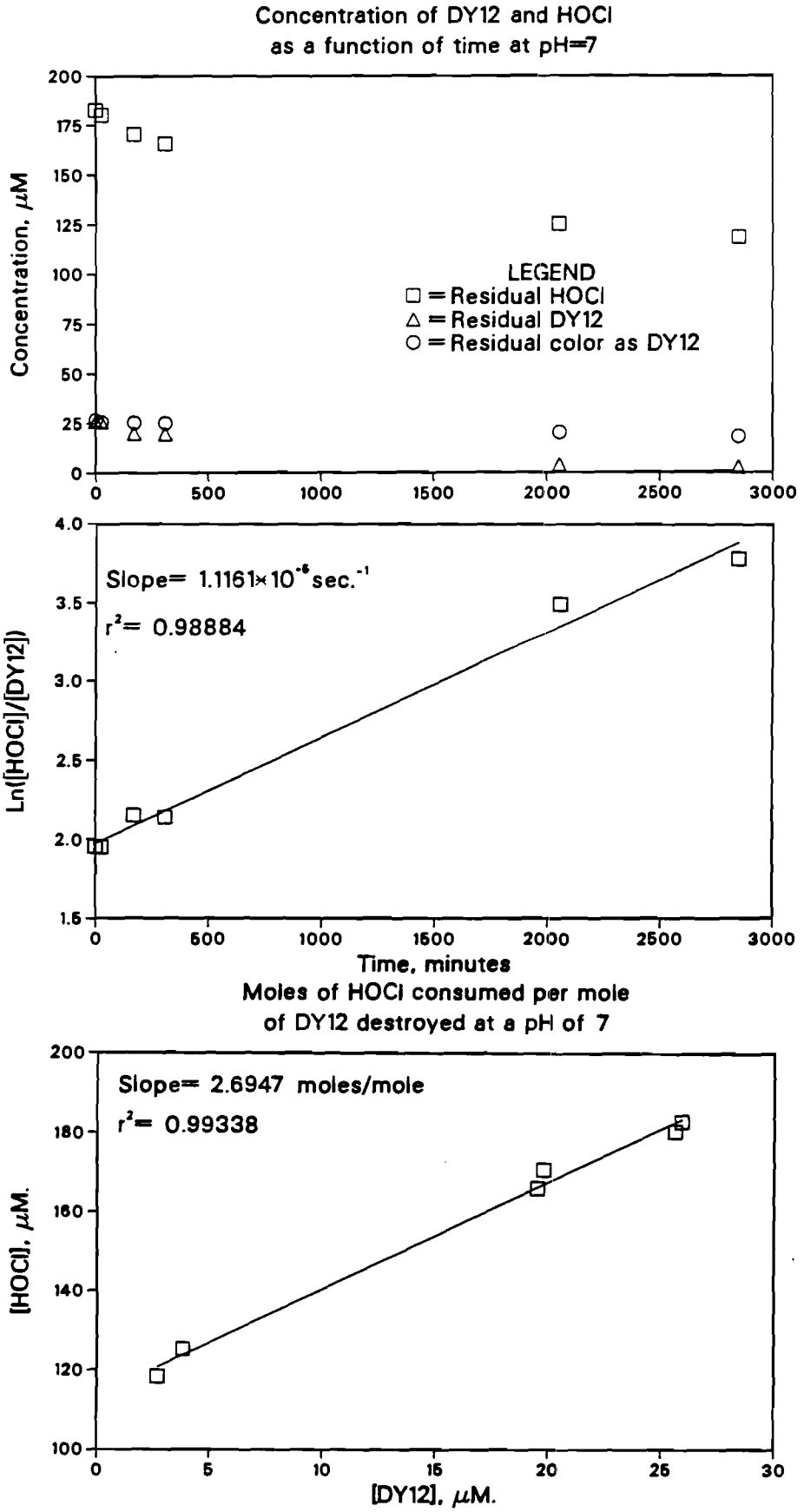
Concentration of DY12 and HOCl
as a function of time at pH=7
Concentration, μM
LEGEND
□ = Residual HOCl
△ = Residual DY12
○ = Residual color as DY12
Ln([HOCl]/[DY12])
Slope= 1.1161×10⁻⁶sec.⁻¹
r²= 0.98884
Time, minutes
Moles of HOCl consumed per mole
of DY12 destroyed at a pH of 7
[HOCl], μM.
Slope= 2.6947 moles/mole
r²= 0.99338
[DY12], μM.

Figure A5.4

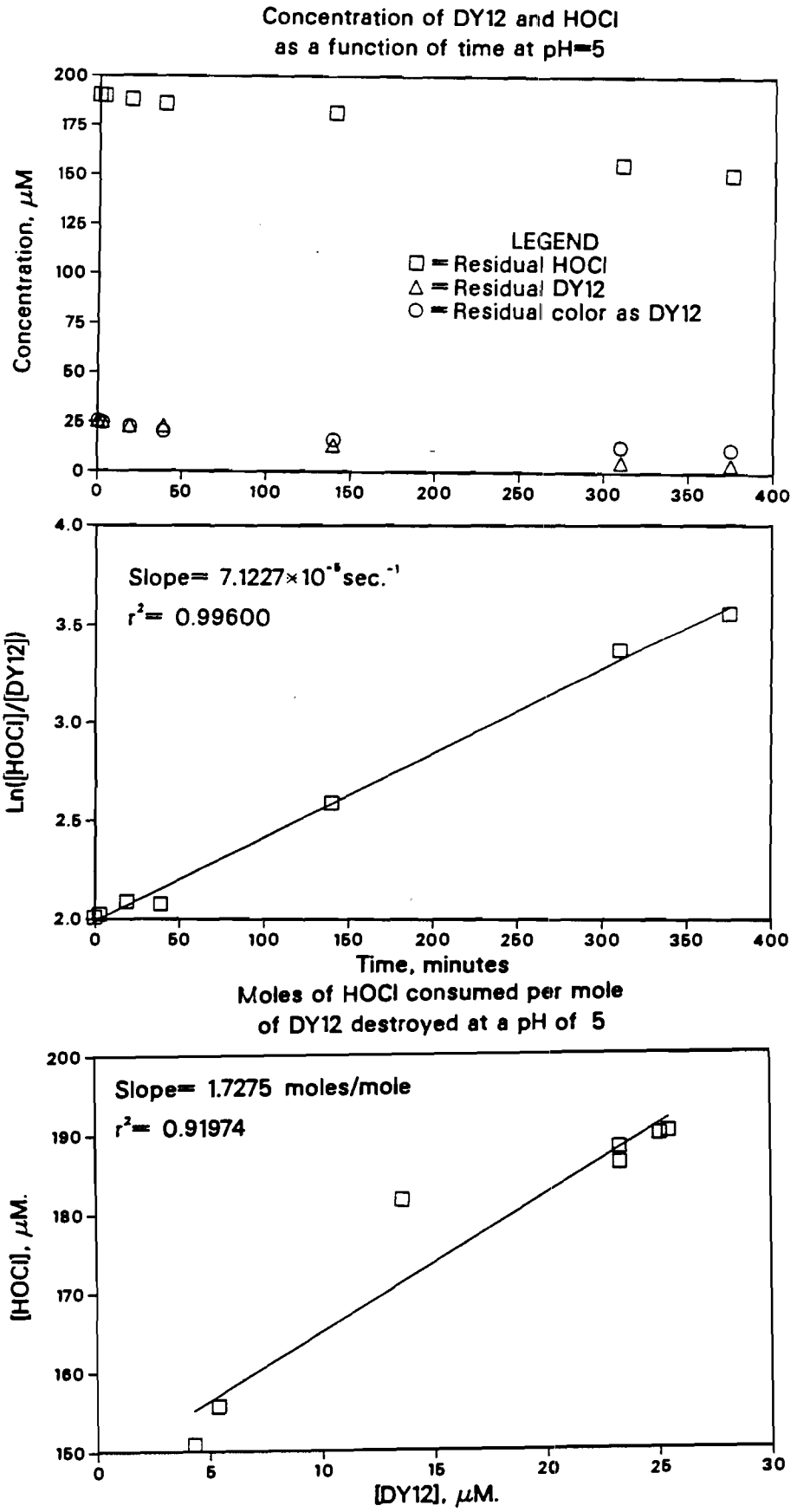
Concentration of DY12 and HOCl
as a function of time at pH=5
Concentration, μM
LEGEND
□ = Residual HOCl
△ = Residual DY12
○ = Residual color as DY12
Slope= 7.1227×10⁻⁵ sec.⁻¹
r²= 0.99600
Ln([HOCl]/[DY12])
Time, minutes
Moles of HOCl consumed per mole
of DY12 destroyed at a pH of 5
Slope= 1.7275 moles/mole
r²= 0.91974
[HOCl], μM.
[DY12], μM.

Figure A5.5

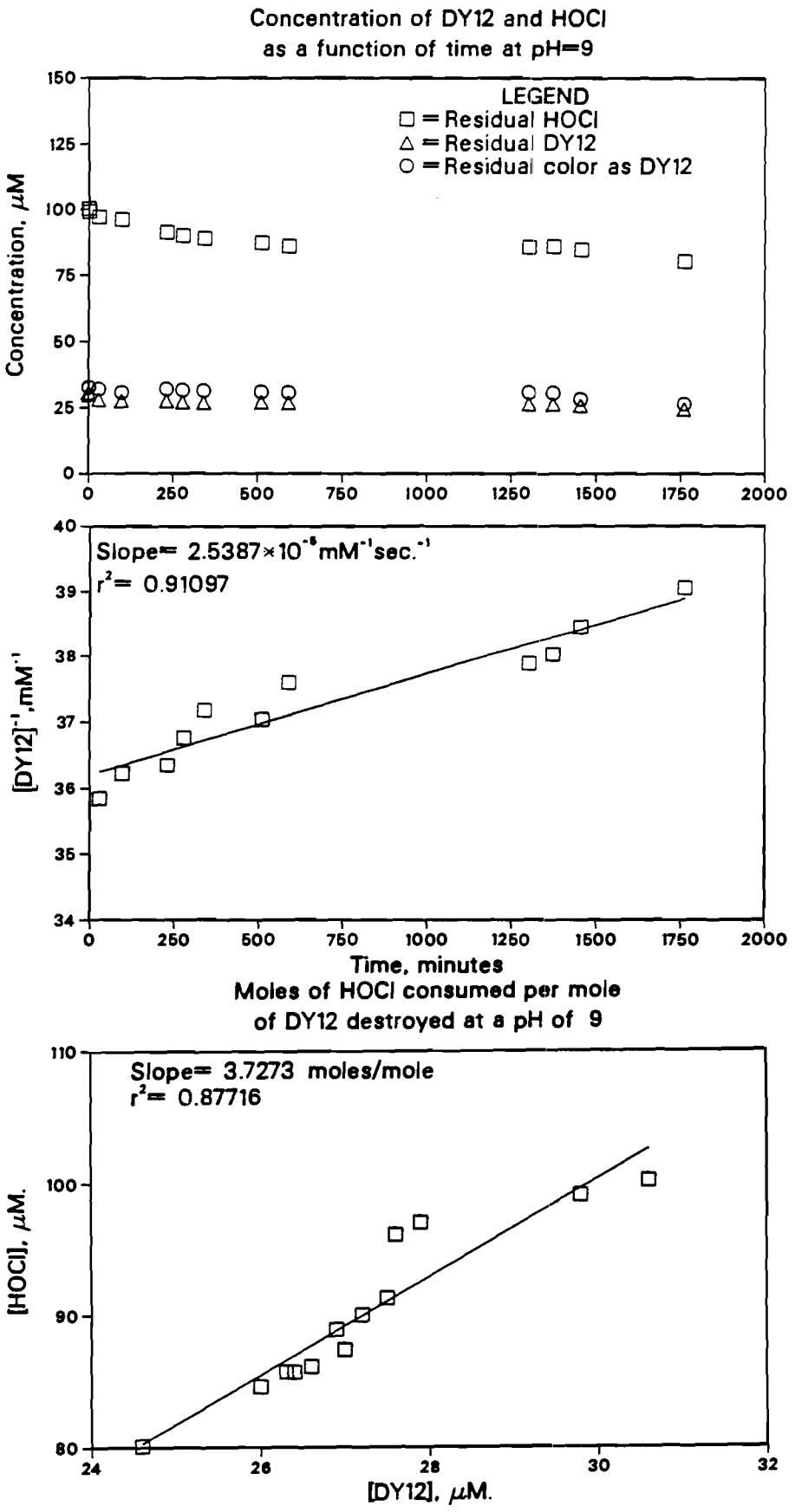
Concentration of DY12 and HOCl
as a function of time at pH=9
LEGEND
□ = Residual HOCl
△ = Residual DY12
○ = Residual color as DY12
Concentration, μM
150
125
100
75
50
25
0
0
250
500
750
1000
1250
1500
1750
2000
Slope= 2.5387×10⁻⁶mM⁻¹sec.⁻¹
r²= 0.91097
[DY12]⁻¹,mM⁻¹
40
39
38
37
36
35
34
Time, minutes
Moles of HOCl consumed per mole
of DY12 destroyed at a pH of 9
Slope= 3.7273 moles/mole
r²= 0.87716
[HOCl], μM.
110
100
90
80
24
26
28
30
32
[DY12], μM.

Figure A5.6

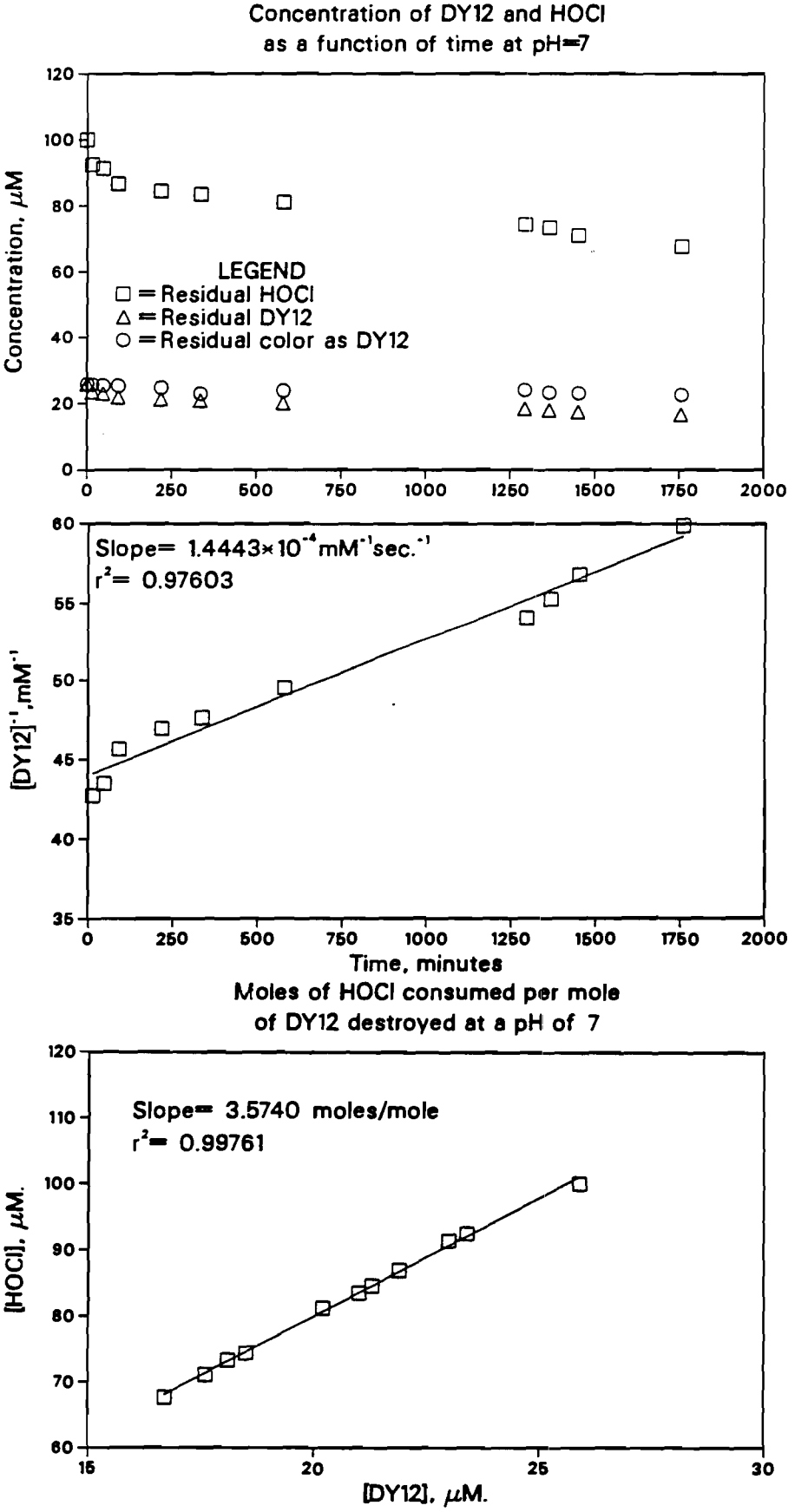
Concentration of DY12 and HOCl
as a function of time at pH=7
Concentration, μM
LEGEND
□ = Residual HOCl
△ = Residual DY12
○ = Residual color as DY12
Slope= 1.4443×10⁻⁴ mM⁻¹sec.⁻¹
r²= 0.97603
[DY12]⁻¹, mM⁻¹
Time, minutes
Moles of HOCl consumed per mole
of DY12 destroyed at a pH of 7
Slope= 3.5740 moles/mole
r²= 0.99761
[HOCl], μM.
[DY12], μM.

Figure A5.7

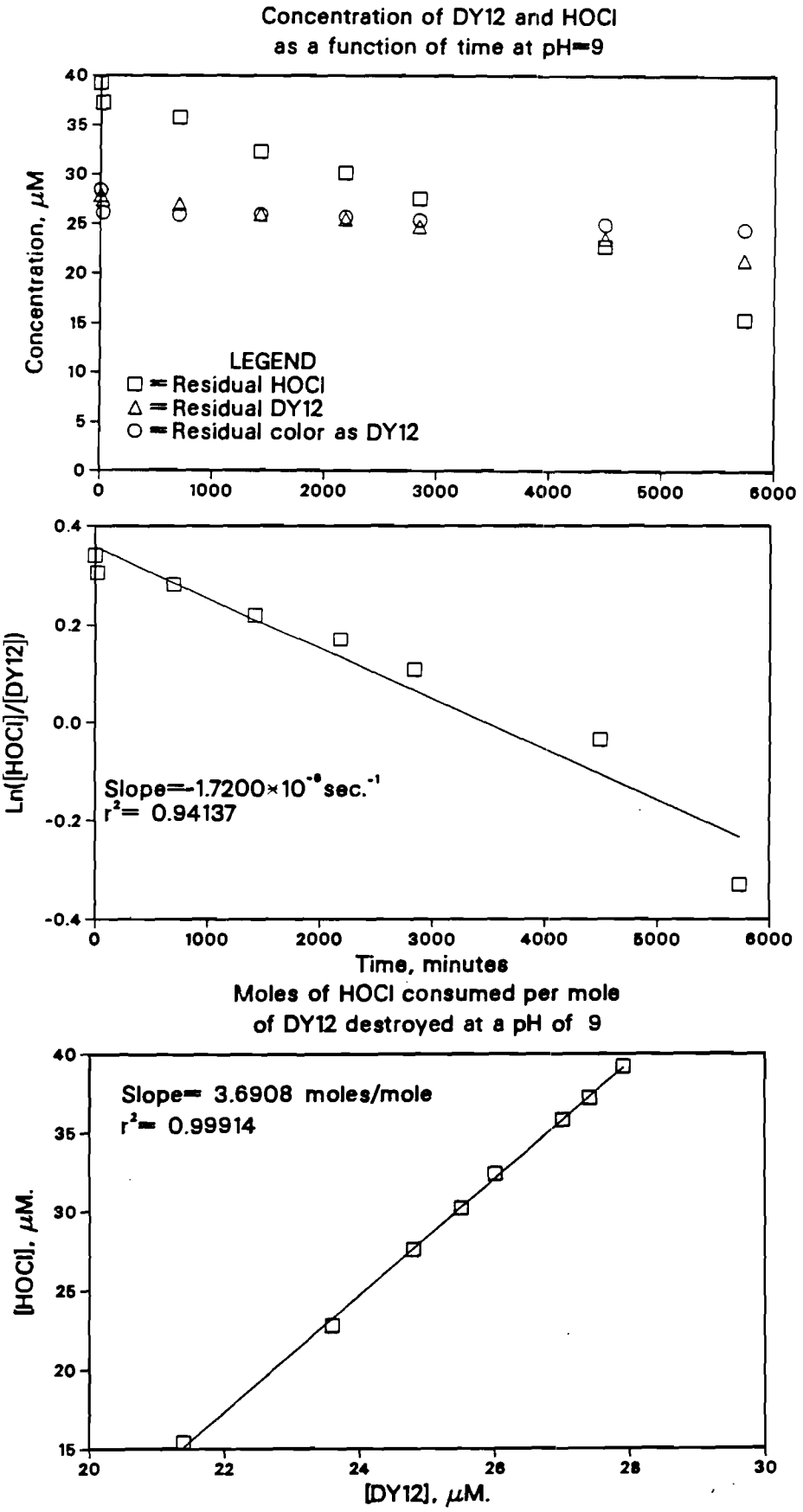
Concentration of DY12 and HOCl
as a function of time at pH=9
Concentration, μM
LEGEND
□ = Residual HOCl
△ = Residual DY12
○ = Residual color as DY12
Ln([HOCl]/[DY12])
Slope=-1.7200×10⁻⁶sec.⁻¹
r²= 0.94137
Time, minutes
Moles of HOCl consumed per mole
of DY12 destroyed at a pH of 9
Slope= 3.6908 moles/mole
r²= 0.99914
[HOCl], μM.
[DY12], μM.

Figure A5.8

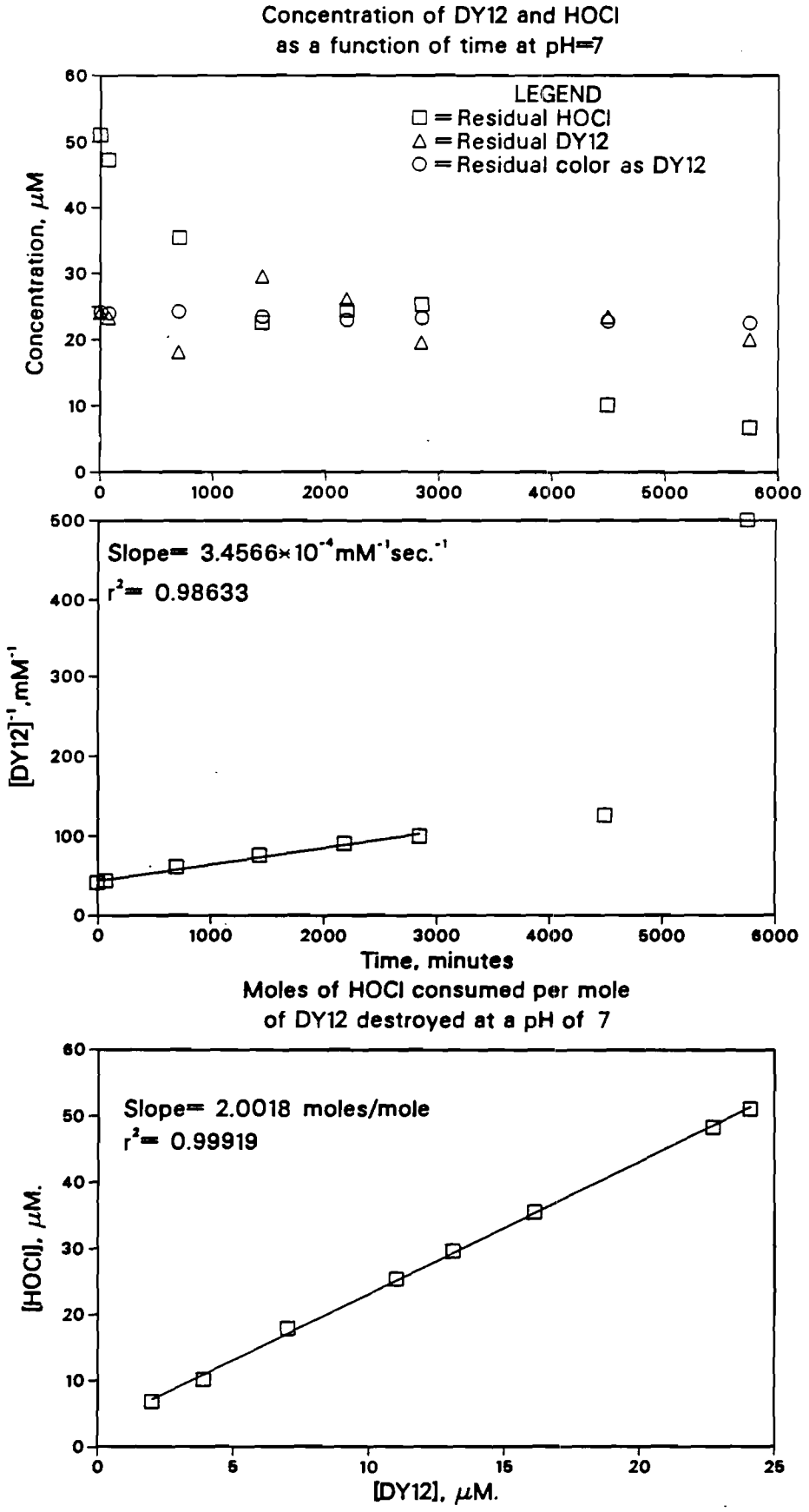
Concentration of DY12 and HOCl
as a function of time at pH=7
LEGEND
□ = Residual HOCl
△ = Residual DY12
○ = Residual color as DY12
Concentration, μM
Slope= 3.4566×10⁻⁴mM⁻¹sec.⁻¹
r²= 0.98633
[DY12]⁻¹,mM⁻¹
Time, minutes
Moles of HOCl consumed per mole
of DY12 destroyed at a pH of 7
Slope= 2.0018 moles/mole
r²= 0.99919
[HOCl], μM.
[DY12], μM.

Figure A5.9

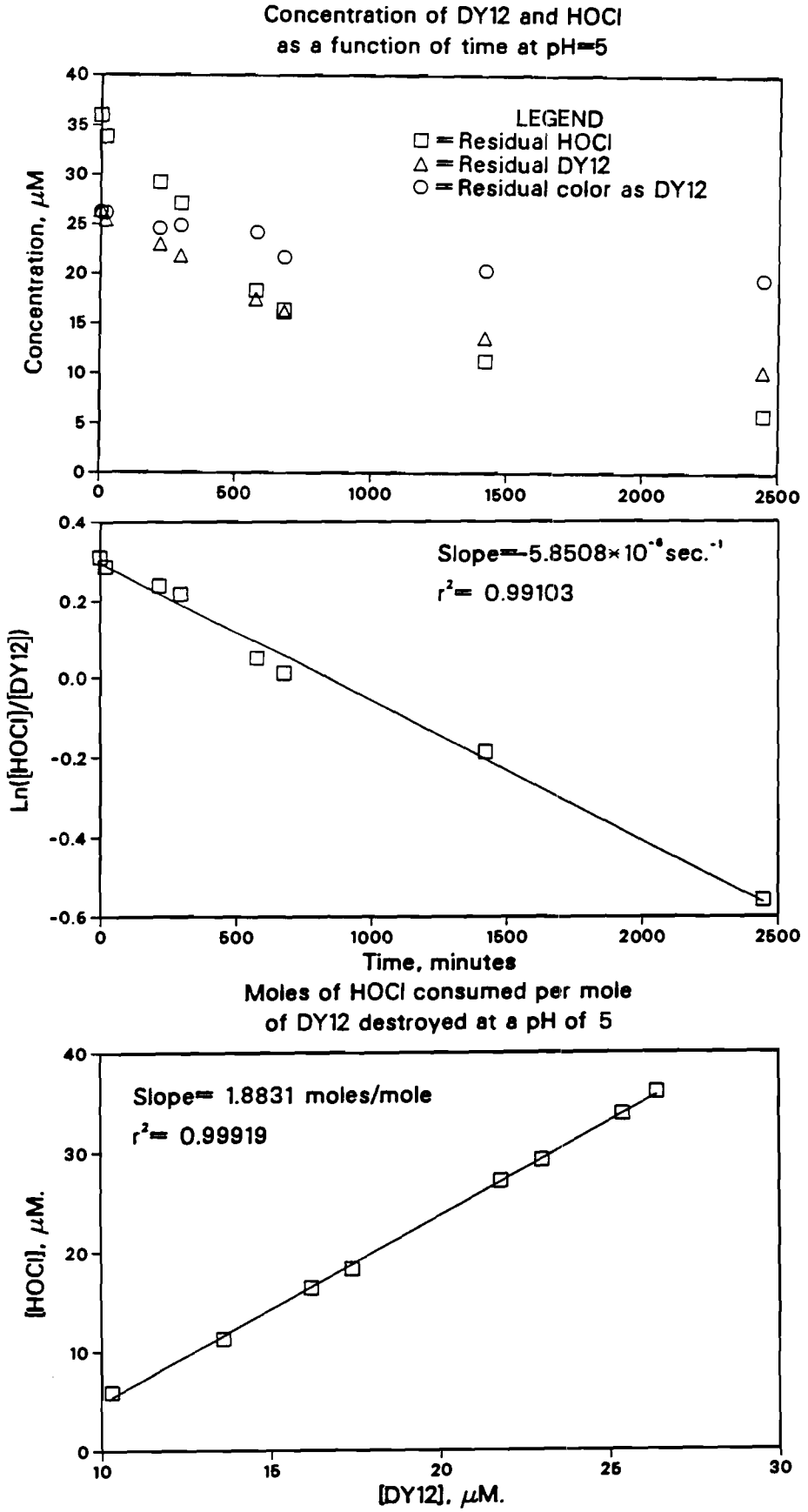
Concentration of DY12 and HOCl
as a function of time at pH=5
LEGEND
□ = Residual HOCl
△ = Residual DY12
○ = Residual color as DY12
Concentration, μM
Slope=-5.8508×10⁻⁶sec.⁻¹
r²= 0.99103
Ln([HOCl]/[DY12])
Time, minutes
Moles of HOCl consumed per mole
of DY12 destroyed at a pH of 5
Slope= 1.8831 moles/mole
r²= 0.99919
[HOCl], μM.
[DY12], μM.

Figure A5.10

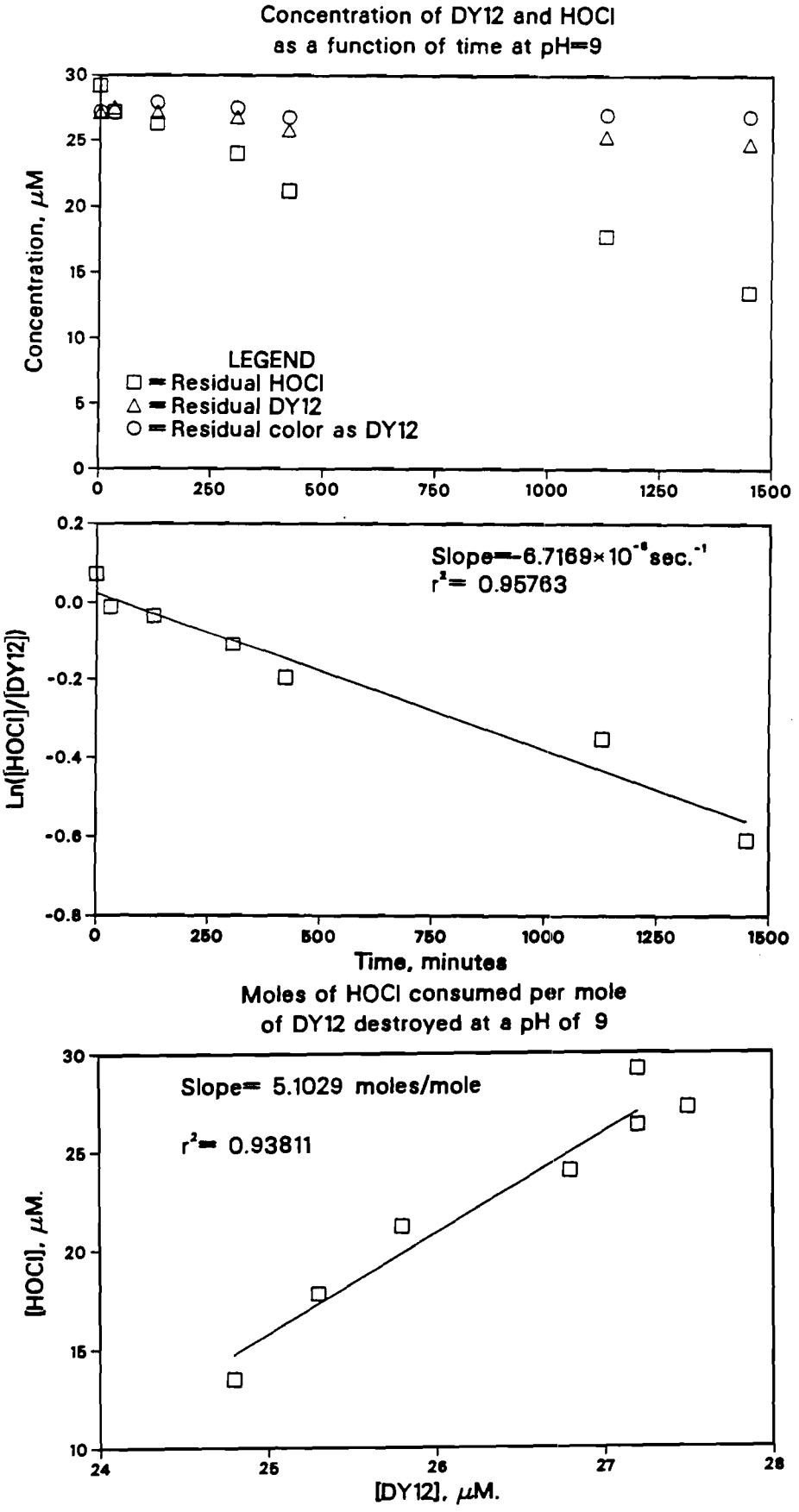
Concentration of DY12 and HOCl
as a function of time at pH=9
Concentration, μM
LEGEND
□ = Residual HOCl
△ = Residual DY12
○ = Residual color as DY12
Slope=-6.7169×10⁻⁴sec.⁻¹
r²= 0.95763
Ln([HOCl]/[DY12])
Time, minutes
Moles of HOCl consumed per mole
of DY12 destroyed at a pH of 9
Slope= 5.1029 moles/mole
r²= 0.93811
[HOCl], μM.
[DY12], μM.

Figure A5.11

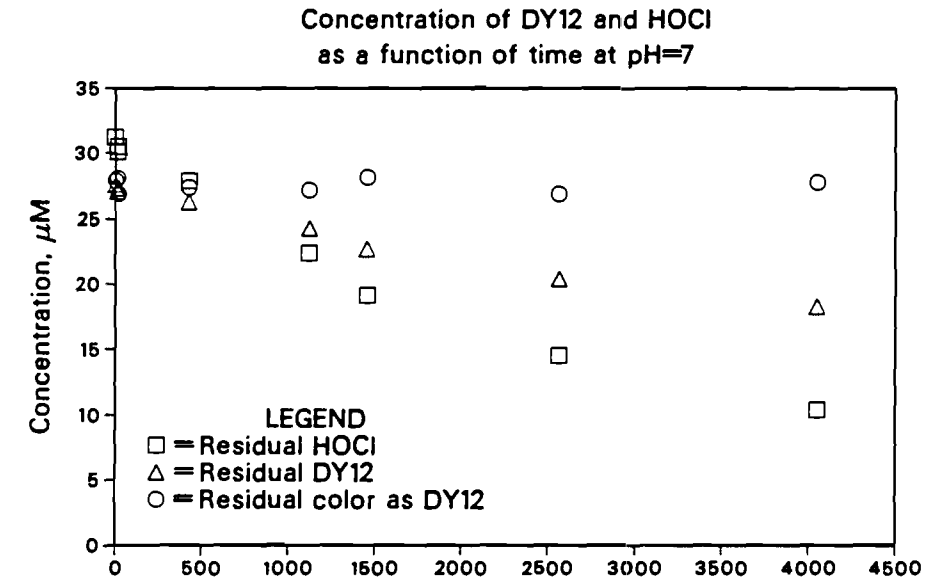
Concentration of DY12 and HOCl
as a function of time at pH=7
Concentration, μM
LEGEND
□ = Residual HOCl
△ = Residual DY12
○ = Residual color as DY12

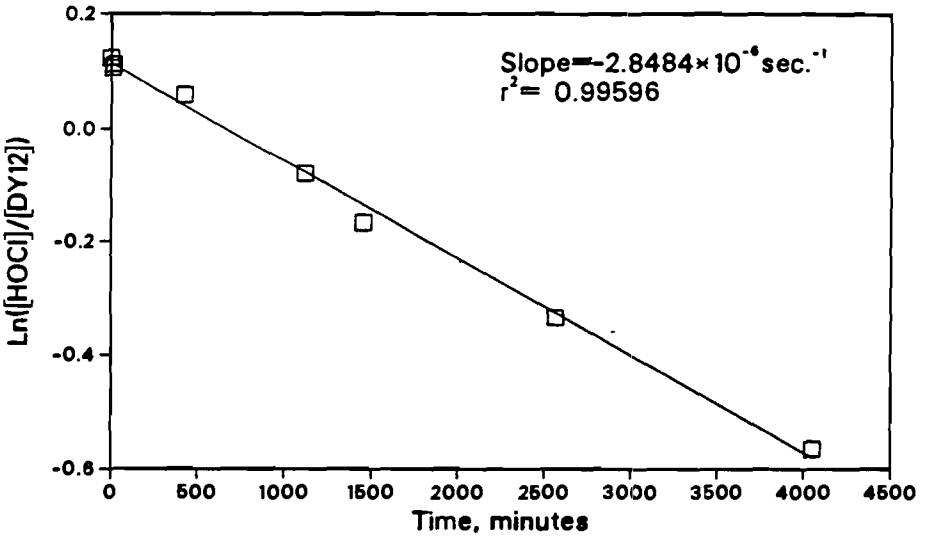
Slope=-2.8484×10⁻⁶ sec.⁻¹
r² = 0.99596
Ln([HOCl]/[DY12])
Time, minutes

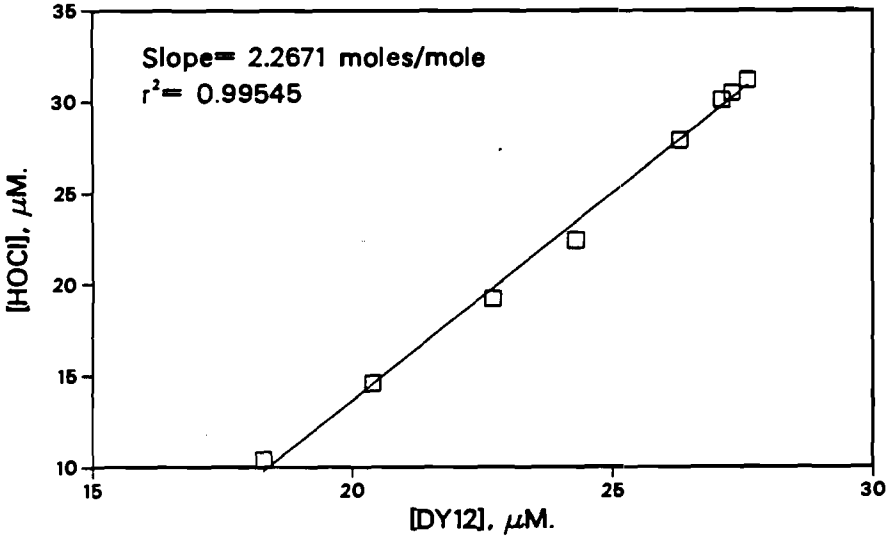
Moles of HOCl consumed per mole
of DY12 destroyed at a pH of 7
Slope= 2.2671 moles/mole
r² = 0.99545
[HOCl], μM.
[DY12], μM.

Figure A5.12

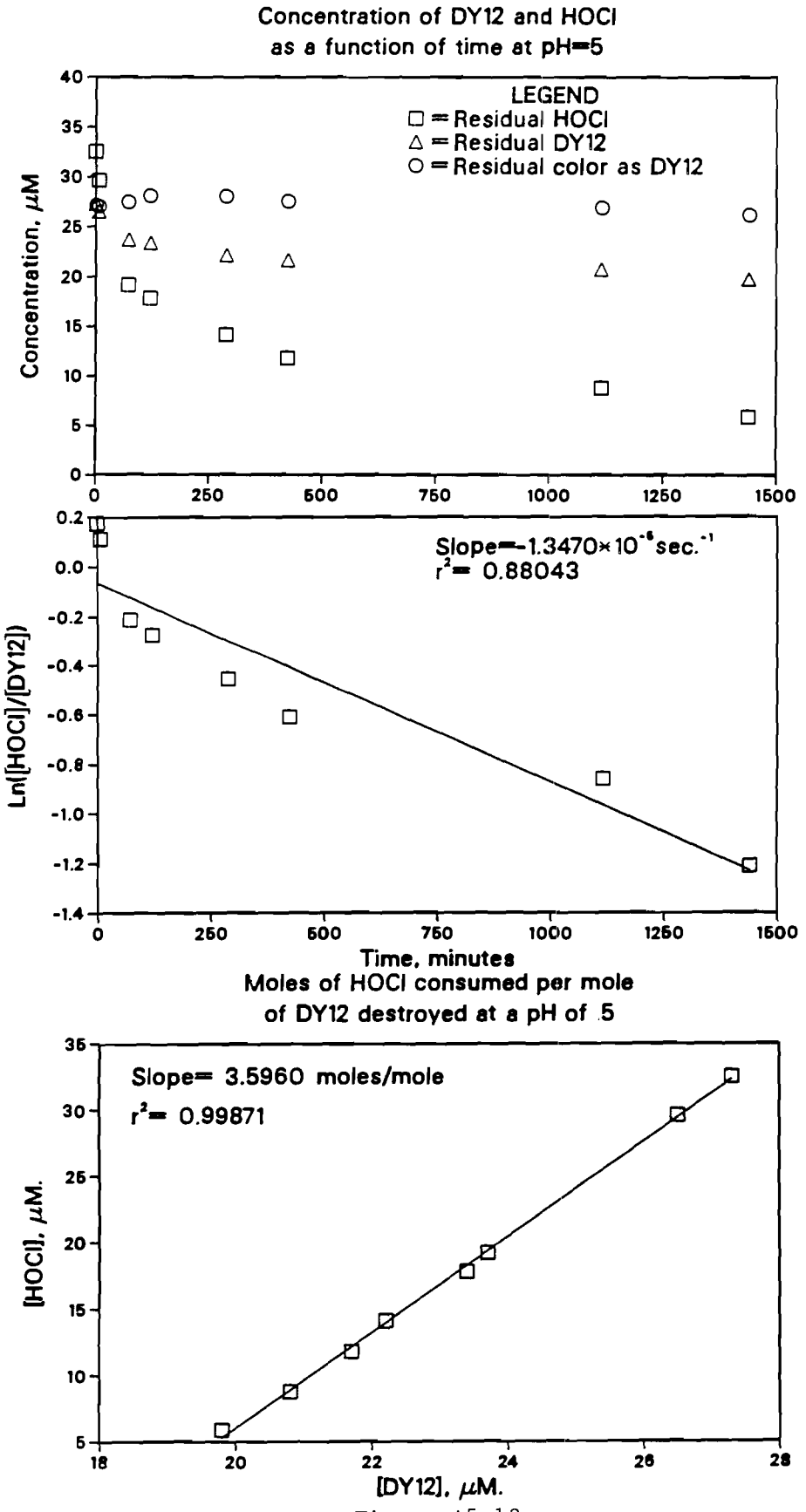
Concentration of DY12 and HOCl
as a function of time at pH=5
LEGEND
□ = Residual HOCl
△ = Residual DY12
○ = Residual color as DY12
Concentration, μM
Slope=-1.3470×10⁻⁵sec.⁻¹
r²= 0.88043
Ln[[HOCl]/[DY12]]
Time, minutes
Moles of HOCl consumed per mole
of DY12 destroyed at a pH of 5
Slope= 3.5960 moles/mole
r²= 0.99871
[HOCl], μM.
[DY12], μM.

Figure A5.13

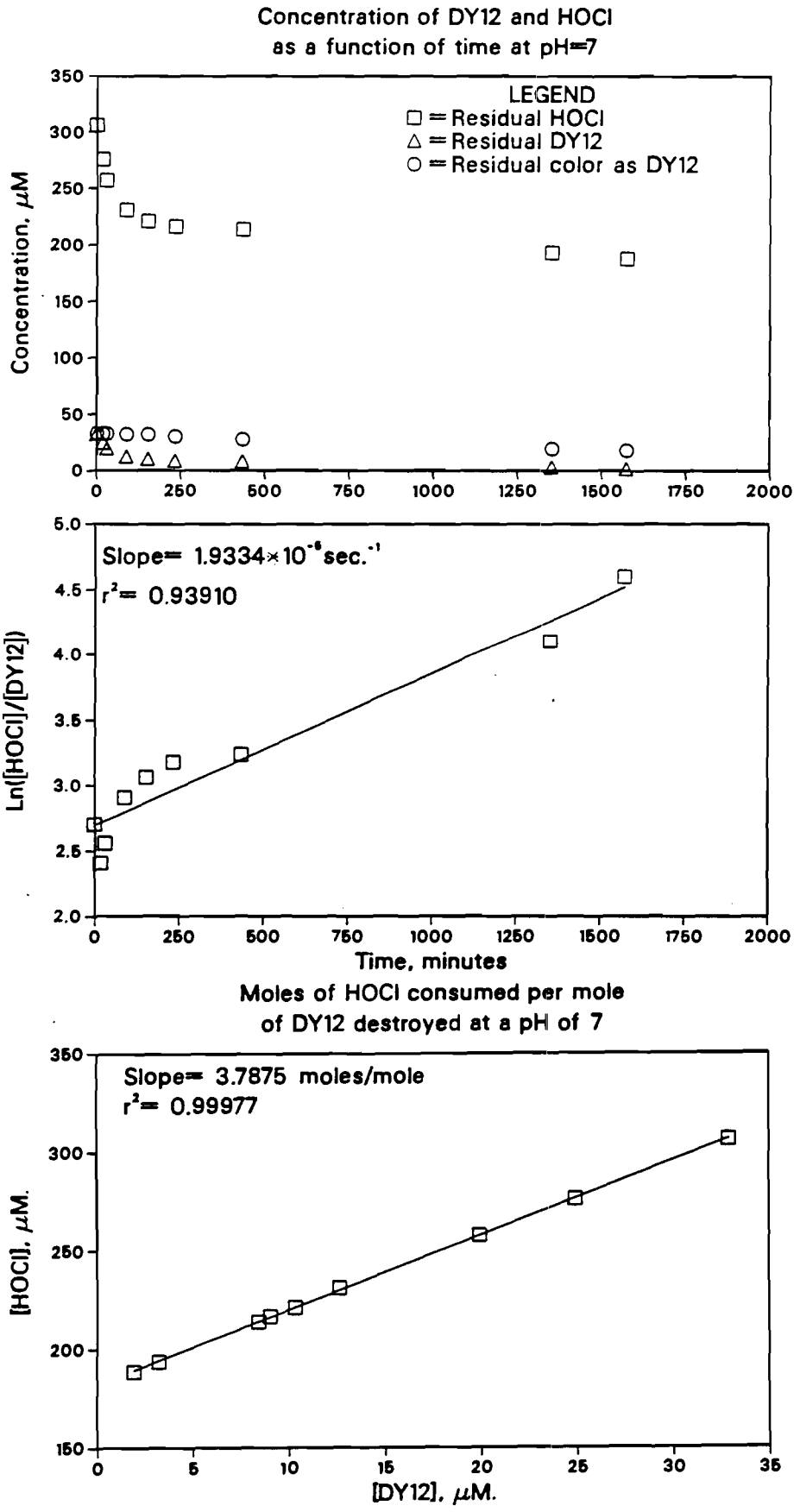
Concentration of DY12 and HOCl
as a function of time at pH=7
LEGEND
□ = Residual HOCl
△ = Residual DY12
○ = Residual color as DY12
Concentration, μM
350
300
250
200
150
100
50
0
0
250
500
750
1000
1250
1500
1750
2000
Slope= 1.9334×10⁻⁶ sec.⁻¹
r²= 0.93910
Ln([HOCl]/[DY12])
5.0
4.5
4.0
3.5
3.0
2.5
2.0
Time, minutes
Moles of HOCl consumed per mole
of DY12 destroyed at a pH of 7
Slope= 3.7875 moles/mole
r²= 0.99977
[HOCl], μM.
350
300
250
200
150
0
5
10
15
20
25
30
35
[DY12], μM.

Figure A5.14

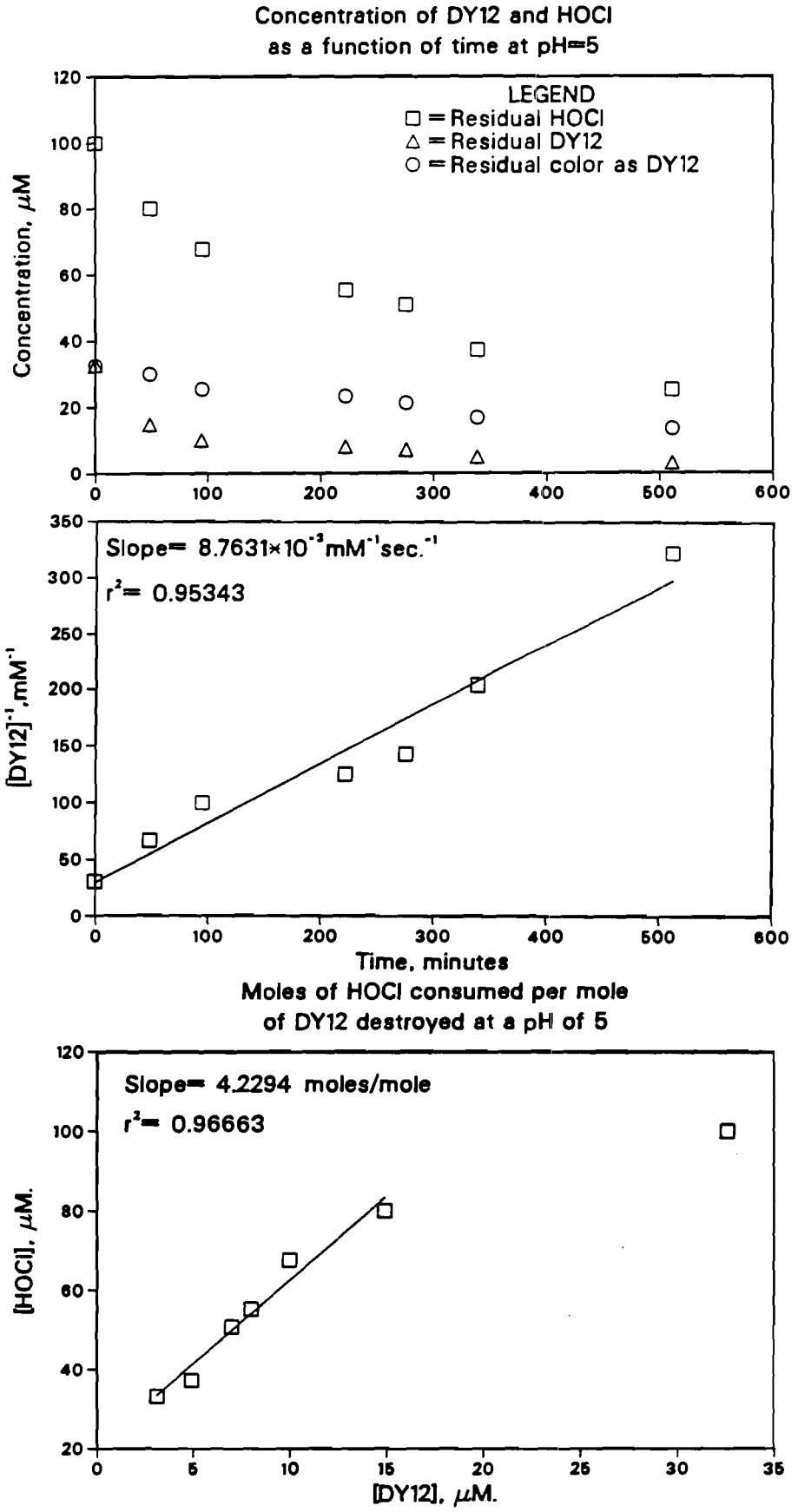
Concentration of DY12 and HOCl
as a function of time at pH=5
LEGEND
□ = Residual HOCl
△ = Residual DY12
○ = Residual color as DY12
Concentration, μM
Slope= 8.7631×10⁻³mM⁻¹sec.⁻¹
r²= 0.95343
[DY12]⁻¹,mM⁻¹
Time, minutes
Moles of HOCl consumed per mole
of DY12 destroyed at a pH of 5
Slope= 4.2294 moles/mole
r²= 0.96663
[HOCl], μM.
[DY12], μM.

Figure A5.15